



Computationally aided direct electrophilic trifluoromethylation and trifluoromethylthiolation *via* sulfonimidamides

By

Lloyd Christopher Chetty

214533430

A dissertation submitted in fulfilment of the academic requirements for the
degree of

Master of Medical Science in Pharmaceutical Chemistry

School of Health Sciences
College of Health Sciences,
The University of KwaZulu-Natal,
Durban, South Africa

January 2020

Computationally aided direct electrophilic trifluoromethylation and trifluoromethylthiolation *via* sulfonimidamides

Lloyd Christopher Chetty

214533430

2020

A thesis submitted to the School of Health Sciences, College of Health Sciences, University of KwaZulu-Natal, for the degree of Master of Medical Science in Pharmaceutical Chemistry.

This is the thesis in which the chapters are written as a set of discrete research publications with an overall introduction and final summary. Typically, these chapters will have been published or submitted in internationally recognized, peer-reviewed journals.

This is to certify that the contents of this thesis are the original research work of Mr. Lloyd Christopher Chetty, carried out under our supervision at the Catalysis and Peptide Research Unit, Westville campus, University of KwaZulu-Natal, Durban, South Africa.

Supervisor:



Signed: -----Name: **Prof. T Naicker** Date: -----

Co-Supervisor:

Signed: -----Name: **Prof. H G Kruger** Date: -----

Abstract

Fluorination chemistry is of interest due to fluorine being recognized as a crucial element in pharmaceuticals, and agrochemicals, with 30% of new small molecule drugs incorporating fluorine. The trifluoromethylation and trifluoromethylthiolation of the active pharmaceutical ingredients formed the basis for the modern trend of fluorination of pharmaceutical compounds.

The incorporation of a trifluoromethyl group (CF_3) into an organic molecule has a significant effect on its lipophilicity, permeability, and metabolic stability. Radical mediated trifluoromethylation facilitated by photoredox catalysis offers mild and highly selective reaction conditions. While there are several commercially available trifluoromethylation reagents, some limitations include the use of gaseous, volatile, and expensive reagents. Therefore, the development of cheaper and safer trifluoromethylation reagents is crucial. The utilisation of computational chemistry can facilitate the design of new potential agents. This study focused on the computational design and thereafter, the synthesis of sulfonimidamides as potential radical trifluoromethylation agents via photoredox catalysis.

Despite all efforts to synthesise trifluoromethylated sulfonimidamides being unsuccessful, the synthesis and characterisation of precursors compounds **5a-d** were successful and resulted in 6 novel X-ray crystal structures. In addition, a simple yet efficient computational method for calculating redox potentials was developed. The decision was then to synthesise trifluoromethylthiolated sulfonimidamides based on the success of sulfonamides as trifluoromethylthiolating agents.

The trifluoromethylthio group (SCF_3) has attracted particular interest in medicinal chemistry due to its remarkable lipophilicity. Due to its high lipophilicity and strong electron-withdrawing ability, the SCF_3 greatly improves the pharmacokinetic properties of lead compounds. Among the various electrophilic reagents available, N-SCF_3 reagents are the most utilised. Previously developed reagents require a strong Brønsted or Lewis acid for activation of the reaction. To address this problem, the second part of this study focused on the computational design and thereafter synthesis of more efficient sulfonimidamide based electrophilic trifluoromethylthiolation agents.

Sulfonimidamides **5c**, **f** were successfully trifluoromethylthiolated, resulting in the corresponding *N*-trifluoromethylthio sulfonimidamides **7c**, **f**. Novel X-ray crystal structures for **5e** and **5f** are also obtained. The computationally calculated SCF_3 electrophilic donation

potential of sulfonimidamides **7c**, **e**, **f** revealed that sulfonimidamide **7c** possessed the greatest potential for donation (36.51 Kcal mol⁻¹) and has the potential to be more electrophilic than previously applied delivering agents (ranging from 9.8-59.1 Kcal mol⁻¹). Therefore, sulfonimidamide **7c** was chosen as the donating agent for the further electrophilic trifluoromethylthiolation of ethyl cyanoacetate and 2,4-dimethylpyrrole. The results from the trifluoromethylthiolation model reactions indicated that sulfonimidamide **7c** is a potentially new SCF₃ donating agent, due to the trifluoromethylthio group leaving from sulfonimidamide **7c** as confirmed by crude ¹⁹F NMR and LC-MS analysis. However, further method optimisation is required and is ongoing to determine the substrate scope and reaction conditions.

Various characterisation techniques were used to confirm the chemical synthesis of the compounds which include liquid chromatography-mass spectrometry (LC-MS), nuclear magnetic resonance (NMR), high resolution mass spectrometry (HRMS), X-ray powder diffraction (XRD), and infrared spectrometry (IR).

A potential future recommendation for the *N*-trifluoromethylthiolation of the sp² type nitrogen's and *N*-trifluoromethylation of sulfonimidamides is the use of trifluoromethylthiolated and trifluoromethylated amines for the amination of the sulfonimidoyl chlorides.

Declaration 1: plagiarism

I, **Lloyd Christopher Chetty**, declare that

1. The research reported in this thesis, except otherwise indicated, is my original research.
2. This thesis has not been submitted for any degree or examination at any other university.
3. This thesis does not contain other person's data, pictures, graphs or other information, unless specifically acknowledged as being sourced from other persons.
4. This thesis does not contain other persons' writing, unless specifically acknowledged as being sourced from other researchers. Where other written sources have quoted, then:
 - a. Their words have been re-written but the general information attributed to them has been referenced.
 - b. Where their exact words have been used, then their writing have been placed in italics and inside quotation marks, and referenced.
5. This thesis does not contain text, graphics or tables copied and pasted from the Internet, unless specifically acknowledged, and the source being detailed in the thesis and in the References sections.
6. A detailed contribution to publications that form part and/or include research presented in this thesis is stated (include publications submitted, accepted, in press and published)

Signed: _____

Declaration 2: publications

Details of contribution to publications that form part and/or include research presented in this thesis (include publications in preparation, submitted, in press and published and give details of the contributions of each author to the experimental work and writing of each publication)

List of publications

Lloyd C. Chetty, Kamal K. Rajbongshi, Thavendran Govender, Hendrik G. Kruger, Per I. Arvidsson and Tricia Naicker

Computationally aided direct electrophilic trifluoromethylation and trifluoromethylthiolation *via* sulfonimidamides. *In preparation, 2020*

Lloyd C. Chetty synthesised and characterised all the compounds, computed all the computational calculations, processed the experimental data, performed the analysis and drafted the entire manuscript with the supporting information.

Kamal K. Rajbongshi aided in the design of the experiments.

The remaining authors are supervisors

Acknowledgements

I would like to express sincere gratitude and appreciation to the following individuals:

My supervisors; Professor Tricia Naicker for her patience, constant assistance, and guidance, Professor H.G. Kruger for his important insight, and corrections, Professor Per I. Arvidsson for his vital suggestions and contributions in the design of the project.

Dr G. Maguire for his critiques and suggestions.

Dr Kamal K. Rajbongshi for crucial guidance and assistance in the laboratory.

The entire Catalysis and Peptide Research Unit (CPRU) group for their advice, assistance, and guidance during the course of my degree.

My friends and family for their motivation and support.

Ms. Alicia Pillay for her indispensable proofreading abilities, suggestions and encouragement.

Mr. Sizwe Zamisa for performing the X-ray crystallography experiments

The Centre for High Performance Computing (www.chpc.ac.za) for computational resources.

The National Research Foundation (NRF) for funding to allow me to pursue my Masters degree.

You are never alone or helpless. The force that guides the stars guides you too. - Shrii Shrii Anandamurti

Table of Contents

Abstract.....	i
Declaration 1: plagiarism	iii
Declaration 2: publications	iv
Acknowledgements	v
List of abbreviations	ix
List of schemes and figures	xi
Chapter 1	1
1. Introduction.....	1
1.1 Fluorine in Pharmaceutical Applications	1
1.2 Trifluoromethylation	1
1.2.1 Nucleophilic trifluoromethylation	2
1.2.2 Electrophilic trifluoromethylation	2
1.2.3 Radical trifluoromethylation.....	3
1.3 Photoredox catalysis.....	4
1.3.1 Transition-metal complexes	6
1.3.2 Organic dyes	7
1.4 Limitations of current trifluoromethylation agents.....	7
1.5 Computational design of trifluoromethylation agents.....	7
1.6 Trifluoromethylthiolation.....	9
1.6.1 Nucleophilic trifluoromethylthiolation.....	10
1.6.2 Radical trifluoromethylthiolation	10
1.6.3 Electrophilic trifluoromethylthiolation.....	11
1.7 Sulfonimidamides	12
1.8 Computational design of trifluoromethylthiolation agents	13
1.9 Computational chemistry	14
1.9.1 Computational methods and background	14
1.9.1.1 Molecular mechanics	15
1.9.1.2 Electronic structure methods.....	15
1.9.1.3 Semi-empirical and empirical methods	15
1.9.1.4 Ab initio methods.....	15
1.9.1.5 Density functional methods	15
1.9.1.6 M06-2X.....	16
1.9.1.7 Basis sets in computational chemistry	16

1.9.1.8 Solvation models in computational chemistry	16
1.10 Experimental techniques utilised.....	17
1.10.1 Nuclear magnetic resonance (NMR) spectroscopy	17
1.10.2 Infrared (IR) spectroscopy	19
1.10.3 Liquid chromatography-mass spectrometry LC-MS).....	20
1.10.4 Supercritical fluid chromatography	22
1.10.5 Microwave-assisted reactions	24
Aims.....	25
Objectives.....	25
1.11 Outline of thesis	26
References	27
Chapter 2	33
2. Sulfonimidamides as trifluoromethylating agents	33
2.1 Trifluoromethyl radical donor abilities (TR•DAs) of sulfonimidamides	33
2.2 Calculated electrochemical potentials	35
2.3 Choice of photocatalyst.....	36
2.4 Synthesis of sulfonimidamides.....	36
2.5 Model photochemical reactions	39
2.6 Attempted trifluoromethylation of sulfonimidamides.....	40
2.7 Conclusion and outlook.....	41
References	42
Chapter 3	45
3. Computationally aided direct electrophilic trifluoromethylthiolation <i>via</i> sulfonimidamides	45
3.1. Introduction	45
3.2 Results and Discussion	47
3.2.1 Trifluoromethylthio cation donor abilities (Tt+DAs) of sulfonimidamides.....	47
3.2.2 Synthesis of sulfonimidamides	48
3.2.3 Trifluoromethylthiolation of sulfonimidamides	51
3.2.4 Direction electrophilic trifluoromethylthiolation <i>via</i> sulfonimidamides.....	55
3.3 Conclusion.....	57
References	58
Chapter 4	60
Conclusion and outlook.....	60
Chapter 5	62

5. Experimental Details	62
5.1 Computational details	62
5.1.1 Calculation of homolytic and heterolytic dissociation enthalpies	62
5.1.2 Calculation of solution phase electrochemical redox potential	62
5.2 General experimental methods	62
5.2.1 Synthesis of TBS protected sulfonamides (2a,b).....	63
5.2.2 Synthesis of TBS protected sulfonimidamides (4)	65
5.2.3 Deprotection of sulfonimidamides (5).....	69
5.2.4 <i>N</i> -trifluoromethylation of sulfonimidamides (6)	72
5.2.5 <i>N</i> -trifluoromethylthiolation of sulfonimidamides (7).....	74
References	78
Appendix 1. Supplementary material for Chapter 2	80
Appendix 2. Supplementary material for Chapter 3	83
Appendix 3. Supplementary material for Chapter 5.....	86

A CD accompanying this thesis includes the following:

- Text containing Chapters 1-5 and appendices (including References).
- All spectra and XRD data.
- All computational files.

List of abbreviations

ACN	Acetonitrile
^1H	Hydrogen-1 isotope
^{13}C	Carbon-13 isotope
^{15}N	Nitrogen-15 isotope
^{19}F	Flourine-19 isotope
^{31}P	Phosphorine-31 isotope
Ag_2CO_3	Silver carbonate
AgF	Silver fluoride
AgSCF_3	Silver trifluoromethanethiolate
CDCl_3	Deuterated chloroform
CF_3	Trifluoromethyl group
$\text{CF}_3\text{SO}_2\text{Na}$	Sodium triflinate
CI	Chemical ionisation
CO_2	Carbon dioxide
COSY	Correlation spectroscopy
CPU	Central processing unit
$\text{Cu}(\text{OAc})_2$	Copper acetate
DCM	Dichloromethane
DEPT	Distortionless enhancement by polarization transfer
DFT	Density functional theory
DMSO-d_6	Deuterated dimethyl sulfoxide
E	Energy
$E_{1/2}^{\text{ox}}$	Oxidation potential
$E_{1/2}^{\text{red}}$	Reduction potential
EI	Electron ionisation
EtOAc	Ethyl Acetate
eq.	Equivalence
eV	Electronvolt
F	Faraday constant
GC	Gas chromatography
H	Hour
H_2O	Water
HCl	Hydrochloric acid
HMBC	Heteronuclear multiple bond coherence spectroscopy
HPLC	High performance liquid chromatography
HSQC	Heteronuclear single quantum coherence
IR	Infrared
LC	Liquid chromatography
LC-HRMS	Liquid chromatography-high resolution mass spectrometry
LC-MS	Liquid chromatography–mass spectrometry
m/z	Mass to charge ratio
MeOH	Methanol

mg	Miligram
MgSO ₄	Magnesium sulphate
MHz	Megahertz
mL	Milliliters
MM	Molecular mechanics
mmol	Milimoles
mp	Melting point
MS	Mass spectrometry
MW	Microwave
N ₂	Molecular nitrogen
NBS	<i>N</i> -Bromosuccinimide
NCS	<i>N</i> -Chlorosuccinimide
NMR	Nuclear magnetic resonance
O ₂	Molecular oxygen
Ox	Oxidant
PC	Photocatalyst
Ph ₃ P	Triphenylphosphine
QM	Quantum mechanics
Red	Reductant
R _f	Retention factor
rt	Room temperature
SCE	Saturated calomel electrode
SCF ₃	trifluoromethylthio group
SET	Single electron transfer
SFC	Supercritical fluid chromatograph
SHE	Standard hydrogen electrode
Sub	Substrate
Tan δ	Loss tangent
TBS-Cl	<i>Tert</i> -Butyldimethylsilyl chloride
^t BuOCl	<i>Tert</i> -butyl hypochlorite
TC ⁺ DA	Trifluoromethyl cation-donating abilities
TEA	Triethylamine
TLC	Thin Layer Chromatography
TMSCF ₃	Trifluoromethyltrimethylsilane
TR•DAs	Trifluoromethyl radical donating ability
Tt ⁺ DA	Trifluoromethylthio cation donor abilities
Tt•DAs	Trifluoromethylthio radical donating ability
UV	Ultraviolet
W	Watts
ΔG	Change in Gibbs energy
μL	Microliters
°C	Degree celsius

List of schemes and figures

Chapter 1

Figure 1: The general mechanism for oxidative or reductive quenching cycles of a photoredox catalyst, adapted from literature.	5
Figure 2: Commonly used Ir(III) and Ru(II) photocatalysts.....	6
Figure 3: Commonly used organic photocatalysts.....	7
Figure 4: SCF ₃ containing biologically active compounds.....	10
Figure 5: Electrophilic trifluoromethylthiolating reagents.	12
Figure 6: Comparison between sulfonamide and analogue sulfonimidamide.....	12
Figure 7: The shielding effect by electrons on the nucleus from an applied magnetic field, adapted from literature.	17
Figure 8: The effect of shielding on the resonance frequency of protons, adapted from literature.	18
Figure 9: 1-bromopropane possesses three different sets of chemically equivalent protons, adapted from literature.	18
Figure 10: Examples of stretching and bending vibrations of bonds, adapted from literature.	19
Figure 11: Separation of a mixture of analytes A and B by HPLC chromatography adapted from literature.	21
Figure 12: The ionisation of a molecule by an electron beam.	21
Figure 13: Schematic diagram of a quadrupole mass analyser, adapted from literature.	22
Figure 14: Schematic of preparative SFC system, adapted from literature.	23
Figure 15: Schematic of sample heating by conduction versus heating by microwaves, adapted from literature.	25
 Scheme 1: Potential pathways of trifluoromethylation.....	2
Scheme 2: Nucleophilic trifluoromethylation of <i>gem</i> -difluoroalkenes.	2
Scheme 3: Electrophilic <i>ortho</i> -trifluoromethylation of heterocycle-substituted arenes.	3
Scheme 4: Proposed mechanism for the radical <i>N</i> -trifluoromethylation of sulfoximines.....	4
Scheme 5: A (Metal free trifluoromethylation of β -nitroalkenes), B (Metal based trifluoromethylation of terminal alkenes), C (Visible-light-driven Synthesis of Arylstannanes).	6
Scheme 6: Homolytic and heterolytic bond cleavage of trifluoromethylation agents.....	8
Scheme 7: Comparison of computational and experimental data for the electrophilic trifluoromethylation of β -keto ester.	8
Scheme 8: The effect of a single electron reduction on TR•DAs.	9
Scheme 9: Nucleophilic trifluoromethylthiolation of bromoalkynones.	10
Scheme 10: Radical trifluoromethylthiolation of aryl alkynoate esters.....	11
Scheme 11: Electrophilic N-trifluoromethylthiolation of amines.	11
Scheme 12: Homolytic and heterolytic bond cleavage of trifluoromethylthiolation agents. ..	13
Scheme 13: Electrophilic trifluoromethylthiolation of 2-(naphthalen-2-yl)ethanol.....	13
Scheme 14: The effect of a single electron reduction on Tt•DAs values.	14

Scheme 15: Evaluation between microwave and conventional heating yields and reaction times.	24
--	----

Chapter 2

Figure 1: Calculated* TR•DAs values of the proposed sulfonimidamides before and after a single electron reduction in acetonitrile. *(SMD-M06-2X/6-31+G(d)// SMD-M06-2X/6-311++G(2df,2p)).....	34
Figure 2: The reported calculated* TR•DAs values of trifluoromethylating reagents after a single electron reduction in acetonitrile. ²⁰ *(SMD-M06-2X/6-31+G(d)// SMD-M06-2X/6-311++G(2df,2p)).....	35
Figure 3: Possible organic photocatalysts for the reduction of the proposed sulfonimidamides.	36
Figure 4: Novel X-ray crystal structures obtained (unpublished results).	39

Scheme 1: Synthesis route for the proposed sulfonimidamides.	38
Scheme 2: Trifluoromethylation of electron rich heteroarenes.	39
Scheme 3: Trifluoromethylation of β -nitroalkenes.....	40
Scheme 4: Trifluoromethylation following Bolm's method.....	40
Scheme 5: Trifluoromethylation following Wang's method.	41
Scheme 6: Trifluoromethylation following Yi's method.....	41

Chapter 3

Figure 1: SCF ₃ containing biologically active compounds.....	45
Figure 2: Electrophilic trifluoromethylthiolating reagents.	46
Figure 3: Calculated* Tt ⁺ DAs values of the proposed sulfonimidamides in acetonitrile. *(SMD-M06-2X/6-31+G(d)// SMD-M06-2X/6-311++G(2df,2p)).....	47
Figure 4: The reported calculated* Tt ⁺ DAs values of electrophilic trifluoromethylthiolation reagents in acetonitrile. *(SMD-M06-2X/6-31+G(d)// SMD-M06-2X/6-311++G(2df,2p))....	48
Figure 5: Novel X-ray crystal structures obtained (unpublished results).	50
Figure 6: Comparison of reactivities between carbon-centred nucleophiles (N) and SCF ₃ reagents, modified from literature to include Tt ⁺ DA values and sulfonimidamides 7c, e, f . ..	54
Figure 7: Structure of sulfonimidamides 5c, d	56

Scheme 1: Synthesis route for the proposed saccharin based sulfonimidamides 5a-d	49
Scheme 2: Synthesis route for the proposed sulfonimidamides 5e, f	51
Scheme 3: <i>N</i> -trifluoromethylthiolation following Bolm's method.....	52
Scheme 4: Attempted <i>N</i> -trifluoromethylthiolation of sulfonimidamide 5b	53
Scheme 5: Direction electrophilic trifluoromethylthiolation of ethyl cyanoacetate.	55
Scheme 6: Direction electrophilic trifluoromethylthiolation of 2,4-dimethylpyrrole.	56

Chapter 5

Scheme 1: Synthesis of TBS protected sulfonamides (2a,b).....	63
Scheme 2: Synthesis of TBS protected sulfonimidamides 4a-d	65
Scheme 3: Synthesis of TBS protected sulfonimidamides 4e, f	65
Scheme 4: Deprotected of sulfonimidamide 4a-d	69

Scheme 5: Deprotected of sulfonimidamide 4e, f	71
Scheme 6: Attempted <i>N</i> -trifluoromethylation of sulfonimidamides.	72
Scheme 7: Attempted <i>N</i> -trifluoromethylation of sulfonimidamide 5c	73
Scheme 8: Attempted <i>N</i> -trifluoromethylation of sulfonimidamide 5b	73
Scheme 9: <i>N</i> -trifluoromethylation of sulfonimidamides.	74
Scheme 10: Attempted <i>N</i> -trifluoromethylation of sulfonimidamide 5b	74
Scheme 11: Attempted <i>N</i> -trifluoromethylation of sulfonimidamides 5b	75
Scheme 12: The trifluoromethylthiolation of ethyl cyanoacetate.....	76
Scheme 13: the trifluoromethylthiolation of 2,4-dimethylpyrrole.....	77

Chapter 1

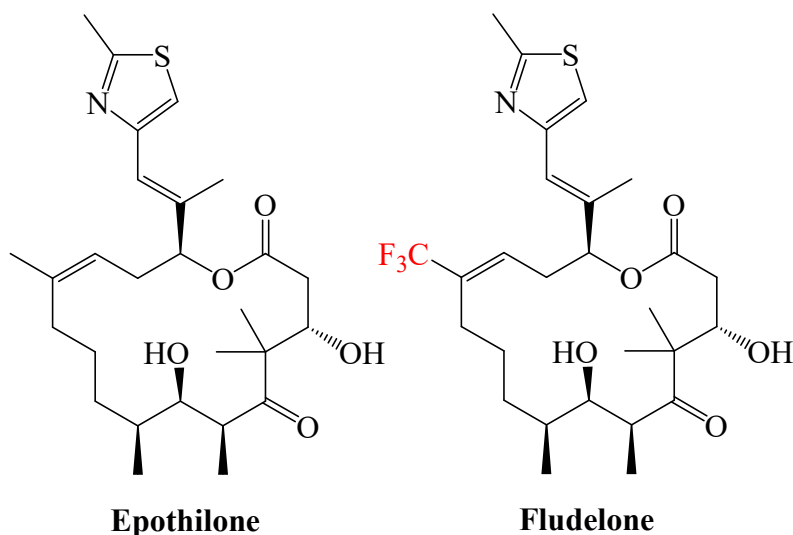
1. Introduction

1.1 Fluorine in Pharmaceutical Applications

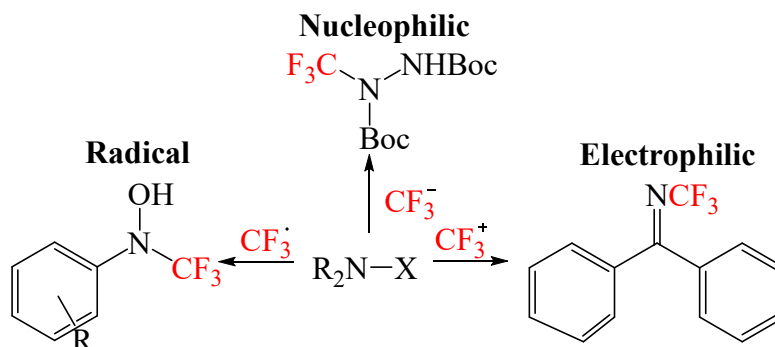
The development of fluorine chemistry began more than 100 years ago, with the first electrophilic and nucleophilic fluorination reactions dating back to the mid-19th century.^{1, 2} Currently, fluorination chemistry is of interest due to fluorine being recognised as a crucial element in pharmaceuticals, agrochemicals, and materials³, with 30% of new small molecule drugs incorporating fluorine.⁴ Prior to 1957, fluorine had not been utilised in drug development. A noticeable increase in the number of fluorine containing drug compounds began in the 1980s.⁵ The trifluoromethylation of the active pharmaceutical ingredients formed the basis for the modern trend of fluorination of pharmaceutical compounds.⁵ At present more than 50% of all current agrochemical and pharmaceutical molecules contain fluorine⁶, with over 150 active ingredients already commercialised.⁵

1.2 Trifluoromethylation

The incorporation of a trifluoromethyl group (CF_3) into an organic molecule has a significant effect on its lipophilicity, permeability, conformational behaviour, and metabolic stability.^{7, 8} Incorporating a CF_3 group into the structure of the anticancer agent epothilone (subsequently renamed fludelone) illustrates how trifluoromethylation can increase metabolic stability and retain comparable cytotoxic potency.⁹



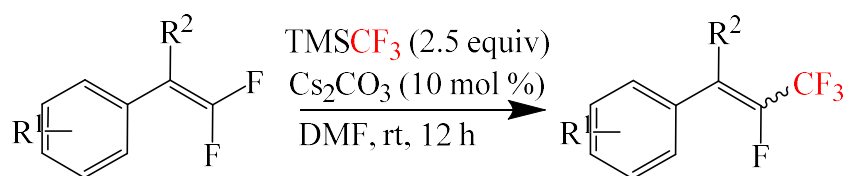
There are three main potential pathways of trifluoromethylation onto a small organic molecule. These are nucleophilic¹⁰, electrophilic¹¹, and free radical trifluoromethylation¹² (Scheme 1).¹³



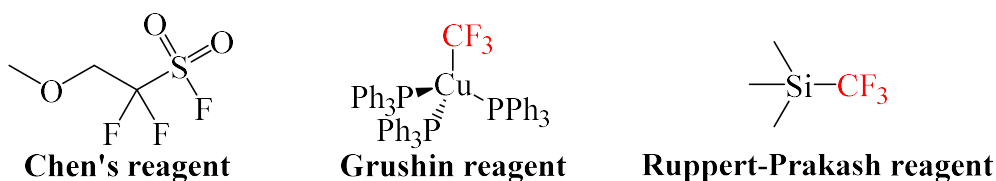
Scheme 1: Potential pathways of trifluoromethylation.¹⁰⁻¹²

1.2.1 Nucleophilic trifluoromethylation

Nucleophilic trifluoromethylation utilises the unstable anion trifluoromethyl anion (CF_3^-) (Scheme 2). The unstable anion rapidly forms a stabilised difluorocarbene and a fluoride anion.¹⁴ The instability of the CF_3^- is due to Coulombian compression.¹⁴ Initially, the instability of the anion hindered the development of nucleophilic trifluoromethylation strategies. However, currently the success of nucleophilic trifluoromethylation reactions are due to the availability of the trifluoromethylation reagents such as the unusual Chen's reagent¹⁵, Ruppert–Prakash reagent^{16, 17} or Grushin reagent.^{18, 3, 19}

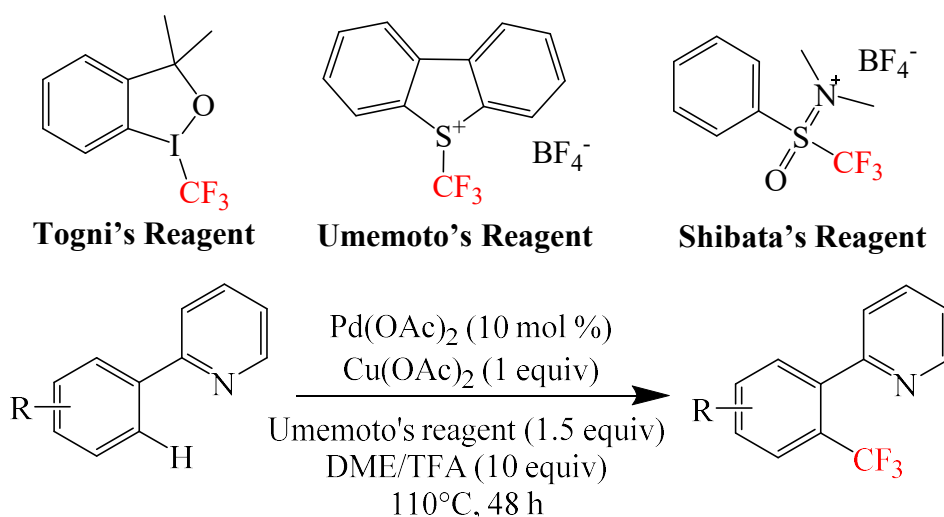


Scheme 2: Nucleophilic trifluoromethylation of *gem*-difluoroalkenes.²⁰



1.2.2 Electrophilic trifluoromethylation

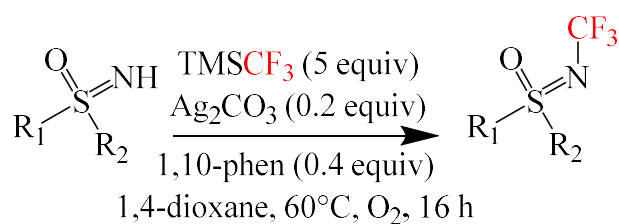
Electrophilic trifluoromethylation makes use of a trifluoromethyl cation (CF_3^+) (Scheme 3). Commonly used electrophilic CF_3 donating agents are Togni's reagent²¹, Umemoto reagent²², or Shibata reagent.^{3, 23} These reagents can react with soft nucleophiles such as thiols, alkenes, and (hetero)arenes. These reagents can also react with hard nucleophiles such as alcohols and nitriles.²⁴ Controversy remains regarding the mechanism of electrophilic trifluoromethylation, whether a single electron transfer (SET) or alternatively a polar substitution pathway occurs.²⁵

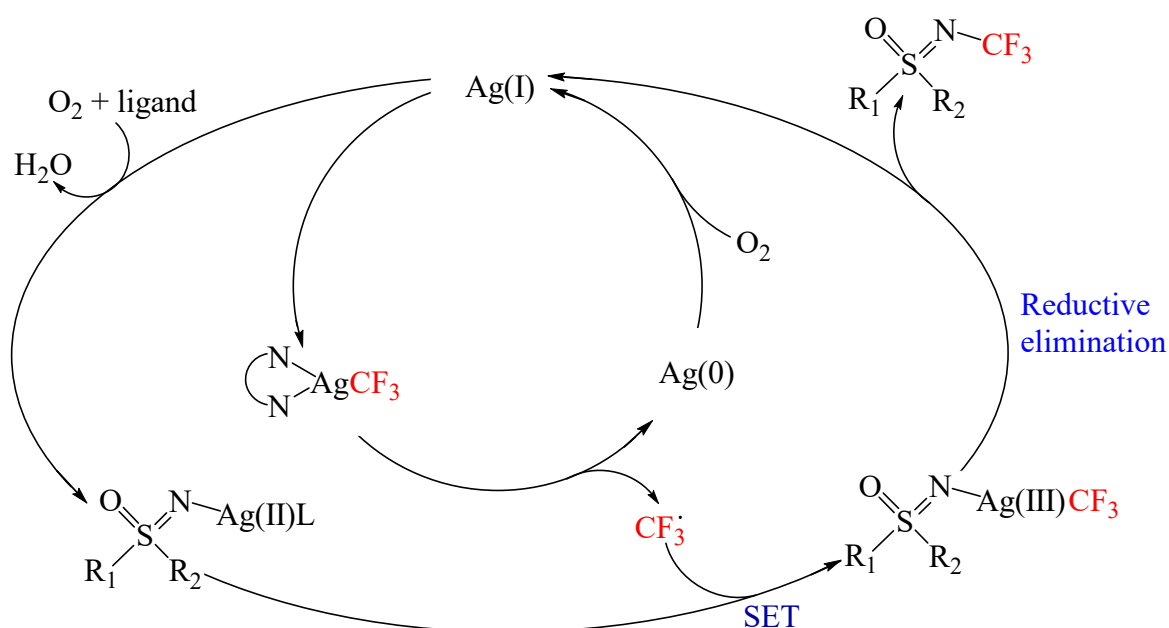


Scheme 3: Electrophilic *ortho*-trifluoromethylation of heterocycle-substituted arenes.²⁶

1.2.3 Radical trifluoromethylation

In the radical trifluoromethylation reactions, the active trifluoromethyl species is the trifluoromethyl radical (CF_3^\bullet) (Scheme 4). The trifluoromethyl radical can be generated under mild, neutral conditions from commercially available reagents²⁷ such as CF_3I ²⁸, $\text{CF}_3\text{SO}_2\text{Cl}$ ²⁹, Togni reagent³⁰, Umemoto reagent³¹, Langlois reagents³², and Ruppert–Prakash reagent.³³ Radical trifluoromethylations can easily be scaled up and proceed with high chemoselectivity.^{34, 35} Photoredox catalysis has provided access to reactive trifluoromethyl radicals.³⁶





Scheme 4: Proposed mechanism for the radical *N*-trifluoromethylation of sulfoximines.⁷

1.3 Photoredox catalysis

The renewed interest in radical-mediated organic synthesis has correspondingly revitalised attention in photochemistry, particularly photoredox catalysis.³⁷ The revived interest is due to the accessibility of species, which would be practically inaccessible by other forms of catalysis. Academics in various chemical fields ranging from organic synthesis to materials science.³⁸⁻⁴² are incorporating photoredox catalysis in order to facilitate unique chemical reactions.⁴³ Photoredox catalysis offers environmental benignity, high selectivity, mild conditions, and can be applied to numerous synthetically important reactions.⁴⁴

Photoredox catalysed reactions follow either an oxidative or reductive quenching cycle (Figure 1). In an oxidative quenching cycle, the photocatalyst in the excited state (PC*) donates an electron to either a substrate (Sub) or an oxidant (ox) present in the reaction and returns to the ground state.⁴³⁻⁴⁵ The photocatalyst (PC^{•+}) is then reduced by a substrate or reductant (red) to complete the cycle. In a reductive quenching cycle, the excited catalyst is quenched by obtaining an electron either from a substrate or a reductant present in the reaction mixture.⁴³⁻⁴⁵ The catalysis is then oxidised by a substrate or oxidant to complete the cycle. Photoredox catalysed reactions are highly controlled as light is required for excitation and for the reaction to occur. The energy put into the system is selective for the photocatalyst instead of the entire system, as most simple organic molecules do not absorb energy in the visible region.⁴³⁻⁴⁵

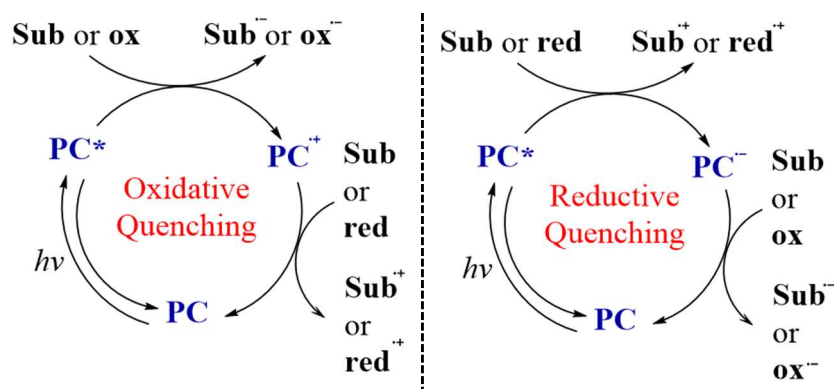


Figure 1: The general mechanism for oxidative or reductive quenching cycles of a photoredox catalyst, adapted from literature.⁴³

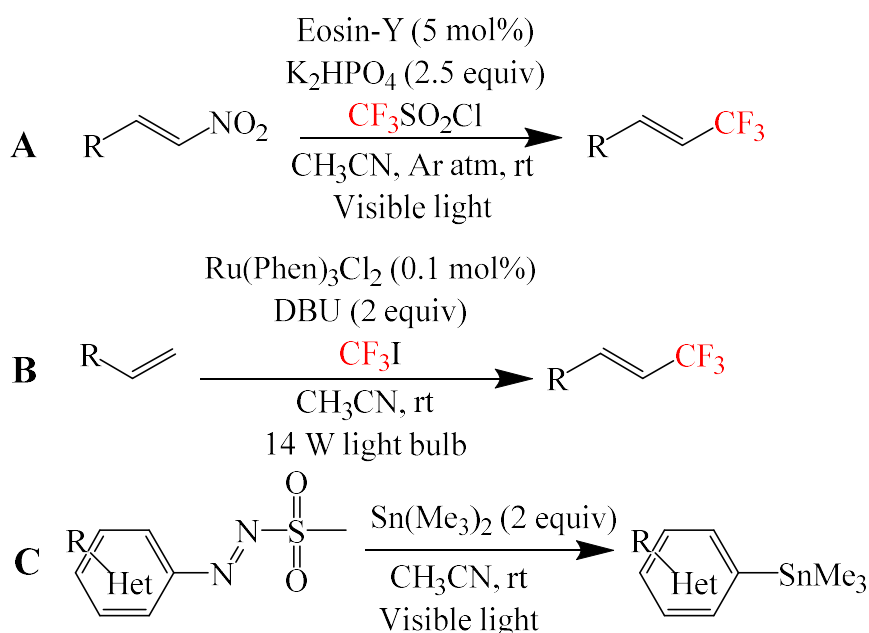
The oxidation potential ($E_{1/2}^{\text{ox}}$) of a donor measures the ability of a species to release an electron. The lower the oxidation potential, the more easily a species is oxidised. The reduction potential ($E_{1/2}^{\text{red}}$) of an acceptor measures its tendency to accept an electron. The higher the reduction potential, the more easily a species is reduced. The oxidation potential of the donor and reduction potential of the acceptor can be utilised to understand the feasibility of a redox reaction between the donor/acceptor pair.⁴³ The Nernst equation (1), is used to relate these two values to free energy, where ΔG is change in free energy, n is the number of electrons transferred, and F is the Faraday constant.⁴⁶

$$\Delta G = -nFE \quad (1)$$

$$E = E_{\frac{1}{2}}^{\text{red}}(A) - E_{\frac{1}{2}}^{\text{ox}}(D)$$

A negative ΔG indicates an exergonic process, for a favourable redox reaction the reduction potential for the acceptor should exceed the oxidation potential of the donor.⁴³

Photoredox processes can be facilitated by organic dye based catalysts⁴⁷ (Scheme 5, A), transition metal-based catalysts⁴⁸ (Scheme 5, B), and photocatalyst free reactions⁴⁹ (Scheme 5, C). However, photocatalyst free reactions are rare.⁵⁰



Scheme 5: A (Metal free trifluoromethylation of β -nitroalkenes), B (Metal based trifluoromethylation of terminal alkenes), C (Visible-light-driven Synthesis of Arylstannanes).

1.3.1 Transition-metal complexes

Since the MacMillan⁵¹ and Yoon⁵² groups simultaneously reported the first use of $[\text{Ru}(\text{bpy})_3]^{2+}$ as a photocatalyst (PC), several other researchers have considered transition-metal based complexes as PCs in organic synthesis.⁵³ Currently, the most popular photocatalysts employed are either Ir(III) or Ru(II) polypyridyl complexes.⁵³

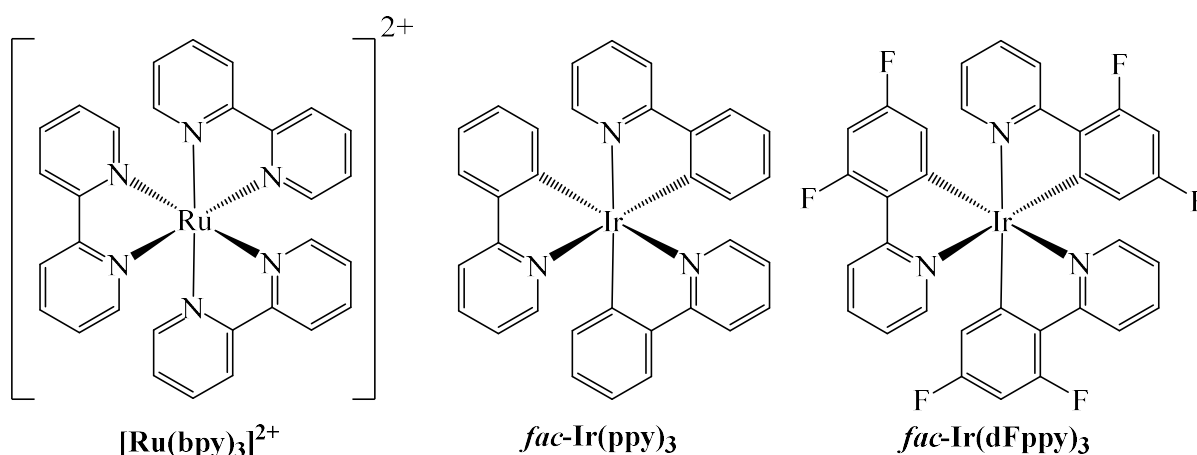


Figure 2: Commonly used Ir(III) and Ru(II) photocatalysts.⁴⁴

Unfortunately, transition-metal based photocatalysts are expensive and the removal of toxic metal impurities are the main disadvantage.⁵⁴

1.3.2 Organic dyes

Organic photoredox catalysts possess a relatively lower cost, greater availability, and can have superior efficiency^{55, 56} when compared to metal based photocatalysts.⁵⁷ Additionally, organic photocatalysts are non-toxic, easy to modify and handle.⁵⁸ Therefore, the development of methodology using metal-free photoredox catalysis such as organic dyes is highly desirable.⁴⁷

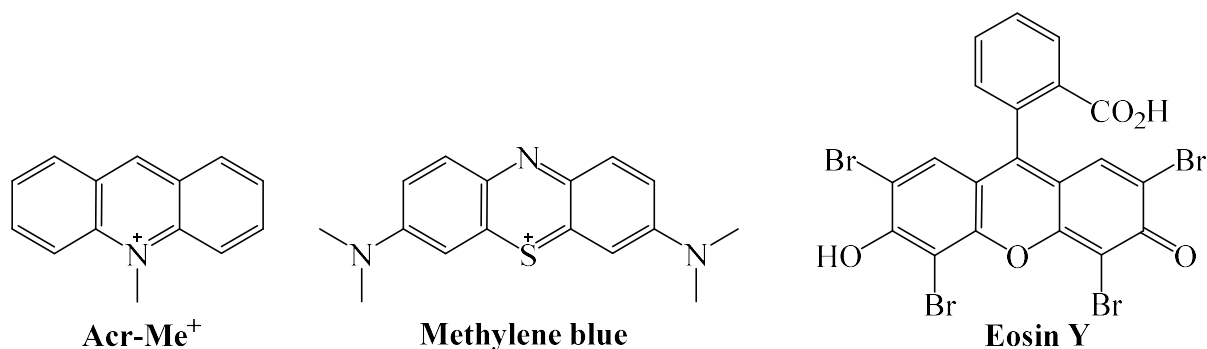


Figure 3: Commonly used organic photocatalysts.⁴³

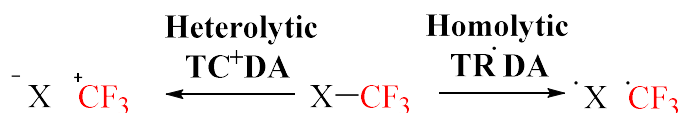
1.4 Limitations of current trifluoromethylation agents

Although there are many commercially available trifluoromethylation reagents, they suffer from limitations such as the gaseous CF₃I²⁸, the volatile CF₃SO₂Cl²⁹, the expensive Togni²¹, Umemoto²², and Rupert-Prakash^{16, 17} reagents.^{32, 59} Therefore, the development of cheaper and safer trifluoromethylation reagents is vital.⁶⁰

The utilisation of computational chemistry can facilitate the design of new potential trifluoromethylation agents.⁶¹⁻⁶³ Coupled with experimental results, computations can lead to more effective reagents than currently available.⁶⁴

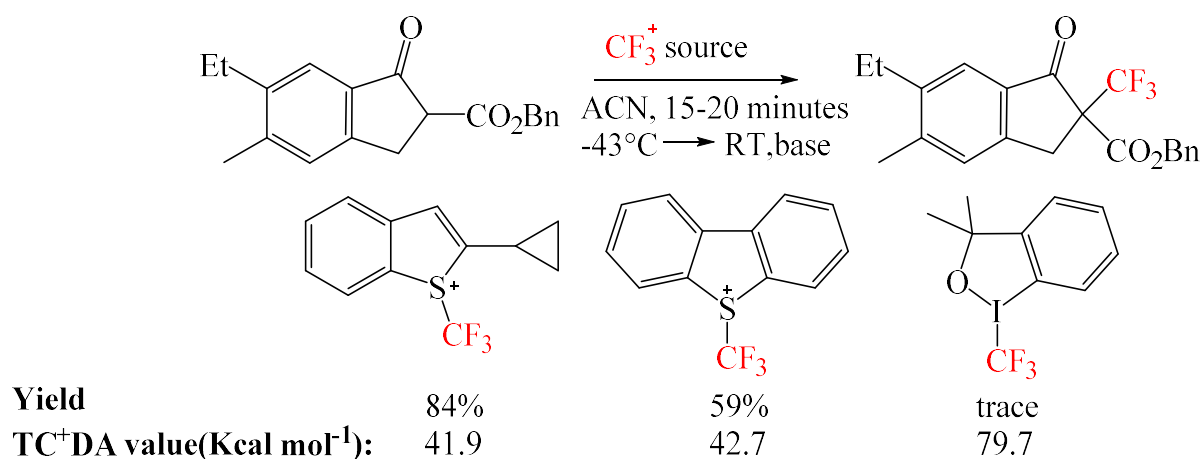
1.5 Computational design of trifluoromethylation agents

Cheng and co-workers computationally studied the radical and electrophilic donating ability of various known trifluoromethylation agents (Scheme 6) by calculating the homolytic and heterolytic bond cleavage.^{61, 63}



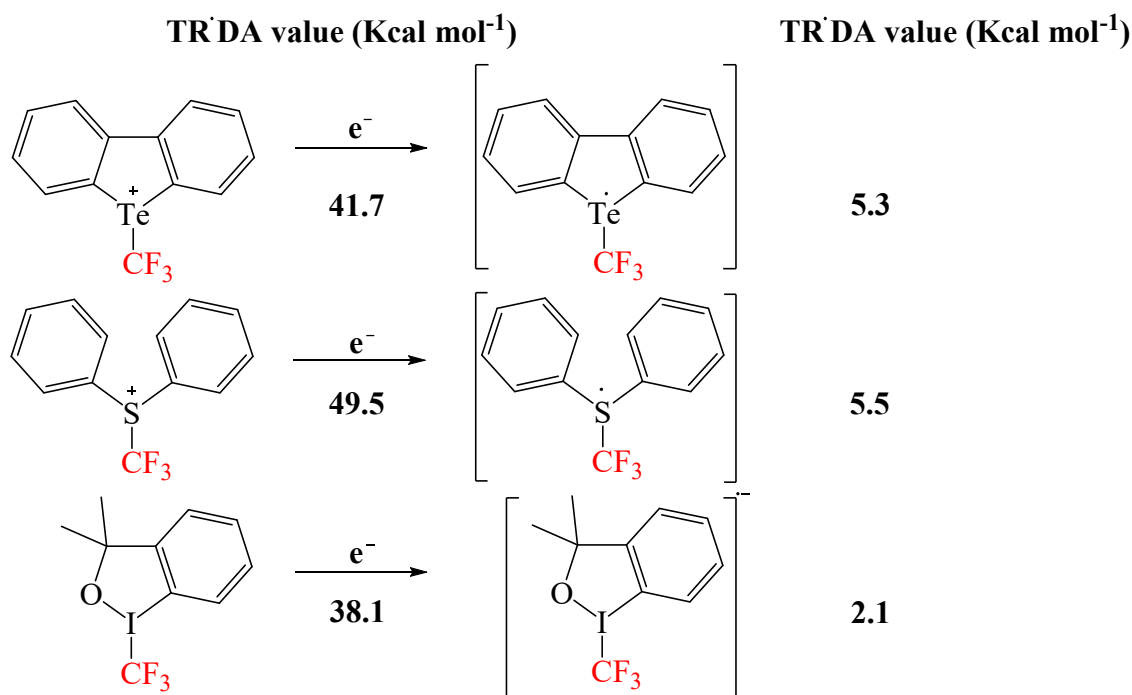
Scheme 6: Homolytic and heterolytic bond cleavage of trifluoromethylation agents.^{61, 63}

Cheng compared the trifluoromethyl cation-donating abilities (TC⁺DA) of various electrophilic trifluoromethylation agents with experimental data for the electrophilic trifluoromethylation of β -keto ester.^{19, 61} Upon comparing the TC⁺DA values with experimental yield, lower TC⁺DA values led to higher yields. Low TC⁺DA values correspond to a weaker bond between the CF₃ group and the donating agent. Therefore, the lower the TC⁺DA value, the greater the ability for donation. Furthermore, Cheng compared the TC⁺DA values for the electrophilic trifluoromethylation of pyrrole and terminal acetylenic carbon and found good correlation.



Scheme 7: Comparison of computational and experimental data for the electrophilic trifluoromethylation of β -keto ester.⁶¹

Cheng and co-workers computationally studied the radical donating ability (TR[•]DAs) of various known trifluoromethylation agents before and after a single electron reduction.⁶³ Single electron reduction was found to activate the X-CF₃ bond as indicated by the significantly reduced TR[•]DAs values (Scheme 8). Single electron reduction can be achieved either photochemically⁶⁵ or electrochemically.⁶⁶



Scheme 8: The effect of a single electron reduction on TR·DAs.⁶³

Computationally calculated bond dissociation enthalpies have also been used in the design of more efficient fluorinating agents.⁶⁴ Computational chemistry has also been implemented in designing new Togni reagents.⁶²

Inspired by the work of Cheng and co-workers^{61, 63}, this study was focused on the computational design and thereafter synthesis of more efficient radical trifluoromethylation agents using photoredox catalysis.

1.6 Trifluoromethylthiolation

The trifluoromethylthio group (SCF₃) has attracted special interest in medicinal chemistry for its incredible lipophilicity (Hansch constants 1.44).⁶⁷⁻⁶⁹ Based on its strong electron-withdrawing ability and high lipophilicity, the trifluoromethylthio group greatly improves the pharmacokinetic properties of lead compounds.^{69, 70} The trifluoromethylthio group is incorporated into several bioactive compounds (Figure 4), such as Tiflorex^{71, 72} (anorectic drug), Toltrazuril^{73, 74} (coccidiostatic drug), and Cefazaflur^{75, 76} (parenteral cephalosporin).^{77, 78} The unique properties possessed by the trifluoromethylthio moiety has prompted much research into the development of efficient methods for its incorporation into desired scaffolds.⁷⁹

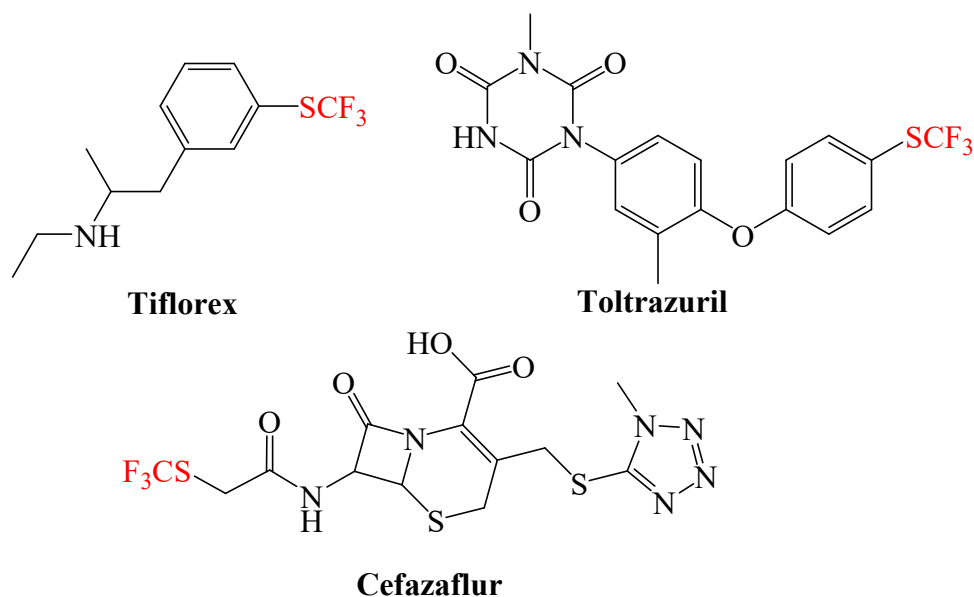
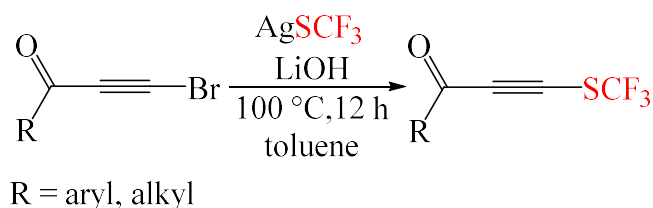


Figure 4: SCF₃ containing biologically active compounds.⁷⁷

The trifluoromethylthio group can be directly incorporated into desired scaffolds using nucleophilic⁸⁰, radical⁸¹, and electrophilic⁸² strategies.

1.6.1 Nucleophilic trifluoromethylthiolation

The use of nucleophilic reagents represents one of the most popular strategies in trifluoromethylthiolation (Scheme 9).⁸³ Amongst the several nucleophilic trifluoromethylthiolating reagents such as Hg(SCF₃)₂,^{84, 85} CuSCF₃,⁸⁶ (bpy)CuSCF₃,⁸⁷ [R₄N]SCF₃,⁸⁸ and CsSCF₃,⁸⁹ the commercially available AgSCF₃⁹⁰ is the most popular.⁹¹ The major advantage of nucleophilic trifluoromethylthiolation is the use of relatively inexpensive SCF₃ sources. However, the major limitation of the strategy is based on prefunctionalization of the substrates.⁹²

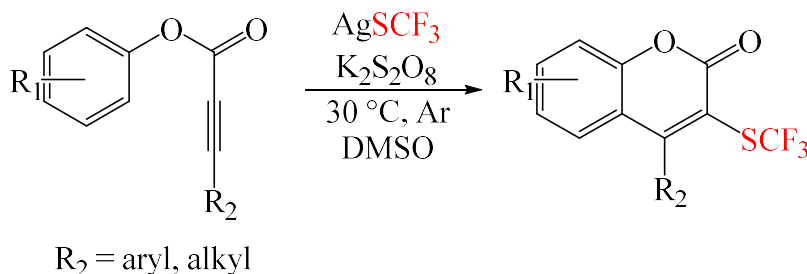


Scheme 9: Nucleophilic trifluoromethylthiolation of bromoalkynones.⁸³

1.6.2 Radical trifluoromethylthiolation

Electrophilic and nucleophilic trifluoromethylthiolation methodologies have also been developed and utilised successfully in the last decade.⁸¹ In contrast, radical trifluoromethylthiolation (Scheme 10) has been studied and applied to a lesser extent due to

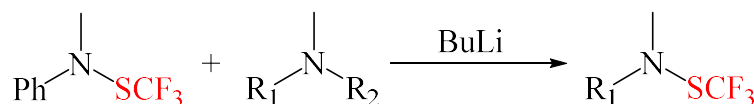
the toxic and gaseous radical reagents (CF_3SH and CF_3SCI).^{78–81} The recent emergence of photoredox catalysis has prompted the revival of radical trifluoromethylthiolations.^{78, 93, 94} The success of photoredox catalysis^{81, 95–98} has been assisted by the recent availability of new shelf-stable and easy to handle electrophilic and nucleophilic reagents.⁹⁹



Scheme 10: Radical trifluoromethylthiolation of aryl alkynoate esters.¹⁰⁰

1.6.3 Electrophilic trifluoromethylthiolation

Electrophilic trifluoromethylthiolation offers a straightforward method for direct trifluoromethylthiolation (Scheme 11).



Scheme 11: Electrophilic N-trifluoromethylthiolation of amines.¹⁰¹

Among the various electrophilic reagents available, N- SCF_3 reagents are the most interesting, with the main reagents based on saccharin, succinimide, and phthalimide scaffolds^{78, 79} (Figure 5). The reagents PhNHSCF_3 (Figure 5, **A**) and PhN(Me)SCF_3 (Figure 5, **B**) developed by Billard and Langlois^{102, 103} are effective for trifluoromethylthiolation of alkenes¹⁰², indole¹⁰⁴, Grignard reagents⁸², and alkynes.¹⁰⁵ However, a strong Brønsted or Lewis acid is required for the activation of the reaction.⁷⁹ To address this problem, Shen and co-workers developed the highly electrophilic, shelf-stable N-trifluoromethylthiosaccharin¹⁰⁶ (Figure 5, **E**) and N-trifluoromethylthio-dibenzene-sulfonimide¹⁰⁷ (Figure 5, **F**). Both reagents have been shown to be highly electrophilic in both computational¹⁰⁸ and experimental⁷⁰ studies. These reagents have been shown to possess a greater reactivity than previous reagents with a broader substrate scope while under milder conditions.^{79, 106–109}

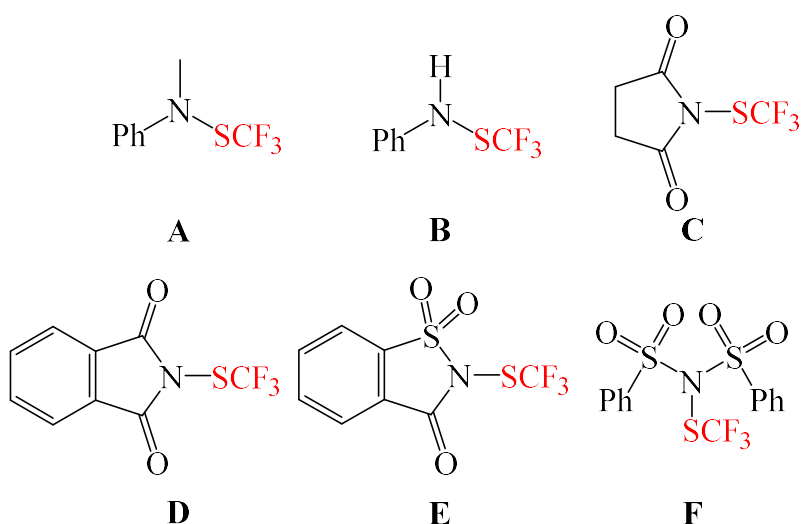


Figure 5: Electrophilic trifluoromethylthiolating reagents.¹⁰⁷

1.7 Sulfonimidamides

Sulfonimidamides are the aza-analogues of sulfonamides, where one of the oxygen atoms have been replaced by a nitrogen¹¹⁰ (Figure 6). Sulfonimidamides have received less attention compared to sulfonamides presumably due to the lack of commercial availability and synthetic methods.^{111, 112}

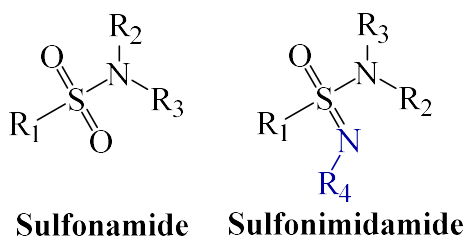
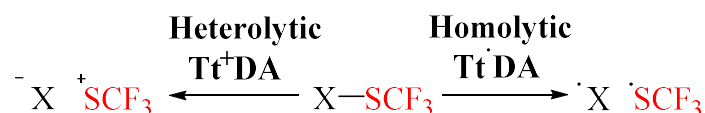


Figure 6: Comparison between sulfonamide and analogue sulfonimidamide.¹¹³

Levchenko *et al.* first reported sulfonimidamides in the early 1960's.¹¹⁴⁻¹¹⁷ However, only in the last decade has interest increased in the applications and reactivity of sulfonimidamides in the fields of biological and synthetic chemistry.¹¹⁸⁻¹²¹ Studies have shown that sulfonamides have the ability to act as highly electrophilic trifluoromethylthiolating reagent.¹⁰⁶⁻¹⁰⁸ Therefore, this study was focused on designing highly electrophilic sulfonimidamides based trifluoromethylthiolating reagents.

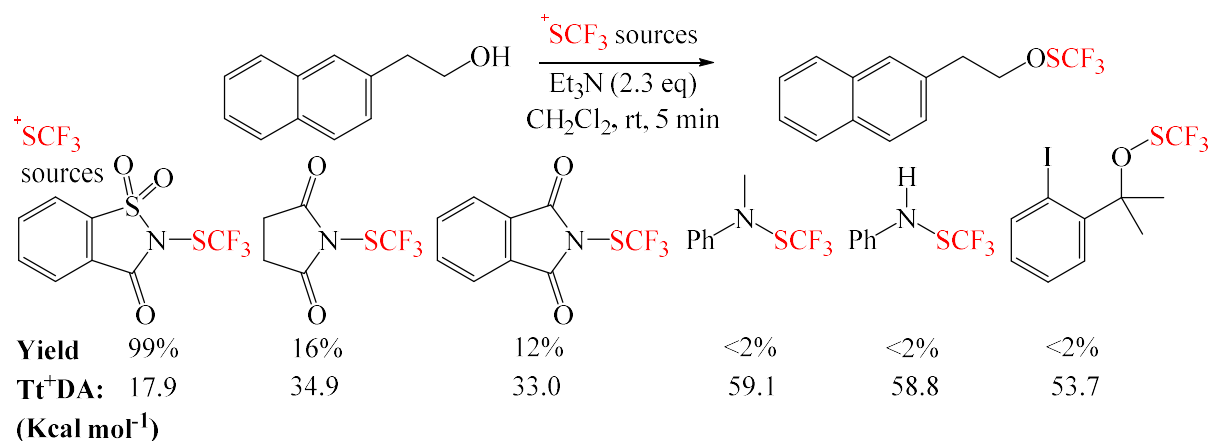
1.8 Computational design of trifluoromethylthiolation agents

Cheng and co-workers additionally studied the electrophilic and radical donating ability of various known trifluoromethylthiolation agents (Scheme 12) by computationally calculating the homolytic and heterolytic bond cleavage.^{108, 122}



Scheme 12: Homolytic and heterolytic bond cleavage of trifluoromethylthiolation agents.^{108, 122}

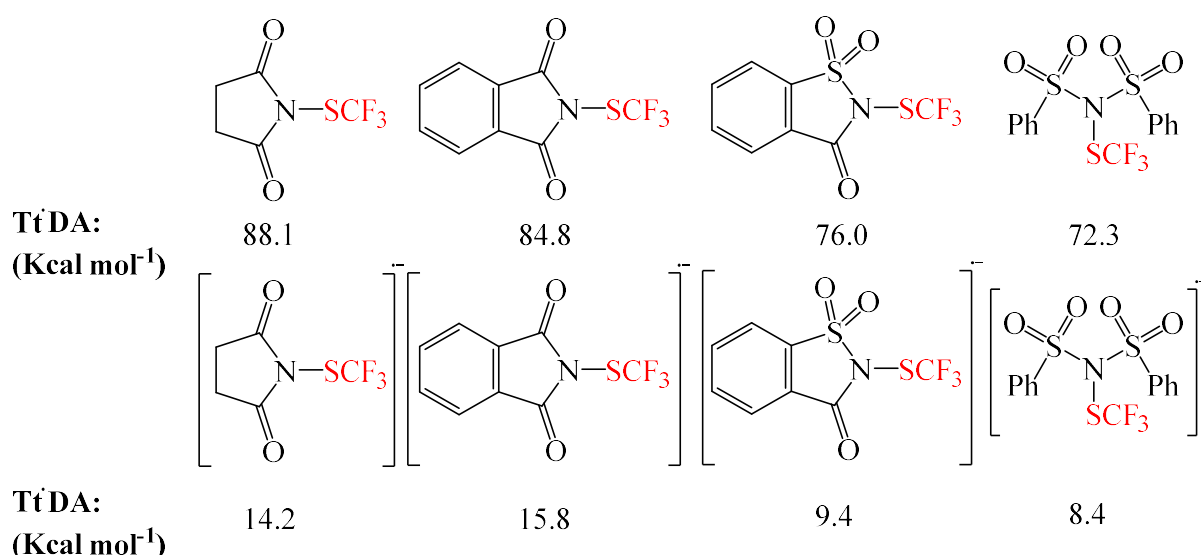
Cheng observed a good correlation between the computed Tt^+DA values and experimental reactivity of the various electrophilic trifluoromethylthiolation agents (Scheme 13).



Scheme 13: Electrophilic trifluoromethylthiolation of 2-(naphthalen-2-yl)ethanol.^{79, 106, 108}

In an additional study, Cheng and co-workers experimentally determined the electrophilicity parameters of various trifluoromethylthiolation agents, which correlated well with Tt^+DA values.⁷⁰

Cheng and co-workers additionally computed the radical donating ability ($\text{Tt}^\bullet\text{DA}$ s) of various known electrophilic trifluoromethylthiolation agents before and after a single electron reduction.¹²² Single electron reduction was found to activate the $\text{X}-\text{SCF}_3$ bond as indicated by significantly reduced $\text{Tt}^\bullet\text{DA}$ s values (Scheme 14). Single electron reduction can be achieved either photochemically⁸¹ or electrochemically.



Scheme 14: The effect of a single electron reduction on Tt•DAs values.¹²²

Inspired by the work of Cheng and co-workers^{108, 122} and Shen and associates^{106, 107}, this study was focused on the computational design and thereafter, synthesis of more efficient sulfonimidamide based electrophilic trifluoromethylthiolation agents.

1.9 Computational chemistry

Chemistry is a branch of science pertaining to the transformation, construction, and properties of molecules.¹²³ Computational chemistry comprises of quantum mechanics, molecular mechanics, simulations and other computational methods for understanding and predicting the behaviour of molecular systems. Computational chemistry has become an invaluable tool in modern industrial and academic chemistry. The solution of chemical problems otherwise extremely difficult or even impossible experimentally is possible due to the processing power of modern computers. Given a set of nuclei and electrons, computational chemistry can attempt to calculate things such as the geometrical arrangements of the nuclei corresponding to stable molecules, relative energies, dipole moment, polarizability, NMR coupling constants, and how different molecules will interact. To achieve this computational chemists use complex computational software that enables them to achieve an understanding of chemical processes, and avoid time-consuming expensive experiments.¹²⁴⁻¹²⁷

1.9.1 Computational methods and background

Chemical systems are modelled using a set of approximations, this is referred to as a theoretical model or method. These approximations in combination with an algorithm are applied to atomic orbitals in order to calculate molecular orbitals and energy.^{128, 129} Modelling of chemical

structures are based on two different methods which form the backbone of computational chemistry. These are molecular mechanics (MM) also known as force field methods and electronic structure methods.¹²⁷

1.9.1.1 Molecular mechanics

MM utilises the laws of classical mechanics to determine molecular structures and properties. MM computations do not consider the electrons for a molecular system. Rather, calculations are centred on nuclei interactions. As a result of this approximation, MM calculations are computationally inexpensive. However, MM methods are not applicable to chemical problems in which electronic effects predominate. The numerous MM methods are characterised based on their particular force field.^{126, 127, 130}

1.9.1.2 Electronic structure methods

Electronic structure methods utilise the laws of quantum mechanics (QM) instead of classical mechanics as the foundation for calculations. QM states that the energy and related molecular properties can be acquired by solving Schrödinger's equation. The three classes of electronic structure methods are semi-empirical, *ab initio*, and density functional.^{127, 128, 130}

1.9.1.3 Semi-empirical and empirical methods

Semi-empirical computations are set up where certain pieces of information are approximated or entirely removed. Therefore, to rectify the introduced errors, the method is parameterized. These calculations only consider the valence electrons and are therefore quicker than *ab initio* computations. However, results can be erratic.¹²⁶⁻¹²⁸

1.9.1.4 *Ab initio* methods

Ab initio computations are derived exclusively from theory, containing no experimental data. The approximations used are generally mathematical. *Ab initio* methods systematically approach the correct "answer" as the basis set size and level of theory are increased. However, *ab initio* computations require massive amounts of computer disk space, CPU time, and memory.^{127, 128}

1.9.1.5 Density functional methods

Kohn, Sham and Hohenberg^{131, 132} proposed the use of density functional models in order to design an improved electronic structure method. Density functional theory (DFT) methods can attain a substantially greater increase in accuracy, as compared to Hartree-Fock theory. This improvement comes with a moderate rise in computational cost. This is obtained by including

certain electron correlation effects, which are less expensive as compared to traditional correlation methods.^{127, 128}

DFT methods compute electron correlation *via* the use of a general functional of the electron density. The DFT functionals compute electronic energy by partitioning it into numerous components. The partitioned components are then computed separately. Functionals are distinguished by their treatment of the exchange and correlation components.

A prominent disadvantage in density functional development is that the functionals are not systematically improvable. Therefore, improvements to satisfy constraints or provide more flexible functional forms will not necessarily lead to improvement for all interactions. Presently no functional is universally accurate. The main limitations of density functionals are their treatment of nonlocal exchange and correlation.¹³³ The accuracy of DFT computations are dependent on the basis set and density functional selected. DFT methods have improved due to the utilisation of hybrid functionals.¹²⁷⁻¹³⁰

1.9.1.6 M06-2X

The M06^{134, 135} suit of density functionals have gained recent attention for studies in which accurate calculations of molecular properties could be performed with improved accuracy in comparison with experiments.¹³⁶⁻¹³⁸ Truhlar and co-workers recommend the M06-2X¹³⁹ functional for calculations involving main-group thermochemistry.¹³⁹ The M06-2X functional has shown accuracy in thermochemistry calculations involving systems which contain halogens, oxygen, and carbon atoms.¹³⁷

1.9.1.7 Basis sets in computational chemistry

A basis set is a mathematical description of the orbitals in a molecular system and is utilised to execute calculations. The larger the basis set, the more accurate the approximated orbitals. This is due to a small number of restrictions imposed on electron locations in space.¹²⁷⁻¹²⁹

1.9.1.8 Solvation models in computational chemistry

The solute properties which depend on energy, such as geometry, and total energy, are dependent on the solvent due to the interaction energy between solute and solvent¹²⁶. Solvent effects are included in computational calculations using both discrete¹⁴⁰⁻¹⁴⁶ and continuum¹⁴⁷⁻¹⁴⁹ solvent models. Discrete methods work well on problems using chemical intuition. However, discrete methods are computational costly even for simple systems. In continuum models, the explicit solvent structure is not considered.¹⁵⁰ Therefore, the solute's electronic distribution can be treated quantitatively and polarization effects can be assessed at a minimal

computational cost. The PCM method is commonly used for solvent modeling since it is flexible and robust¹²⁶. The SMD solvation model is recommended by Gaussian for the ΔG of solvation¹⁵¹ and is one of the most commonly used solvation model in recent literature.^{61, 63, 69, 108, 122, 152}

1.10 Experimental techniques utilised

1.10.1 Nuclear magnetic resonance (NMR) spectroscopy

In the 1940s, NMR spectroscopy was developed in order to study the properties of nuclei.¹⁵³⁻¹⁵⁵ NMR spectroscopy can aid in the identification of the carbon-hydrogen framework of organic compounds.¹⁵⁶ Nuclei that possess spin (an odd number of protons and, or neutrons) permits them to be analysed by NMR techniques (^1H , ^{13}C , ^{15}N , ^{19}F , and ^{31}P).¹⁵⁷ Due to the nucleus possessing charge, nuclei with spin have a magnetic moment and generates a magnetic field. When there is no applied magnetic field, the magnetic moments of these nuclei are randomly oriented. However, when there is an applied magnetic field, the magnetic moments of these nuclei line up either with or against the applied magnetic field.^{156, 158} The frequency of an NMR signal is dependent on the strength of the applied magnetic field experienced by the nucleus. If all of the protons in an organic compound experienced the same magnetic field, then all of the protons would produce a single signal of the same frequency.¹⁵⁶ Nuclei are surrounded by electrons, which circulate about the nuclei and in a magnetic field induce a local magnetic field which opposes the applied magnetic field and therefore, subtracts from it¹⁵⁹ (Figure 7). The electron density partly shields the protons from the applied magnetic field. The shielding varying for different hydrogens, all of the protons in an organic compound do not experience the same applied magnetic field. The greater the electron density of the proton's environment, the greater the shielding from the applied magnetic field (diamagnetic shielding).^{156, 160}

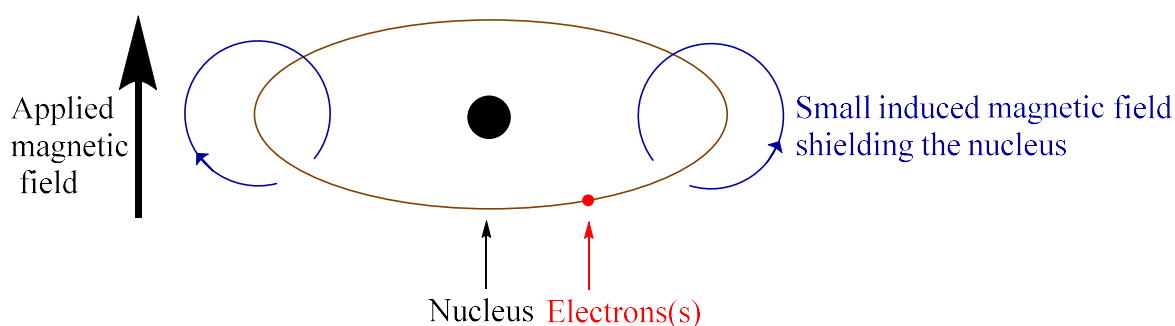


Figure 7: The shielding effect by electrons on the nucleus from an applied magnetic field, adapted from literature.¹⁵⁹

In electron-rich environments, protons are more shielded and resonate at lower frequencies (upfield). Whereas in electron-poor environments, protons are less shielded and resonate at higher frequencies (downfield). In NMR spectra high frequency appears on the left-hand side (Figure 8).¹⁵⁶

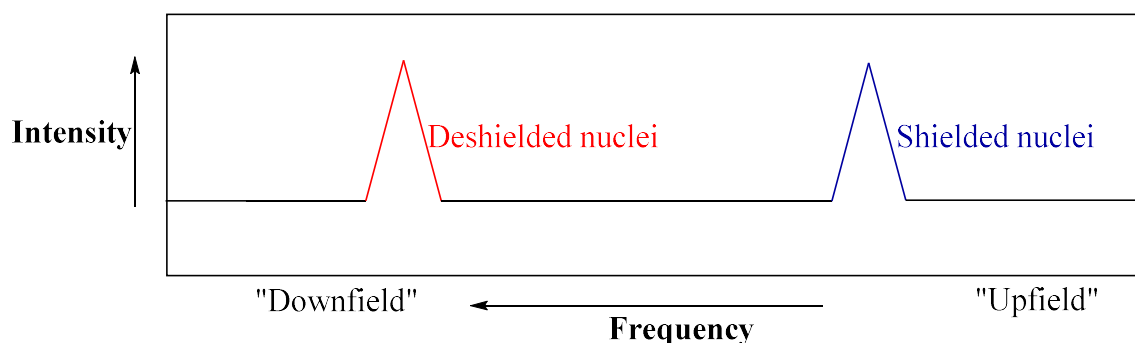


Figure 8: The effect of shielding on the resonance frequency of protons, adapted from literature.¹⁵⁶

When protons are in the same environment, they are chemically equivalent (Figure 9). Therefore, they produce the same signal in an NMR spectrum. Therefore, non-chemically equivalent protons produce a unique signal in NMR spectra. The ^1H NMR spectrum of 1-bromopropane possesses three signals due to three sets of chemically equivalent protons being present.¹⁵⁶

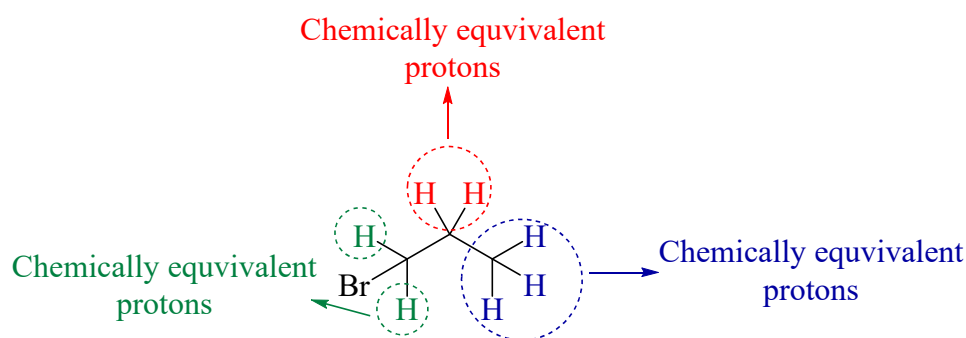


Figure 9: 1-bromopropane possesses three different sets of chemically equivalent protons, adapted from literature.¹⁵⁶

In the ^1H NMR spectrum, integration of the area under a signal can determine the relative number of protons responsible for producing that signal. The number of peaks in a signal is the multiplicity of that signal. Splitting is due to protons that are bonded to adjacent carbons.^{156, 160} In ^{13}C NMR spectra, the number of signals indicates how many different kinds of carbons a compound has, similar to ^1H NMR spectra the number of signals reveals the number of

non-chemically equivalent hydrogens a compound has. The principles behind ^1H NMR and ^{13}C NMR spectroscopy are essentially the same.¹⁵⁶

Complex molecules which are difficult to analyse by conventional ^1H NMR and ^{13}C NMR spectroscopy because of signals overlapping can be analysed by special techniques. These include DEPT (distortionless enhancement by polarization transfer) ^{13}C NMR which distinguishes between CH , CH_2 , and CH_3 groups.¹⁵⁶ Two-dimensional NMR spectroscopy techniques such as COSY (Correlation spectroscopy), HSQC (heteronuclear single quantum coherence), and HMBC (heteronuclear multiple bond coherence spectroscopy). COSY is used to observe ^1H – ^1H correlations. HSQC is used to observe ^1H – ^{13}C correlations resulting from one-bond couplings. HMBC is used to observe ^1H – ^{13}C correlations resulting from two-bond and three-bond coupling.^{160, 161} Currently, even 3-D and 4-D NMR spectroscopy techniques have been employed in the elucidation of highly complex molecules.¹⁵⁶

1.10.2 Infrared (IR) spectroscopy

IR radiation (4000 to 600 cm^{-1}) corresponds to the frequencies associated with the bending and stretching vibrations of bonds (Figure 10). Each of these bond vibrations has a characteristic frequency. When a molecule is irradiated and the radiation of a frequency matches the characteristic frequency required for vibration, the molecule absorbs energy.¹⁵⁶

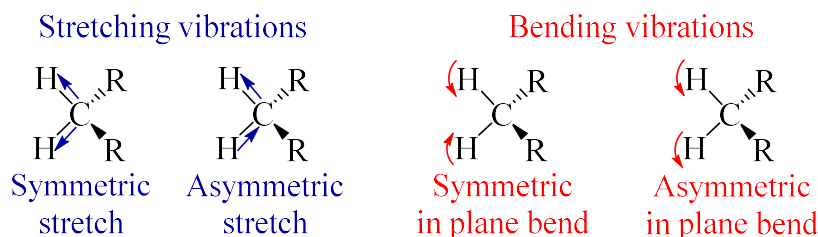


Figure 10: Examples of stretching and bending vibrations of bonds, adapted from literature.¹⁶²

IR spectroscopy provides a way of identifying functional groups.¹⁵⁹ An IR spectrum, which is produced by irradiating a sample with IR radiation, is a graph of the percent transmission of radiation against the wavenumber (inverse of wavelength) of the radiation transmitted. At 100% transmission, all IR radiation at a specific wavelength passes through the compound. The lower the value of percent transmission, the more energy is absorbed by the molecule.¹⁶³ Each absorption band in an IR spectrum represents energy absorption. Absorption bands are produced by the stretching and bending vibrations of each bond in the compound. The intensity of an absorption band depends on the change in dipole moment. The more intense the

absorption, the greater the change. The stronger the bond or the heavier the atom, the greater the energy required to stretch it. Lighter atoms and stronger bonds absorb at larger wavenumbers.¹⁵⁶

An IR spectrum may be separated into two regions. The functional group region (4000-1400 cm^{-1}) is where the majority of organic functional groups produce absorption bands. Organic chemists generally focus on the functional group region. The fingerprint region (1400-600 cm^{-1}) is characteristic of the whole molecule. The fingerprint region of the spectrum can be used to identify a compound by comparing the spectrum of a known sample of the compound.¹⁶² Stretching a bond requires more energy than to bending a bond. Consequently, absorption bands produced from stretching vibrations appear in the functional group region of the spectrum, whereas absorption bands produced from bending vibrations normally appear in the fingerprint region.¹⁵⁶

1.10.3 Liquid chromatography-mass spectrometry LC-MS)

The combination of chromatography and mass spectrometry (MS) allows purified compounds to be introduced into a mass spectrometer. Therefore, the combination of high-performance liquid chromatography (HPLC) and MS permits for more definitive qualitative and quantitative analysis than each individual technique.¹⁶⁴

The most utilised of all the analytical separation techniques is liquid chromatography (LC). This is due to its accurate quantitative determinations, sensitivity, and ease of automation.¹⁶⁵ In LC separations the sample is dissolved in a liquid mobile phase. This mobile phase is then passed through an immiscible stationary phase. The relative interaction of the analyte with both phases determines the analytes retention characteristics. Analytes that interact strongly with the stationary phase more are retained longer in this phase. In contrast, analytes that interact weakly with the stationary phase travel quickly with the mobile phase and are less retained. These differences in migration rates allow for sample components to separate (Figure 11).¹⁶⁴ The majority of HPLC separations utilise reversed-phase chromatography. In reversed-phase chromatography, the mobile phase is more polar than the stationary phase. Therefore, the more polar the analytes, the lower the retention.¹⁶⁴

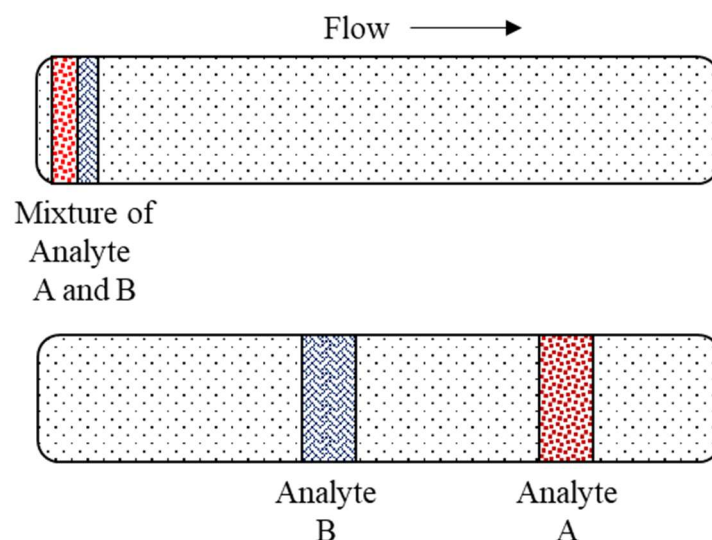


Figure 11: Separation of a mixture of analytes A and B by HPLC chromatography adapted from literature.¹⁶⁵

In mass spectrometry, a small amount of an analyte is vaporized and then ionised (Figure 12).¹⁵⁶

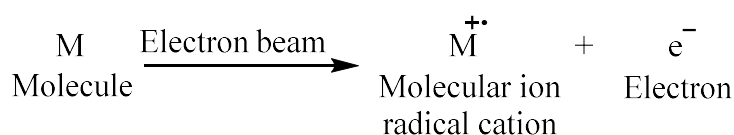


Figure 12: The ionisation of a molecule by an electron beam.¹⁵⁶

There are several different types of ionisation methods. Amongst the most popular methods are electron ionisation (EI) and chemical ionisation (CI).¹⁶⁴ In EI, the analyte is bombarded with high-energy electrons (generally 70 eV). A major disadvantage of EI is that the excess energy utilised during electron bombardment can cause rapid fragmentation which results in the molecular ion not being detected in the mass spectrum. In contrast, CI was developed to specifically enhance the production of the molecular ion. In CI, the analyte is introduced into a mass spectrometer source containing a reagent gas. The mixture is thereby ionised with an electron beam. Thereafter, Ion–molecule reactions occur between the neutral analyte molecules and the ionised reagent gas. During fragmentation, weaker bonds break in preference to stronger bonds, and bond breakage that leads to the formation of more stable fragments is preferred to those that lead to less stable fragments being formed.¹⁶⁴

After ionisation, an electric field accelerates the ions and then the ions pass into the mass analyser, which separates the ion in accordance to their mass-to-charge (m/z) ratios. In a quadrupole mass analyser (Figure 13), four solid rods are arranged parallel to the direction of the ion beam. A direct current voltage and a radiofrequency are applied to the rods, generating

an oscillating electrostatic field between the rods. Depending on the ratio of the radiofrequency amplitude to the direct current voltage, ions acquire an oscillation in this electrostatic field. Ions of an incorrect m/z ratio experience an unstable oscillation. The amplitude of the oscillation continuously increases until the ion strikes into one of the quadrupole rods. Ions possessing the correct m/z ratio experience a stable oscillation. These ions do not strike the rods but pass through the analyser to reach the detector.¹⁵⁷

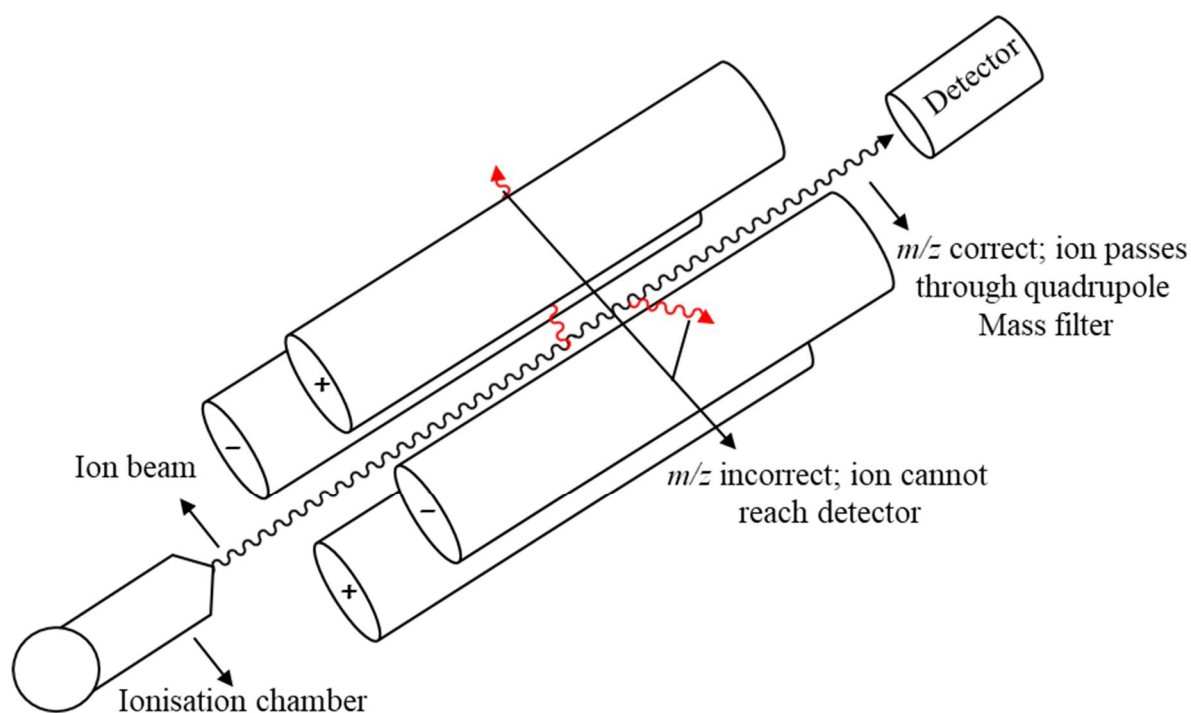


Figure 13: Schematic diagram of a quadrupole mass analyser, adapted from literature.¹⁵⁷

1.10.4 Supercritical fluid chromatography

Supercritical fluid chromatography (SFC) is a hybrid of gas chromatography (GC) and HPLC, combining the best features of each respective technique and can even offer superiority in specific applications.¹⁶⁵ SFC can be chosen over GC for nonpolar and thermally labile compounds with higher molecular weights.¹⁶⁵ SFC began gaining popularity upon becoming the favoured method for chiral separations, and thereby replacing chromatographic methods utilising normal phase chromatography and hydrocarbons. In contrast, SFC uses a solvent system that is greener, comprising of an organic modifier and supercritical CO₂. In SFC, the mobile phase is a supercritical fluid.¹⁶⁶ At pressures and temperatures above its critical pressure and temperature, a substance is called a supercritical fluid.¹⁶⁷ Neat CO₂ is a nonpolar fluid suitable for dissolving and separating nonpolar compounds. However, more polar compounds require the addition of a polar organic modifier (e.g. methanol, ethanol, and acetonitrile).¹⁶⁶

The most common mobile phase used is CO₂, as it is as readily available, non-toxic, inert, and miscible with numerous solvents.^{166, 167} The most commonly used modifier is methanol.¹⁶⁷ The modifier decreases the retention characteristics of more polar compounds. The modifier also affects the density, and viscosity of the fluid mixture. Acidic or basic additives can also be added to the modifier, these attach to the active sites on the stationary phase. The additives can increase the stationary phases polarity and enhanced peak shape for polar compounds.¹⁶⁶ Figure 14 depicts a general schematic of a preparative SFC system. The mobile phase is delivered by two different pumps. The first pump is for liquid CO₂, the pump head and incoming CO₂ are chilled to ensure liquid CO₂ is pumped. The second pump is for the organic modifier. After the mixing of the two streams, the mobile phase travels to the injector. Analyte from the injector is then carried to the column, and thereafter to the UV detector and finally the back pressure regulator. The back pressure regulator maintains the mobile phase in a dense state. The fraction collection system collects eluted bands. After the pressure is dropped, the CO₂ vented or recycled, and the modifier waste is collected in an enclosed container.¹⁶⁶

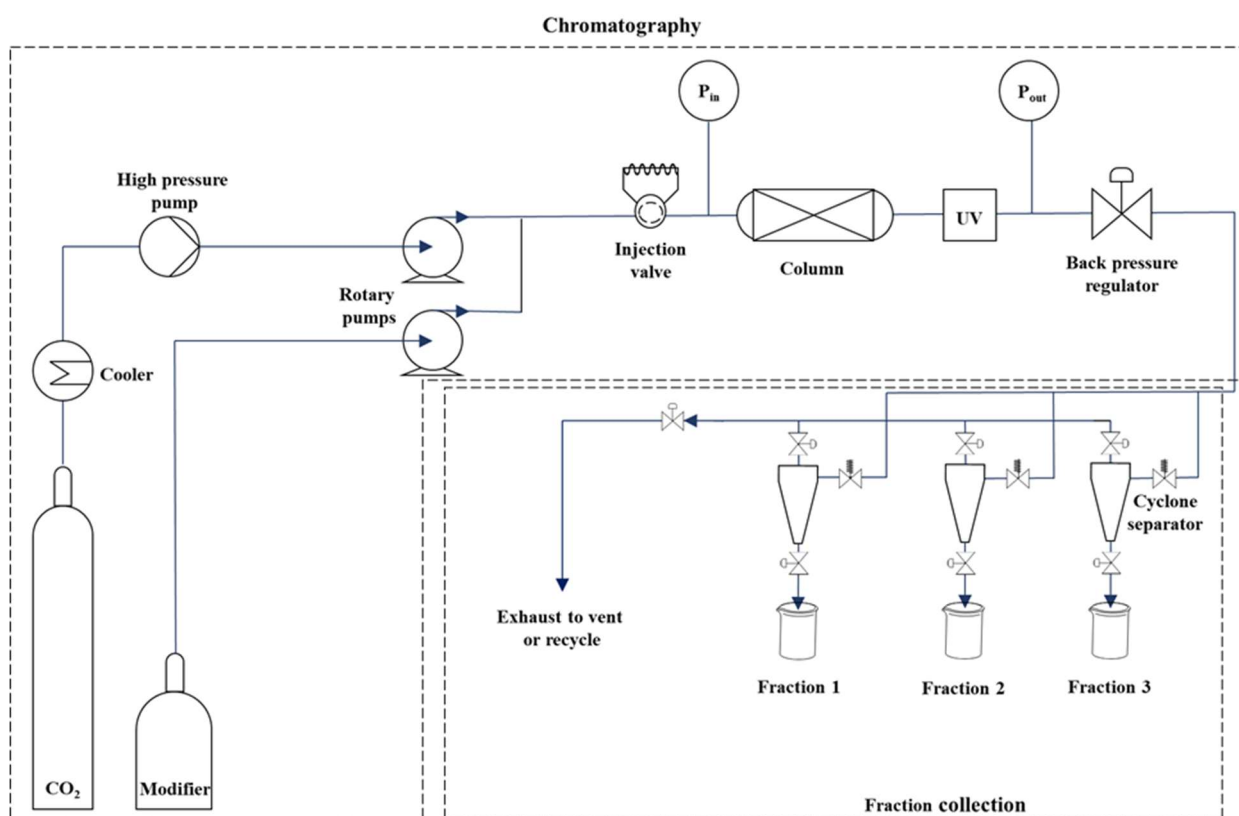
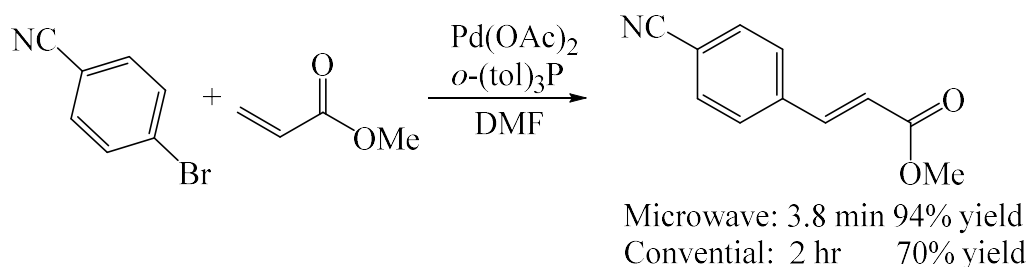


Figure 14: Schematic of preparative SFC system, adapted from literature.¹⁶⁸

1.10.5 Microwave-assisted reactions

Gedye *et al.* and Giguere *et al.* were the first to report on the utilisation of microwave irradiation in organic synthesis in 1986.^{169, 170} Since then numerous studies have shown microwave-assisted reactions have the potential to increase product yield, decrease reaction times and undesirable side reactions over conventional thermal heating methods (Scheme 15).¹⁷¹



Scheme 15: Evaluation between microwave and conventional heating yields and reaction times.¹⁷²

The energy of the microwave photon (0.0016 eV) cannot cleave molecular bonds.¹⁷³ Therefore, microwave-assisted reactions rely on the efficient heating of materials by microwave dielectric heating effects. These depend on the material's ability (solvent or reagent) to absorb microwave energy and convert that energy into heat.¹⁷⁴

The ability of a particular material to generate heat upon microwave irradiation depends on the dielectric properties of that material. The loss tangent ($\tan \delta$) determines the ability of a particular substance to convert electromagnetic energy into heat at a given frequency and temperature.¹⁷⁵ A high $\tan \delta$ is necessary for efficient rapid heating and absorption. A material with a high dielectric constant may not necessarily possess a high $\tan \delta$ value.¹⁷⁵ Generally, solvents may be categorised as high ($\tan \delta > 0.5$, polar organic solvents), medium ($\tan \delta$ 0.1–0.5), or low microwave absorbing ($\tan \delta < 0.1$, non-polar organic solvents). A low $\tan \delta$ value may not necessarily exclude a solvent from being utilised in microwave-assisted reactions.¹⁷⁴ Since the reagents or substrates may be polar, the overall dielectric properties of the reaction medium will generally allow for necessary heating by microwave irradiation.¹⁷⁴

Traditional organic synthesis is performed using conductive heating from an external heat source, typically a heating mantle or oil-bath. Conductive heating is relatively inefficient and slow method for energy transfer into the system since its depends on the involved materials thermal conductivity and convection currents. As a result, the reaction vessel typically possesses a higher temperature versus the reaction mixture. Whereas microwave-assisted

reactions allow for effective internal heating by utilising direct microwave irradiation of molecules (solvents, and reagents) in the reaction. Microwave irradiation increases the temperature of the whole reaction mixture concurrently. In contrast to conventional heating, where heating first occurs with the reaction solution in contact with the vessel wall (Figure 15).¹⁷⁴

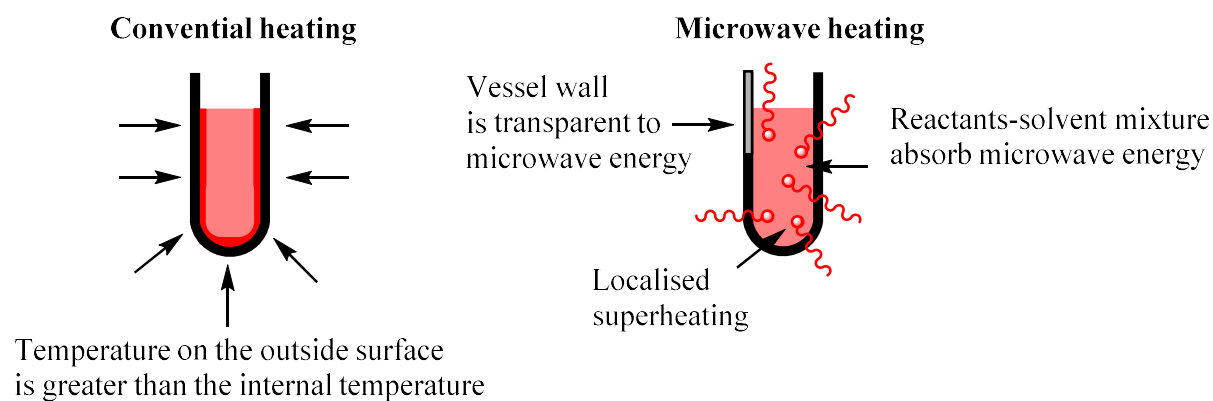


Figure 15: Schematic of sample heating by conduction versus heating by microwaves, adapted from literature.¹⁷⁶

Aims

The aims of the study are stated as follows:

To determine if sulfonimidamides are suitable trifluoromethyl and trifluoromethylthiol donating agents using DFT computational methods. To synthesise sulfonimidamides based trifluoromethyl and trifluoromethylthiol donating agents. To evaluate these agents on a model photoredox trifluoromethylation reaction and a model electrophilic trifluoromethylthiolation reaction (Chapter 2-3).

Objectives

- To perform homolytic and heterolytic DFT bond enthalpy calculations on the N-CF₃ and N-SCF₃ bonds in various sulfonimidamides before and after single electron reduction (Chapter 2-3).
- To synthesise the most promising sulfonimidamide based trifluoromethyl and trifluoromethylthiol donating agents (Chapter 2-3).
- To perform DFT calculations and experimental measurements to determine the redox potentials for the selected trifluoromethyl donating agents (Chapter 2).
- To compare various potential photoredox catalysts for trifluoromethylation (Chapter 2).

- To evaluate the sulfonimidamide based trifluoromethyl donating agents on a model photoredox trifluoromethylation reaction (Chapter 2).
- To evaluate the sulfonimidamide based trifluoromethylthiol donating agents on an electrophilic trifluoromethylthiolation reaction (Chapter 3).
- To compare all computational and experimental values for correlation (Chapter 2-3).

1.11 Outline of thesis

This thesis consists of 5 chapters that are presented as follows:

Chapter 1 presents a literature review of the background information pertaining to this study.

Chapter 2 presents the attempted use of sulfonimidamides as trifluoromethylating agents.

Chapter 3 presents the direct electrophilic trifluoromethylthiolation *via* sulfonaimidamines and is in progress for submission.

Chapter 4 provides a summary and conclusion.

Chapter 5 provides the experimental procedures and spectra.

References

1. A. Borodine, *Justus Liebigs Annalen der Chemie*, 1863, **126**, 58-62.
2. O. Wallach, *Justus Liebigs Annalen der Chemie*, 1886, **235**, 233-255.
3. H. Shen, Z. Liu, P. Zhang, X. Tan, Z. Zhang and C. Li, *Journal of the American Chemical Society*, 2017, **139**, 9843-9846.
4. M. Imiolek, G. Karunanithy, W.-L. Ng, A. J. Baldwin, V. Gouverneur and B. G. Davis, *Journal of the American Chemical Society*, 2018, **140**, 1568-1571.
5. H. Groult, F. Leroux and A. Tressaud, *Modern synthesis processes and reactivity of fluorinated compounds*, 2017.
6. A. Tressaud, 2006.
7. F. Teng, J. Cheng and C. Bolm, *Organic Letters*, 2015, **17**, 3166-3169.
8. S. P. Midya, J. Rana, T. Abraham, B. Aswin and E. Balaraman, *Chemical Communications*, 2017, **53**, 6760-6763.
9. A. Rivkin, K. Biswas, T.-C. Chou and S. J. Danishefsky, *Organic Letters*, 2002, **4**, 4081-4084.
10. A. van der Werf, M. Hribersek and N. Selander, *Organic Letters*, 2017, **19**, 2374-2377.
11. G. Zheng, X. Ma, J. Li, D. Zhu and M. Wang, *The Journal of Organic Chemistry*, 2015, **80**, 8910-8915.
12. M. Mamone, E. Morvan, T. Milcent, S. Ongeru and B. Crousse, *The Journal of Organic Chemistry*, 2015, **80**, 1964-1971.
13. Y. Macé and E. Magnier, *European Journal of Organic Chemistry*, 2012, **2012**, 2479-2494.
14. B. R. Langlois, T. Billard and S. Roussel, *Journal of Fluorine Chemistry*, 2005, **126**, 173-179.
15. Q.-Y. Chen and S.-W. Wu, *Journal of the Chemical Society, Chemical Communications*, 1989, DOI: 10.1039/C39890000705, 705-706.
16. G. K. S. Prakash, R. Krishnamurti and G. A. Olah, *Journal of the American Chemical Society*, 1989, **111**, 393-395.
17. I. Ruppert, K. Schlich and W. Volbach, *Tetrahedron Letters*, 1984, **25**, 2195-2198.
18. O. A. Tomashenko, E. C. Escudero-Adán, M. Martínez Belmonte and V. V. Grushin, *Angewandte Chemie International Edition*, 2011, **50**, 7655-7659.
19. N. Shibata, A. Matsnev and D. Cahard, *Beilstein J Org Chem*, 2010, **6**, 65.
20. L.-F. Jiang, B.-T. Ren, B. Li, G.-Y. Zhang, Y. Peng, Z.-Y. Guan and Q.-H. Deng, *The Journal of Organic Chemistry*, 2019, **84**, 6557-6564.
21. P. Eisenberger, S. Gischig and A. Togni, *Chemistry – A European Journal*, 2006, **12**, 2579-2586.
22. T. Umemoto and S. Ishihara, *Journal of the American Chemical Society*, 1993, **115**, 2156-2164.
23. S. Noritake, N. Shibata, S. Nakamura, T. Toru and M. Shiro, *European Journal of Organic Chemistry*, 2008, **2008**, 3465-3468.
24. S. Barata-Vallejo, B. Lantaño and A. Postigo, *Chemistry – A European Journal*, 2014, **20**, 16806-16829.
25. J.-A. Ma and D. Cahard, *Journal of Fluorine Chemistry*, 2007, **128**, 975-996.
26. X. Wang, L. Truesdale and J.-Q. Yu, *Journal of the American Chemical Society*, 2010, **132**, 3648-3649.
27. G.-B. Li, C. Zhang, C. Song and Y.-D. Ma, *Beilstein J Org Chem*, 2018, **14**, 155-181.
28. Z. Su, Y. Guo, Q.-Y. Chen, Z.-G. Zhao and B.-Y. Nian, *Chinese Journal of Chemistry*, 2019, **37**, 597-604.

29. K. Maeda, T. Kurahashi and S. Matsubara, *European Journal of Organic Chemistry*, 2019, **2019**, 4613-4616.
30. J. Wang, K. Sun, X. Chen, T. Chen, Y. Liu, L. Qu, Y. Zhao and B. Yu, *Organic Letters*, 2019, **21**, 1863-1867.
31. H. Oh, A. Park, K.-S. Jeong, S. B. Han and H. Lee, *Advanced Synthesis & Catalysis*, 2019, **361**, 2136-2140.
32. K. G. Ghosh, P. Chandu, S. Mondal and D. Sureshkumar, *Tetrahedron*, 2019, **75**, 4471-4478.
33. H. Yu, M. Jiao, X. Fang and P. Xuan, *RSC Advances*, 2018, **8**, 23919-23923.
34. D. J. Wilger, N. J. Gesmundo and D. A. Nicewicz, *Chemical Science*, 2013, **4**, 3160-3165.
35. A. Sato, J. Han, T. Ono, A. Wzorek, J. L. Aceña and V. A. Soloshonok, *Chemical Communications*, 2015, **51**, 5967-5970.
36. S. P. Pitre, C. D. McTiernan, H. Ismaili and J. C. Scaiano, *ACS Catalysis*, 2014, **4**, 2530-2535.
37. R. Lekkala, R. Lekkala, B. Moku, K. P. Rakesh and H.-L. Qin, *European Journal of Organic Chemistry*, 2019, **2019**, 2769-2806.
38. C. Han, M.-Y. Qi, Z.-R. Tang, J. Gong and Y.-J. Xu, *Nano Today*, 2019, DOI: <https://doi.org/10.1016/j.nantod.2019.05.001>.
39. F. Amir, K. P. Liles, A. O. Delawder, N. D. Colley, M. S. Palmquist, H. R. Linder, S. A. Sell and J. C. Barnes, *ACS Applied Materials & Interfaces*, 2019, **11**, 24627-24638.
40. A. Bagheri, C. Bainbridge and J. Jin, *ACS Applied Polymer Materials*, 2019, **1**, 1896-1904.
41. A. G. Herraiz and M. G. Suero, *Synthesis*, 2019, **51**, 2821-2828.
42. T.-H. Zhu, Z.-Y. Zhang, J.-Y. Tao, K. Zhao and T.-P. Loh, *Organic Letters*, 2019, DOI: 10.1021/acs.orglett.9b02361.
43. N. A. Romero and D. A. Nicewicz, *Chemical Reviews*, 2016, **116**, 10075-10166.
44. T. Chatterjee, N. Iqbal, Y. You and E. J. Cho, *Accounts of Chemical Research*, 2016, **49**, 2284-2294.
45. T. Koike and M. Akita, *Topics in Catalysis*, 2014, **57**, 967-974.
46. A. S. Feiner and A. J. McEvoy, *Journal of Chemical Education*, 1994, **71**, 493.
47. S. P. Midya, J. Rana, T. Abraham, B. Aswin and E. Balaraman, *Chemical Communications*, 2017, **53**, 6760-6763.
48. N. Iqbal, S. Choi, E. Kim and E. J. Cho, *The Journal of Organic Chemistry*, 2012, **77**, 11383-11387.
49. C. Lian, G. Yue, J. Mao, D. Liu, Y. Ding, Z. Liu, D. Qiu, X. Zhao, K. Lu, M. Fagnoni and S. Protti, *Organic Letters*, 2019, **21**, 5187-5191.
50. H. Wang, Y. Cheng and S. Yu, *Science China Chemistry*, 2016, **59**, 195-198.
51. D. A. Nicewicz and D. W. C. MacMillan, *Science*, 2008, **322**, 77.
52. M. A. Ischay, M. E. Anzovino, J. Du and T. P. Yoon, *Journal of the American Chemical Society*, 2008, **130**, 12886-12887.
53. C. K. Prier, D. A. Rankic and D. W. C. MacMillan, *Chemical Reviews*, 2013, **113**, 5322-5363.
54. A. K. Yadav and K. N. Singh, *Chemical Communications*, 2018, **54**, 1976-1979.
55. D. P. Hari and B. König, *Chemical Communications*, 2014, **50**, 6688-6699.
56. S. P. Pitre, C. D. McTiernan, H. Ismaili and J. C. Scaiano, *Journal of the American Chemical Society*, 2013, **135**, 13286-13289.
57. D. A. Nicewicz and T. M. Nguyen, *ACS Catalysis*, 2014, **4**, 355-360.
58. S. Arumugam, A. Brandstädt, T. Nishizeki and K. Thulasiraman, *Handbook of graph theory, combinatorial optimization, and algorithms*, Chapman and Hall/CRC, 2016.

59. E. Torti, S. Protti and M. Fagnoni, *Chemical Communications*, 2018, **54**, 4144-4147.
60. Y. Ouyang, X.-H. Xu and F.-L. Qing, *Angewandte Chemie International Edition*, 2018, **57**, 6926-6929.
61. M. Li, X.-S. Xue, J. Guo, Y. Wang and J.-P. Cheng, *The Journal of Organic Chemistry*, 2016, **81**, 3119-3126.
62. H. Jiang, T.-Y. Sun, Y. Chen, X. Zhang, Y.-D. Wu, Y. Xie and H. F. Schaefer, *Chemical Communications*, 2019, **55**, 5667-5670.
63. M. Li, Y. Wang, X.-S. Xue and J.-P. Cheng, *Asian Journal of Organic Chemistry*, 2017, **6**, 235-240.
64. D. Meyer, H. Jangra, F. Walther, H. Zipse and P. Renaud, *Nature Communications*, 2018, **9**, 4888.
65. G. Zou and X. Wang, *Organic & Biomolecular Chemistry*, 2017, **15**, 8748-8754.
66. F.-Y. Li, D.-Z. Lin, T.-J. He, W.-Q. Zhong and J.-M. Huang, *ChemCatChem*, 2019, **11**, 2350-2354.
67. A. Leo, C. Hansch and D. Elkins, *Chemical Reviews*, 1971, **71**, 525-616.
68. C. Hansch, A. Leo, S. H. Unger, K. H. Kim, D. Nikaitani and E. J. Lien, *Journal of Medicinal Chemistry*, 1973, **16**, 1207-1216.
69. M. Li, X.-S. Xue and J.-P. Cheng, *ACS Catalysis*, 2017, **7**, 7977-7986.
70. J. Zhang, J.-D. Yang, H. Zheng, X.-S. Xue, H. Mayr and J.-P. Cheng, *Angewandte Chemie International Edition*, 2018, **57**, 12690-12695.
71. T. Silverstone, J. Fincham and J. Plumley, *Br J Clin Pharmacol*, 1979, **7**, 353-356.
72. J. N. André, L. G. Dring, G. Gillet and C. Mas-Chamberlin, *Br J Pharmacol*, 1979, **66**, 506P-506P.
73. P. Pommier, A. Keita, S. Wessel-Robert, B. Dellac and H. Mundt, *Revue de Médecine Vétérinaire (France)*, 2003.
74. P. Laczay, G. Vörös and G. Semjén, *International Journal for Parasitology*, 1995, **25**, 753-756.
75. G. W. Counts, D. Gregory, D. Zeleznik and M. Turck, *Antimicrobial agents and chemotherapy*, 1977, **11**, 708-711.
76. N. Aswapokee and H. C. Neu, *Antimicrobial agents and chemotherapy*, 1979, **15**, 444-446.
77. X.-H. Xu, K. Matsuzaki and N. Shibata, *Chemical Reviews*, 2015, **115**, 731-764.
78. M. Horvat, M. Jereb and J. Iskra, *European Journal of Organic Chemistry*, 2018, **2018**, 3837-3843.
79. X. Shao, C. Xu, L. Lu and Q. Shen, *Accounts of Chemical Research*, 2015, **48**, 1227-1236.
80. S. Munavalli, G. W. Wagner, A. Bashir Hashemi, D. K. Rohrbaugh and H. D. Durst, *Synthetic Communications*, 1997, **27**, 2847-2851.
81. G. Dagousset, C. Simon, E. Anselmi, B. Tuccio, T. Billard and E. Magnier, *Chemistry – A European Journal*, 2017, **23**, 4282-4286.
82. F. Baert, J. Colomb and T. Billard, *Angewandte Chemie International Edition*, 2012, **51**, 10382-10385.
83. H. Jiang, R. Zhu, C. Zhu, F. Chen and W. Wu, *Organic & Biomolecular Chemistry*, 2018, **16**, 1646-1650.
84. A. Haas and K. W. Kempf, *Tetrahedron*, 1984, **40**, 4963-4972.
85. W. J. Middleton, *The Journal of Organic Chemistry*, 1984, **49**, 919-922.
86. A. Haas and H.-U. Krächter, *Chemische Berichte*, 1988, **121**, 1833-1840.
87. Z. Weng, W. He, C. Chen, R. Lee, D. Tan, Z. Lai, D. Kong, Y. Yuan and K.-W. Huang, *Angewandte Chemie International Edition*, 2013, **52**, 1548-1552.

88. C.-P. Zhang and D. A. Vicic, *Journal of the American Chemical Society*, 2012, **134**, 183-185.
89. K.-Y. Ye, X. Zhang, L.-X. Dai and S.-L. You, *The Journal of Organic Chemistry*, 2014, **79**, 12106-12110.
90. H. J. Emeléus and D. E. MacDuffie, *Journal of the Chemical Society (Resumed)*, 1961, 2597-2599.
91. H. Zheng, Y. Huang and Z. Weng, *Tetrahedron Letters*, 2016, **57**, 1397-1409.
92. S. Kovács, B. Bayarmagnai and L. J. Goossen, *Advanced Synthesis & Catalysis*, 2017, **359**, 250-254.
93. A.-L. Barthelemy, E. Magnier and G. Dagousset, *Synthesis*, 2018, **50**, 4765-4776.
94. Y. Li, T. Koike and M. Akita, *Asian Journal of Organic Chemistry*, 2017, **6**, 445-448.
95. M. Zhu, W. Fu, W. Guo, Y. Tian, Z. Wang and B. Ji, *Organic & Biomolecular Chemistry*, 2019, **17**, 3374-3380.
96. R. Honeker, R. A. Garza-Sanchez, M. N. Hopkinson and F. Glorius, *Chemistry – A European Journal*, 2016, **22**, 4395-4399.
97. D. Koziakov, M. Majek and A. Jacobi von Wangelin, *European Journal of Organic Chemistry*, 2017, **2017**, 6722-6725.
98. S. Mukherjee, B. Maji, A. Tlahuext-Aca and F. Glorius, *Journal of the American Chemical Society*, 2016, **138**, 16200-16203.
99. C. Ghiazza, T. Billard and A. Tlili, *Chemistry – A European Journal*, 2019, **25**, 6482-6495.
100. Y.-F. Zeng, D.-H. Tan, Y. Chen, W.-X. Lv, X.-G. Liu, Q. Li and H. Wang, *Organic Chemistry Frontiers*, 2015, **2**, 1511-1515.
101. S. Alazet, K. Ollivier and T. Billard, *Beilstein J Org Chem*, 2013, **9**, 2354-2357.
102. A. Ferry, T. Billard, B. R. Langlois and E. Bacqué, *The Journal of Organic Chemistry*, 2008, **73**, 9362-9365.
103. F. Toulgoat, S. Alazet and T. Billard, *European Journal of Organic Chemistry*, 2014, **2014**, 2415-2428.
104. A. Ferry, T. Billard, E. Bacqué and B. R. Langlois, *Journal of Fluorine Chemistry*, 2012, **134**, 160-163.
105. A. Ferry, T. Billard, B. R. Langlois and E. Bacqué, *Angewandte Chemie International Edition*, 2009, **48**, 8551-8555.
106. C. Xu, B. Ma and Q. Shen, *Angewandte Chemie International Edition*, 2014, **53**, 9316-9320.
107. P. Zhang, M. Li, X.-S. Xue, C. Xu, Q. Zhao, Y. Liu, H. Wang, Y. Guo, L. Lu and Q. Shen, *The Journal of organic chemistry*, 2016, **81**, 7486-7509.
108. M. Li, J. Guo, X.-S. Xue and J.-P. Cheng, *Organic letters*, 2016, **18**, 264-267.
109. H. Chachignon and D. Cahard, *Chinese Journal of Chemistry*, 2016, **34**, 445-454.
110. G. C. Nandi and P. I. Arvidsson, *Advanced Synthesis & Catalysis*, 2018, **360**, 2976-3001.
111. F. Izzo, M. Schäfer, R. Stockman and U. Lücking, *Chemistry – A European Journal*, 2017, **23**, 15189-15193.
112. Y. Chen and J. Gibson, *RSC Advances*, 2015, **5**, 4171-4174.
113. P. K. Chinthakindi, T. Naicker, N. Thota, T. Govender, H. G. Kruger and P. I. Arvidsson, *Angewandte Chemie International Edition*, 2017, **56**, 4100-4109.
114. E. Levchenko and A. Kirsanov, *Zhurnal Obshchei Khimii*, 1960, **30**, 1553-1561.
115. E. Levchenko, E. Kozlov and A. Kirsanov, *ZHURNAL OBSHCHEI KHIMII*, 1962, **32**, 882-886.
116. E. Levchenko, N. Y. Derkach and A. Kirsanov, *Zh Obshch Khim*, 1962, **32**, 1208-1212.
117. E. Levchenko, I. Sheinkman and A. Kirsanov, *Zh Obshch Khim*, 1960, **30**, 1941-1946.

118. S. V. Zasukha, V. M. Timoshenko, A. A. Tolmachev, V. O. Pivnytska, O. Gavrylenko, S. Zherish, Y. Shermolovich and O. O. Grygorenko, *Chemistry – A European Journal*, 2019, **25**, 6928-6940.
119. U. Lücking, *Organic Chemistry Frontiers*, 2019, **6**, 1319-1324.
120. E. L. Briggs, A. Tota, M. Colella, L. Degennaro, R. Luisi and J. A. Bull, *Angewandte Chemie International Edition*, 2019, **58**, 14303-14310.
121. G. C. Nandi, *European Journal of Organic Chemistry*, 2017, **2017**, 6633-6638.
122. M. Li, B. Zhou, X.-S. Xue and J.-P. Cheng, *The Journal of organic chemistry*, 2017, **82**, 8697-8702.
123. E. J. Neth, P. Flowers, K. H. Theopold, W. R. Robinson, R. Langley, O. College and R. University, *Chemistry: Atoms First*, OpenStax College, 2016.
124. F. Jensen, *Introduction to computational chemistry*, John Wiley & Sons, Chichester, England ;, 2nd ed. edn., 2007.
125. S. M. Bachrach, *Computational organic chemistry*, Wiley-Interscience, Hoboken, N.J., 2007.
126. D. C. Young, *Computational chemistry : a practical guide for applying techniques to real world problems*, Wiley, New York, 2001.
127. J. B. Foresman and A. Frisch, *Exploring chemistry with electronic structure methods*, Gaussian, Inc., Wallingford, CT, Third edition. edn., 2015.
128. A. Tomberg.
129. W. J. Hehre, *A Guide to Molecular Mechanics and Quantum Chemical Calculations*, Wavefunction, 2003.
130. F. Jensen, *Introduction to Computational Chemistry*, Wiley, 2006.
131. P. Hohenberg and W. Kohn, *Physical Review*, 1964, **136**, B864-B871.
132. W. Kohn and L. J. Sham, *Physical Review*, 1965, **140**, A1133-A1138.
133. N. Mardirossian and M. Head-Gordon, *Molecular Physics*, 2017, **115**, 2315-2372.
134. Y. Zhao, N. González-García and D. G. Truhlar, *The Journal of Physical Chemistry A*, 2005, **109**, 2012-2018.
135. Y. Zhao and D. G. Truhlar, *Accounts of Chemical Research*, 2008, **41**, 157-167.
136. M. M. Lawal, T. Govender, G. E. M. Maguire, B. Honarparvar and H. G. Kruger, *Journal of Molecular Modeling*, 2016, **22**, 235.
137. M. M. Lawal, T. Govender, G. E. M. Maguire, H. G. Kruger and B. Honarparvar, *International Journal of Quantum Chemistry*, 2018, **118**, e25497.
138. M. Walker, A. J. A. Harvey, A. Sen and C. E. H. Dessent, *The Journal of Physical Chemistry A*, 2013, **117**, 12590-12600.
139. Y. Zhao and D. G. Truhlar, *Theoretical Chemistry Accounts*, 2008, **120**, 215-241.
140. K. Coutinho and S. Canuto, *The Journal of Chemical Physics*, 2000, **113**, 9132-9139.
141. B. Mennucci, J. M. Martínez and J. Tomasi, *The Journal of Physical Chemistry A*, 2001, **105**, 7287-7296.
142. J. Zeng, J. Craw, N. Hush and J. Reimers, *The Journal of chemical physics*, 1993, **99**, 1482-1495.
143. J. Zeng, N. Hush and J. Reimers, *The Journal of chemical physics*, 1993, **99**, 1508-1521.
144. F. Zhang and R. Brüschweiler, *Journal of the American Chemical Society*, 2002, **124**, 12654-12655.
145. D. Chesnut and B. Rusiloski, *Journal of Molecular Structure: THEOCHEM*, 1994, **314**, 19-30.
146. M. Pecul and J. Sadlej, *Chemical physics*, 1998, **234**, 111-119.
147. C. J. Cramer and D. G. Truhlar, *Chemical Reviews*, 1999, **99**, 2161-2200.

148. D. M. Dolney, G. D. Hawkins, P. Winget, D. A. Liotard, C. J. Cramer and D. G. Truhlar, *Journal of Computational Chemistry*, 2000, **21**, 340-366.
149. J. Tomasi and M. Persico, *Chemical Reviews*, 1994, **94**, 2027-2094.
150. L. Onsager, *Journal of the American Chemical Society*, 1936, **58**, 1486-1493.
151. Gaussian, SCRF, <https://gaussian.com/scrf/>, (accessed 07/11/2019, 2019).
152. B. Thapa and H. B. Schlegel, *The Journal of Physical Chemistry A*, 2016, **120**, 8916-8922.
153. G. E. Pake, *American Journal of Physics*, 1950, **18**, 438-452.
154. G. E. Pake, *American Journal of Physics*, 1950, **18**, 473-486.
155. I. I. Rabi, J. R. Zacharias, S. Millman and P. Kusch, *Physical Review*, 1938, **53**, 318-318.
156. P. Y. Bruice, *Organic chemistry*, Pearson, Harlow, Essex, Seventh edition. Pearson new international edition. edn., 2014.
157. D. L. Pavia, G. M. Lampman, G. S. Kriz, Jr. and J. R. Vyvyan, *Introduction to spectroscopy*, Cengage Learning, Stamford, CT, Fifth edition, [2nd printing]. edn., 2015.
158. A.-u. Rahman, M. I. Choudhary and A.-t. Wahab, *Journal*, 2016.
159. J. Clayden, N. Greeves and S. G. Warren, *Organic chemistry*, Oxford University Press, Oxford ;, 2nd ed. edn., 2012.
160. J. H. Simpson, in *NMR Case Studies*, ed. J. H. Simpson, Elsevier, Boston, 2017, DOI: <https://doi.org/10.1016/B978-0-12-803342-5.00001-6>, pp. 1-9.
161. A. M. Anderson-Wile, *Journal of Chemical Education*, 2016, **93**, 699-703.
162. J. M. Thompson, *Infrared Spectroscopy*, Jenny Stanford Publishing, 2018.
163. B. H. Stuart, *Infrared Spectroscopy: Fundamentals and Applications*, Wiley, 2004.
164. R. E. Ardrey, *Liquid Chromatography - Mass Spectrometry: An Introduction*, Wiley, 2003.
165. D. A. Skoog, F. J. Holler and S. R. Crouch, *Principles of Instrumental Analysis*, Cengage Learning, 2017.
166. C. F. Poole, *Supercritical Fluid Chromatography*, Elsevier Science, 2017.
167. E. Lundanes, L. Reubsaet and T. Greibrokk, *Chromatography: Basic Principles, Sample Preparations and Related Methods*, Wiley, 2013.
168. A. Rajendran, *Journal of Chromatography A*, 2012, **1250**, 227-249.
169. R. J. Giguere, T. L. Bray, S. M. Duncan and G. Majetich, *Tetrahedron Letters*, 1986, **27**, 4945-4948.
170. R. Gedye, F. Smith, K. Westaway, H. Ali, L. Baldisera, L. Laberge and J. Rousell, *Tetrahedron Letters*, 1986, **27**, 279-282.
171. B. Wathey, J. Tierney, P. Lidström and J. Westman, *Drug Discovery Today*, 2002, **7**, 373-380.
172. M. Larhed and A. Hallberg, *The Journal of Organic Chemistry*, 1996, **61**, 9582-9584.
173. C. O. Kappe, in *Comprehensive Medicinal Chemistry II*, eds. J. B. Taylor and D. J. Triggle, Elsevier, Oxford, 2007, DOI: <https://doi.org/10.1016/B0-08-045044-X/00109-7>, pp. 837-860.
174. C. O. Kappe, D. Dallinger and S. S. Murphree, *Practical Microwave Synthesis for Organic Chemists: Strategies, Instruments, and Protocols*, Wiley, 2008.
175. M. Larhed and A. Hallberg, *Drug Discovery Today*, 2001, **6**, 406-416.
176. B. L. Hayes, *Microwave Synthesis: Chemistry at the Speed of Light*, CEM Pub., 2002.

Chapter 2

2. Sulfonimidamides as trifluoromethylating agents

The introduction of a trifluoromethyl group (CF_3) into an organic molecule can significantly affect its lipophilicity, conformational behaviour, and metabolic stability.^{1, 2} Radical mediated trifluoromethylation facilitated by photoredox catalysis offers mild and highly selective reaction conditions.³⁻⁵ Organic photocatalysts possess a lower cost, greater availability, and can have superior efficiency^{6, 7} when compared to metal based photocatalysts.^{8, 9} Therefore, the development of methodologies using organic photocatalysts is currently highly advantageous.¹⁰

While there are several commercially available trifluoromethylation reagents, some limitations include the use of gaseous CF_3I ¹¹, volatile $\text{CF}_3\text{SO}_2\text{Cl}$ ¹², and expensive Togni¹³, Umemoto¹⁴, or Rupert-Prakash^{15, 16} reagents.^{17, 18} Therefore, the development of cheaper and safer trifluoromethylation reagents is vital.¹⁹

Cheng and co-worker's computational study illustrated that a single electron reduction can significantly reduce the radical donating ability ($\text{TR}^\bullet\text{DAs}$)²⁰, which corresponds to a weaker bond. Single electron reduction can be achieved either photochemically²¹ or electrochemically.²²

Inspired by the work of Cheng and co-workers^{20, 23}, this study focused on the computational design and thereafter synthesis of sulfonimidamides as potential radical trifluoromethylation agents *via* photoredox catalysis.

2.1 Trifluoromethyl radical donor abilities ($\text{TR}^\bullet\text{DAs}$) of sulfonimidamides

All calculations were performed with the Gaussian 16 software package.²⁴ Optimisations were performed with the M06-2X²⁵ functional and 6-31+G(d)^{26, 27} basis set, using the SMD solvation model²⁸ to account for solvation in dichloromethane. Thereafter, single point energy was calculated at the M06-2X/6-311++G(2df,2p)^{29, 30} level of theory on the pre-optimised structures. The $\text{TR}^\bullet\text{DAs}$ of the proposed sulfonimidamides before and after a single electron reduction were calculated (Figure 1).

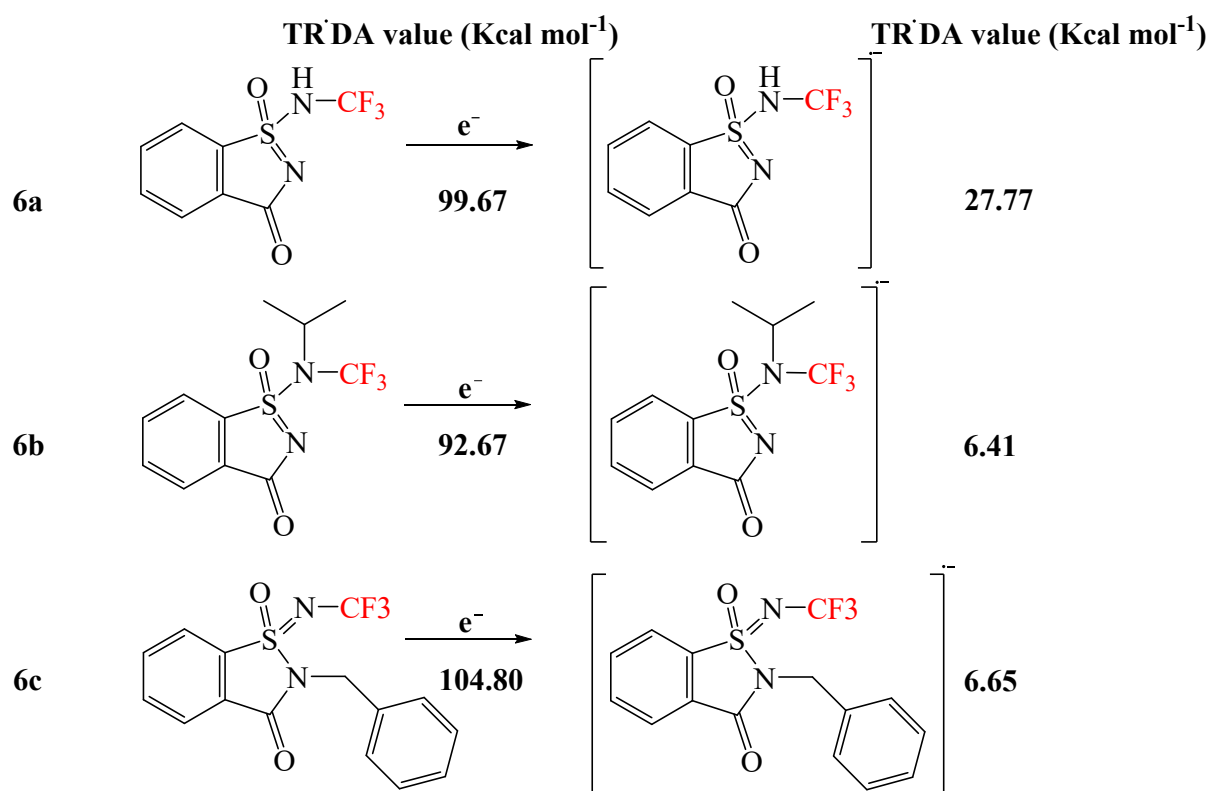


Figure 1: Calculated* TR[•]DAs values of the proposed sulfonimidamides before and after a single electron reduction in acetonitrile. *(SMD-M06-2X/6-31+G(d)// SMD-M06-2X/6-311++G(2df,2p))

Single electron reduction significantly lowered the TR[•]DAs values. Figure 1 illustrates that sulfonimidamides possess (**6a-c**) the potential to deliver a trifluoromethyl group comparable to known delivering agents (Figure 2). The trifluoromethyl cation donating abilities (TC⁺DA) of the proposed sulfonimidamides were also calculated (Appendix 1, Figure S1). However, the TC⁺DA values indicated poor donation potentials as compared to known electrophilic trifluoromethylating reagents (Appendix 1, Figure S2).

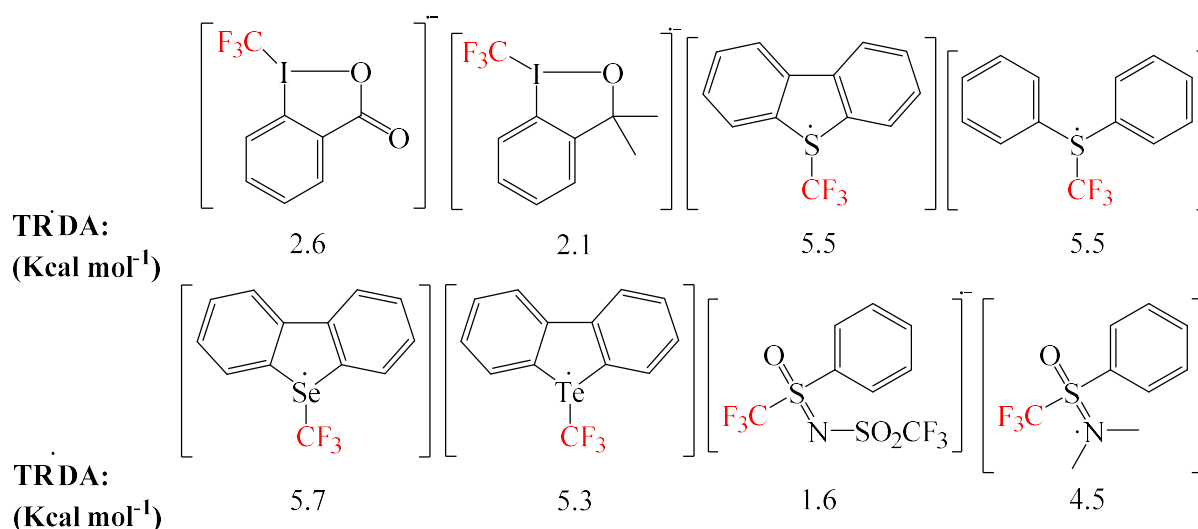


Figure 2: The reported calculated* TR•DAs values of trifluoromethylating reagents after a single electron reduction in acetonitrile.²⁰ *(SMD-M06-2X/6-31+G(d)// SMD-M06-2X/6-311++G(2df,2p))

The computations illustrate that the proposed sulfonimidamides (**6a-c**, Figure 1) have the potential to donate a trifluoromethyl group upon single electron reduction, comparable to known delivering agents (Figure 2). Therefore, redox potentials were calculated to identify a suitable photocatalyst to reduce the sulfonimidamides.

2.2 Calculated electrochemical potentials

All calculations were performed using the Gaussian 09 software package.³¹ The reduction potentials ($E_{1/2}^{\text{red}}$) and oxidation potentials ($E_{1/2}^{\text{ox}}$) of the proposed sulfonimidamides were calculated by utilising an improved method initially developed by Nicewicz and co-workers³² and are referenced to the saturated calomel electrode (SCE) (Table 1). The initial method utilised the CPCM solvation model^{33, 34} for the M06-2X and B3LYP³⁵ functionals with the 6-31+G(d,p) basis set. The M06-2X functional tends to overestimate the redox potentials, while the B3LYP functional underestimates the potentials. The average potentials of both functional provides a potential close to the experimental value. The improved method utilised the SMD solvation model for the M06-2X and HSEH1PBE³⁶⁻⁴² functionals with and 6-31+G(d) basis set. The SMD solvation model is recommended by Gaussian for the ΔG of solvation⁴³ and is one of the most commonly used solvation model in recent literature.^{20, 23, 44-47} The complete procedure for calculations can be found in Chapter 5, while the complete method optimisation can be found in Appendix 3 (Table S1-3).

Table 1: Redox potentials of the proposed sulfonimidamides in acetonitrile (V vs SCE)

	(E _{1/2} ^{red}) ^b	(E _{1/2} ^{ox})	(E _{1/2} ^{red}) ^c	(E _{1/2} ^{ox})	Average	Average
Sulfonimidamide ^a	M06-2X	M06-2X	HSEH1PBE	HSEH1PBE	(E _{1/2} ^{red})	(E _{1/2} ^{ox})
	(V)	(V)	(V)	(V)	(V)	(V)
6a	-1.48	3.15	-1.36	3.00	-1.42	3.07
6b	-1.66	3.10	-1.39	2.99	-1.53	3.04
6c	-1.49	2.40	-1.34	2.42	-1.41	2.41

^aStructure number as designated in Figure 1.

^bSMD-M062X/6-31+G(d)

^cCPCM-HSEH1PBE/6-31+G(d)

Table 1 illustrates that the proposed sulfonimidamides possess high oxidation potentials and relatively high reduction potentials. Therefore, a highly reducing photocatalysts is required for the photochemical reduction.

2.3 Choice of photocatalyst

Utilising the Nernst equation (1)⁴⁸ in order to obtain a negative ΔG (spontaneous electron transfer) for the reduction of the sulfonimidamides, the reduction potential of the sulfonimidamides should be greater than the oxidation potential of the photocatalysts.⁴⁹

$$\Delta G = -nFE \quad (1)$$

$$E = E_1^{\text{red}}(A) - E_1^{\text{ox}}(D)$$

Possible organic photocatalysts are xanthone and 10-phenylphenothiazine (Figure 3) whose excited state oxidation values are $E_{1/2}^{\text{ox}} = -1.61$ ^{50, 51} and $E_{1/2}^{\text{ox}} = -2.1$ ⁵² respectively.

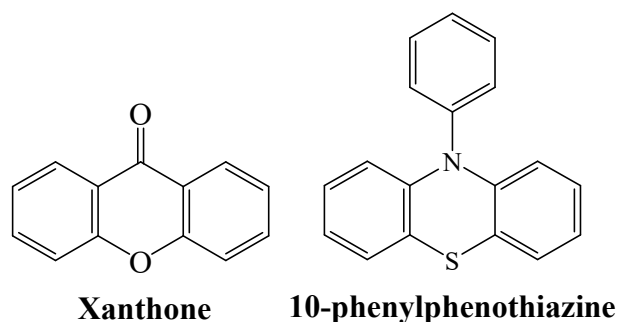
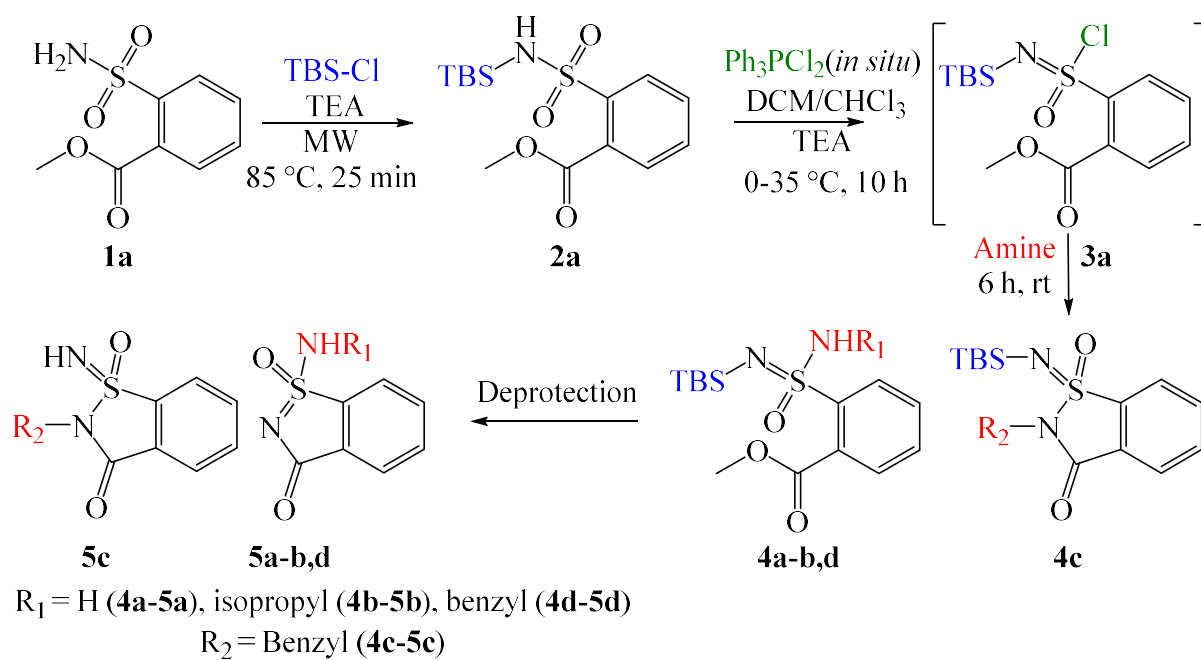


Figure 3: Possible organic photocatalysts for the reduction of the proposed sulfonimidamides.

2.4 Synthesis of sulfonimidamides

The various sulfonimidamides were synthesised according to an adapted method developed by Chen *et al.*⁵³ (Scheme 1). The protection of sulfonamide (**1a**, Figure 4, **A**) was performed over

25 minutes using a microwave method (85 °C, 200 W) instead of the reported 20 hour room temperature reaction, the protected sulfonimidamide (**2a**) was confirmed by ¹H, ¹³C NMR spectroscopy and LC-MS analysis. *Tert*-butyldimethyl-silyl (TBS) protection was necessary to prevent a reaction between the primary amine that could form and the *in situ* formed sulfonimidoyl chloride (**3a**). Bulkier silyl protecting groups (TBS and *tert*-butyldiphenylsilyl) generate more stable sulfonimidoyl chlorides and increased yields, as shown in studies by Chen and Gibson⁵⁴ and Chinthakindi *et al.*⁵⁵ The deoxychlorination of the protected sulfonamide (**2a**) using Ph₃PCl₂ was initially reported by Roy⁵⁶, using tri-methylsilyl protected sulfonamides. The amination step of the sulfonimidoyl chloride (**3a**) can result in the formation of products with ring closure (**4c**, Figure 5, **B**) or without ring closure (**4a, b, d**), which is dependent on the reaction conditions as shown in literature.⁵³ Compounds **4a-d** were confirmed by novel X-ray crystal structures, ¹H, ¹³C NMR spectroscopy and LC-MS analysis. Deprotection eventually leads to ring closure obtaining the final sulfonimidamides (**5a-c**) without an imine nitrogen present, confirmed by novel X-ray crystal structures, ¹H, ¹³C NMR spectroscopy and LC-MS analysis. Deprotection of the ring closed products lead to a sulfonimidamide with an imine nitrogen present (**5c**), confirmed by ¹H, ¹³C NMR spectroscopy and LC-MS analysis. Compound **5d** (Figure 4, **D**) was obtained in trace amounts during the synthesis of compound **5c** and was therefore, not considered further. Compounds **4b** and **5b** (Figure 4, **C**) are novel. Novel X-ray crystal structures for **4a** and **5a** are currently under analysis. A detailed experimental procedure is provided in Chapter 5.



Scheme 1: Synthesis route for the proposed sulfonimidamides.

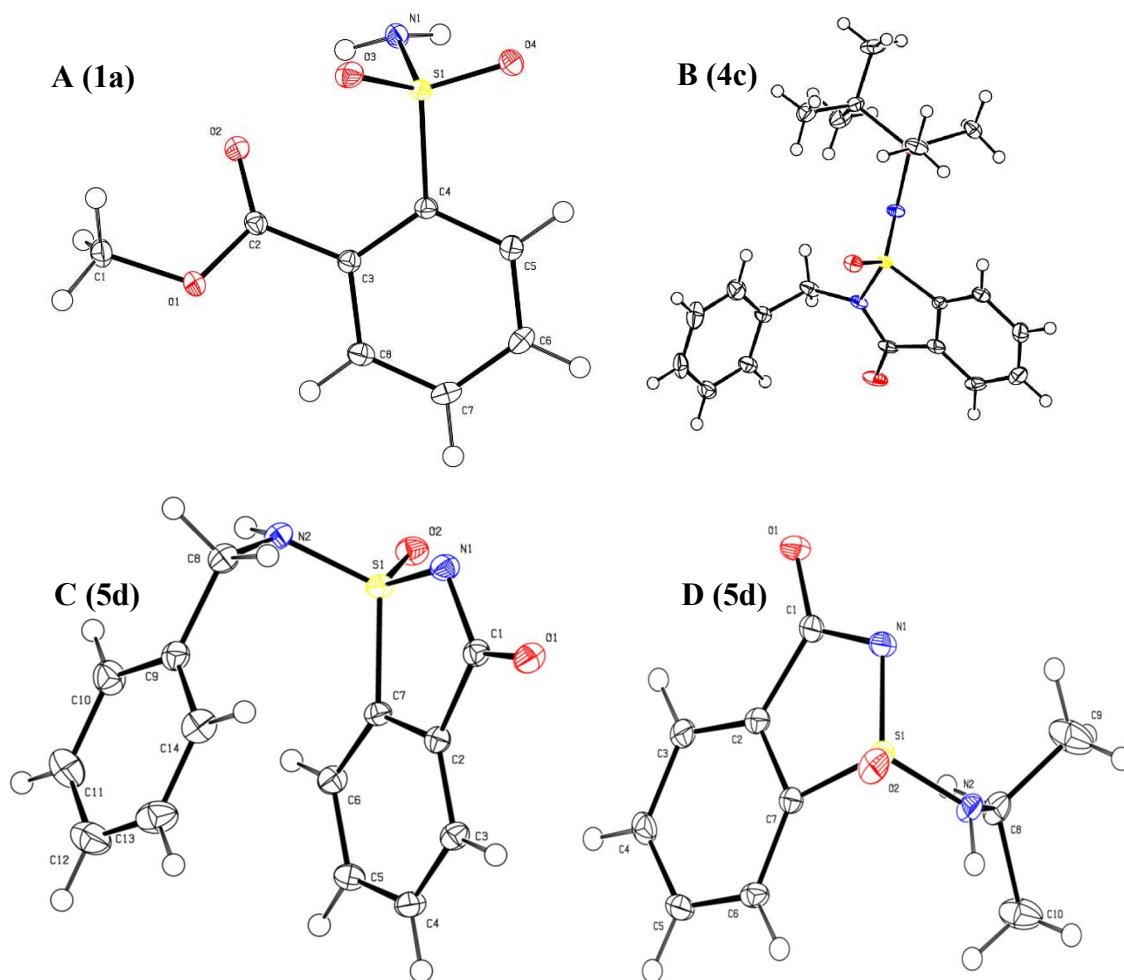
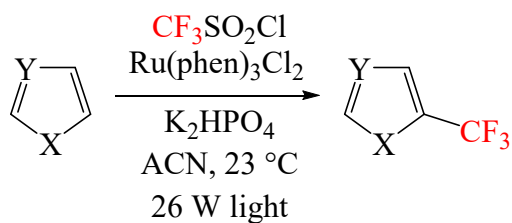


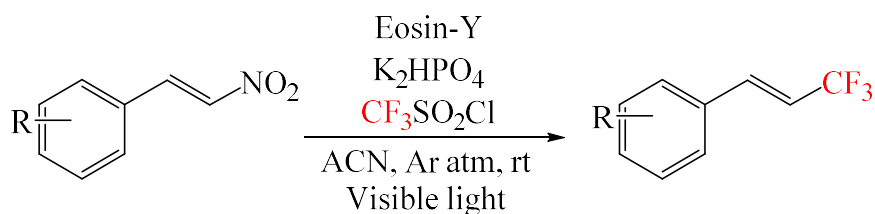
Figure 4: Novel X-ray crystal structures obtained (unpublished results).

2.5 Model photochemical reactions

The following photoredox reactions (Scheme 2-3) were the proposed model reactions to evaluate the effectiveness of the proposed sulfonimidamides as trifluoromethylating agents.



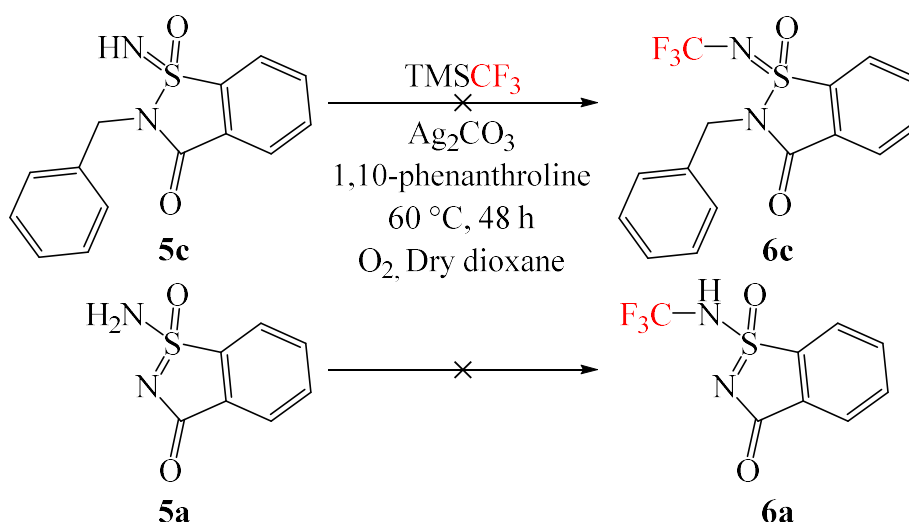
Scheme 2: Trifluoromethylation of electron rich heteroarenes.⁵⁷



Scheme 3: Trifluoromethylation of β -nitroalkenes.²

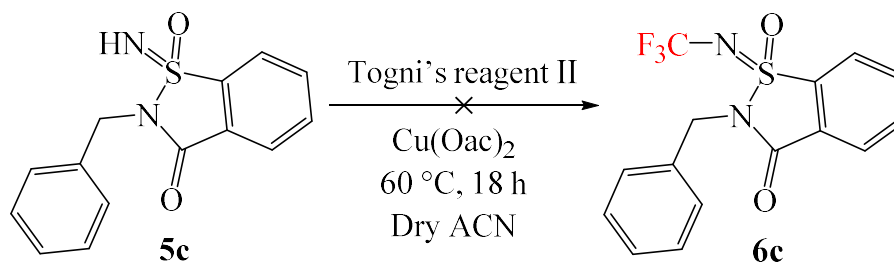
2.6 Attempted trifluoromethylation of sulfonimidamides

Bolm and co-workers¹ initially developed a method for the *N*-trifluoromethylation of the sulfoximines, which was then adapted by Lücking and associates⁵⁸ for the *N*-trifluoromethylation of sulfonimidamides. This method was utilised for the trifluoromethylation of the sulfonimidamides in Scheme 4. In the reaction of sulfonimidamide **5c**, incomplete conversion with side product formation was observed from TLC analysis. Despite all efforts to improve the conversion, no formation of **6c** was observed. In the reaction of sulfonimidamide **5a** using the same conditions as **5c**, no conversion of **5a** occurred from TLC analysis. A detailed experimental procedure is provided in Chapter 5.



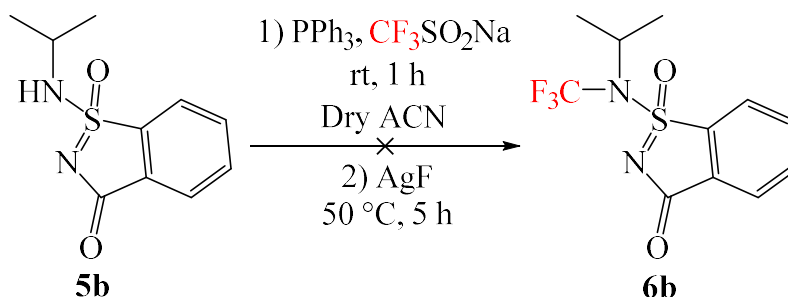
Scheme 4: Trifluoromethylation following Bolm's method.^{1, 58}

Thereafter, a method developed by Wang and co-workers for the electrophilic *N*-trifluoromethylation of *N*-H ketimines was attempted⁵⁹ (Scheme 5). However, again no formation of the desired product (**6c**) was achieved as **5c** remain unreacted as observed from TLC analysis. A detailed experimental procedure is provided in Chapter 5.



Scheme 5: Trifluoromethylation following Wang's method.⁵⁹

Finally, a recent method developed by Yi and associates for the *N*-trifluoromethylation of amines was attempted⁶⁰ (Scheme 6). However, no formation of the desired product (**6b**) was achieved as no conversion of **5b** occurred as observed from TLC analysis. A detailed experimental procedure is provided in Chapter 5.



Scheme 6: Trifluoromethylation following Yi's method.⁶⁰

2.7 Conclusion and outlook

Despite all efforts to synthesise trifluoromethylated sulfonimidamides (Scheme 4-6) being unsuccessful, the synthesis and characterisation of compounds **5a-d** were successful and resulted in 6 novel X-ray crystal structures. In addition, a simple yet efficient computational method for calculating redox potentials was also developed. The decision was then to synthesise trifluoromethylthiolated sulfonimidamides based on the success of sulfonamides as trifluoromethylthiolating agents and will be presented in Chapter 3. A potential future recommendation to synthesise the trifluoromethylated sulfonimidamides is the use of trifluoromethylated amines for the amination of the sulfonimidoyl chlorides (Scheme 1). The detailed experimental procedures for Schemes 4-6 are provided in Chapter 5.

References

1. F. Teng, J. Cheng and C. Bolm, *Organic Letters*, 2015, **17**, 3166-3169.
2. S. P. Midya, J. Rana, T. Abraham, B. Aswin and E. Balaraman, *Chemical Communications*, 2017, **53**, 6760-6763.
3. S. P. Pitre, C. D. McTiernan, H. Ismaili and J. C. Scaiano, *ACS Catalysis*, 2014, **4**, 2530-2535.
4. G.-B. Li, C. Zhang, C. Song and Y.-D. Ma, *Beilstein J Org Chem*, 2018, **14**, 155-181.
5. T. Chatterjee, N. Iqbal, Y. You and E. J. Cho, *Accounts of Chemical Research*, 2016, **49**, 2284-2294.
6. D. P. Hari and B. König, *Chemical Communications*, 2014, **50**, 6688-6699.
7. S. P. Pitre, C. D. McTiernan, H. Ismaili and J. C. Scaiano, *Journal of the American Chemical Society*, 2013, **135**, 13286-13289.
8. D. A. Nicewicz and T. M. Nguyen, *ACS Catalysis*, 2014, **4**, 355-360.
9. S. Arumugam, A. Brandstädt, T. Nishizeki and K. Thulasiraman, *Handbook of graph theory, combinatorial optimization, and algorithms*, Chapman and Hall/CRC, 2016.
10. S. P. Midya, J. Rana, T. Abraham, B. Aswin and E. Balaraman, *Chemical Communications*, 2017, **53**, 6760-6763.
11. Z. Su, Y. Guo, Q.-Y. Chen, Z.-G. Zhao and B.-Y. Nian, *Chinese Journal of Chemistry*, 2019, **37**, 597-604.
12. K. Maeda, T. Kurahashi and S. Matsubara, *European Journal of Organic Chemistry*, 2019, **2019**, 4613-4616.
13. P. Eisenberger, S. Gischig and A. Togni, *Chemistry – A European Journal*, 2006, **12**, 2579-2586.
14. T. Umemoto and S. Ishihara, *Journal of the American Chemical Society*, 1993, **115**, 2156-2164.
15. I. Ruppert, K. Schlich and W. Volbach, *Tetrahedron Letters*, 1984, **25**, 2195-2198.
16. G. K. S. Prakash, R. Krishnamurti and G. A. Olah, *Journal of the American Chemical Society*, 1989, **111**, 393-395.
17. K. G. Ghosh, P. Chandu, S. Mondal and D. Sureshkumar, *Tetrahedron*, 2019, **75**, 4471-4478.
18. E. Torti, S. Protti and M. Fagnoni, *Chemical Communications*, 2018, **54**, 4144-4147.
19. Y. Ouyang, X.-H. Xu and F.-L. Qing, *Angewandte Chemie International Edition*, 2018, **57**, 6926-6929.
20. M. Li, Y. Wang, X.-S. Xue and J.-P. Cheng, *Asian Journal of Organic Chemistry*, 2017, **6**, 235-240.
21. G. Zou and X. Wang, *Organic & Biomolecular Chemistry*, 2017, **15**, 8748-8754.
22. F.-Y. Li, D.-Z. Lin, T.-J. He, W.-Q. Zhong and J.-M. Huang, *ChemCatChem*, 2019, **11**, 2350-2354.
23. M. Li, X.-S. Xue, J. Guo, Y. Wang and J.-P. Cheng, *The Journal of Organic Chemistry*, 2016, **81**, 3119-3126.
24. M. J. Frisch, G. W. Trucks, H. B. Schlegel, G. E. Scuseria, M. A. Robb, J. R. Cheeseman, G. Scalmani, V. Barone, G. A. Petersson, H. Nakatsuji, X. Li, M. Caricato, A. V. Marenich, J. Bloino, B. G. Janesko, R. Gomperts, B. Mennucci, H. P. Hratchian, J. V. Ortiz, A. F. Izmaylov, J. L. Sonnenberg, Williams, F. Ding, F. Lipparini, F. Egidi, J. Goings, B. Peng, A. Petrone, T. Henderson, D. Ranasinghe, V. G. Zakrzewski, J. Gao, N. Rega, G. Zheng, W. Liang, M. Hada, M. Ehara, K. Toyota, R. Fukuda, J. Hasegawa, M. Ishida, T. Nakajima, Y. Honda, O. Kitao, H. Nakai, T. Vreven, K. Throssell, J. A. Montgomery Jr., J. E. Peralta, F. Ogliaro, M. J. Bearpark, J. J. Heyd, E. N. Brothers, K. N. Kudin, V. N. Staroverov, T. A. Keith, R. Kobayashi, J. Normand,

- K. Raghavachari, A. P. Rendell, J. C. Burant, S. S. Iyengar, J. Tomasi, M. Cossi, J. M. Millam, M. Klene, C. Adamo, R. Cammi, J. W. Ochterski, R. L. Martin, K. Morokuma, O. Farkas, J. B. Foresman and D. J. Fox, *Journal*, 2016.
25. Y. Zhao and D. G. Truhlar, *Theoretical Chemistry Accounts*, 2008, **120**, 215-241.
26. R. Krishnan, J. S. Binkley, R. Seeger and J. A. Pople, *J. Chem. Phys.*, 1980, **72**, 650.
27. A. D. McLean and G. S. Chandler, *J. Chem. Phys.*, 1980, **72**, 5639.
28. A. V. Marenich, C. J. Cramer and D. G. Truhlar, *The Journal of Physical Chemistry B*, 2009, **113**, 6378-6396.
29. R. Krishnan, J. S. Binkley, R. Seeger and J. A. Pople, *The Journal of Chemical Physics*, 1980, **72**, 650-654.
30. A. McLean and G. Chandler, *The Journal of Chemical Physics*, 1980, **72**, 5639-5648.
31. M. J. Frisch, G. W. Trucks, H. B. Schlegel, G. E. Scuseria, M. A. Robb, J. R. Cheeseman, G. Scalmani, V. Barone, B. Mennucci, G. A. Petersson, H. Nakatsuji, M. Caricato, X. Li, H. P. Hratchian, A. F. Izmaylov, J. Bloino, G. Zheng, J. L. Sonnenberg, M. Hada, M. Ehara, K. Toyota, R. Fukuda, J. Hasegawa, M. Ishida, T. Nakajima, Y. Honda, O. Kitao, H. Nakai, T. Vreven, J. A. Montgomery, Jr., J. E. Peralta, F. Ogliaro, M. Bearpark, J. J. Heyd, E. Brothers, K. N. Kudin, V. N. Staroverov, R. Kobayashi, J. Normand, K. Raghavachari, A. Rendell, J. C. Burant, S. S. Iyengar, J. Tomasi, M. Cossi, N. Rega, J. M. Millam, M. Klene, J. E. Knox, J. B. Cross, V. Bakken, C. Adamo, J. Jaramillo, R. Gomperts, R. E. Stratmann, O. Yazyev, A. J. Austin, R. Cammi, C. Pomelli, J. W. Ochterski, R. L. Martin, K. Morokuma, V. G. Zakrzewski, G. A. Voth, P. Salvador, J. J. Dannenberg, S. Dapprich, A. D. Daniels, Ö. Farkas, J. B. Foresman, J. V. Ortiz, J. Cioslowski and D. J. Fox, *Gaussian 09, Revision E.01*, Gaussian Inc, Wallingford, 2009.
32. H. G. Roth, N. A. Romero and D. A. Nicewicz, *Synlett*, 2016, **27**, 714-723.
33. V. Barone and M. Cossi, *J. Phys. Chem. A*, 1998, **102**, 1995.
34. M. Cossi, N. Rega, G. Scalmani and V. Barone, *J. Comput. Chem.*, 2003, **24**, 669.
35. P. J. Stephens, F. Devlin, C. Chabalowski and M. J. Frisch, *The Journal of physical chemistry*, 1994, **98**, 11623-11627.
36. A. V. Krukau, O. A. Vydrov, A. F. Izmaylov and G. E. Scuseria, *The Journal of Chemical Physics*, 2006, **125**, 224106.
37. J. Heyd, G. E. Scuseria and M. Ernzerhof, *The Journal of Chemical Physics*, 2006, **124**, 219906.
38. J. Heyd and G. E. Scuseria, *The Journal of Chemical Physics*, 2004, **120**, 7274-7280.
39. J. Heyd and G. E. Scuseria, *The Journal of Chemical Physics*, 2004, **121**, 1187-1192.
40. J. Heyd, J. E. Peralta, G. E. Scuseria and R. L. Martin, *The Journal of Chemical Physics*, 2005, **123**, 174101.
41. A. F. Izmaylov, G. E. Scuseria and M. J. Frisch, *The Journal of Chemical Physics*, 2006, **125**, 104103.
42. T. M. Henderson, A. F. Izmaylov, G. Scalmani and G. E. Scuseria, *The Journal of Chemical Physics*, 2009, **131**, 044108.
43. Gaussian, SCRF, <https://gaussian.com/scrf/>, (accessed 07/11/2019, 2019).
44. B. Thapa and H. B. Schlegel, *The Journal of Physical Chemistry A*, 2016, **120**, 8916-8922.
45. M. Li, J. Guo, X.-S. Xue and J.-P. Cheng, *Organic letters*, 2016, **18**, 264-267.
46. M. Li, B. Zhou, X.-S. Xue and J.-P. Cheng, *The Journal of organic chemistry*, 2017, **82**, 8697-8702.
47. M. Li, X.-S. Xue and J.-P. Cheng, *ACS Catalysis*, 2017, **7**, 7977-7986.
48. A. S. Feiner and A. J. McEvoy, *Journal of Chemical Education*, 1994, **71**, 493.
49. N. A. Romero and D. A. Nicewicz, *Chemical Reviews*, 2016, **116**, 10075-10166.

50. H.-J. Timpe, K.-P. Kronfeld, U. Lammel, J.-P. Fouassier and D.-J. Lougnot, *Journal of Photochemistry and Photobiology A: Chemistry*, 1990, **52**, 111-122.
51. H.-J. Timpe and K.-P. Kronfeld, *Journal of Photochemistry and Photobiology A: Chemistry*, 1989, **46**, 253-267.
52. N. J. Treat, H. Sprafke, J. W. Kramer, P. G. Clark, B. E. Barton, J. Read de Alaniz, B. P. Fors and C. J. Hawker, *Journal of the American Chemical Society*, 2014, **136**, 16096-16101.
53. Y. Chen, C.-J. Aurell, A. Pettersen, R. J. Lewis, M. A. Hayes, M. Lepistö, A. C. Jonson, H. Leek and L. Thunberg, *ACS medicinal chemistry letters*, 2017, **8**, 672-677.
54. Y. Chen and J. Gibson, *RSC Advances*, 2015, **5**, 4171-4174.
55. P. K. Chinthakindi, A. Benediktsdottir, A. Ibrahim, A. Wared, C. J. Aurell, A. Pettersen, E. Zamaratski, P. I. Arvidsson, Y. Chen and A. Sandström, *European Journal of Organic Chemistry*, 2019, **2019**, 1045-1057.
56. A. K. Roy, *Journal of the American Chemical Society*, 1993, **115**, 2598-2603.
57. D. A. Nagib and D. W. MacMillan, *Nature*, 2011, **480**, 224.
58. F. Izzo, M. Schäfer, P. Lienau, U. Ganzer, R. Stockman and U. Lücking, *Chemistry–A European Journal*, 2018, **24**, 9295-9304.
59. G. Zheng, X. Ma, J. Li, D. Zhu and M. Wang, *The Journal of organic chemistry*, 2015, **80**, 8910-8915.
60. S. Liang, J. Wei, L. Jiang, J. Liu, Y. Mumtaz and W.-b. Yi, *Chemical Communications*, 2019.

Chapter 3

3. Computationally aided direct electrophilic trifluoromethylthiolation *via* sulfonimidamides

3.1. Introduction

The trifluoromethylthio group (SCF_3) has attracted special interest in medicinal chemistry due to its remarkable lipophilicity (Hansch constants 1.44).¹⁻³ Due to its high lipophilicity and strong electron-withdrawing ability, the trifluoromethylthio group greatly improves the pharmacokinetic properties of lead compounds.^{3, 4} The trifluoromethylthio group is incorporated in several bioactive compounds (Figure 1), such as Tiflorex^{5, 6} (anorectic drug), Toltrazuril^{7, 8} (coccidiostatic drug), and Cefazaflur^{9, 10} (parenteral cephalosporin).^{11, 12} The unique properties possessed by the trifluoromethylthio group has prompted research into the development of efficient methods for the incorporation into desired scaffolds.¹³

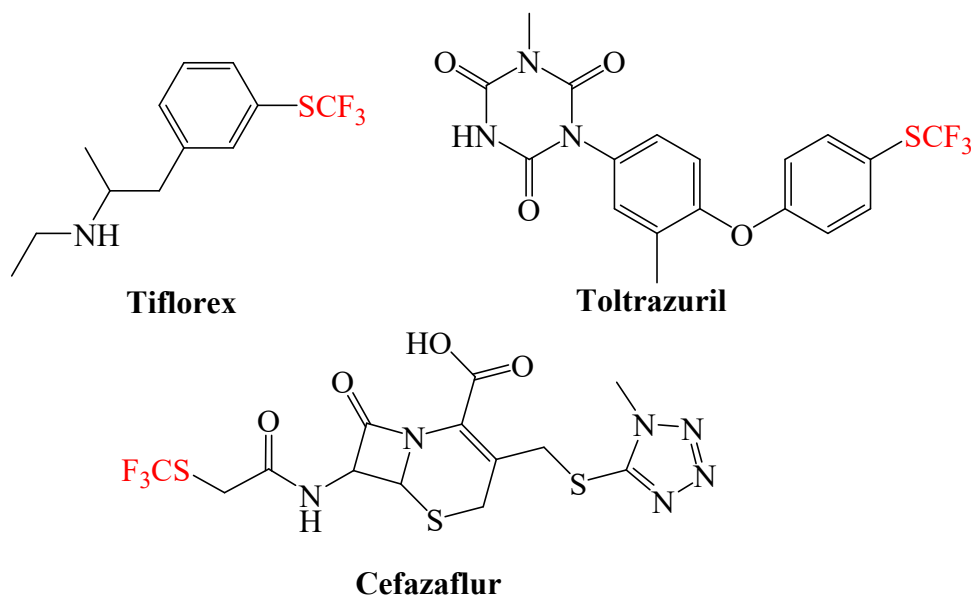


Figure 1: SCF_3 containing biologically active compounds.¹¹

Among the various electrophilic reagents available, N- SCF_3 reagents are the most utilised^{12, 13} (Figure 2). The reagents $\text{PhN}(\text{Me})\text{SCF}_3$ (Figure 2, **A**) and PhNHSCF_3 (Figure 2, **B**), developed by Billard and Langlois,^{14, 15} are effective for trifluoromethylthiolation of various substrates.^{14, 16-18} However, a strong Brønsted or Lewis acid is required for the activation of the reaction.¹³ To address this problem, Shen and associates developed sulphonamide based N-trifluoromethylthiosaccharin¹⁹ (Figure 2, **E**) and N-trifluoromethylthio-dibenzenesulfonimide²⁰ (Figure 2, **F**). Both reagents have been shown to be highly electrophilic

in both computational²¹ and experimental⁴ studies. These reagents have been shown to possess a greater reactivity than previous reagents with a broad substrate scope under mild conditions.^{13, 19-22}

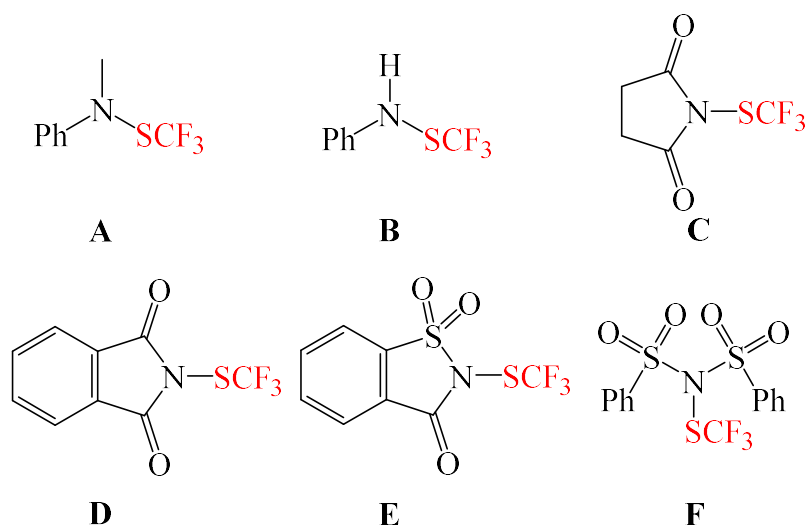


Figure 2: Electrophilic trifluoromethylthiolating reagents.²⁰

Sulfonimidamides are the aza-analogues of sulfonamides, where one of the oxygen atoms have been replaced by a nitrogen.²³ Sulfonimidamides have received less attention compared to sulfonamides, presumably to the lack of commercial availability and synthetic methods.^{24, 25} Based on the success sulfonamides have had as highly electrophilic trifluoromethylthiolating reagent¹⁹⁻²¹, this study was focused on designing highly electrophilic sulfonimidamide based trifluoromethylthiolating reagents.

Cheng and co-workers studied the electrophilic donating ability ($Tt^{+}DA$) of various trifluoromethylthiolation agents by computationally calculating bond dissociation enthalpies cleavage.^{21, 26} Good correlation was observed between the computed $Tt^{+}DA$ values and experimental reactivity. In an additional study, Cheng and co-workers experimentally determined the electrophilicity parameters of various trifluoromethylthiolation agents, these also correlated well with $Tt^{+}DA$ values.⁴

Inspired by the work of Cheng and co-workers^{21, 26} and Shen and associates^{19, 20}, this study was focused on the computational design and thereafter synthesis of more efficient sulfonimidamide based electrophilic trifluoromethylthiolation agents.

3.2 Results and Discussion

3.2.1 Trifluoromethylthio cation donor abilities (Tt⁺DAs) of sulfonimidamides

All calculations were performed with the Gaussian 16 software package.²⁷ Optimisations were performed with the M06-2X²⁸ functional and 6-31+G(d)^{29, 30} basis set, using the SMD solvation model³¹ to account for solvation in acetonitrile. Thereafter, single point energy was calculated at the M06-2X/6-311++G(2df,2p)^{32, 33} level of theory on the pre-optimised structures. The Tt⁺DAs of the proposed sulfonimidamides were calculated (Figure 3). Figure 3 illustrates that sulfonimidamides (**7a-c**, **e**, **f**) possess the potential to deliver a trifluoromethylthio group comparable to known delivering agents (Figure 4). The Tt⁺DAs values of the proposed sulfonimidamides illustrate that they have the potential to be more electrophilic than previously applied delivering agents.

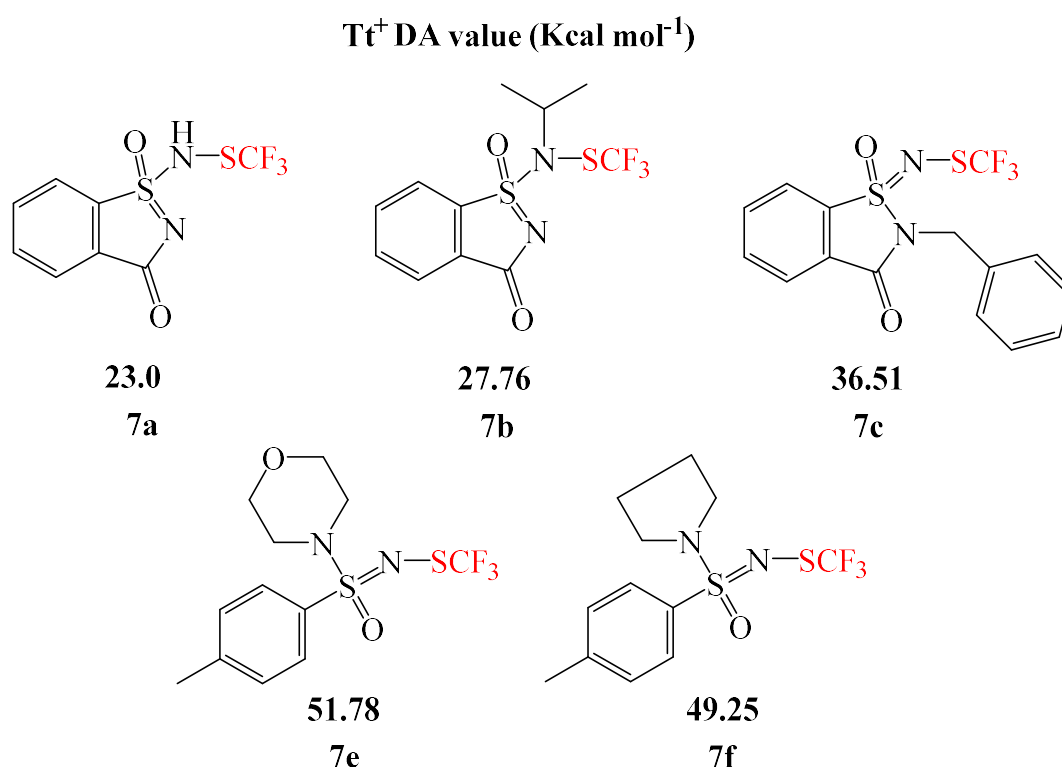


Figure 3: Calculated* Tt⁺DAs values of the proposed sulfonimidamides in acetonitrile.

*(SMD-M06-2X/6-31+G(d)// SMD-M06-2X/6-311++G(2df,2p))

The trifluoromethylthio radical donating abilities (Tt[•]DA) of the proposed sulfonimidamides were also calculated (Appendix 2, Figure S1). The Tt[•]DA values indicated the potential to

deliver a trifluoromethylthio group comparable to known delivering agents (Appendix 2, Figure S2).

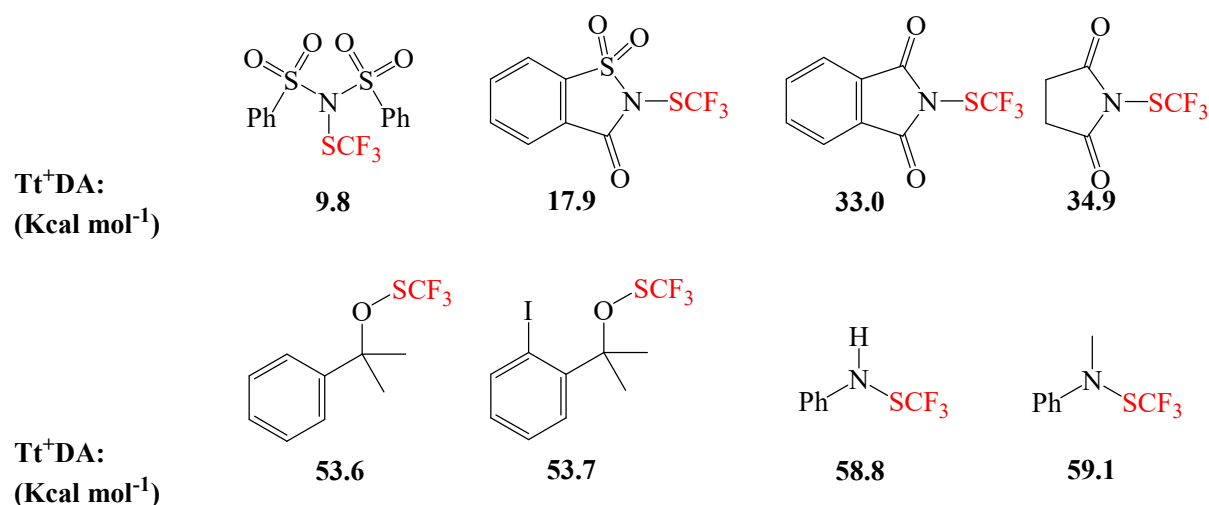
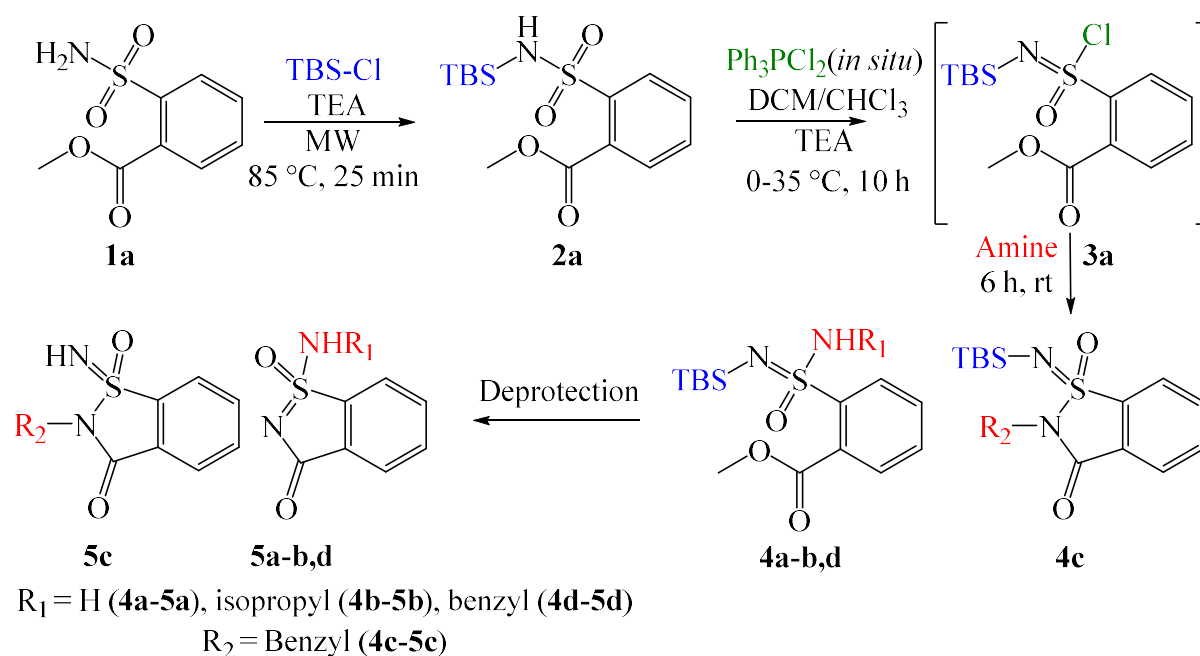


Figure 4: The reported calculated* Tt^+DA s values of electrophilic trifluoromethylthiolation reagents in acetonitrile.^{20, 21} * (SMD-M06-2X/6-31+G(d)// SMD-M06-2X/6-311++G(2df,2p))

3.2.2 Synthesis of sulfonimidamides

The various sulfonimidamides were synthesised according to an adapted method developed by Chen *et al.*³⁴ (Scheme 1). The protection of sulfonamide (**1a**, Figure 5, **A**) was performed over 25 minutes using a microwave method (85 °C, 200 W) instead of the reported 20 hour room temperature reaction, the protected sulfonimidamide (**2a**) was confirmed by ^1H , ^{13}C NMR spectroscopy and LC-MS analysis. *Tert*-butyldimethyl-silyl (TBS) protection was necessary to prevent a reaction between the primary amine that could form and the *in situ* formed sulfonimidoyl chloride (**3a**). Bulkier silyl protecting groups (TBS and *tert*-butyldiphenylsilyl) generate more stable sulfonimidoyl chlorides and increased yields, as shown in studies by Chen and Gibson²⁵ and Chinthakindi *et al.*³⁵ The deoxychlorination of the protected sulfonamide (**2a**) using Ph_3PCl_2 was initially reported by Roy³⁶, using tri-methylsilyl protected sulfonamides. The amination step of the sulfonimidoyl chloride (**3a**) can result in the formation of products with ring closure (**4c**, Figure 5, **B**) or without ring closure (**4a**, **b**, **d**), which is dependent on the reaction conditions as shown in literature.³⁴ Compounds **4a-d** were confirmed by novel X-ray crystal structures, ^1H , ^{13}C NMR spectroscopy and LC-MS analysis. Deprotection eventually leads to ring closure obtaining the final sulfonimidamides (**5a-c**) without an imine nitrogen present, confirmed by novel X-ray crystal structures, ^1H , ^{13}C NMR spectroscopy and LC-MS analysis. Deprotection of the ring closed products lead to a sulfonimidamide with an imine nitrogen present (**5c**), confirmed by ^1H , ^{13}C NMR spectroscopy

and LC-MS analysis. Compound **5d** (Figure 5, **D**) was obtained in trace amounts during the synthesis of compound **5c** and was therefore, not considered further. Compounds **4b** and **5b** (Figure 5, **C**) are novel. Novel X-ray crystal structures for **4a** and **5a** are currently under analysis. A detailed experimental procedure is provided in Chapter 5.



Scheme 1: Synthesis route for the proposed saccharin based sulfonimidamides **5a-d**.

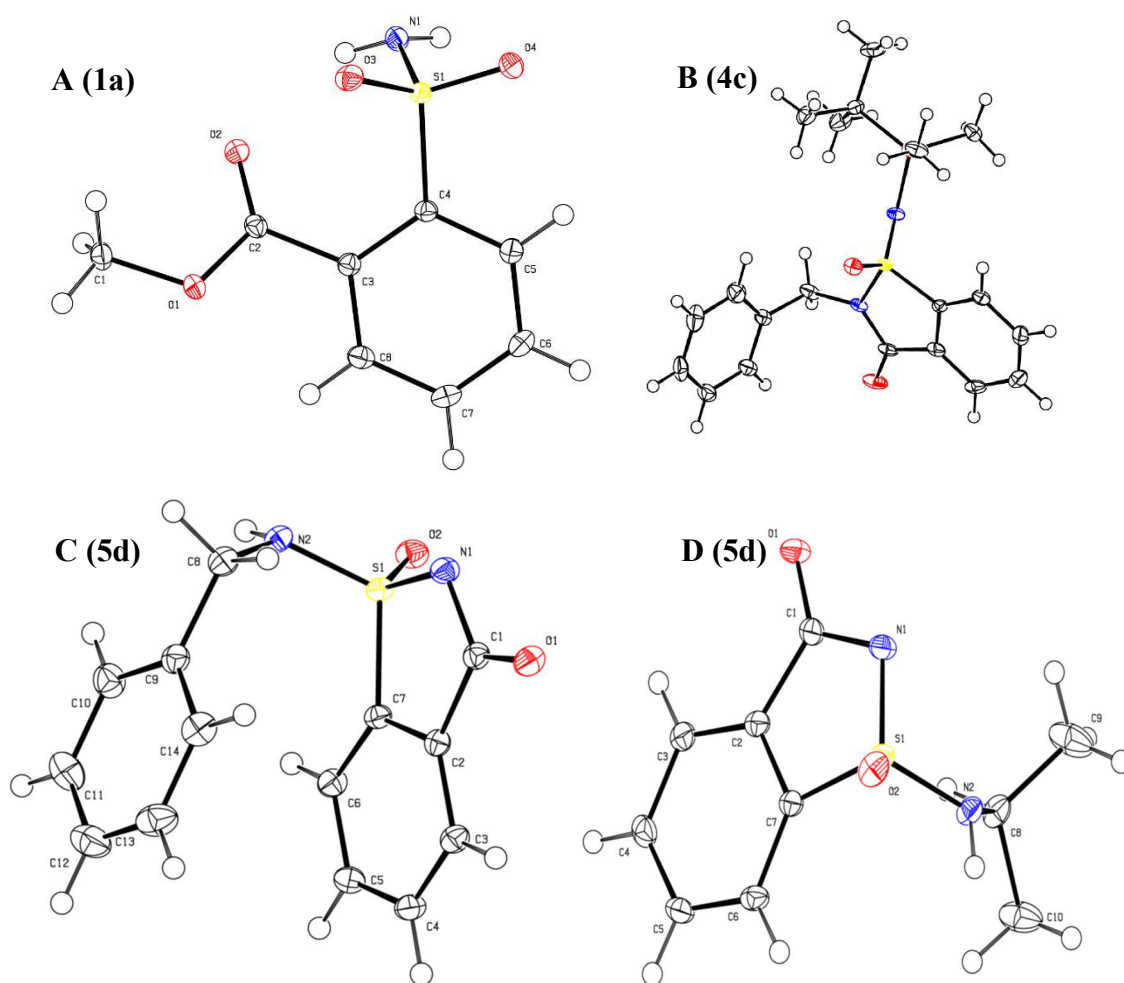
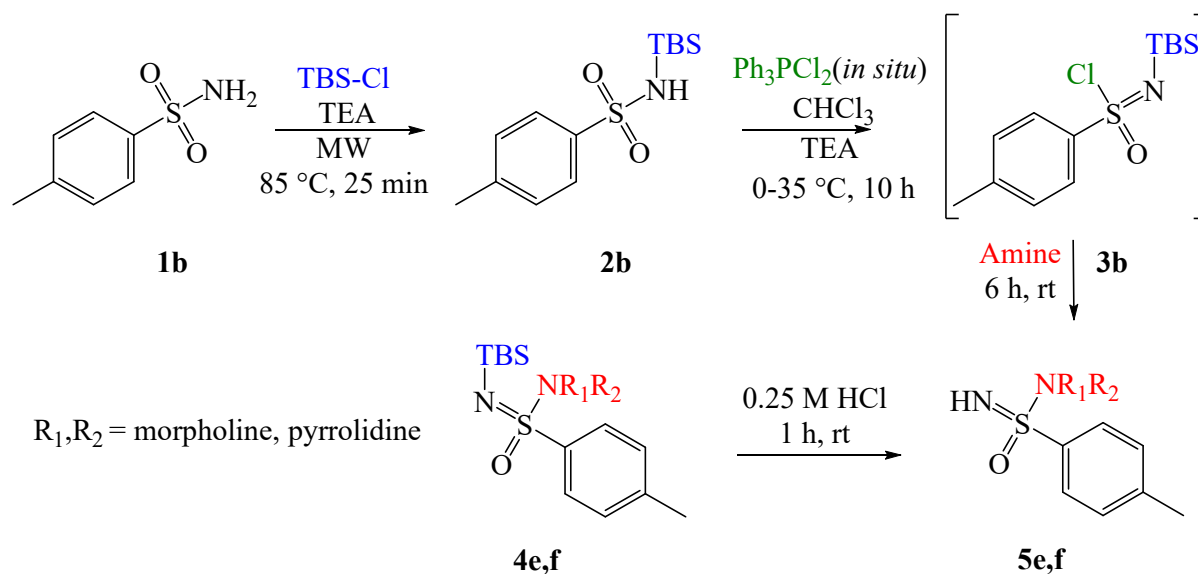


Figure 5: Novel X-ray crystal structures obtained (unpublished results).

Additional sulfonimidamides were synthesised according to an adapted method developed by Chen *et al.*²⁵ (Scheme 2). The protection of sulfonamide **1b** was performed in 25 minutes under ambient conditions using microwave instead of the previously reported three day air and moisture conditions. The protected sulfonimidamide (**2b**) was confirmed by ¹H, ¹³C NMR spectroscopy and LC-MS analysis. Protection was necessary due to the reasons previously stated for the saccharin based sulfonimidamides. The deoxychlorination of the protected sulfonamide **2b** was performed using *in situ* generated Ph₃PCl₂. The amination of the sulfonimidoyl chloride **3b** resulted in the formation of protected sulfonimidamides **4e, f**. Compounds **4e, f** were confirmed by ¹H, ¹³C NMR spectroscopy and LC-MS analysis. Deprotection of the compounds **4e, f** led to the final products **5e, f**, which was confirmed by ¹H, ¹³C NMR spectroscopy and LC-MS analysis. A detailed synthesis procedure is provided in Chapter 5.

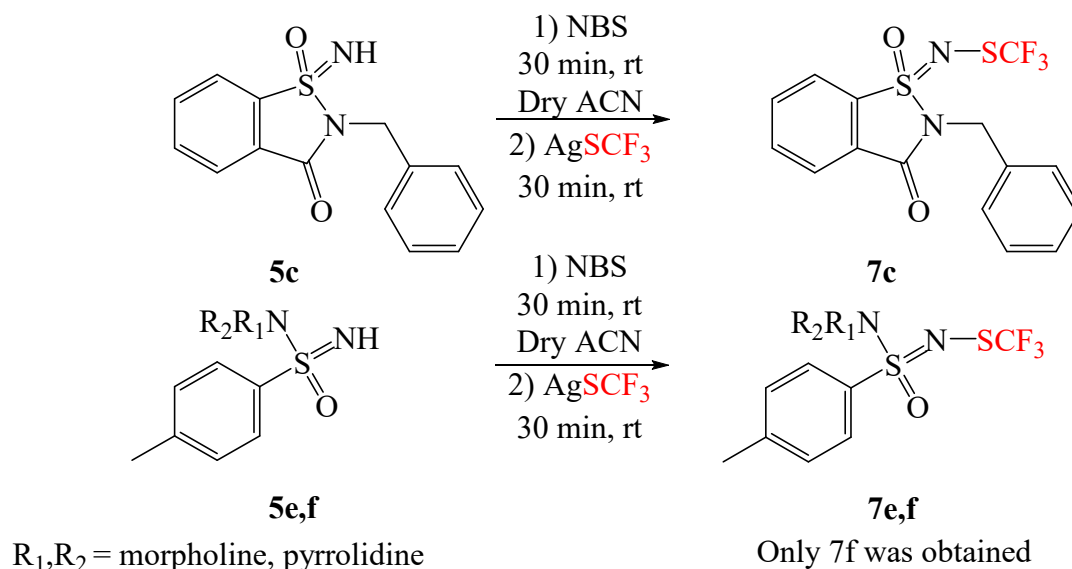


Scheme 2: Synthesis route for the proposed sulfonimidamides **5e, f**.

Sulfonimidamides **5a-f** were successfully synthesised. All of which possessed the potential to deliver a trifluoromethylthio group comparable to known delivering agents (Figure 3,4). Therefore, all of the synthesised sulfonimidamides with the exception of **5d** (obtained in trace amounts) were selected for further *N*-trifluoromethylthiolation.

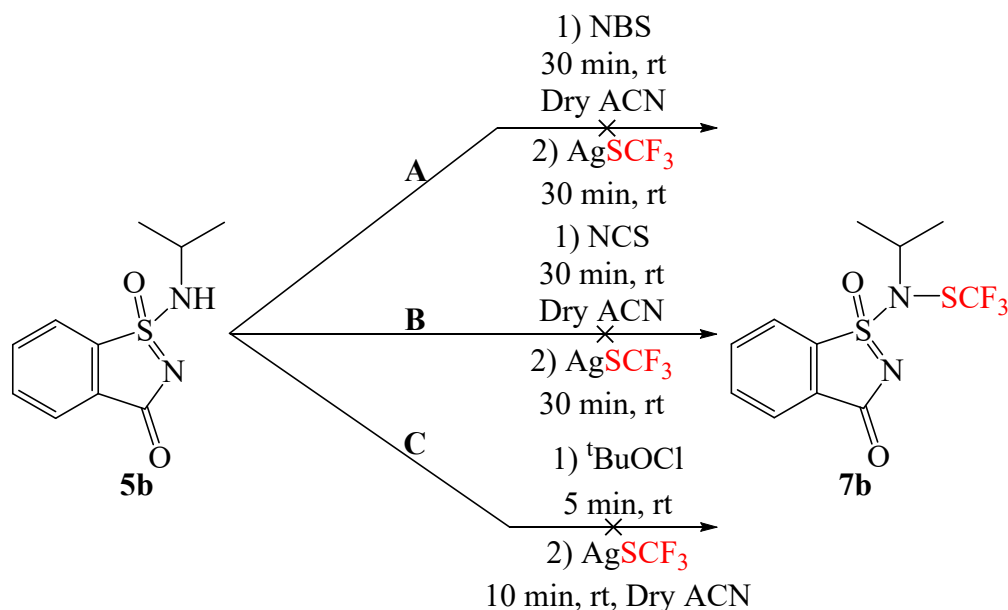
3.2.3 Trifluoromethylthiolation of sulfonimidamides

Bolm and co-workers³⁷ initially developed a method for the *N*-trifluoromethylthiolation of the sulfoximines, which was then adapted by Arvidsson and associates³⁸ for the *N*-trifluoromethylthiolation of sulfonimidamides. This method was utilised successfully for trifluoromethylthiolation of the sulfonimidamides in Scheme 3. In the reaction the following sulfonimidamides reacted with the *N*-bromosuccinimide (NBS) to form *N*-bromosulfonimidamides. The usually nucleophilic imine nitrogen of the sulfonimidamides was subjected to “umpolung” through bromination and thereafter nucleophilic replacement with the CF₃S anion occurred.³⁸ The formation of AgBr is suspected of promoting the *N*-trifluoromethylthiolations of the sulfonimidamides.³⁷ The trifluoromethylthiolation of the sulfonimidamides (**5c, e, f**) was confirmed by ¹H, ¹³C NMR spectroscopy and LC-MS analysis. A detailed experimental procedure is provided in Chapter 5.



Scheme 3: *N*-trifluoromethylthiolation following Bolm's method.^{37, 38}

The *N*-trifluoromethylthiolation of the sp^2 type nitrogen's were also attempted on derivative **5b**. Initially, the method developed by Bolm and co-workers³⁷ was attempted (Scheme 4, path A). However, no bromination occurred as observed from TLC analysis. Thereafter, the NBS was replaced with *N*-chlorosuccinimide (NCS) following a method developed for the trifluoromethylthiolation of amines by Besset and co-workers (Scheme 4, path B).³⁹ The sulfonimidamide **5b** was chlorinated by the NCS, however, upon addition of the AgSCF_3 only starting material was observed from LC-MS analysis. Finally the method developed by Shen and co-workers for the trifluoromethylthiolation of sulfonamides was attempted (Scheme 4, path C).^{19, 20} However, no conversion of the starting material (**5b**) occurred as observed from TLC analysis. A detailed experimental procedure is provided in Chapter 5.



Scheme 4: Attempted *N*-trifluoromethylthiolation of sulfonimidamide **5b**.

Despite all attempts, the *N*-trifluoromethylthiolation of sulfonimidamide **5b** could not be achieved. Therefore, *N*-trifluoromethylthiolation on sulfonimidamide **5a** was not attempted. Despite compound **5e** possessing an imine nitrogen, compound **7e** did not form. Sulfonimidamide **7c, f** were successfully synthesised.

Cheng and co-workers experimentally determined the electrophilicity parameters (*E*) of various trifluoromethylthiolation agents, which correlated well with the computational $Tt^{+}DA$ values (Figure 5).⁴ This is in agreement with previous reports stating Shen's reagents being the most reactive.^{19, 20} The lower the *E* parameter and $Tt^{+}DA$ values, the more electrophilic the trifluoromethylthiolation agent. Figure 5 also depicts reactivities of carbon-centred nucleophiles. The higher the *N* parameter the more nucleophilic the carbon-centred nucleophiles. Each respective trifluoromethylthiolation agent should react with nucleophiles on the same or lower level at room temperature. Utilising the $Tt^{+}DA$ values as a guide sulfonimidamide **7c, e, f** were positioned in the graph and therefore, should react with a correspondingly similar or lower placed nucleophiles. The computationally calculated $Tt^{+}DA$ s values of the proposed sulfonimidamides (Figure 3) illustrate that sulfonimidamide **7c** possessed the greatest potential for donation as compared to sulfonimidamides **7e, f**. Therefore, **7c** was chosen as the donating agent for direction electrophilic trifluoromethylthiolation.

Using Figure 5 as a guide ethyl cyanoacetate and 2,4-dimethylpyrrole were chosen as the model substrates to evaluate the reactivity of sulfonimidamide **7c**. The trifluoromethylthiolation of

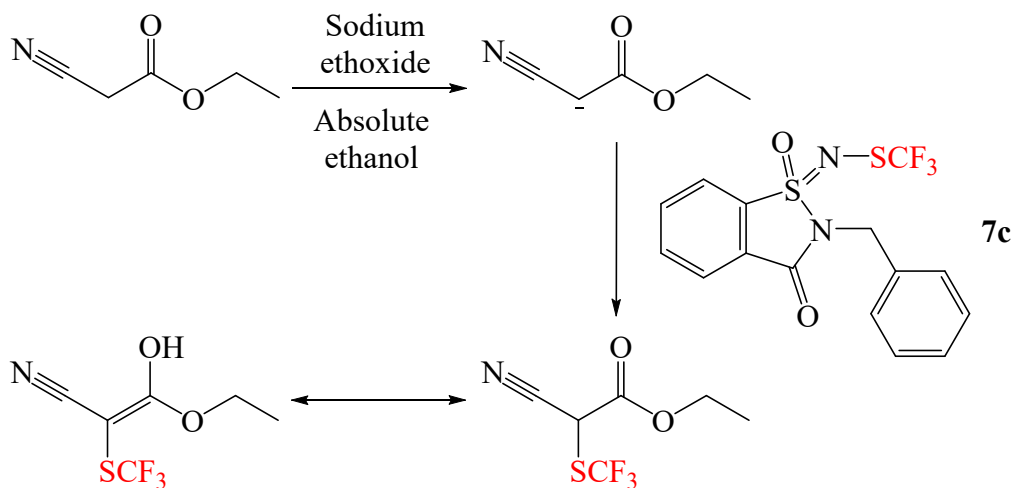
Figure 1 displays a vertical energy scale from 1 to 20 kcal/mol, with N and E arrows. Various chemical structures are plotted along this scale, including alkenes, aromatics, and organosulfur compounds. Some structures are highlighted in red or blue. Energy values are provided for many structures, and reaction energies are given for several transformations.

Energy (kcal/mol)	Structure	Energy (kcal/mol)	Structure
1.11	Isobutylene	-3.72	Phenyl cation
0.78	Styrene	-5.17	Me-N ⁺ Ph
1.33	Furan	-5.91	Ph-S ⁺ -Ph
1.70	p-Methoxystyrene	-6.06	Ph-SO ₂ -N(SCF ₃)-SO ₂ -Ph
2.30	Cyclopentadiene	-6.48	Ph-isoindole-1-one-SCF ₃
3.09	2-Methyl-2-butene	-6.48	Ph-isoindole-1-one-SCF ₃
3.61	2-Methoxyfuran	-6.48	Ph-isoindole-1-one-SCF ₃
3.92	EtOCH=CH ₂	-6.48	Ph-isoindole-1-one-SCF ₃
4.41	SiMe ₃ -CH=CH ₂	-6.48	Ph-isoindole-1-one-SCF ₃
4.90	Ph-N ⁺ C ⁻	-6.48	Ph-isoindole-1-one-SCF ₃
5.85	2-Methylpyrrole	-6.48	Ph-isoindole-1-one-SCF ₃
5.75	Indole	-6.48	Ph-isoindole-1-one-SCF ₃
5.55	Indole	-6.48	Ph-isoindole-1-one-SCF ₃
6.57	SiMe ₃ -O-Cyclopentadiene	-6.48	Ph-isoindole-1-one-SCF ₃
6.91	Indole	-6.48	Ph-isoindole-1-one-SCF ₃
8.01	2-Methyl-2-pyrrole	-6.48	Ph-isoindole-1-one-SCF ₃
9.01	Ph-N ⁺ C ⁻	-6.48	Ph-isoindole-1-one-SCF ₃
9.35	Ph-N ⁺ C ⁻	-6.48	Ph-isoindole-1-one-SCF ₃
9.56	Ph-N ⁺ C ⁻	-6.48	Ph-isoindole-1-one-SCF ₃
9.90	SiMe ₃ -O-Cyclopentadiene	-6.48	Ph-isoindole-1-one-SCF ₃
10.67	Indole	-6.48	Ph-isoindole-1-one-SCF ₃
11.99	Ph-N ⁺ C ⁻	-6.48	Ph-isoindole-1-one-SCF ₃
14.91	Indole	-6.48	Ph-isoindole-1-one-SCF ₃
16.03	Ph-CO-CH ₂ -COMe	-6.48	Ph-isoindole-1-one-SCF ₃
17.52	Ph-CO-CH ₂ -CO ₂ Et	-6.48	Ph-isoindole-1-one-SCF ₃
19.67	Ph-CO-CH ₂ -CN	-6.48	Ph-isoindole-1-one-SCF ₃
23.32	Ph-N ⁺ C ⁻	-6.48	Ph-isoindole-1-one-SCF ₃

21

3.2.4 Direction electrophilic trifluoromethylthiolation *via* sulfonimidamides

Ethyl cyanoacetate was deprotonated to form the highly nucleophilic ethyl cyanoacetate anion using sodium ethoxide in ethanol. Thereafter, sulfonimidamide **7c** was added. After 12 hours LC-MS analysis indicated complete consumption of **7c**. Interestingly, sulfonimidamide **5d** was obtained as a by-product of the reaction and not **5c** (Figure 7), as confirmed by ^1H NMR and LC-MS analysis. This indicates a migration of the benzyl group after the trifluoromethylthio group leaves. The suspected product possesses two peaks in the ^{19}F NMR indicating possible resonance between keto-enol forms of the desired product. This was similarly observed in the trifluoromethylthiolation of 1-phenylbutane-1,3-dione and ethyl 3-oxo-3-phenylpropanoate.⁴ LC-MS analysis indicated the formation of the trifluoromethylthiolated ethyl cyanoacetate. Purification was attempted using gravity chromatography and supercritical fluid chromatography. However, a clean ^1H and ^{13}C NMR could not be achieved. All attempts to isolate the trifluoromethylthiolated ethyl cyanoacetate resulted in a mixture of the suspected product and sulfonimidamide **5c** as indicated by ^1H and LC-MS analysis. Further optimization towards the desired products is ongoing. A detailed experimental procedure is provided in Chapter 5.



Scheme 5: Direction electrophilic trifluoromethylthiolation of ethyl cyanoacetate.

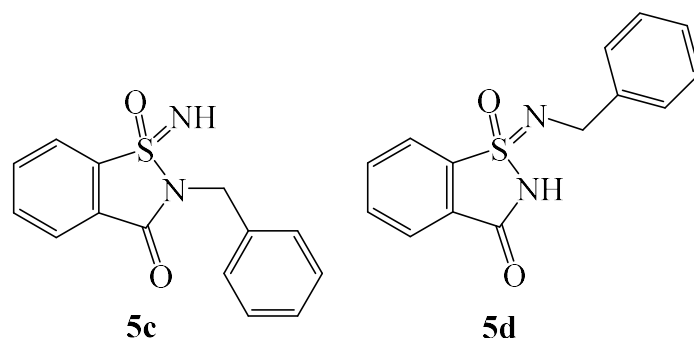
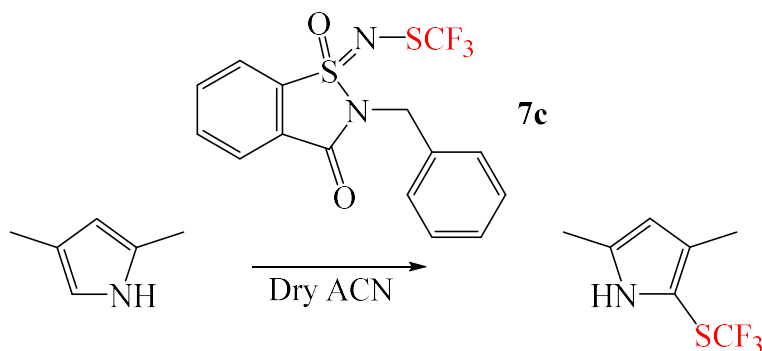


Figure 7: Structure of sulfonimidamides **5c**, **d**.

Additionally, the trifluoromethylthiolation of 2,4-dimethylpyrrole was also attempted to evaluate the reactivity of sulfonimidamide **7c**. After 12 hours LC-MS analysis indicated complete consumption of **7c** to form sulfonimidamide **5c**. The ^{19}F NMR of the crude reaction mixture revealed a single peak which corresponded to chemical shift reported in literature.⁴⁰⁻⁴² However, all attempts at purification of the desired product were unsuccessful and a clean ^1H and ^{13}C NMR could not be achieved. All attempts to isolate the trifluoromethylthiolated 2,4-dimethylpyrrole resulted in a mixture compounds as indicated by ^1H NMR and LC-MS analysis. Further optimization towards the desired products is ongoing. A detailed experimental procedure is provided in Chapter 5.



Scheme 6: Direction electrophilic trifluoromethylthiolation of 2,4-dimethylpyrrole.

The results from the trifluoromethylthiolation of ethyl cyanoacetate and 2,4-dimethylpyrrole indicate that sulfonimidamide **7c** has the potential to be a new SCF_3 donating agent. Due to the trifluoromethylthio group leaving as confirmed by crude ^{19}F NMR and LC-MS analysis. However, further optimization is ongoing in our laboratory.

Additionally, these sulfonimidamide based trifluoromethylthiolating agents have the indicated potential to deliver a trifluoromethylthio radical comparable to known delivering agents as indicated by calculated T^*DA values (Appendix 2, Figure S1-2). *N*-trifluoromethylthio sulfonimidamides have been reported to show high antimycobacterial activity comparable to

ethambutol, a first line antibiotic for tuberculosis infection recommended by the world health organization. Interestingly, other work in our lab revealed a structure activity relationship using matched pair analysis, that concluded that the trifluoromethylthio moiety as compared to the trifluoromethyl moiety on sulfoximines was responsible for superior biological activity against bacterial presumably to the lability of the N-SCF₃ bond.³⁸ This result correlates to our experimental observation of losing the SCF₃ group. Therefore, sulfonimidamides **7a-c** have the potential to be biological active as well as potential trifluoromethylthio delivering agents.

3.3 Conclusion

Sulfonimidamides **5c, f** were successfully trifluoromethylthiolated, resulting in the corresponding *N*-trifluoromethylthio sulfonimidamides **7c, f**. Novel X-ray crystal structures for **5e** and **5f** are currently under analysis. The computationally calculated Tt⁺DAs values of sulfonimidamides **7c, e, f** (Figure 3) illustrate that sulfonimidamide **7c** possessed the greatest potential for donation (36.51 Kcal mol⁻¹) and has the potential to be more electrophilic than previously applied delivering agents (Figure 4). Therefore, sulfonimidamide **7c** was chosen as the donating agent for the further electrophilic trifluoromethylthiolation of ethyl cyanoacetate and 2,4-dimethylpyrrole. The results from the trifluoromethylthiolation model reactions indicated that sulfonimidamide **7c** is a potentially new SCF₃ donating agent. Due to the trifluoromethylthio group leaving from sulfonimidamide **7c** as confirmed by crude ¹⁹F NMR and LC-MS analysis. However, method optimisation is required and is ongoing to determine the substrate scope and reaction conditions.

A potential future recommendation for the *N*-trifluoromethylthiolation of the sp² type nitrogen's is the use of trifluoromethylthiolated amines for the amination of the sulfonimidoyl chlorides (Scheme 1). This could lead to the synthesis of sulfonimidamides **7a, b** which possess greater Tt⁺DAs values as compared to sulfonimidamide **7c** (Figure 3).

References

1. A. Leo, C. Hansch and D. Elkins, *Chemical Reviews*, 1971, **71**, 525-616.
2. C. Hansch, A. Leo, S. H. Unger, K. H. Kim, D. Nikaitani and E. J. Lien, *Journal of Medicinal Chemistry*, 1973, **16**, 1207-1216.
3. M. Li, X.-S. Xue and J.-P. Cheng, *ACS Catalysis*, 2017, **7**, 7977-7986.
4. J. Zhang, J.-D. Yang, H. Zheng, X.-S. Xue, H. Mayr and J.-P. Cheng, *Angewandte Chemie International Edition*, 2018, **57**, 12690-12695.
5. T. Silverstone, J. Fincham and J. Plumley, *Br J Clin Pharmacol*, 1979, **7**, 353-356.
6. J. N. André, L. G. Dring, G. Gillet and C. Mas-Chamberlin, *Br J Pharmacol*, 1979, **66**, 506P-506P.
7. P. Pommier, A. Keita, S. Wessel-Robert, B. Dellac and H. Mundt, *Revue de Médecine Vétérinaire (France)*, 2003.
8. P. Laczay, G. Vörös and G. Semjén, *International Journal for Parasitology*, 1995, **25**, 753-756.
9. G. W. Counts, D. Gregory, D. Zeleznik and M. Turck, *Antimicrobial agents and chemotherapy*, 1977, **11**, 708-711.
10. N. Aswapokee and H. C. Neu, *Antimicrobial agents and chemotherapy*, 1979, **15**, 444-446.
11. X.-H. Xu, K. Matsuzaki and N. Shibata, *Chemical Reviews*, 2015, **115**, 731-764.
12. M. Horvat, M. Jereb and J. Iskra, *European Journal of Organic Chemistry*, 2018, **2018**, 3837-3843.
13. X. Shao, C. Xu, L. Lu and Q. Shen, *Accounts of Chemical Research*, 2015, **48**, 1227-1236.
14. A. Ferry, T. Billard, B. R. Langlois and E. Bacqué, *The Journal of Organic Chemistry*, 2008, **73**, 9362-9365.
15. F. Toulgoat, S. Alazet and T. Billard, *European Journal of Organic Chemistry*, 2014, **2014**, 2415-2428.
16. A. Ferry, T. Billard, E. Bacqué and B. R. Langlois, *Journal of Fluorine Chemistry*, 2012, **134**, 160-163.
17. F. Baert, J. Colomb and T. Billard, *Angewandte Chemie International Edition*, 2012, **51**, 10382-10385.
18. A. Ferry, T. Billard, B. R. Langlois and E. Bacqué, *Angewandte Chemie International Edition*, 2009, **48**, 8551-8555.
19. C. Xu, B. Ma and Q. Shen, *Angewandte Chemie International Edition*, 2014, **53**, 9316-9320.
20. P. Zhang, M. Li, X.-S. Xue, C. Xu, Q. Zhao, Y. Liu, H. Wang, Y. Guo, L. Lu and Q. Shen, *The Journal of organic chemistry*, 2016, **81**, 7486-7509.
21. M. Li, J. Guo, X.-S. Xue and J.-P. Cheng, *Organic letters*, 2016, **18**, 264-267.
22. H. Chachignon and D. Cahard, *Chinese Journal of Chemistry*, 2016, **34**, 445-454.
23. G. C. Nandi and P. I. Arvidsson, *Advanced Synthesis & Catalysis*, 2018, **360**, 2976-3001.
24. F. Izzo, M. Schäfer, R. Stockman and U. Lücking, *Chemistry – A European Journal*, 2017, **23**, 15189-15193.
25. Y. Chen and J. Gibson, *RSC Advances*, 2015, **5**, 4171-4174.
26. M. Li, B. Zhou, X.-S. Xue and J.-P. Cheng, *The Journal of organic chemistry*, 2017, **82**, 8697-8702.
27. M. J. Frisch, G. W. Trucks, H. B. Schlegel, G. E. Scuseria, M. A. Robb, J. R. Cheeseman, G. Scalmani, V. Barone, G. A. Petersson, H. Nakatsuji, X. Li, M. Caricato, A. V. Marenich, J. Bloino, B. G. Janesko, R. Gomperts, B. Mennucci, H. P. Hratchian,

- J. V. Ortiz, A. F. Izmaylov, J. L. Sonnenberg, Williams, F. Ding, F. Lipparini, F. Egidi, J. Goings, B. Peng, A. Petrone, T. Henderson, D. Ranasinghe, V. G. Zakrzewski, J. Gao, N. Rega, G. Zheng, W. Liang, M. Hada, M. Ehara, K. Toyota, R. Fukuda, J. Hasegawa, M. Ishida, T. Nakajima, Y. Honda, O. Kitao, H. Nakai, T. Vreven, K. Throssell, J. A. Montgomery Jr., J. E. Peralta, F. Ogliaro, M. J. Bearpark, J. J. Heyd, E. N. Brothers, K. N. Kudin, V. N. Staroverov, T. A. Keith, R. Kobayashi, J. Normand, K. Raghavachari, A. P. Rendell, J. C. Burant, S. S. Iyengar, J. Tomasi, M. Cossi, J. M. Millam, M. Klene, C. Adamo, R. Cammi, J. W. Ochterski, R. L. Martin, K. Morokuma, O. Farkas, J. B. Foresman and D. J. Fox, *Journal*, 2016.
28. Y. Zhao and D. G. Truhlar, *Theoretical Chemistry Accounts*, 2008, **120**, 215-241.
 29. R. Krishnan, J. S. Binkley, R. Seeger and J. A. Pople, *J. Chem. Phys.*, 1980, **72**, 650.
 30. A. D. McLean and G. S. Chandler, *J. Chem. Phys.*, 1980, **72**, 5639.
 31. A. V. Marenich, C. J. Cramer and D. G. Truhlar, *The Journal of Physical Chemistry B*, 2009, **113**, 6378-6396.
 32. R. Krishnan, J. S. Binkley, R. Seeger and J. A. Pople, *The Journal of Chemical Physics*, 1980, **72**, 650-654.
 33. A. McLean and G. Chandler, *The Journal of Chemical Physics*, 1980, **72**, 5639-5648.
 34. Y. Chen, C.-J. Aurell, A. Pettersen, R. J. Lewis, M. A. Hayes, M. Lepistö, A. C. Jonson, H. Leek and L. Thunberg, *ACS medicinal chemistry letters*, 2017, **8**, 672-677.
 35. P. K. Chinthakindi, A. Benediktsdottir, A. Ibrahim, A. Wared, C. J. Aurell, A. Pettersen, E. Zamaratski, P. I. Arvidsson, Y. Chen and A. Sandström, *European Journal of Organic Chemistry*, 2019, **2019**, 1045-1057.
 36. A. K. Roy, *Journal of the American Chemical Society*, 1993, **115**, 2598-2603.
 37. C. Bohnen and C. Bolm, *Organic letters*, 2015, **17**, 3011-3013.
 38. N. Thota, P. Makam, K. K. Rajbongshi, S. Nagiah, N. S. Abdul, A. A. Chuturgoon, A. Kaushik, G. Lamichhane, A. M. Somboro and H. G. Kruger, *ACS Medicinal Chemistry Letters*, 2019, **10**, 1457-1461.
 39. H.-Y. Xiong, X. Pannecoucke and T. Besset, *Organic Chemistry Frontiers*, 2016, **3**, 620-624.
 40. L. Jiang, J. Qian, W. Yi, G. Lu, C. Cai and W. Zhang, *Angewandte Chemie International Edition*, 2015, **54**, 14965-14969.
 41. Z. Huang, Y.-D. Yang, E. Tokunaga and N. Shibata, *Organic letters*, 2015, **17**, 1094-1097.
 42. H. Chachignon, M. Maeno, H. Kondo, N. Shibata and D. Cahard, *Organic letters*, 2016, **18**, 2467-2470.

Chapter 4

Conclusion and outlook

The computational calculated trifluoromethyl radical donor abilities of sulfonimidamides **6a-c** illustrate the potential to deliver a trifluoromethyl group comparable to known delivering agents (Chapter 2, Figure 1-2). The synthesis and characterisation of compounds **5a-d** were successful and resulted in 6 novel X-ray crystal structures, however, despite all efforts to synthesis of the trifluoromethylated sulfonimidamides (Chapter 2, Scheme 4-6) were unsuccessful. In addition, a simple yet efficient computational method for calculating redox potentials was also developed. A future recommendation is to synthesise the trifluoromethylated sulfonimidamides is the use of trifluoromethylated amines for the amination of the sulfonimidoyl chlorides (Chapter 2, Scheme 1).

The decision was then to synthesise trifluoromethylthiolated sulfonimidamides based on the success of sulfonamides as trifluoromethylthiolating agents. Sulfonimidamides **5c, f** were successfully trifluoromethylthiolated, resulting in *N*-trifluoromethylthio sulfonimidamides **7c, f**. Novel X-ray crystal structures for **5e** and **5f** are currently under analysis. The computationally calculated Tt^+ DAs values of sulfonimidamides **7c, e, f** (Chapter 3, Figure 3) illustrated that sulfonimidamide **7c** possessed the greatest potential for donation ($36.51 \text{ Kcal mol}^{-1}$) and has the potential to be more electrophilic than previously applied delivering agents (Chapter 3, Figure 4). Therefore, sulfonimidamide **7c** was chosen as the donating agent for direction electrophilic trifluoromethylthiolation of ethyl cyanoacetate and 2,4-dimethylpyrrole. The results from the trifluoromethylthiolation model reactions indicated that sulfonimidamide **7c** is a potentially new SCF_3 donating agent. Due to the trifluoromethylthio group leaving from sulfonimidamide **7c** as confirmed by crude ^{19}F NMR and LC-MS analysis. However, further method optimisation is ongoing to determine an ideal substrate scope and reaction conditions.

Various characterisation techniques were used to confirm the chemical synthesis of the compounds which include liquid chromatography-mass spectrometry (LC-MS), nuclear magnetic resonance (NMR), high resolution mass spectrometry (HRMS), X-ray powder diffraction (XRD) and infrared spectrometry (IR).

A future recommendation for the *N*-trifluoromethylthiolation of the sp^2 type nitrogen's is the use of trifluoromethylthiolated amines for the amination of the sulfonimidoyl chlorides

(Chapter 3, Scheme 1). This could lead to the synthesis of sulfonimidamides **7a, b** which possess greater Tt^+DA s values as compared to sulfonimidamide **7c** (Chapter 3, Figure 3).

Additionally, these sulfonimidamide based trifluoromethylthiolating agents have the indicated potential to deliver a trifluoromethylthio radical comparable to known delivering agents as indicated by calculated Tt^+DA values (Appendix 2, Figure S1-2). Further studies can be performed on photochemical and electrochemical reactions to generate a trifluoromethylthio radical from sulfonimidamide based trifluoromethylthiolating agents. *N*-trifluoromethylthio sulfonimidamides have been reported to show high antimycobacterial activity and the saccharin scaffold is commonly utilised in drug discovery. Therefore, sulfonimidamides **7a-c** have the potential to be biological active as well as potential trifluoromethylthio delivering agents. Further studies can be performed on the biological activity of these compounds.

Chapter 5

5. Experimental Details

5.1 Computational details

5.1.1 Calculation of homolytic and heterolytic dissociation enthalpies

All calculations were performed with the Gaussian 16 software package.¹ Geometry optimisations and vibrational frequencies were performed with the M06-2X² functional and 6-31+G(d)^{3, 4} basis set, using the SMD solvation model⁵ to account for solvation in acetonitrile for trifluoromethylating agents and in dichloromethane for trifluoromethylthiolating agents. Thereafter, single point energy was calculated at the M06-2X/6-311++G(2df, 2p) level of theory on the pre-optimised structures.

5.1.2 Calculation of solution phase electrochemical redox potential

All calculations were performed using the Gaussian 09 software package.⁶ Geometry optimisations and vibrational frequencies were performed with the HSEH1PBE⁷⁻¹³ and M06-2X functionals and 6-31+G(d) basis set. The CPCM solvation model^{14, 15} was utilised for HSEH1PBE functional while the SMD solvation model was utilised for the M06-2x functional to account for solvation in acetonitrile.

Redox potentials ($E_{\frac{1}{2}}^{o,calc}$) were calculated according to equation 2.

$$E_{\frac{1}{2}}^{o,calc} = \frac{G_{298}(reduced) + G_{298}(oxidised)}{n_e F} - E_{\frac{1}{2}}^{o,SHE} + E_{\frac{1}{2}}^{o,SCE} \quad (2)$$

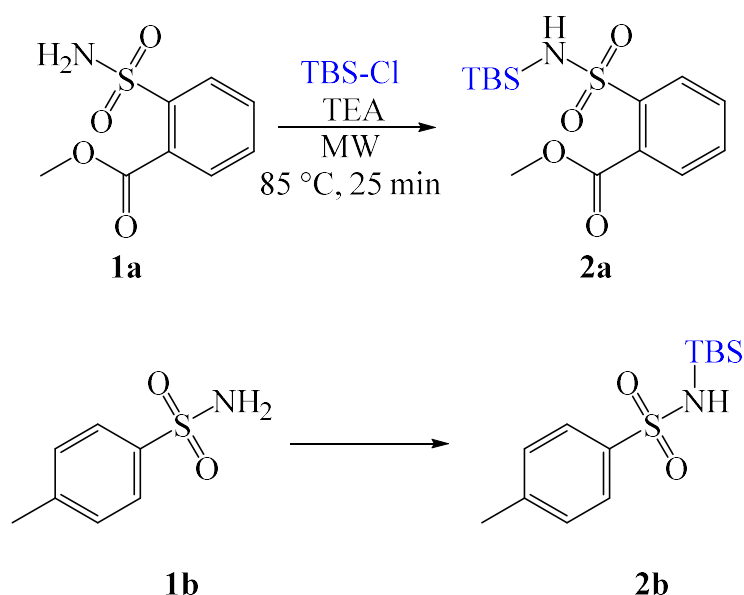
Where n_e is the number of electrons transferred ($n_e = 1$), F is the Faraday constant (value 23.061 kcal mol⁻¹ V⁻¹), $E_{\frac{1}{2}}^{o,SHE}$ is the absolute value for the standard hydrogen electrode (SHE, value = 4.281 V)¹⁶, and $E_{\frac{1}{2}}^{o,SCE}$ is the potential of the saturated calomel electrode (SCE) relative to SHE in acetonitrile (value = -0.141 V)¹⁶, and G_{298} (oxidised) and G_{298} (reduced) are the Gibbs free energies. Method optimisation can be found in Appendix 3 (Table S1-3).

5.2 General experimental methods

Reagents and solvents were purchased from Sigma Aldrich and Merck and unless otherwise noted used without further purification. All solvents were reagent grade or better. Deuterated solvents were used as received. Solvents were dried according to standard procedures.¹⁷ Thin layer chromatography (TLC) was performed using Merck Kieselgel 60 F254 plates. Synthetic steps were characterised using LC-MS (Shimadzu 2020 UFLC-MS, Japan). Purification was

done by gravity column chromatography (mesh particle size, 40-63 μm) and preparatory supercritical fluid chromatography performed on a Sepiatec Prep SFC basic/basic 30 (Germany). High resolution mass spectrometric data were obtained with a Bruker micrOTOF-Q II instrument that operated at ambient temperatures and at a sample concentration of 1 $\mu\text{g/ml}$. Infrared spectrometric data were recorded on a Perkin Elmer spectrum 100 instrument with a universal ATR attachment and optical rotations were measured out on a Bellingham + Stanley Polarimeter (Model 440+). NMR data were recorded using a Bruker AVANCE III 400 MHz at room temperature. Chemical shifts are expressed in ppm. The following abbreviations were used to explain the multiplicities: s = singlet, d = doublet, t = triplet, q = quartet, m = multiplet, br = broad.

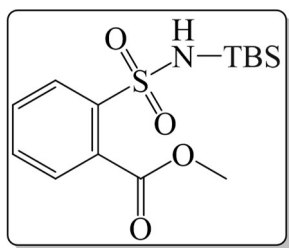
5.2.1 Synthesis of TBS protected sulfonamides (**2a,b**)



Scheme 1: Synthesis of TBS protected sulfonamides (**2a,b**).

A mixture of methyl 2-(aminosulfonyl)benzoate (**1a**, 0.46 mmol), *tert*-Butyldimethylsilyl chloride (TBS-Cl, 1.18 eq.), and triethylamine (TEA, 3 eq.) in dichloromethane (DCM, 2 mL) was subjected to microwave heating (85 °C, 200 watts) for 25 minutes. The reaction progress was monitored with TLC analysis. Upon completion, the mixture was washed with brine (10 mL) and extracted three times with DCM (10 mL). The resultant organic layer was dried over anhydrous MgSO_4 and the solvent was evaporated under reduced pressure. The compound was thereafter dried under vacuum. The same general procedure was applied in the synthesis of sulfonamide **2b**.

Methyl 2-(N-(tert-butyldimethylsilyl)sulfamoyl)benzoate (**2a**)



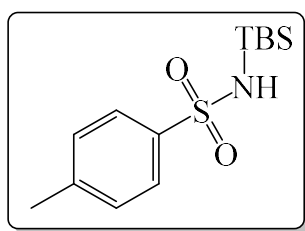
Compound **2a** was prepared according to the preceding general procedure. White solid. Yield: 100%.

R_f = 0.5 (20:80 EtOAc/Hexane)

^1H NMR (400 MHz, CDCl_3): δ = 8.10 (d, 1H), 8.08 (d, 1H), 7.55-7.84 (m, 2H), 6.18 (s, 1H), 3.98 (s, 3H), 0.90 (s, 9H), 0.23 (s, 6H).

^{13}C NMR (100 MHz, CDCl_3): δ = 168.3, 143.4, 132.0, 131.7, 130.8, 129.4, 127.6, 53.4, 25.8, 17.3, -4.3

N-(tert-butyldimethylsilyl)-4-methylbenzenesulfonamide (**2b**)



Compound **2b** was prepared according to the preceding general procedure. White solid. Yield: 100%.

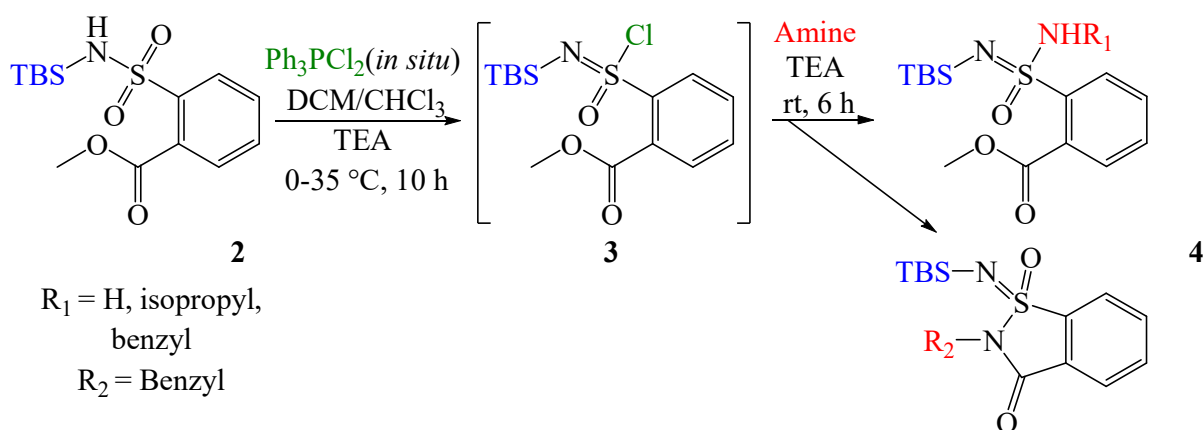
R_f = 0.5 (20:80 EtOAc/Hexane)

^1H NMR (400 MHz, CDCl_3): δ = 7.76-7.74 (m, 2H), 7.28-7.26 (m, 2H), 4.30 (s, 1H), 2.41 (s, 3H), 0.90 (s, 9H), 0.21 (s, 6H).

^{13}C NMR (100 MHz, CDCl_3): δ = 129.6, 128.9, 126.3, 126.1, 25.9, 21.6, 17.4, -4.3

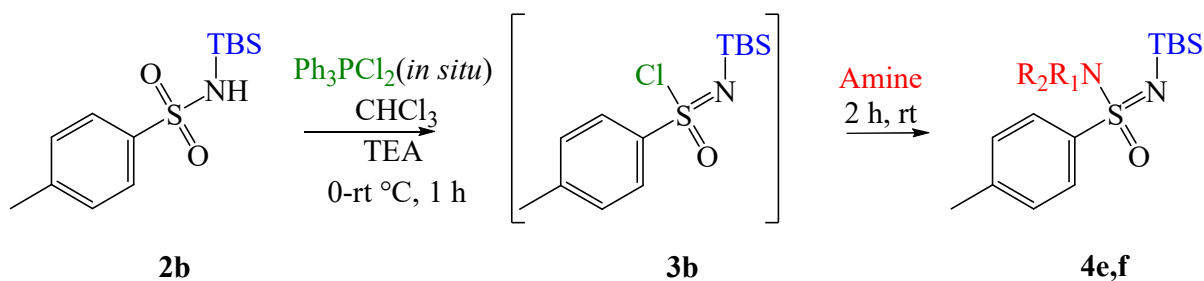
The spectroscopic data are in agreement with those in the literature.¹⁸

5.2.2 Synthesis of TBS protected sulfonimidamides (4)



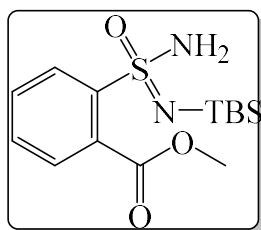
Scheme 2: Synthesis of TBS protected sulfonimidamides **4a-d**.

A mixture of Ph_3P (1.18 eq.), $\text{Cl}_3\text{C}-\text{CCl}_3$ (1.18 eq.) in anhydrous chloroform (CHCl_3) was heated at $85\text{ }^\circ\text{C}$ under N_2 for six hours. A suspension formed immediately upon heating. Thereafter, the suspension was cooled to $0\text{ }^\circ\text{C}$ using an ice bath. A mixture of compound **2** in anhydrous DCM and TEA (3 eq.) was added to the suspension at $0\text{ }^\circ\text{C}$. The reaction mixture was then stirred at $35\text{ }^\circ\text{C}$ overnight. Thereafter, amine (3 eq.) was added to the reaction mixture and the mixture was stirred at room temperature for six hours. The reaction progress was monitored by LC-MS analysis. Upon completion, the reaction mixture was washed with brine (10 mL) and extracted three times with DCM (10 mL). The resultant organic layer was dried over anhydrous MgSO_4 and the solvent was evaporated under reduced pressure. The crude product was purified by gravity chromatography using a gradient of ethyl acetate (EtOAc) in hexane (5 - 25%) as the eluent. The same general procedure was applied in the synthesis of sulfonimidamides **4e, f** with the exception of a shorter reaction times for the deoxychlorination and amination as illustrated in Scheme 3.



Scheme 3: Synthesis of TBS protected sulfonimidamides **4e, f**.

methyl 2-(N'-(tert-butyldimethylsilyl)sulfamidimidoyl)benzoate (4a)



Compound **4a** was prepared according to the preceding general procedure using 32% ammonium hydroxide solution. White solid. Yield: 30%.

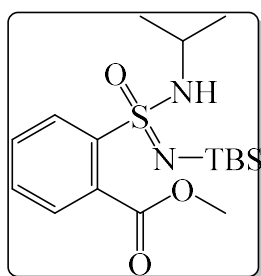
R_f = 0.3 (20:80 EtOAc/Hexane)

¹H NMR (400 MHz, CDCl₃): δ = 8.16-8.14 (m, 1H), 7.67-7.64 (m, 1H), 7.50-7.59 (m, 2H), 5.42 (br, 2H), 4.00 (s, 3H), 0.91 (s, 9H), 0.11-0.14 (d, 6H).

¹³C NMR (100 MHz, CDCl₃): δ = 169.1, 145.6, 131.1, 131.0, 130.3, 129.8, 127.6, 53.2, 25.8, 17.9, -2.8

The spectroscopic data are in agreement with those in the literature.¹⁹

methyl 2-(N'-(tert-butyldimethylsilyl)-N-isopropylsulfamidimidoyl)benzoate (4b)



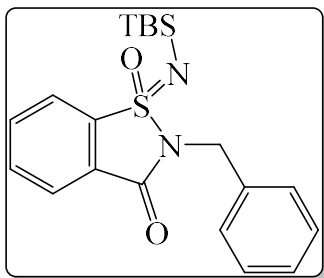
Compound **4b** was prepared according to the general procedure as described above using isopropylamine. Colourless oil. Yield: 70%.

R_f = 0.5 (20:80 EtOAc/Hexane)

¹H NMR (400 MHz, CDCl₃): δ = 8.09-8.07 (m, 1H), 7.62-7.59 (m, 1H), 7.55-7.46 (m, 2H), 5.49-5.47 (d, 1H), 3.93 (s, 3H), 3.45-3.37 (m, 1H), 1.04-1.02 (d, 3H), 0.97-0.95 (d, 3H), 0.90 (s, 9H), 0.11 (s, 3H), 0.09 (s, 3H),

¹³C NMR (100 MHz, CDCl₃): δ = 169.3, 144.2, 130.8, 130.7, 130.3, 129.9, 128.9, 53.1, 46.6, 26.0, 24.0, 23.4, 18.1, -2.56, -2.6

2-benzyl-1-((tert-butyldimethylsilyl)imino)-1,2-dihydro-3H-1 λ ⁴-benzo[d]isothiazol-3-one 1-oxide (4c)



Compound **4c** was prepared according to the general procedure as described above using benzylamine. The crude product was purified by gravity chromatography using neutralised silica *via* a gradient of EtOAc in hexane (5 - 25%) as the eluent. Yellow solid. Yield: 60%.

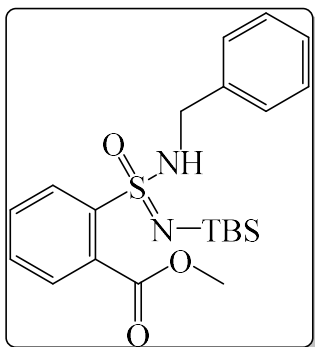
R_f = 0.5 (20:80 EtOAc/Hexane)

¹H NMR (400 MHz, CDCl₃): δ = 7.88-7.86 (m, 1H), 7.65-7.55 (m, 3H), 7.34-7.32 (m, 2H), 7.20-7.12 (m, 3H), 4.70-4.64 (q, 2H), 0.76 (s, 9H), 0.00 (s, 3H), -0.10 (s, 3H),

¹³C NMR (100 MHz, CDCl₃): δ = 159.8, 142.7, 135.6, 134.2, 132.8, 128.5, 128.1, 127.7, 126.7, 124.8, 119.7, 41.6, 25.7, 18.0, -2.8, -2.9

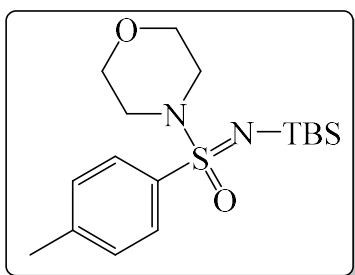
The spectroscopic data are in agreement with those in the literature.¹⁹

Methyl 2-(N-benzyl-N'-((tert-butyldimethylsilyl)sulfamidimidoyl)benzoate (4d)



Compound **4d** was obtained in trace amounts during the synthesis of compound **4c**.

4-(N-(tert-butyldimethylsilyl)-4-methylphenylsulfonimidoyl)morpholine (4e)



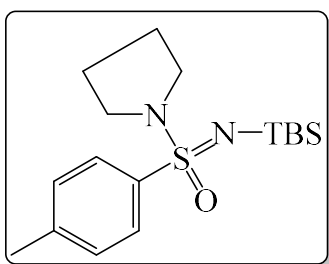
Compound **4e** was prepared according to the general procedure as described above using morpholine. Colourless oil. Yield: 67%. R_f = 0.5 (20:80 EtOAc/Hexane)

^1H NMR (400 MHz, CDCl_3): δ = 7.62 (d, 2H), 7.27 (d, 2H), 3.69-3.67 (m, 4H), 2.86-2.87 (m, 4H), 2.40 (s, 3H), 0.93 (s, 9H), 0.12 (d, 6H).

^{13}C NMR (100 MHz, CDCl_3): δ = 142.3, 135.7, 129.2, 127.9, 66.7, 46.9, 26.1, 21.5, 18.2, -2.5, -2.5.

The spectroscopic data are in agreement with those in the literature.²⁰

1-(N-(tert-butyldimethylsilyl)-4-methylphenylsulfonimidoyl)pyrrolidine (4f)

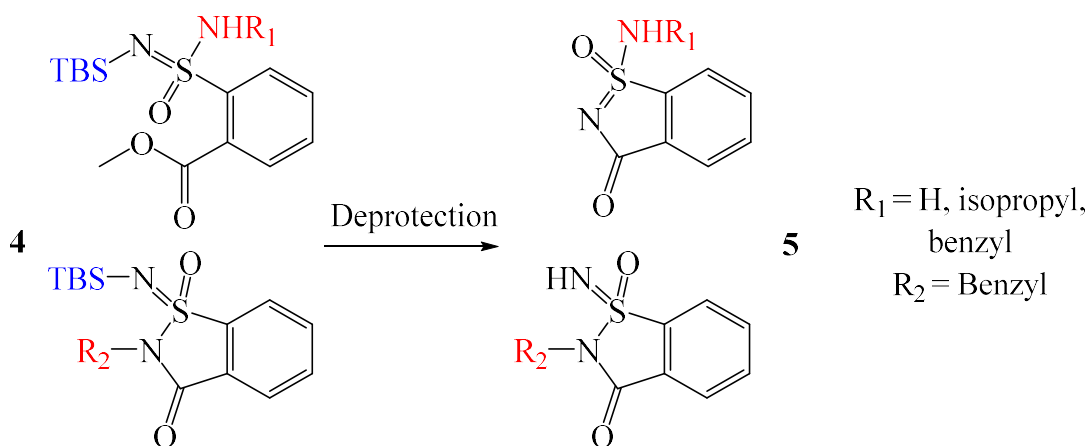


Compound **4f** was prepared according to the general procedure as described above using pyrrolidine. Colourless oil. Yield: 61%. R_f = 0.6 (20:80 EtOAc/Hexane)

^1H NMR (400 MHz, CDCl_3): δ = 7.64 (d, 2H), 7.16 (d, 2H), 3.07-2.97 (m, 4H), 2.32 (s, 3H), 1.59-1.55 (m, 4H), 0.84 (s, 9H), 0.01 (d, 6H).

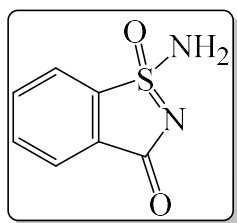
^{13}C NMR (100 MHz, CDCl_3): δ = 141.7, 137.6, 129.1, 127.7, 48.4, 26.1, 25.2, 21.5, 18.2, -2.5.

5.2.3 Deprotection of sulfonimidamides (5)



Scheme 4: Deprotection of sulfonimidamide **4a-d**.

1-amino-3H-1 λ ⁴-benzo[d]isothiazol-3-one 1-oxide (**5a**)



To a round bottom flask containing a solution of **4a** (100 mg, 0.30 mmol) in acetonitrile (1.5 mL), 32% aqueous ammonium hydroxide solution (76.68 μL , 1.3 mmol) was added. Thereafter the reaction mixture was stirred at room temperature for 14 hours. The reaction was monitored by LC-MS analysis. The solvent was then evaporated under reduced pressure and isopropanol (0.5 mL) was added. The mixture was stirred at room temperature for one hour. Subsequently, the product (**5a**) was filtered and dried under vacuum.

White-off solid. Yield: 98%

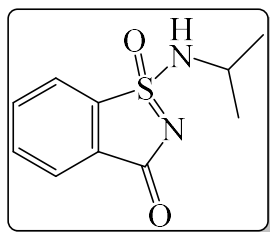
$R_f = 0.04$ (60:40 EtOAc/Hexane)

^1H NMR (400 MHz, DMSO- d_6): $\delta = 8.10$ (br s, 2H), 7.96-7.94 (m, 1H), 7.88-8.82 (m, 3H) NH peaks missing

^{13}C NMR (100 MHz, DMSO- d_6): $\delta = 169.8, 143.7, 134.3, 133.4, 133.4, 123.8, 120.8$.

The spectroscopic data are in agreement with those in the literature.¹⁹

1-(isopropylamino)-3H-1 λ ⁴-benzo[d]isothiazol-3-one 1-oxide (5b)



To a round bottom flask containing a solution of **4b** (100 mg, 0.27 mmol) in methanol (2.0 mL) a stock solution of 0.25 M HCl (1 mL) in MeOH/H₂O (4:1) was added. Thereafter the reaction mixture was stirred at room temperature for one hour. The reaction was monitored by LC-MS analysis. The solvent was then evaporated under reduced pressure to afford the product **5b**.

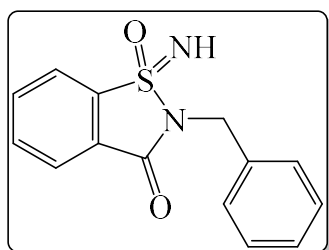
White solid. Yield 99%. *R*_f = 0.2 (60:40 EtOAc/Hexane). mp 80.0 °C.

¹H NMR (400 MHz, DMSO-*d*₆): δ = 8.45 (s, 1H), 8.04-8.01 (m, 1H), 7.88-7.86 (m, 3H), 3.46-3.40 (m, 1H), 1.14 (d, 3H), 0.95 (d, 3H).

¹³C NMR (100 MHz, DMSO-*d*₆): δ = 170.05, 142.4, 134.5, 133.7, 124.1, 121.3, 46.1, 23.2, 23.1.

LC-HRMS: *m/z* calculated for [C₁₀H₁₂N₂O₂S+H]⁺ 225.0653, Found: 225.0563.

2-benzyl-1-imino-1,2-dihydro-3H-1 λ ⁴-benzo[d]isothiazol-3-one 1-oxide (5c)



Compound **4c** was deprotected using the procedure applied for **5b**.

During the synthesis of **4c** trace amounts of **4d** was obtained, after deprotection **5d** was separated from **5c** using prep SFC.

A mixture of **5c**, **d** in acetonitrile was purified utilising prep SFC with the following parameters: Injection volume = 200 μ L, column = silica gel (250x10 mm, 100 Å) at 40 °C, mobile phase = an acetonitrile modifier (10%), with tech grade-wet CO₂ (90%), in 15 minutes, flow rate = 10 mL min⁻¹, stacked injection program with a two minute equilibration time, BPR setting = 150 bar, monitoring and collection at 220 nm.

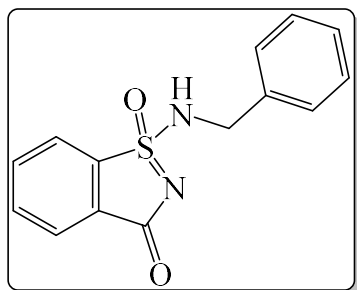
Yellow oil. Yield 99%. *R*_f = 0.6 (60:40 EtOAc/Hexane)

¹H NMR (400 MHz, DMSO-*d*₆): δ = 8.11-7.89 (m, 4H), 7.43-7.26 (m, 5H), 5.92 (s, 1H), 4.76 (q, 2H).

^{13}C NMR (100 MHz, DMSO- d_6): δ = 159.3, 141.1, 136.1, 135.3, 134.2, 128.4, 127.8, 127.4, 126.3, 124.5, 121.4, 40.7.

The spectroscopic data are in agreement with those in the literature.¹⁹

1-(benzylamino)-3H-1 λ^4 -benzo[d]isothiazol-3-one 1-oxide (5d)



During the synthesis of **4c** trace amounts of **4d** was obtained, after deprotection **5d** was separated from **5c** using prep SFC.

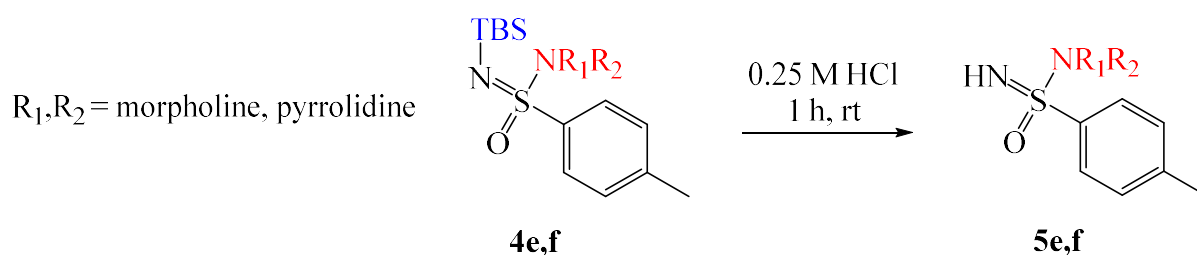
Yellow solid.

R_f = 0.5 (60:40 EtOAc/Hexane)

^1H NMR (400 MHz, CDCl_3): δ = 9.06 (br, 1H), 7.83-7.62 (m, 4H), 7.27-7.21 (m, 5H), 4.20 (m, 4H).

^{13}C NMR (100 MHz, DMSO- d_6): δ = 141.5, 136.5, 134.5, 133.8, 133.4, 128.4, 127.8, 127.6, 124.0, 121.4, 46.0. Carbonyl carbon peak missing.

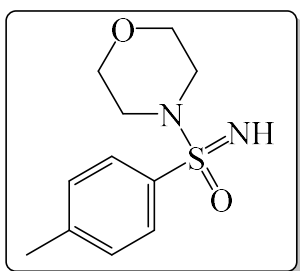
The spectroscopic data are in agreement with those in the literature.¹⁹



Scheme 5: Deprotection of sulfonimidamide **4e,f**.

Sulfonimidamides **4e,f** were deprotected using the procedure applied to sulfonimidamides **4b**, **c**.

4-(4-methylphenylsulfonimidoyl)morpholine (5e)



Compound **4e** was deprotected using the procedure applied for **4b**. White solid. Yield: 99%

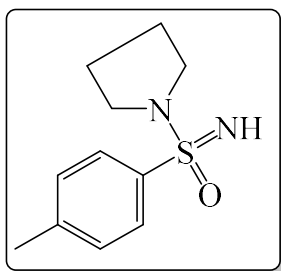
$R_f = 0.4$ (60:40 EtOAc/Hexane)

^1H NMR (400 MHz, DMSO- d_6): $\delta = 7.86\text{--}7.84$ (m, 2H), 7.55-7.53 (m, 3H), 5.56 (br s, NH peak), 3.66-3.62 (m, 4H), 3.06-3.03 (m, 4H), 2.43 (s, 3H).

^{13}C NMR (100 MHz, DMSO- d_6): $\delta = 146.1, 130.7, 130.5, 128.7, 128.1, 65.4, 46.4, 21.3$.

The spectroscopic data are in agreement with those in the literature.¹⁸

1-(4-methylphenylsulfonimidoyl)pyrrolidine (5f)



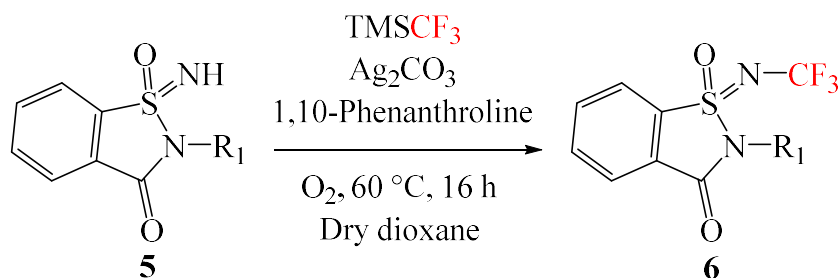
Compound **4f** was deprotected using the procedure applied for **4b**. White solid. Yield: 99%

$R_f = 0.5$ (60:40 EtOAc/Hexane)

^1H NMR (400 MHz, DMSO- d_6): $\delta = 7.89$ (s, 2H), 7.53 (d, 2H), 2.44 (s, 3H), 1.72 (s, 4H). NH peak missing

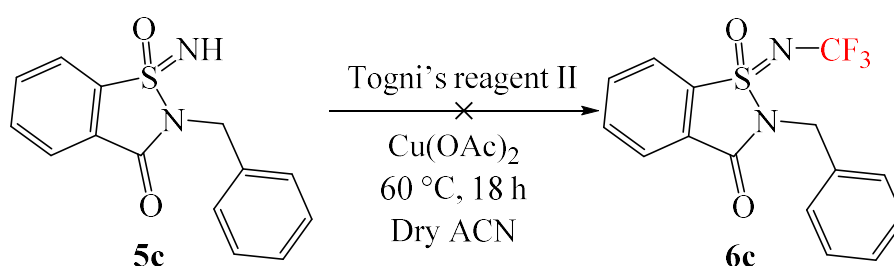
^{13}C NMR (100 MHz, DMSO- d_6): $\delta = 130.2, 128.2, 48.5, 24.9, 21.0$.

5.2.4 *N*-trifluoromethylation of sulfonimidamides (6)



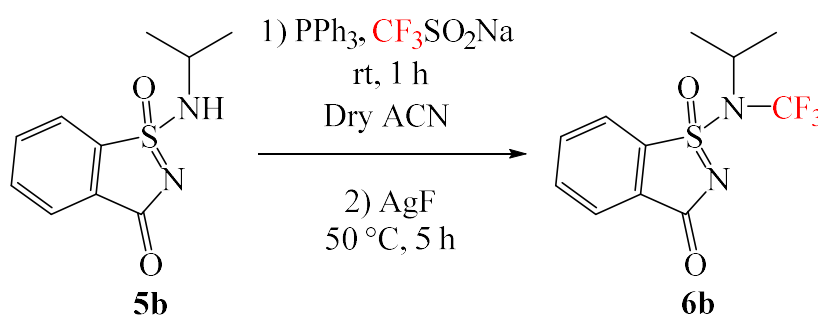
Scheme 6: Attempted *N*-trifluoromethylation of sulfonimidamides.²¹

To a Schlenk tube, sulfonimidamide (**5**, 50 mg), trifluoromethyltrimethylsilane (7 eq.), silver carbonate (0.4 eq.), 1,10- phenanthroline (0.8 eq.), and anhydrous 1,4-dioxane (3 mL) were added. Thereafter, a balloon charged with O₂ was attached. The mixture was then stirred and heated for 16 hours at 60 °C in an oil bath. Thereafter, the reaction mixture was left to cool to room temperature, washed with brine (10 mL) and extracted three times with EtOAc (10 mL). The resultant organic layer was dried over anhydrous MgSO₄ and the solvent was evaporated under reduced pressure. The crude product was purified by gravity chromatography using a gradient of EtOAc in hexane (5 - 25%) as an eluent.



Scheme 7: Attempted *N*-trifluoromethylation of sulfonimidamide **5c**.²²

To a Schlenk tube, sulfonimidamide **5c** (50 mg, 0.18 mmol), anhydrous ACN (2.0 mL), Togni's reagent II (1.51 eq.), and Cu(OAc)₂ (0.05 eq.) were added under argon. Thereafter, the tube was sealed, and the reaction mixture was stirred at 60 °C for 18 hours. The reaction progress was monitored by TLC analysis. To work-up, water was added to the reaction mixture and extracted with DCM (3 × 10 mL). The resultant organic layer was dried over anhydrous MgSO₄ and the solvent was evaporated under reduced pressure. Sulfonimidamide **6c** was not obtained.

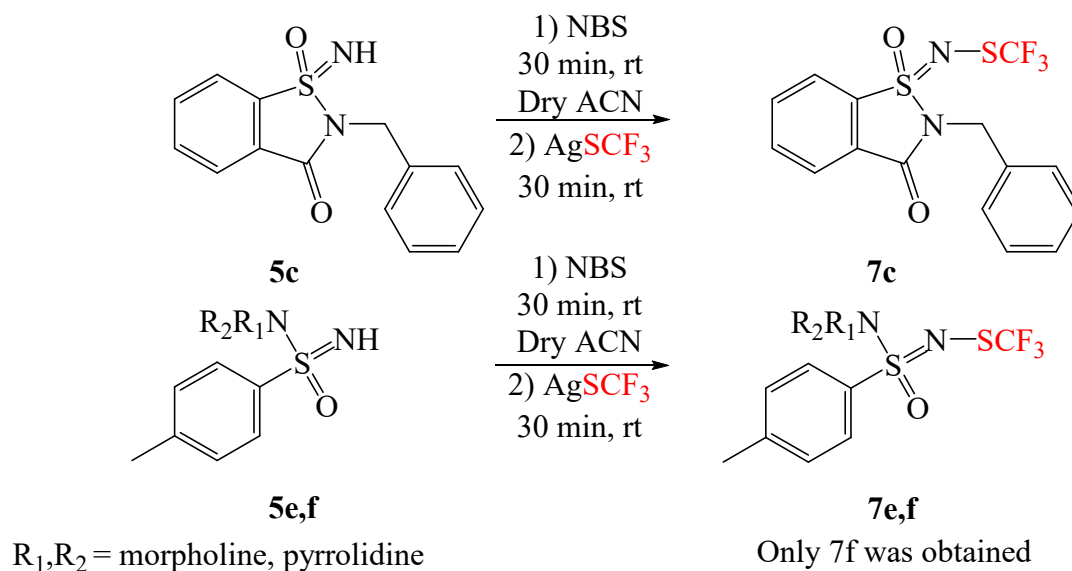


Scheme 8: Attempted *N*-trifluoromethylation of sulfonimidamide **5b**.²³

To a Schlenk tube, sulfonimidamide **5b** (50 mg, 0.22 mmol), CF₃SO₂Na (1.5 eq.), Ph₃P (3 eq.), and anhydrous ACN (2.0 mL) were added under argon. The tube was then sealed, and the reaction mixture was stirred at room temperature for one hour. Thereafter, AgF (4.5 eq.) was added to the tube under positive argon pressure. The reaction mixture was further stirred at 50

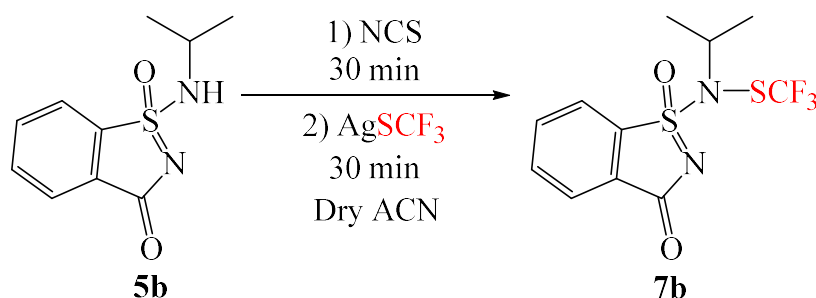
°C for five hours. The reaction progress was monitored by TLC analysis. Sulfonimidamide **6b** was not obtained.

5.2.5 *N*-trifluoromethylthiolation of sulfonimidamides (7)



Scheme 9: *N*-trifluoromethylation of sulfonimidamides.^{24, 25}

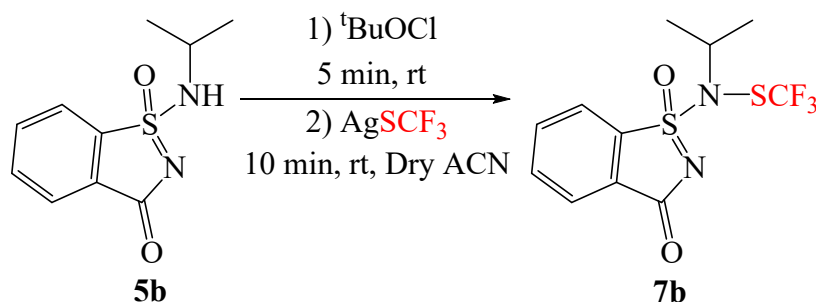
To a round bottom flask containing a solution of the sulfonimidamide (**5c**, 0.37 mmol) in anhydrous ACN (1 mL), *N*-bromosuccinimide (1 eq.) was added. The mixture was stirred at room temperature for 30 minutes. Thereafter, a solution of AgSCF₃ (1.2 eq.) in anhydrous ACN (1 mL) was added dropwise. Subsequently, the reaction mixture was stirred at room temperature for 30 minutes. The crude product was concentrated and purified by gravity chromatography.



Scheme 10: Attempted *N*-trifluoromethylation of sulfonimidamide **5b**.²⁶

To a round bottom flask containing a solution of the sulfonimidamide (**5b**, 0.13 mmol) in anhydrous ACN (1 mL), *N*-chlorosuccinimide (1 eq.) was added. The mixture was stirred at room temperature for 30 minutes. Thereafter, a solution of AgSCF₃ (1.2 eq.) in anhydrous ACN (1 mL) was added dropwise. Subsequently, the reaction mixture was stirred at room

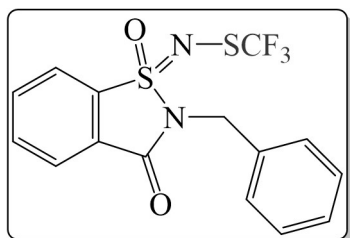
temperature for 30 minutes. The reaction progress was monitored by LC-MS analysis. Sulfonimidamide **7b** was not obtained.



Scheme 11: Attempted *N*-trifluoromethylation of sulfonimidamides **5b**.^{27, 28}

To a round bottom flask containing a stirred suspension of sulfonimidamide (**5b**, 0.13 mmol) in anhydrous ACN (1 mL), *tert*-butyl hypochlorite ($t\text{BuOCl}$, 20.65 μL) was added. Upon addition, a white precipitate formed. Thereafter, the reaction mixture was stirred for five minutes and was left to stand for five minutes. Subsequently, AgSCF_3 (33.58 mg) was added and the reaction mixture was stirred at room temperature for ten minutes. The reaction progress was monitored by TLC analysis. Sulfonimidamide **7b** was not obtained.

2-benzyl-1-(((trifluoromethyl)thio)imino)-1,2-dihydro-3H-114-benzo[d]isothiazol-3-one 1-oxide (**7c**)



Compound **7c** was purified by gravity chromatography using a 5% EtOAc in hexane as the eluent. White solid. Yield: 76%. R_f = 0.4 (20:80 EtOAc/Hexane). mp 160.0 $^{\circ}\text{C}$.

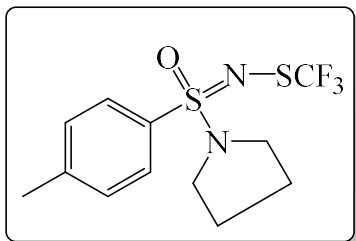
^1H NMR (400 MHz, CDCl_3): δ = 8.08 (d, 2H), 7.90-7.84 (m, 3H), 7.51 (d, 2H), 7.39-7.32 (m, 3H), 4.84 (q, 2H).

^{13}C NMR (100 MHz, CDCl_3): δ = 159.6, 136.3, 135.1, 135.1, 134.0, 131.6, 129.2, 128.8, 128.6, 128.3, 125.3, 122.6, 42.6.

^{19}F NMR (100 MHz, CDCl_3): δ = -50.20

LC-HRMS: m/z calculated for $[\text{C}_{15}\text{H}_{11}\text{F}_3\text{N}_2\text{O}_2\text{S}_2+\text{H}]^+$ 373.0248, Found: 373.0210.

N-(oxo(pyrrolidin-1-yl)(p-tolyl)-l6-sulfaneylidene)-S-(trifluoromethyl)thiohydroxylamine (7f)

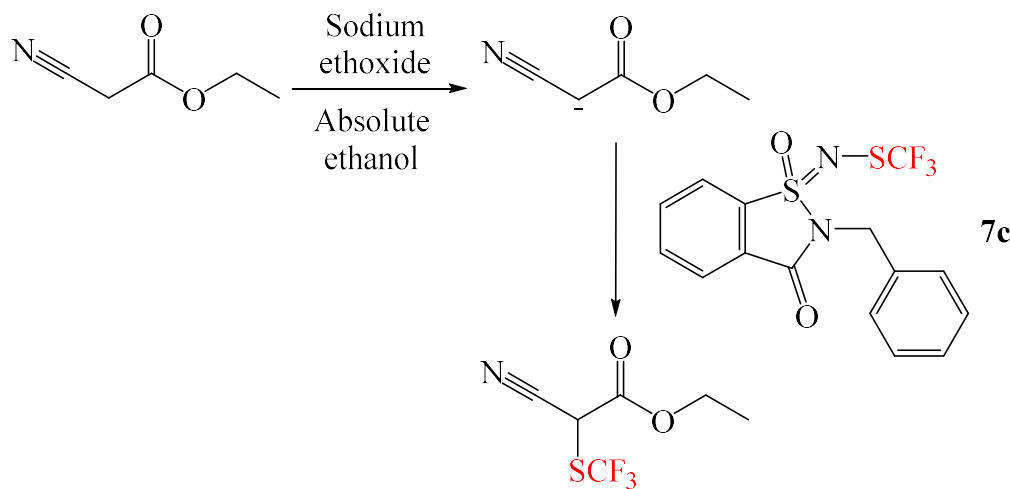


Compound **7f** was purified by gravity chromatography using a 10% EtOAc in hexane as the eluent. White solid. Yield: 80%. $R_f = 0.6$ (20:80 EtOAc/Hexane)

^1H NMR (400 MHz, CDCl_3): $\delta = 7.79$ (d, 2H), 7.33 (d, 2H), 3.28-3.19 (m, 4H), 2.44 (s, 3H), 1.80 (m, 4H).

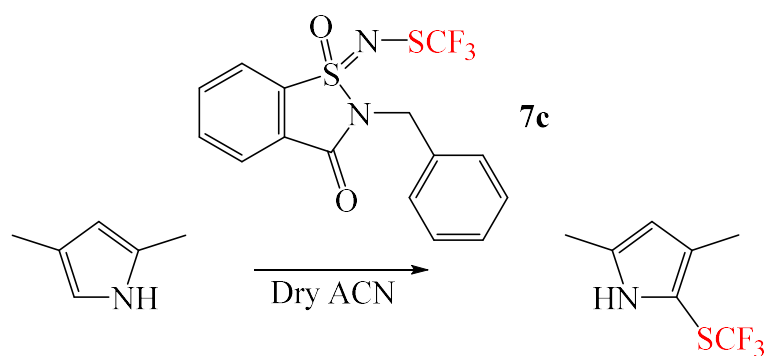
^{19}F NMR (100 MHz, CDCl_3): $\delta = -50.65$

The spectroscopic data are in agreement with those in the literature.²⁴



Scheme 12: The trifluoromethylthiolation of ethyl cyanoacetate.

To a Schlenk tube, ethyl cyanoacetate (4.70 μL , 0.044 mmol), and absolute ethanol (1.0 mL) were added under argon. The tube was then sealed, and the reaction mixture was stirred at room temperature for two hours. Thereafter, sulfonimidamide **7c** (1.2 eq.) in absolute ethanol (1.0 mL) was injected into the tube. The reaction mixture was further stirred at room temperature for 12 hours under argon. The reaction progress was monitored by LC-MS analysis.



Scheme 13: the trifluoromethylthiolation of 2,4-dimethylpyrrole.

To a round bottom flask, 2,4-dimethylpyrrole (4.80 μ L, 0.047 mmol), sulfonimidamide **7c** (1.2 eq.) and anhydrous ACN (1.0 mL) were added. The flask was then sealed, and the reaction mixture was stirred at room temperature for 12 hours. The reaction progress was monitored by LC-MS analysis.

References

1. M. J. Frisch, G. W. Trucks, H. B. Schlegel, G. E. Scuseria, M. A. Robb, J. R. Cheeseman, G. Scalmani, V. Barone, G. A. Petersson, H. Nakatsuji, X. Li, M. Caricato, A. V. Marenich, J. Bloino, B. G. Janesko, R. Gomperts, B. Mennucci, H. P. Hratchian, J. V. Ortiz, A. F. Izmaylov, J. L. Sonnenberg, Williams, F. Ding, F. Lipparini, F. Egidi, J. Goings, B. Peng, A. Petrone, T. Henderson, D. Ranasinghe, V. G. Zakrzewski, J. Gao, N. Rega, G. Zheng, W. Liang, M. Hada, M. Ehara, K. Toyota, R. Fukuda, J. Hasegawa, M. Ishida, T. Nakajima, Y. Honda, O. Kitao, H. Nakai, T. Vreven, K. Throssell, J. A. Montgomery Jr., J. E. Peralta, F. Ogliaro, M. J. Bearpark, J. J. Heyd, E. N. Brothers, K. N. Kudin, V. N. Staroverov, T. A. Keith, R. Kobayashi, J. Normand, K. Raghavachari, A. P. Rendell, J. C. Burant, S. S. Iyengar, J. Tomasi, M. Cossi, J. M. Millam, M. Klene, C. Adamo, R. Cammi, J. W. Ochterski, R. L. Martin, K. Morokuma, O. Farkas, J. B. Foresman and D. J. Fox, *Journal*, 2016.
2. Y. Zhao and D. G. Truhlar, *Theoretical Chemistry Accounts*, 2008, **120**, 215-241.
3. R. Krishnan, J. S. Binkley, R. Seeger and J. A. Pople, *J. Chem. Phys.*, 1980, **72**, 650.
4. A. D. McLean and G. S. Chandler, *J. Chem. Phys.*, 1980, **72**, 5639.
5. A. V. Marenich, C. J. Cramer and D. G. Truhlar, *The Journal of Physical Chemistry B*, 2009, **113**, 6378-6396.
6. M. J. Frisch, G. W. Trucks, H. B. Schlegel, G. E. Scuseria, M. A. Robb, J. R. Cheeseman, G. Scalmani, V. Barone, B. Mennucci, G. A. Petersson, H. Nakatsuji, M. Caricato, X. Li, H. P. Hratchian, A. F. Izmaylov, J. Bloino, G. Zheng, J. L. Sonnenberg, M. Hada, M. Ehara, K. Toyota, R. Fukuda, J. Hasegawa, M. Ishida, T. Nakajima, Y. Honda, O. Kitao, H. Nakai, T. Vreven, J. A. Montgomery, Jr., J. E. Peralta, F. Ogliaro, M. Bearpark, J. J. Heyd, E. Brothers, K. N. Kudin, V. N. Staroverov, R. Kobayashi, J. Normand, K. Raghavachari, A. Rendell, J. C. Burant, S. S. Iyengar, J. Tomasi, M. Cossi, N. Rega, J. M. Millam, M. Klene, J. E. Knox, J. B. Cross, V. Bakken, C. Adamo, J. Jaramillo, R. Gomperts, R. E. Stratmann, O. Yazyev, A. J. Austin, R. Cammi, C. Pomelli, J. W. Ochterski, R. L. Martin, K. Morokuma, V. G. Zakrzewski, G. A. Voth, P. Salvador, J. J. Dannenberg, S. Dapprich, A. D. Daniels, Ö. Farkas, J. B. Foresman, J. V. Ortiz, J. Cioslowski and D. J. Fox, *Gaussian 09, Revision E.01*, Gaussian Inc, Wallingford, 2009.
7. A. V. Krukau, O. A. Vydrov, A. F. Izmaylov and G. E. Scuseria, *The Journal of Chemical Physics*, 2006, **125**, 224106.
8. J. Heyd, G. E. Scuseria and M. Ernzerhof, *The Journal of Chemical Physics*, 2006, **124**, 219906.
9. J. Heyd and G. E. Scuseria, *The Journal of Chemical Physics*, 2004, **120**, 7274-7280.
10. J. Heyd and G. E. Scuseria, *The Journal of Chemical Physics*, 2004, **121**, 1187-1192.
11. J. Heyd, J. E. Peralta, G. E. Scuseria and R. L. Martin, *The Journal of Chemical Physics*, 2005, **123**, 174101.
12. A. F. Izmaylov, G. E. Scuseria and M. J. Frisch, *The Journal of Chemical Physics*, 2006, **125**, 104103.
13. T. M. Henderson, A. F. Izmaylov, G. Scalmani and G. E. Scuseria, *The Journal of Chemical Physics*, 2009, **131**, 044108.
14. V. Barone and M. Cossi, *J. Phys. Chem. A*, 1998, **102**, 1995.
15. M. Cossi, N. Rega, G. Scalmani and V. Barone, *J. Comput. Chem.*, 2003, **24**, 669.
16. A. A. Isse and A. Gennaro, *J. Phys. Chem. B*, 2010, **114**, 7894.
17. W. L. F. Armarego and C. Chai, *Purification of Laboratory Chemicals*, Elsevier Science, 2009.
18. Y. Chen and J. Gibson, *RSC Advances*, 2015, **5**, 4171-4174.

19. Y. Chen, C.-J. Aurell, A. Pettersen, R. J. Lewis, M. A. Hayes, M. Lepistö, A. C. Jonson, H. Leek and L. Thunberg, *ACS medicinal chemistry letters*, 2017, **8**, 672-677.
20. P. K. Chinthakindi, A. Benediktsdottir, A. Ibrahim, A. Wared, C. J. Aurell, A. Pettersen, E. Zamaratski, P. I. Arvidsson, Y. Chen and A. Sandström, *European Journal of Organic Chemistry*, 2019, **2019**, 1045-1057.
21. F. Izzo, M. Schäfer, P. Lienau, U. Ganzer, R. Stockman and U. Lücking, *Chemistry – A European Journal*, 2018, **24**, 9295-9304.
22. G. Zheng, X. Ma, J. Li, D. Zhu and M. Wang, *The Journal of Organic Chemistry*, 2015, **80**, 8910-8915.
23. S. Liang, J. Wei, L. Jiang, J. Liu, Y. Mumtaz and W.-b. Yi, *Chemical Communications*, 2019.
24. N. Thota, P. Makam, K. K. Rajbongshi, S. Nagiah, N. S. Abdul, A. A. Chuturgoon, A. Kaushik, G. Lamichhane, A. M. Somboro and H. G. Kruger, *ACS Medicinal Chemistry Letters*, 2019, **10**, 1457-1461.
25. C. Bohnen and C. Bolm, *Organic letters*, 2015, **17**, 3011-3013.
26. H.-Y. Xiong, X. Pannecoucke and T. Besset, *Organic Chemistry Frontiers*, 2016, **3**, 620-624.
27. P. Zhang, M. Li, X.-S. Xue, C. Xu, Q. Zhao, Y. Liu, H. Wang, Y. Guo, L. Lu and Q. Shen, *The Journal of organic chemistry*, 2016, **81**, 7486-7509.
28. C. Xu, B. Ma and Q. Shen, *Angewandte Chemie International Edition*, 2014, **53**, 9316-9320.

Appendix 1. Supplementary material for Chapter 2

The trifluoromethyl cation donating abilities (TC^+DA) of the proposed sulfonimidamides are shown in Figure S1. The TC^+DA values indicate a poor donation potential as compared to known electrophilic trifluoromethylating reagents (Figure S2).

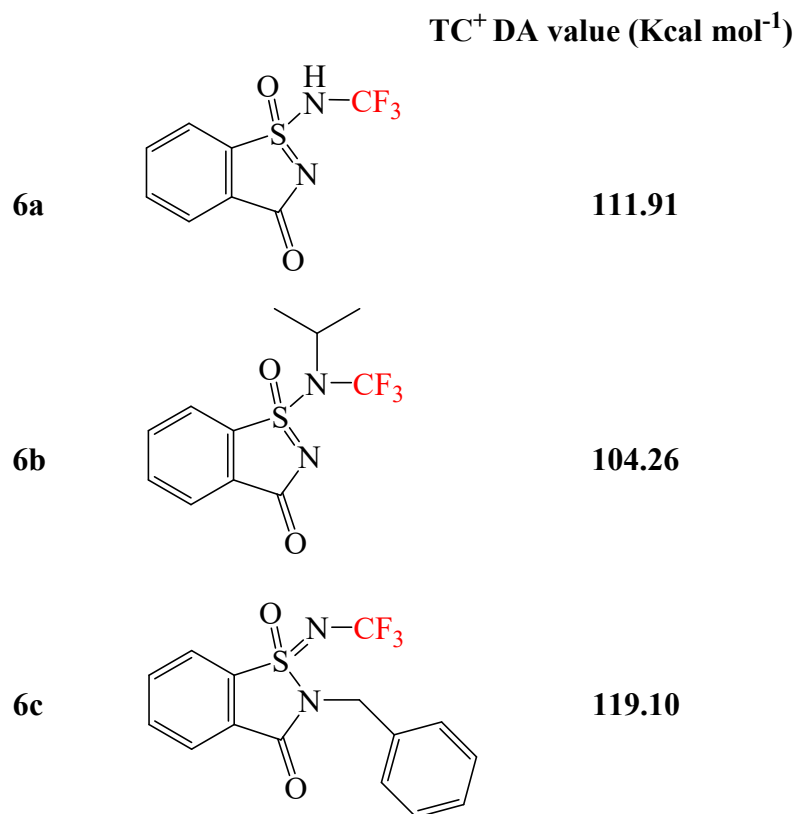


Figure S1: Calculated* TC^+DA s values of the proposed sulfonimidamides in acetonitrile.

*(SMD-M06-2X/6-31+G(d)// SMD-M06-2X/6-311++G(2df,2p))

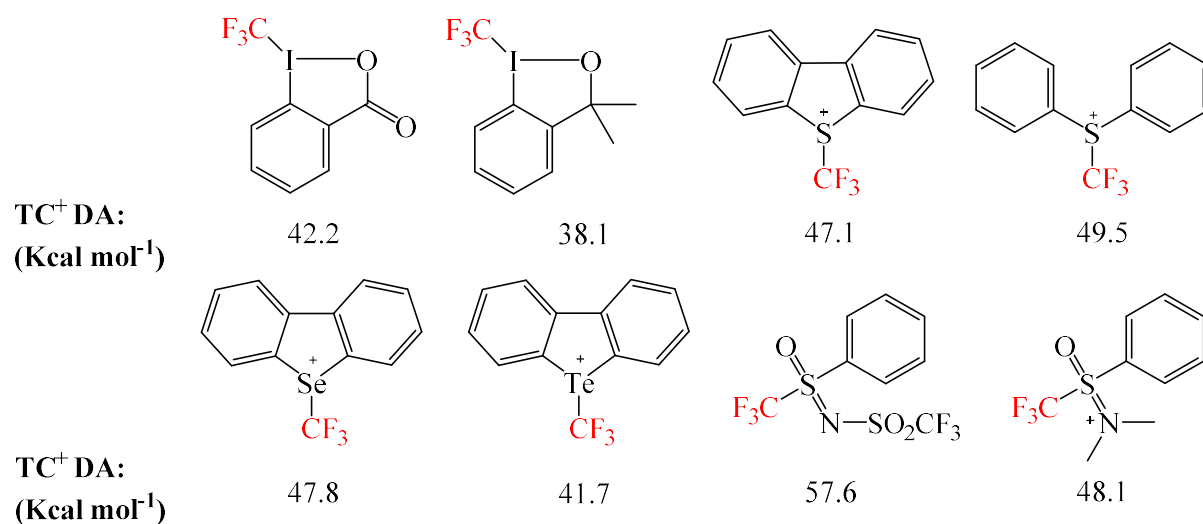


Figure S2: The reported calculated* TC⁺DAs values of common electrophilic trifluoromethylating reagents in acetonitrile.^{1*}(SMD-M06-2X/6-31+G(d)// SMD-M06-2X/6-311++G(2df,2p))

References

1. M. Li, Y. Wang, X.-S. Xue and J.-P. Cheng, *Asian Journal of Organic Chemistry*, 2017, **6**, 235-240.

Appendix 2. Supplementary material for Chapter 3

The trifluoromethylthio radical donating abilities (Tt[•]DA) of the proposed sulfonimidamides are shown in Figure S1. The Tt[•]DA values indicate an excellent donation potential as compared to known electrophilic trifluoromethylating reagents (Figure S2).

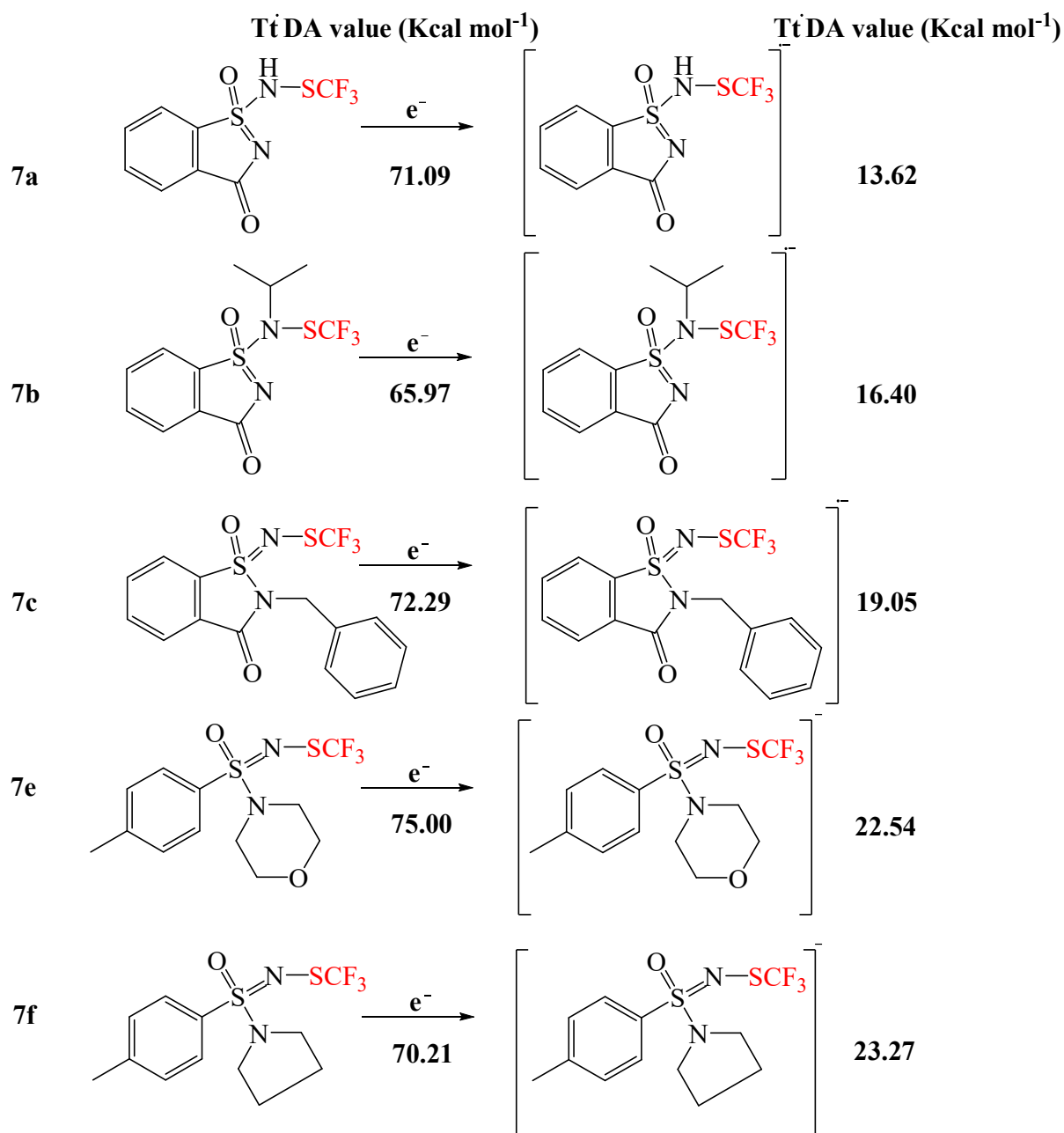


Figure S1: Calculated* Tt[•]DA values of the proposed sulfonimidamides in dichloromethane.

*(SMD-M06-2X/6-31+G(d)// SMD-M06-2X/6-311++G(2df,2p))

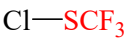

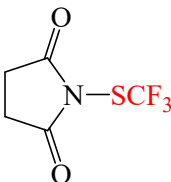
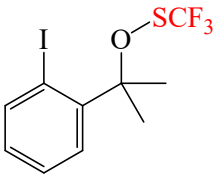
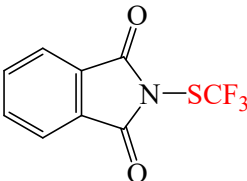
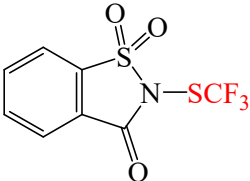
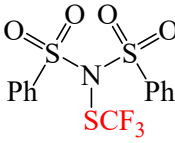
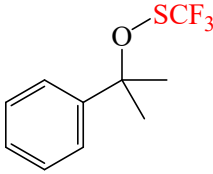
	Tt*DA: (Kcal mol ⁻¹)			
				
Before reduction	65.2	66.1	88.1	61.3
After reduction	15.4	20.9	14.2	32.2
				
Before reduction	84.8	76.0	72.3	64.5
After reduction	15.8	9.4	8.4	31.6

Figure S2: The reported calculated* Tt*DA values of common electrophilic trifluoromethylating reagents in dichloromethane.¹ *(SMD-M06-2X/6-31+G(d)// SMD-M06-2X/6-311++G(2df,2p))

References

1. M. Li, B. Zhou, X.-S. Xue and J.-P. Cheng, *The Journal of organic chemistry*, 2017, **82**, 8697-8702.

Appendix 3. Supplementary material for Chapter 5

Method optimisation for theoretical redox potentials

To develop a suitable method for the computational calculation of redox potentials, the oxidation potential of phenol was chosen as a model. Firstly, different density functional theory (DFT) functionals and *ab initio* methods using the SMD solvation model¹ were compared using a 6-31+G(d)^{2,3} basis set. The results were compared against calculations by Nicewicz and co-workers.⁴ The SMD solvation model was found to decrease the oxidation potential. Thereafter, the CPCM solvation model^{5,6} was used with the HSEH1PBE⁷⁻¹³ DFT functional, as expected this led to an increase in the oxidation potential. An increase in the size of the basis set resulted in an oxidation potential further from the experimental value. Single point energy calculations on a pre-optimised structure resulted in an oxidation potential further from the experimental value. Therefore, SMD-M062X¹⁴/6-31+G(d) and CPCM-HSEH1PBE/6-31+G(d) were chosen as the optimal methods and solvation model for further calculations (Table S1).

Table S1: Method optimisation for the theoretical oxidation potential of phenol

Method	E _{1/2} ^{ox}	Experimental ⁴
CPCM-M062X/6-31+G(d)	1.99 ⁴	1.63
CPCM-B3LYP ¹⁵ /6-31+G(d)	1.79 ⁴	
SMD-M062X/6-31+G(d)	1.73	
SMD-B3LYP/6-31+G(d)	1.52	
SMD-PBEPBE ¹⁶ /6-31+G(d)	1.24	
SMD-CAM-B3LYP ¹⁷ /6-31+G(d)	1.57	
SMD-HSEH1PBE/6-31+G(d)	1.53	
SMD-MP2 ¹⁸⁻²¹ /6-31+G(d)	2.06	
SMD-G3 ²² /6-31+G(d)	1.84	
CPCM-HSEH1PBE/6-31+G(d)	1.79	
SMD- M062X /6-311++G(2d,2p) ^{23, 24}	1.75	
SMD- M062X /6-311++G(2d,2pf)	1.77	
SMD- HSEH1PBE /6-311++G(2d,2p)	1.55	
SMD-CCSD(T) ²⁵⁻²⁸ /6-31+g(d,p)//SMD- M062X /6-311++G(2d,2p)	1.45	

The M06-2X functional tends to overestimate the redox potentials, while the B3LYP and HSEH1PBE functionals underestimates the potentials. Therefore, the average potentials of both functional provides a potential close to the experimental value. To compare the newly developed method to Nicewicz and co-workers⁴ method, the average oxidation potential of the SMD-M062X/6-31+G(d) and CPCM-HSEH1PBE/6-31+G(d) calculations were compared against the CPCM-M062X/6-31+G(d) and CPCM-B3LYP/6-31+G(d) calculations by Nicewicz and associates (Table S2). Bolded values indicate oxidation potentials closer to the experimental value. Percent error was calculated according to equation 3.

$$\text{Percent error} = \left| \frac{\text{computational average value} - \text{experimental value}}{\text{experimental value}} \right| \times 100 \quad (3)$$

The Percent error was calculated for each compound and then averaged. The average percent error of the oxidation potentials for the new method was 5.31% as compared to the percent error for Nicewicz's method was 7.74%.

Table S2: Comparison between the optimised method and the literature method for the calculations of oxidation potentials

Compound	Average $E_{1/2}^{\text{ox}}$	Average from literature ⁴ $E_{1/2}^{\text{ox}}$	Experimental ⁴
1,4-Dioxane	2.40	2.31	2.50
Diphenyl ether	1.74	1.86	1.88
3,4-Dihydro-2H-pyran	1.36	1.54	1.51
m-Dimethoxybenzene	1.54	1.58	1.50
1,3-Di(iso-propoxy)benzene	1.48	1.49	1.47
o-Dimethoxybenzene	1.31	1.34	1.43
2-Methoxynaphthalene	1.30	1.37	1.32
p-Dimethoxybenzene	1.10	1.22	1.30
4-Cyanophenol	2.19	2.33	2.08
4-Bromophenol	1.79	1.88	1.69
Phenol	1.76	1.89	1.63
3,4-Dimethylphenol	1.42	1.54	1.43
Guaiacol	1.32	1.49	1.41
2-Naphthol	1.37	1.47	1.40
2,4,6-Trimethylphenol	1.28	1.44	1.35
4-Methoxyphenol	1.17	1.30	1.17

Hydroquinone	1.25	1.40	1.14
p-Anisaldehyde	1.96	2.09	2.06
p-Hydroxybenzaldehyde	2.01	2.25	1.95

Reduction potentials were also compared between the newly developed method and Nicewicz's method (Table S3). Bolded values indicate reduction potentials closer to the experimental value. The average percent error of the reduction potentials for the new method was 5.66% as compared to the percent error for Nicewicz's method was 11.68%.

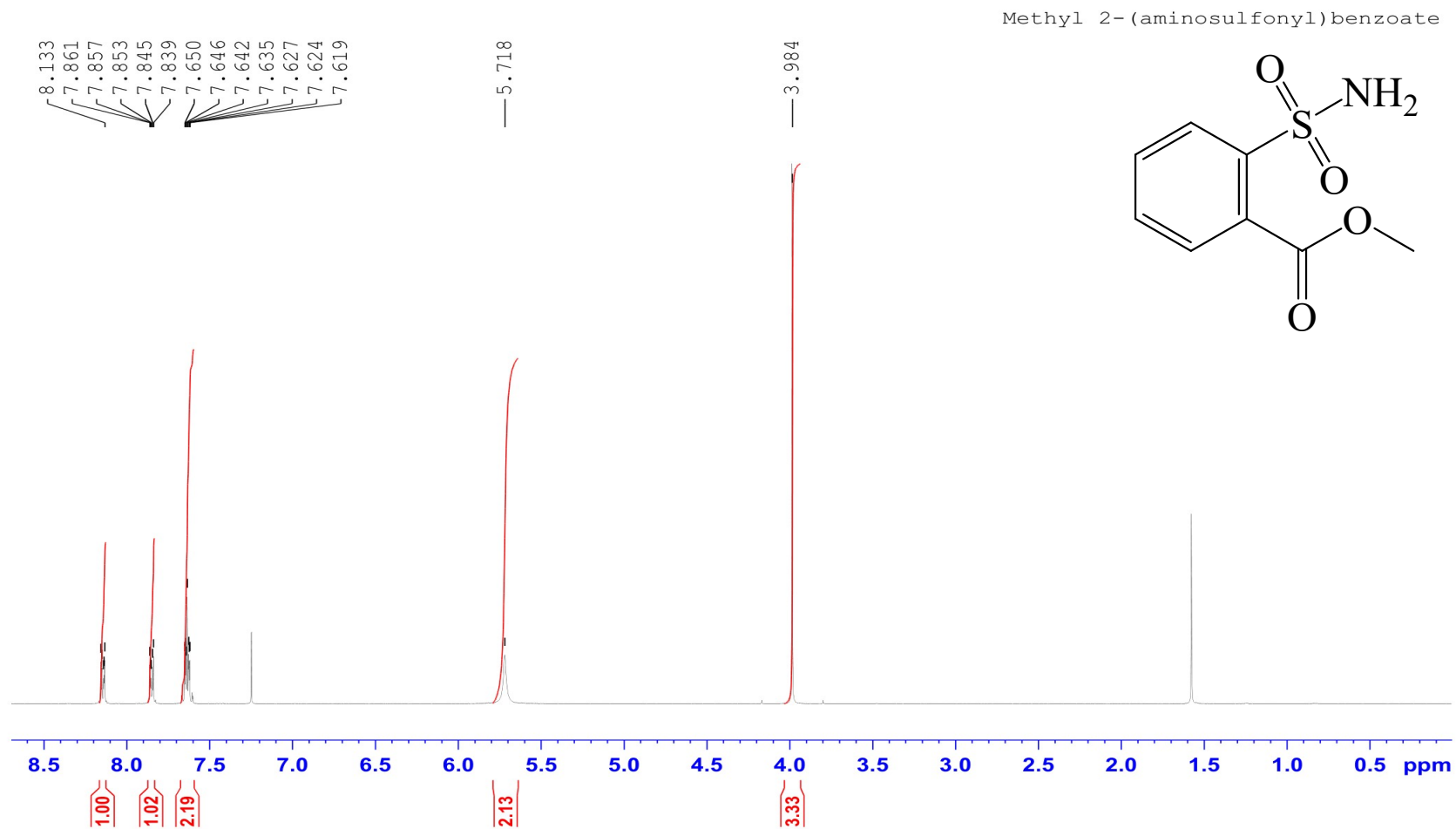
Table S3: Comparison between the optimised method and the literature method for the calculations of reduction potentials

Compound	Average $E_{1/2}^{\text{red}}$	Average from literature ⁴ $E_{1/2}^{\text{red}}$	Experimental ⁴
p-Nitrobenzaldehyde	-0.72	-0.58	-0.86
p-Cyanobenzaldehyde	-1.33	-1.26	-1.42
p-Trifluoromethylbenzaldehyde	-1.56	-1.45	-1.66
Biphenyl-4-carboxaldehyde	-1.76	-1.70	-1.72
2-Naphthaldehyde	-1.79	-1.63	-1.73
p-Chlorobenzaldehyde	-1.79	-1.71	-1.85
Benzaldehyde	-1.91	-1.84	-1.93
o-Tolualdehyde	-1.82	-1.82	-1.94
3-Methylbutyraldehyde	-2.28	-2.70	-2.24
Cyclohexanecarboxaldehyde	-2.71	-2.73	-2.28

References

1. A. V. Marenich, C. J. Cramer and D. G. Truhlar, *The Journal of Physical Chemistry B*, 2009, **113**, 6378-6396.
2. R. Krishnan, J. S. Binkley, R. Seeger and J. A. Pople, *J. Chem. Phys.*, 1980, **72**, 650.
3. A. D. McLean and G. S. Chandler, *J. Chem. Phys.*, 1980, **72**, 5639.
4. H. G. Roth, N. A. Romero and D. A. Nicewicz, *Synlett*, 2016, **27**, 714-723.
5. V. Barone and M. Cossi, *J. Phys. Chem. A*, 1998, **102**, 1995.
6. M. Cossi, N. Rega, G. Scalmani and V. Barone, *J. Comput. Chem.*, 2003, **24**, 669.
7. A. V. Krukau, O. A. Vydrov, A. F. Izmaylov and G. E. Scuseria, *The Journal of Chemical Physics*, 2006, **125**, 224106.
8. J. Heyd, J. E. Peralta, G. E. Scuseria and R. L. Martin, *The Journal of Chemical Physics*, 2005, **123**, 174101.
9. J. Heyd and G. E. Scuseria, *The Journal of Chemical Physics*, 2004, **121**, 1187-1192.
10. J. Heyd and G. E. Scuseria, *The Journal of Chemical Physics*, 2004, **120**, 7274-7280.
11. J. Heyd, G. E. Scuseria and M. Ernzerhof, *The Journal of Chemical Physics*, 2006, **124**, 219906.
12. A. F. Izmaylov, G. E. Scuseria and M. J. Frisch, *The Journal of Chemical Physics*, 2006, **125**, 104103.
13. T. M. Henderson, A. F. Izmaylov, G. Scalmani and G. E. Scuseria, *The Journal of Chemical Physics*, 2009, **131**, 044108.
14. Y. Zhao and D. G. Truhlar, *Accounts of Chemical Research*, 2008, **41**, 157-167.
15. P. J. Stephens, F. Devlin, C. Chabalowski and M. J. Frisch, *The Journal of physical chemistry*, 1994, **98**, 11623-11627.
16. C. Adamo and V. Barone, *The Journal of chemical physics*, 1999, **110**, 6158-6170.
17. T. Yanai, D. P. Tew and N. C. Handy, *Chemical Physics Letters*, 2004, **393**, 51-57.
18. M. Head-Gordon, J. A. Pople and M. J. Frisch, *Chemical Physics Letters*, 1988, **153**, 503-506.
19. S. Sæbø and J. Almlöf, *Chemical Physics Letters*, 1989, **154**, 83-89.
20. M. J. Frisch, M. Head-Gordon and J. A. Pople, *Chemical physics letters*, 1990, **166**, 281-289.
21. M. J. Frisch, M. Head-Gordon and J. A. Pople, *Chemical Physics Letters*, 1990, **166**, 275-280.
22. L. A. Curtiss, K. Raghavachari, P. C. Redfern, V. Rassolov and J. A. Pople, *The Journal of chemical physics*, 1998, **109**, 7764-7776.
23. R. Krishnan, J. S. Binkley, R. Seeger and J. A. Pople, *The Journal of Chemical Physics*, 1980, **72**, 650-654.
24. A. McLean and G. Chandler, *The Journal of Chemical Physics*, 1980, **72**, 5639-5648.
25. P. Sandars, *Advances in chemical physics*, 1969, 365-419.
26. G. D. Purvis III and R. J. Bartlett, *The Journal of Chemical Physics*, 1982, **76**, 1910-1918.
27. G. E. Scuseria, C. L. Janssen and H. F. Schaefer Iii, *The Journal of Chemical Physics*, 1988, **89**, 7382-7387.
28. G. E. Scuseria and H. F. Schaefer III, *The Journal of Chemical Physics*, 1989, **90**, 3700-3703.

¹H and ¹³C NMR spectra, HRMS spectra, IR spectra, and XRD data



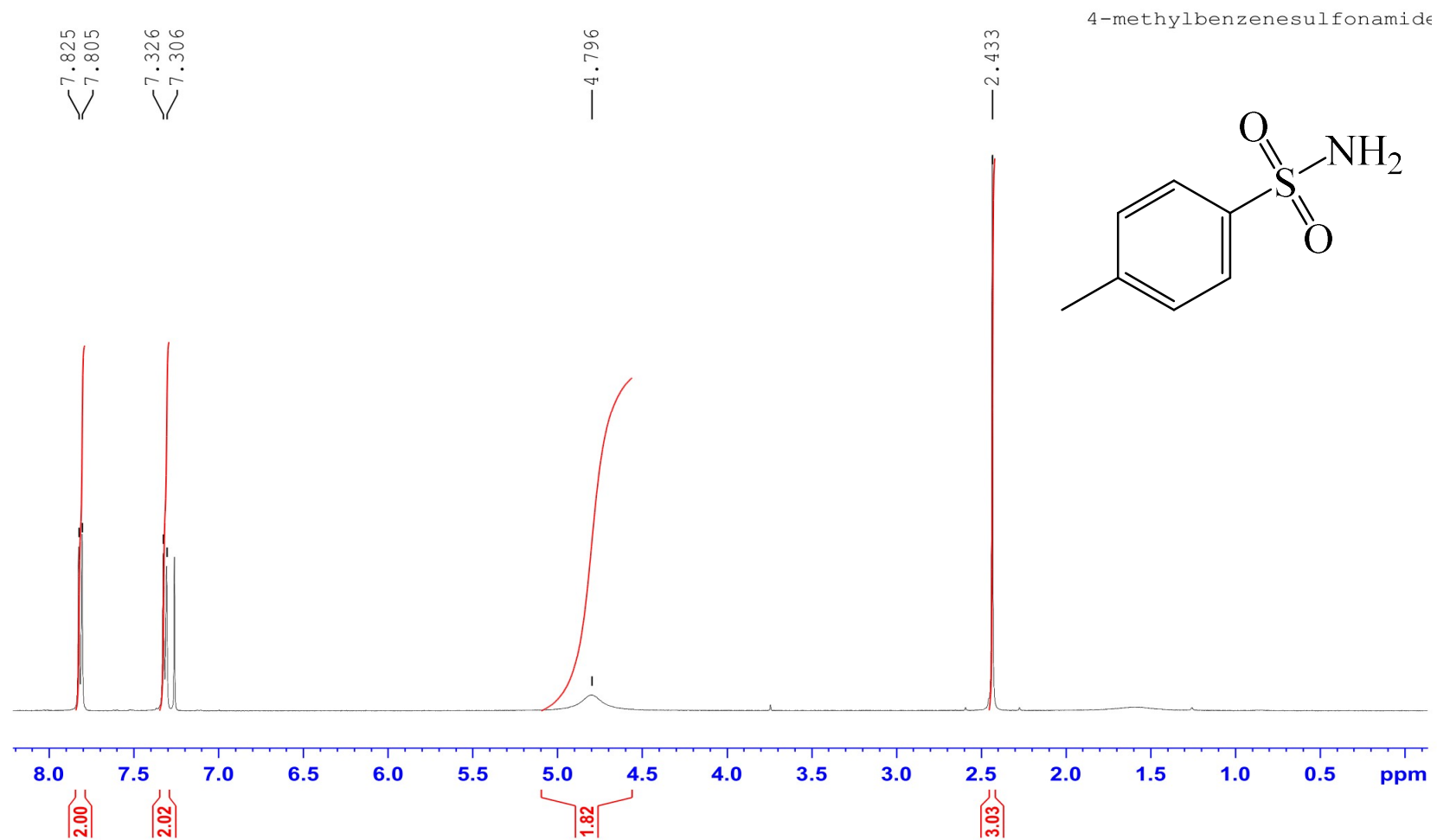
¹H NMR of methyl 2-(aminosulfonyl)benzoate in CDCl₃ (1a)

Table 1: Crystal data and structure refinement for methyl 2-(aminosulfonyl)benzoate.

Empirical formula	C ₈ H ₉ NO ₄ S
Formula weight	215.22
Temperature/K	100.01
Crystal system	orthorhombic
Space group	Pbca
a/Å	15.2056(7)
b/Å	7.4587(3)
c/Å	16.1330(8)
$\alpha/^\circ$	90
$\beta/^\circ$	90
$\gamma/^\circ$	90
Volume/Å ³	1829.71(14)
Z	8
$\rho_{\text{calc}}/\text{cm}^3$	1.563
μ/mm^{-1}	0.341
F(000)	896.0
Crystal size/mm ³	0.28 × 0.22 × 0.13
Radiation	MoK α (λ = 0.71073)
2 Θ range for data collection/ $^\circ$	9.174 to 56.586
Index ranges	-19 ≤ h ≤ 19, -6 ≤ k ≤ 9, -20 ≤ l ≤ 21
Reflections collected	8962
Independent reflections	2235 [R_{int} = 0.0165, R_{sigma} = 0.0137]
Data/restraints/parameters	2235/0/134
Goodness-of-fit on F ²	1.041
Final R indexes [$I \geq 2\sigma(I)$]	R_1 = 0.0289, wR_2 = 0.0786
Final R indexes [all data]	R_1 = 0.0324, wR_2 = 0.0821
Largest diff. peak/hole / e Å ⁻³	0.36/-0.49

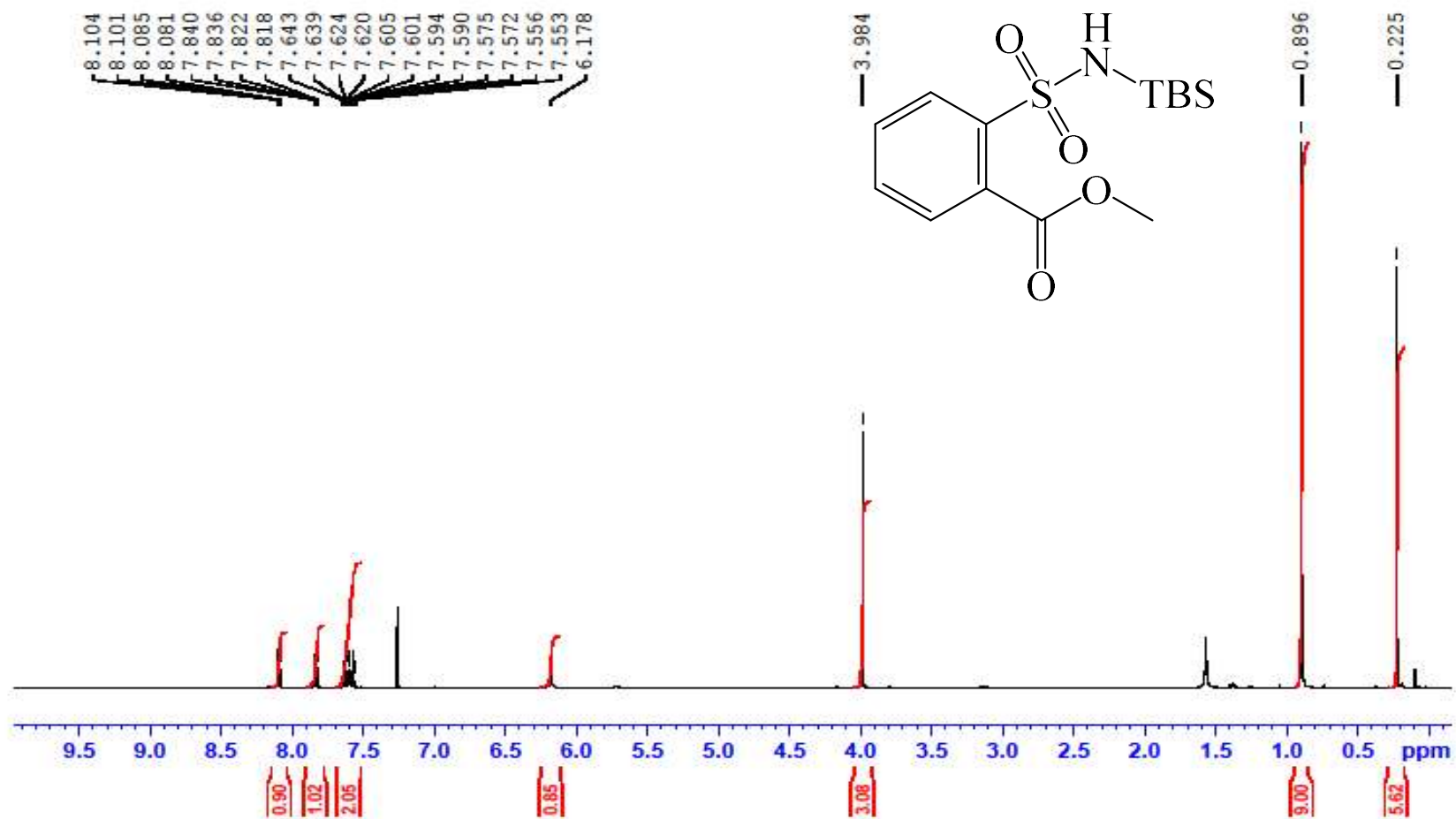
Table 2: Fractional atomic coordinates ($\times 10^4$) and equivalent isotropic displacement parameters ($\text{\AA}^2 \times 10^3$) for methyl 2-(aminosulfonyl)benzoate. U_{eq} is defined as 1/3 of the trace of the orthogonalised U_{IJ} tensor.

Atom	x	y	z	U(eq)
S1	3462.6(2)	2452.6(3)	3835.6(2)	11.17(10)
O1	6349.6(6)	2925.7(12)	3618.0(5)	15.35(19)
O2	5341.9(6)	1437.0(12)	4367.4(5)	16.83(19)
O3	3840.4(6)	3809.2(11)	4353.8(5)	16.59(19)
O4	2568.9(6)	2682.3(12)	3557.0(5)	16.4(2)
N1	3481.9(7)	583.6(14)	4334.4(6)	13.7(2)
C1	6902.9(8)	3018.3(16)	4346.5(7)	16.3(2)
C2	5570.8(8)	2128.3(16)	3724.2(7)	12.2(2)
C3	5047.0(7)	2176.9(14)	2941.1(7)	12.0(2)
C4	4120.2(7)	2252.5(14)	2926.0(7)	11.5(2)
C5	3674.3(8)	2254.2(16)	2172.1(8)	14.9(2)
C6	4138.3(9)	2162.2(17)	1429.3(7)	16.9(2)
C7	5047.5(9)	2078.4(17)	1438.6(7)	16.3(2)
C8	5496.7(8)	2099.5(16)	2186.8(7)	15.0(2)

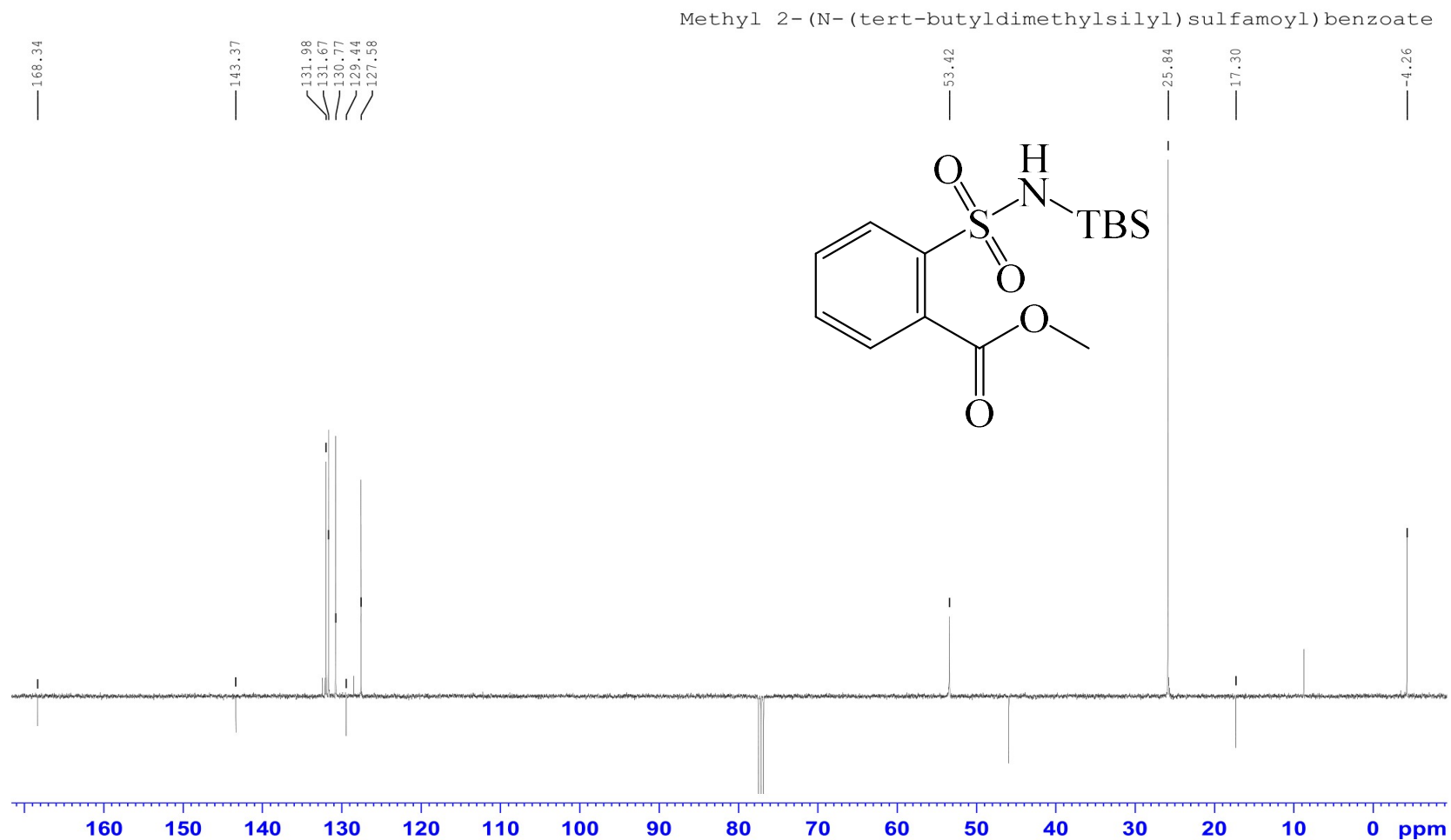


¹H NMR of 4-methylbenzenesulfonamide in CDCl₃ (1b)

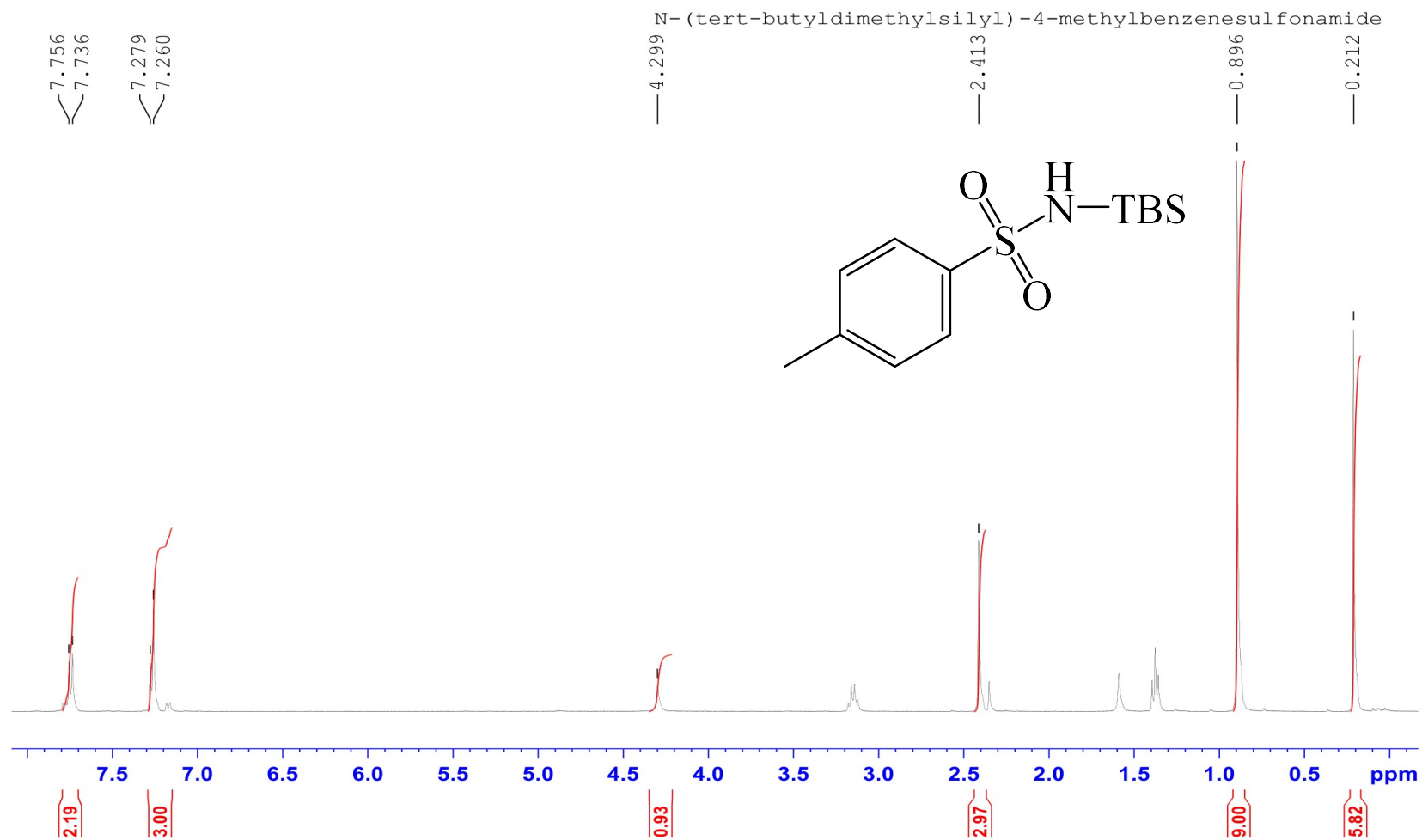
Methyl 2-(N-(tert-butyldimethylsilyl)sulfamoyl)benzoate



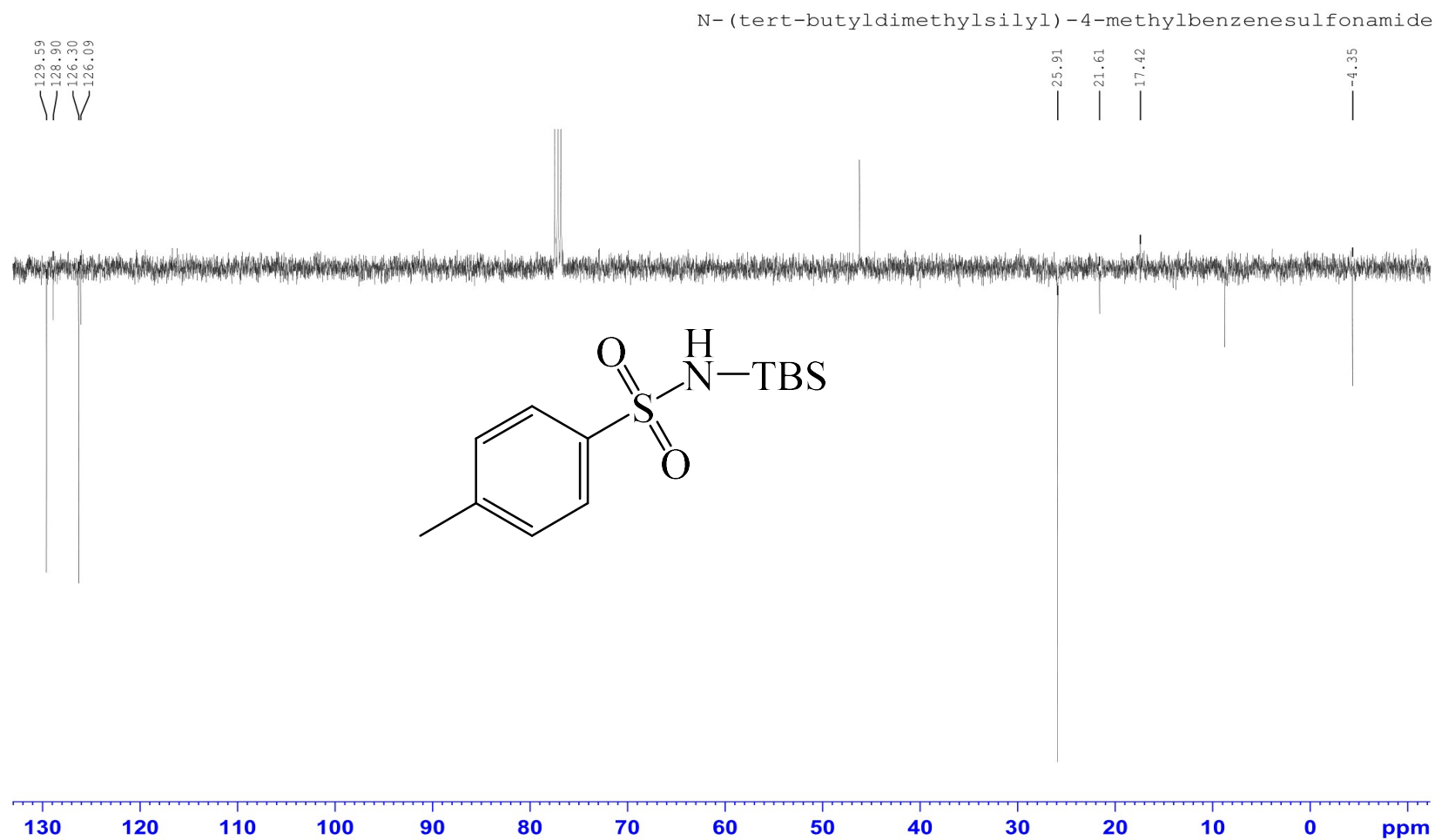
¹H NMR of methyl 2-(N-(tert-butyldimethylsilyl)sulfamoyl)benzoate in CDCl₃ (2a)



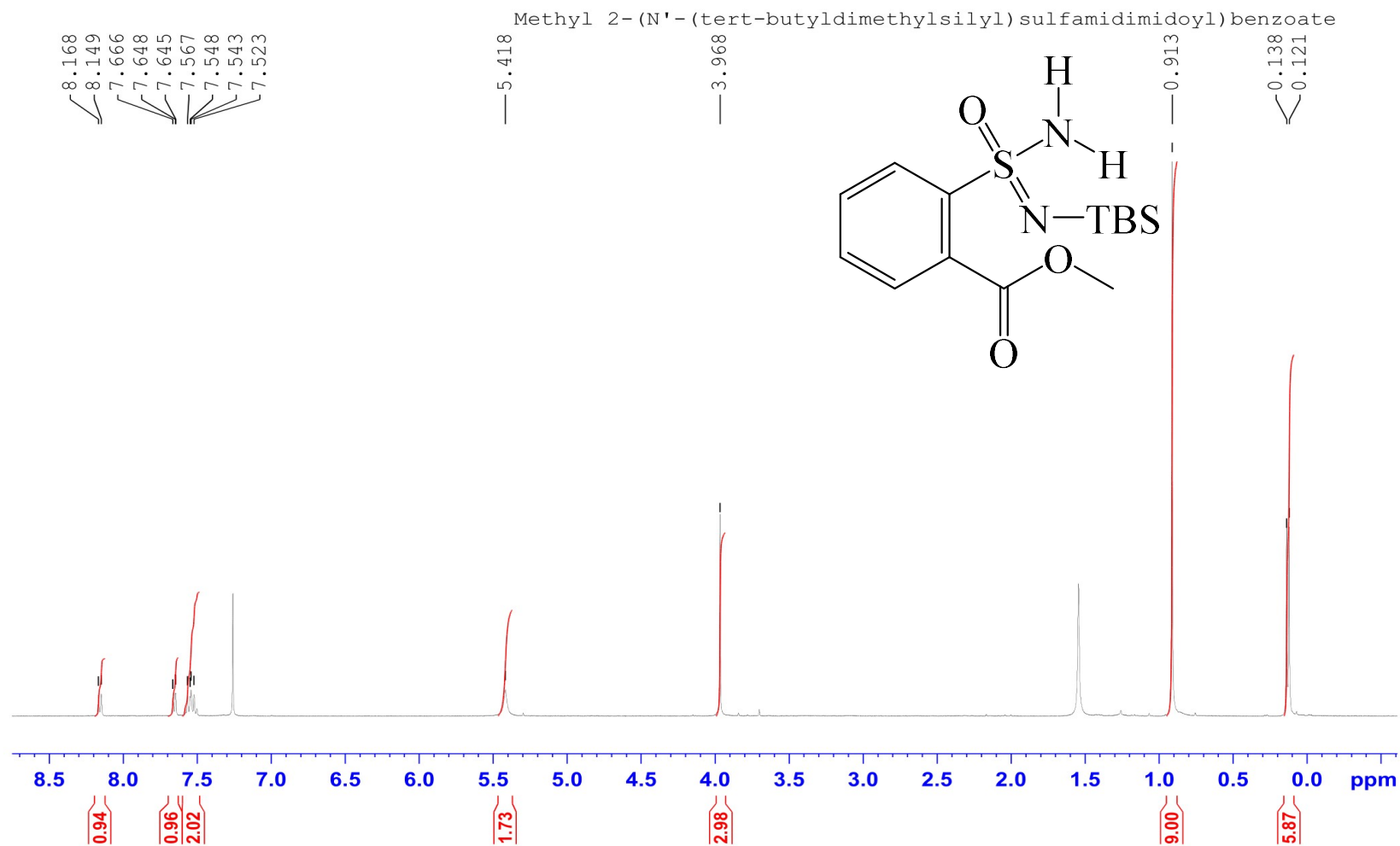
¹³C NMR of methyl 2-(N-(tert-butyldimethylsilyl)sulfamoyl)benzoate in CDCl₃ (2a)



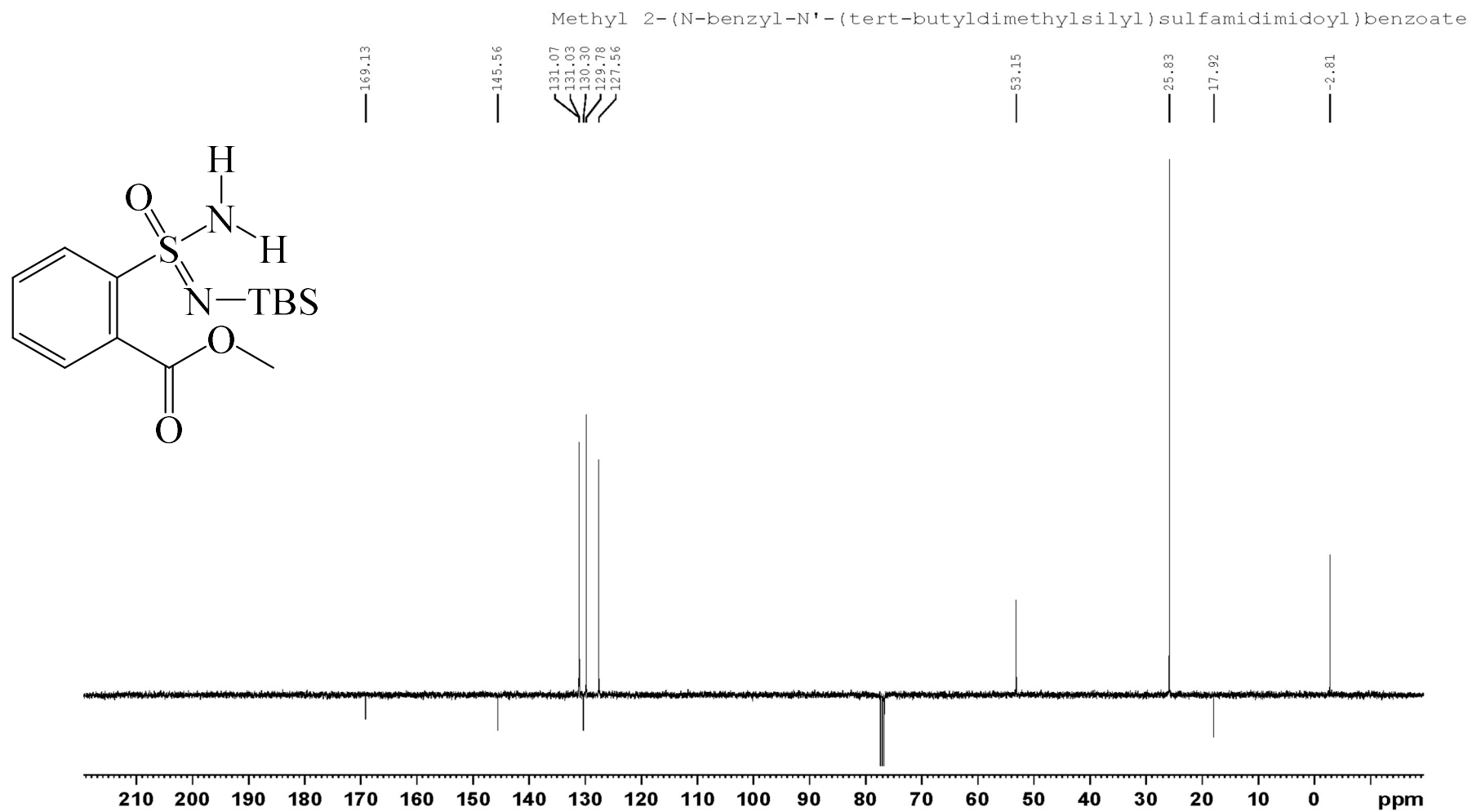
¹H NMR of N-(tert-butyldimethylsilyl)-4-methylbenzenesulfonamide in CDCl₃ (2b)



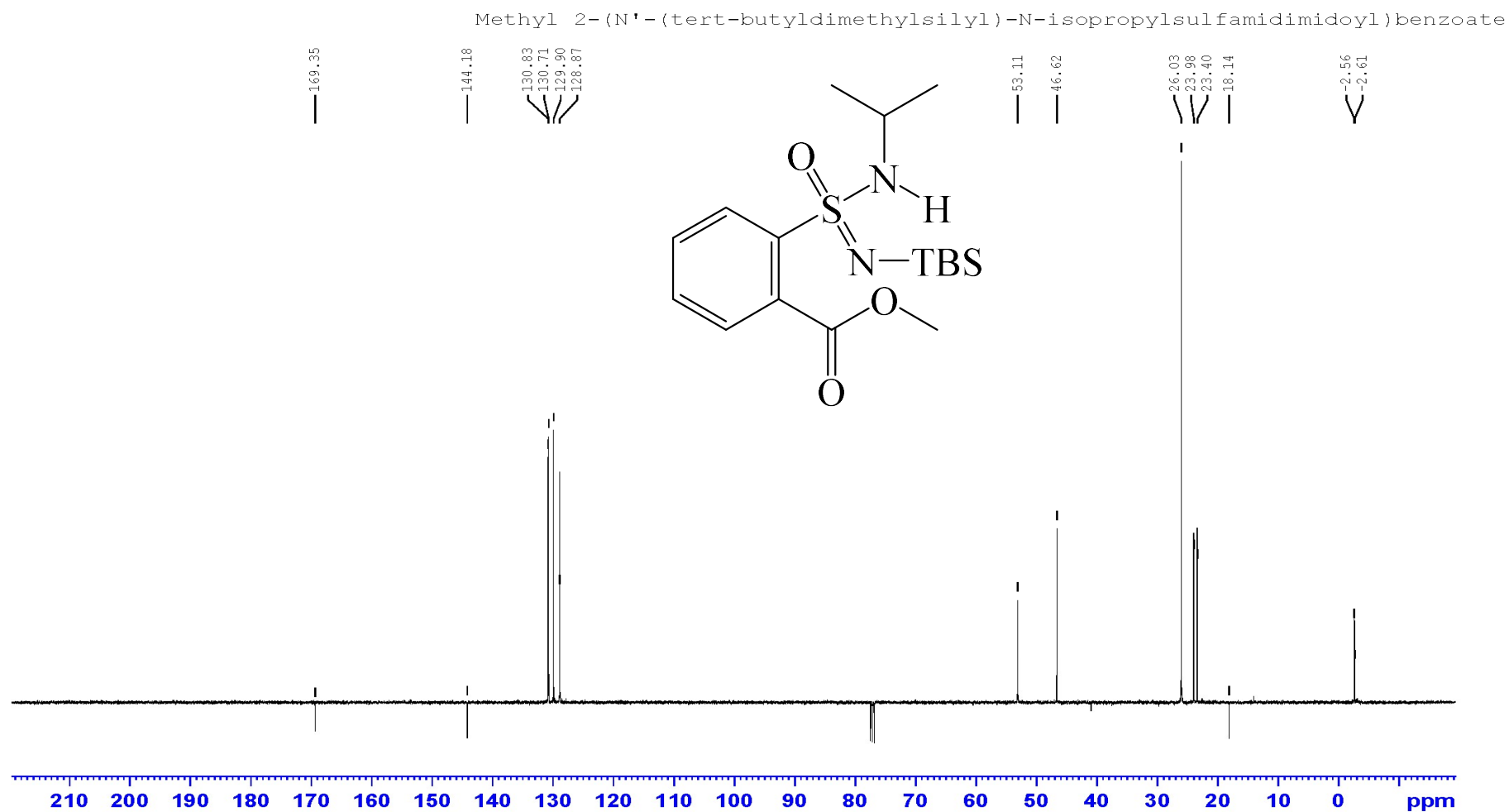
¹³C NMR of N-(tert-butyldimethylsilyl)-4-methylbenzenesulfonamide in CDCl₃ (2b)



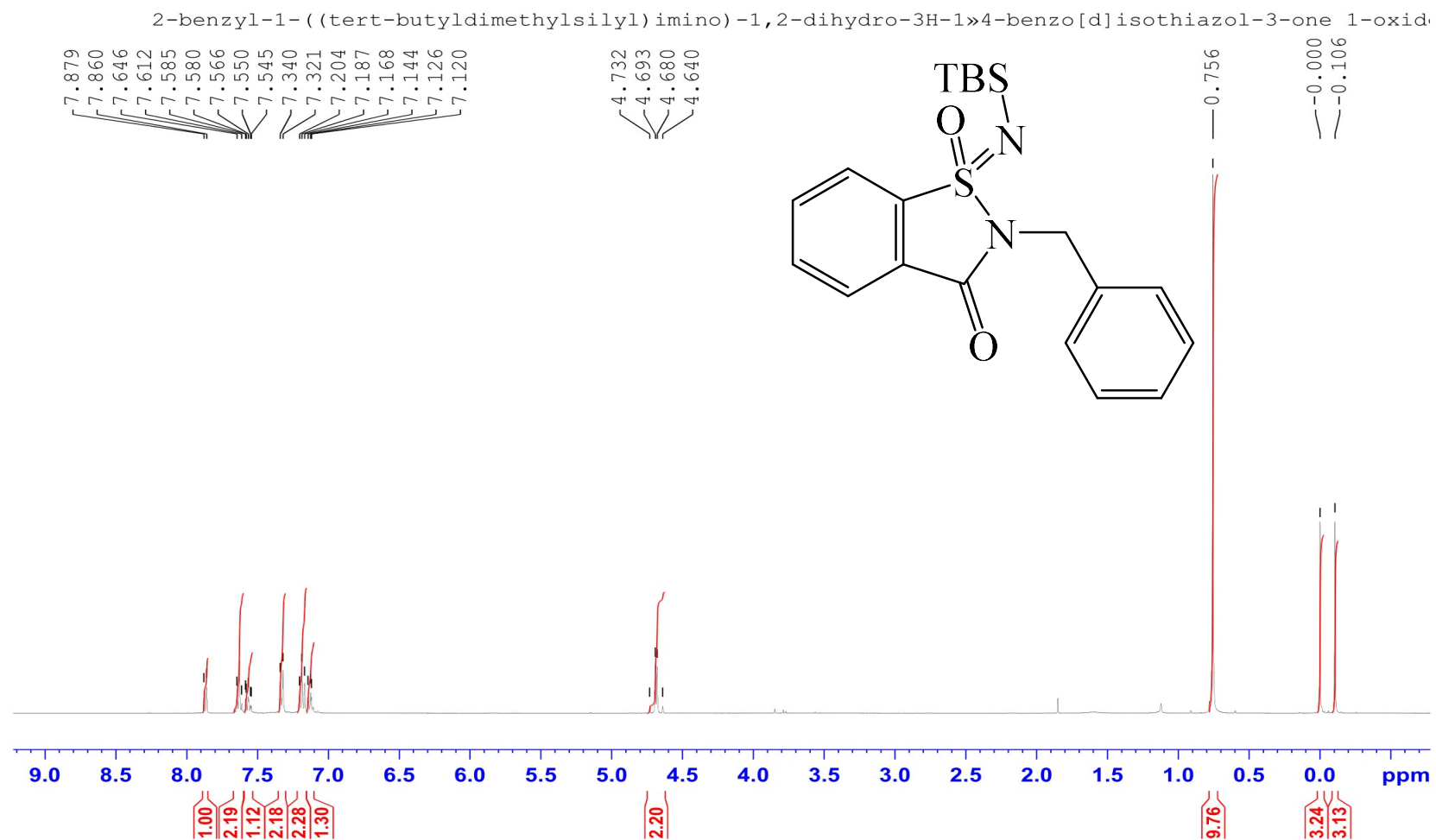
¹H NMR of methyl 2-(N'-(tert-butyldimethylsilyl)sulfamidimidoyl)benzoate in CDCl₃ (4a)



¹³C NMR of methyl 2-(N'-(tert-butyldimethylsilyl)sulfamidimidoyl)benzoate in CDCl₃ (4a)

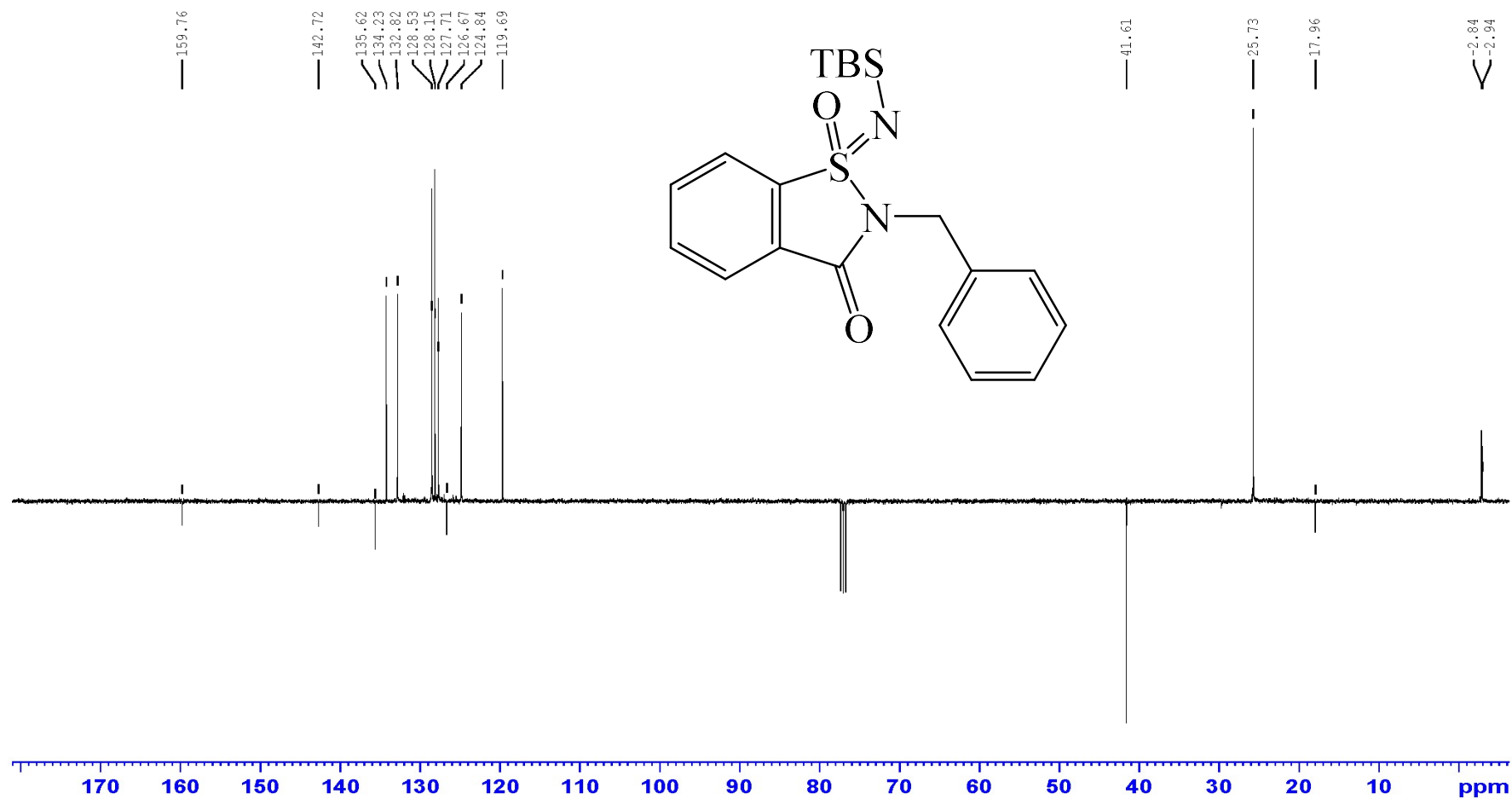


¹³C NMR of methyl 2-(N'-(tert-butyldimethylsilyl)-N-isopropylsulfamidimidoyl)benzoate in CDCl₃ (4b)



¹H NMR of 2-benzyl-1-((tert-butyldimethylsilyl)imino)-1,2-dihydro-3H-1λ⁴-benzo[d]isothiazol-3-one 1-oxide in CDCl₃ (4c)

2-benzyl-1-((tert-butyldimethylsilyl)imino)-1,2-dihydro-3H-1λ⁴-benzo[d]isothiazol-3-one 1-oxide



¹³C NMR of 2-benzyl-1-((tert-butyldimethylsilyl)imino)-1,2-dihydro-3H-1λ⁴-benzo[d]isothiazol-3-one 1-oxide in CDCl₃ (4c)

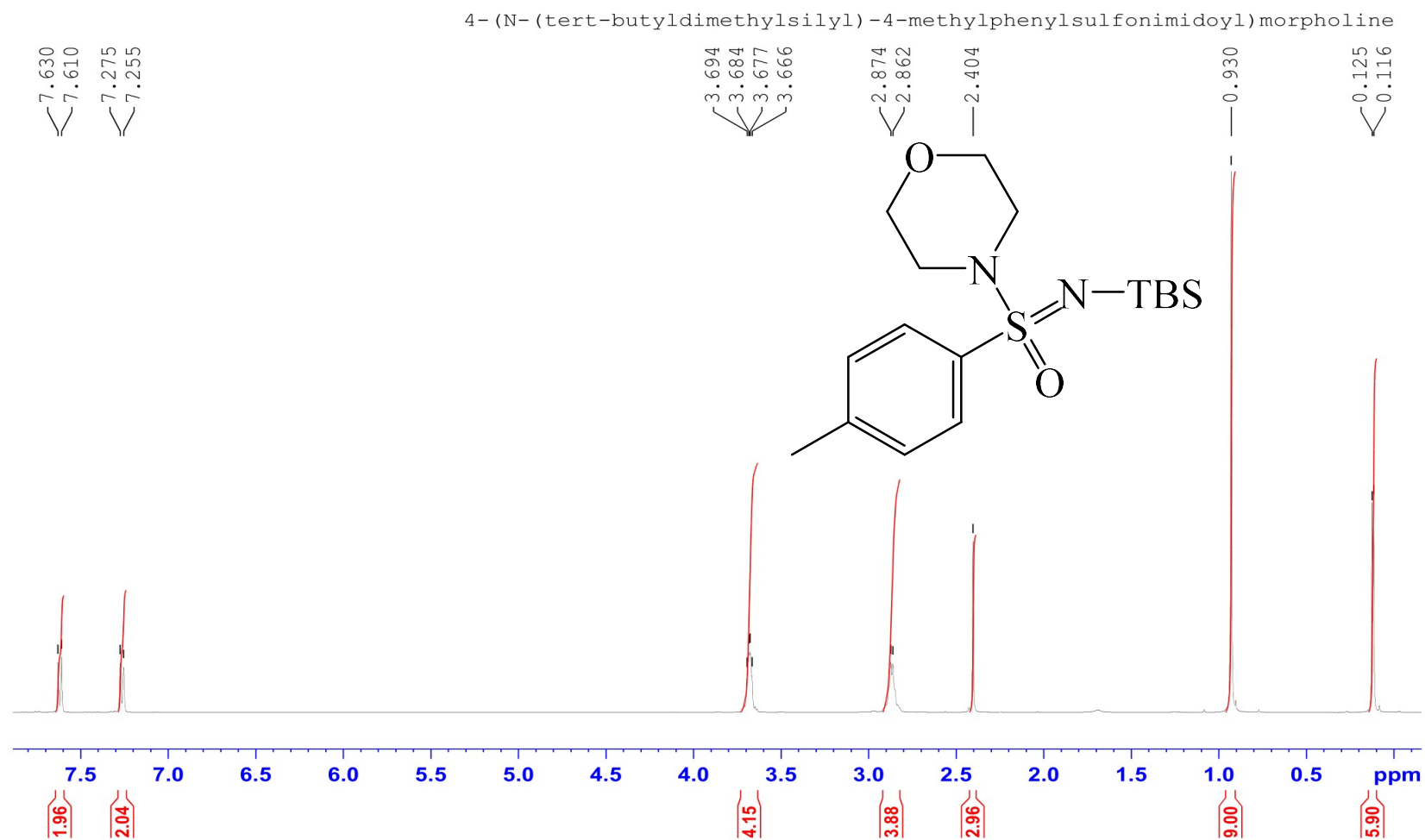
Table 3: Crystal data and structure refinement for 2-benzyl-1-((tert-butyl)dimethylsilyl)imino)-1,2-dihydro-3H-1λ4-benzo[d]isothiazol-3-one 1-oxide.

Empirical formula	C ₂₀ H ₂₆ N ₂ O ₂ SSi
Formula weight	386.58
Temperature/K	104.08
Crystal system	triclinic
Space group	P-1
a/Å	6.8505(2)
b/Å	10.5306(4)
c/Å	28.4395(10)
α/°	94.355(2)
β/°	91.264(2)
γ/°	96.252(2)
Volume/Å ³	2032.58(12)
Z	4
ρ _{calc} /cm ³	1.263
μ/mm ⁻¹	0.235
F(000)	824.0
Crystal size/mm ³	0.31 × 0.18 × 0.12
Radiation	MoKα (λ = 0.71073)
2Θ range for data collection/°	1.436 to 54.298
Index ranges	-8 ≤ h ≤ 8, -13 ≤ k ≤ 12, -36 ≤ l ≤ 36
Reflections collected	21113
Independent reflections	8737 [R _{int} = 0.0253, R _{sigma} = 0.0363]
Data/restraints/parameters	8737/0/480
Goodness-of-fit on F ²	1.072
Final R indexes [I ≥ 2σ (I)]	R ₁ = 0.0558, wR ₂ = 0.1556
Final R indexes [all data]	R ₁ = 0.0630, wR ₂ = 0.1626
Largest diff. peak/hole / e Å ⁻³	0.64/-0.32

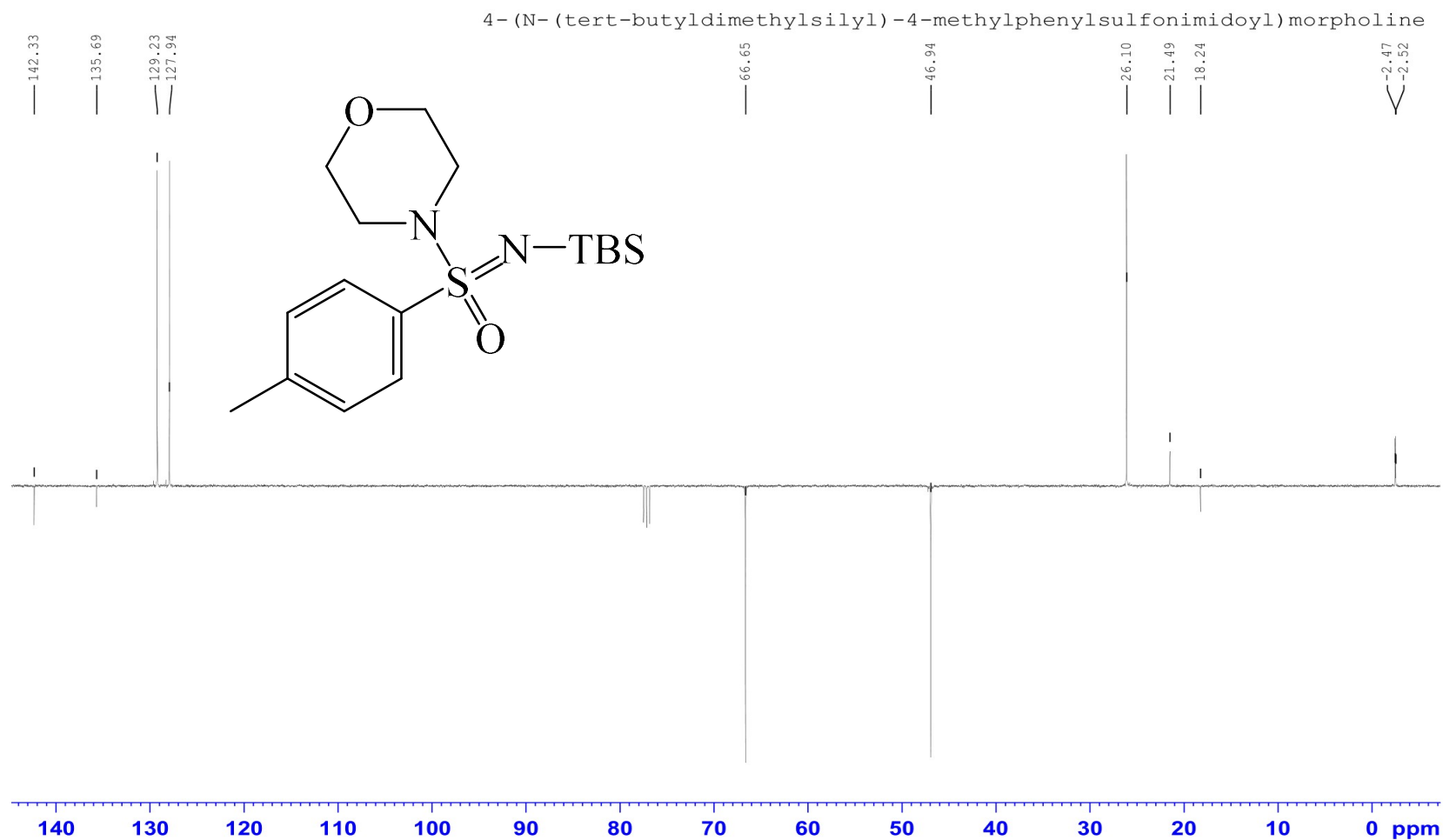
Table 4: Fractional atomic coordinates ($\times 10^4$) and equivalent isotropic displacement parameters ($\text{\AA}^2 \times 10^3$) for 2-benzyl-1-((tert-butyl)dimethylsilyl)imino)-1,2-dihydro-3H-1 λ 4-benzo[d]isothiazol-3-one 1-oxide. U_{eq} is defined as 1/3 of the trace of the orthogonalised U_{ij} tensor.

Atom	x	y	z	U_{eq}
S1	2788.0(11)	6956.3(7)	5789.8(3)	12.34(16)
Si1	778.4(12)	9300.5(8)	5947.0(3)	13.79(19)
O1	4746(3)	7429(2)	5963.6(9)	18.2(5)
O2	1581(4)	3369(2)	5650.5(10)	24.9(6)
N1	1099(4)	7689(3)	5903.2(10)	15.8(5)
N2	2208(4)	5462(2)	5952.2(10)	15.7(5)
C1	-1330(5)	9472(3)	5542.6(13)	21.5(7)
C2	3030(5)	10299(3)	5774.4(14)	23.3(7)
C3	163(5)	9734(3)	6579.1(12)	21.4(7)
C4	2036(6)	9869(4)	6896.0(14)	31.8(9)
C5	-1316(6)	8685(4)	6752.5(14)	31.8(9)
C6	-750(6)	11012(4)	6606.8(16)	32.3(9)
C7	2876(4)	6386(3)	5191.7(11)	14.2(6)
C8	3317(5)	7119(3)	4818.2(12)	18.9(7)
C9	3301(5)	6466(4)	4373.0(13)	24.9(8)
C10	2881(5)	5152(4)	4312.0(13)	25.6(8)
C11	2452(5)	4419(3)	4694.1(13)	22.0(7)
C12	2450(4)	5057(3)	5138.7(12)	16.7(6)
C13	2028(4)	4485(3)	5590.6(12)	16.9(6)
C14	1807(5)	5236(3)	6445.0(12)	19.9(7)
C15	3614(5)	4907(3)	6704.2(12)	17.5(6)
C16	4944(6)	5853(4)	6934.1(14)	28.7(8)
C17	6648(7)	5526(4)	7149.8(14)	33.6(9)
C18	7033(6)	4260(4)	7136.1(13)	29.2(8)
C19	5703(6)	3322(4)	6912.8(13)	25.7(8)
C20	4002(5)	3635(3)	6699.2(13)	21.8(7)
S2	7692.8(11)	6649.0(7)	9210.0(3)	13.19(17)

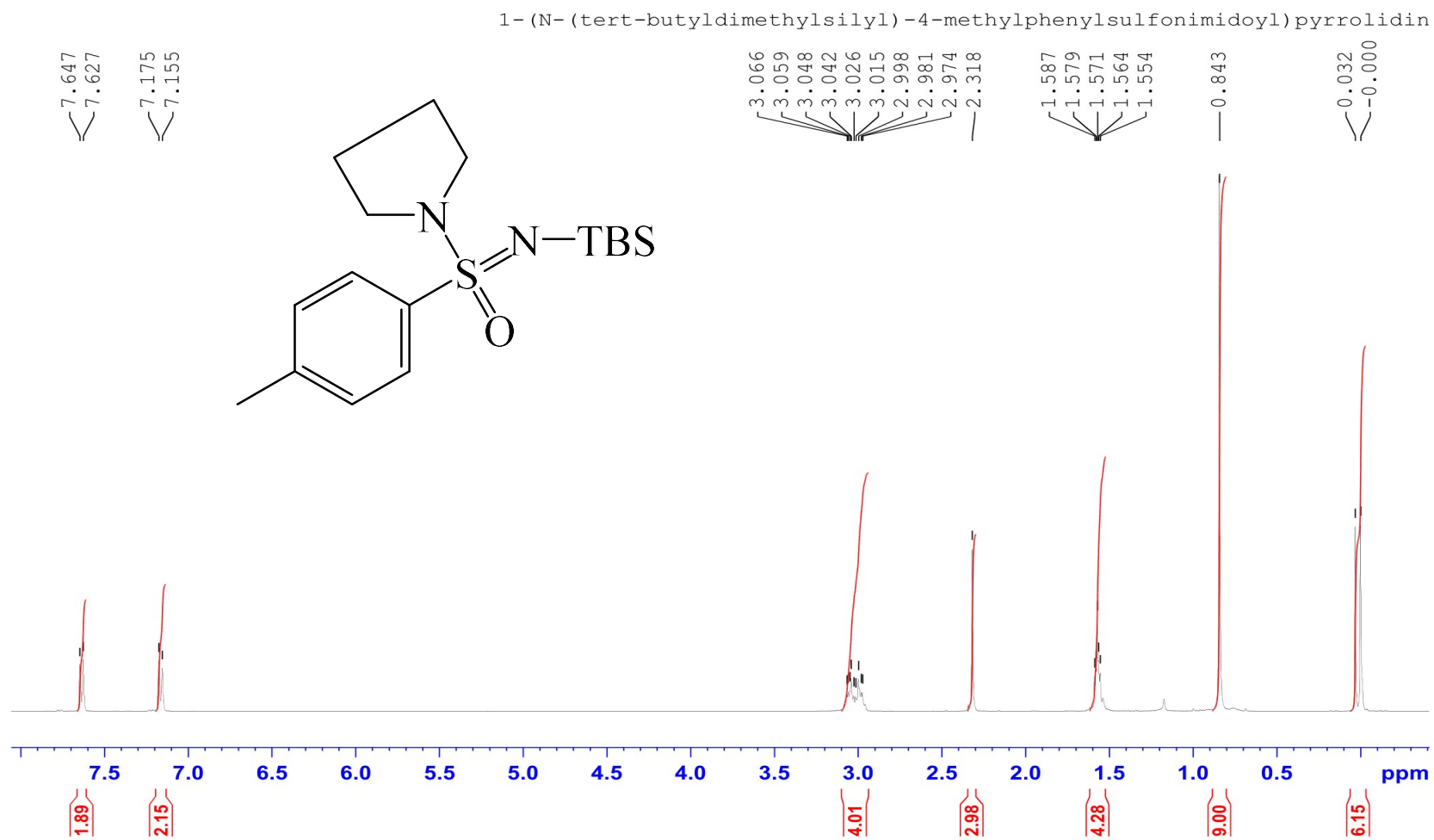
Si2	5630.5(13)	8919.5(8)	9059.3(3)	14.44(19)
O3	9635(3)	7107(2)	9066.1(9)	18.4(5)
O4	6611(4)	3086(2)	9281.7(9)	22.2(5)
N3	5978(4)	7318(2)	9085.3(10)	16.2(5)
N4	7176(4)	5091(2)	9018.0(10)	14.4(5)
C21	7931(5)	9983(3)	9233.5(14)	24.1(7)
C22	3639(5)	9242(3)	9469.3(13)	21.1(7)
C23	3239(6)	8057(4)	8254.0(14)	28.0(8)
C24	6582(6)	9132(4)	8108.2(15)	33.5(9)
C25	4818(5)	9141(3)	8434.2(12)	19.2(7)
C26	3957(6)	10428(3)	8424.3(15)	27.1(8)
C27	7811(4)	6261(3)	9802.7(12)	15.4(6)
C28	8226(5)	7114(3)	10195.5(12)	20.5(7)
C29	8219(5)	6588(4)	10631.0(13)	26.5(8)
C30	7817(5)	5273(4)	10668.3(13)	25.3(8)
C31	7424(5)	4439(4)	10267.1(13)	21.4(7)
C32	7425(4)	4952(3)	9829.7(12)	16.1(6)
C33	7026(4)	4230(3)	9364.9(12)	16.6(6)
C34	6790(5)	4701(3)	8517.8(12)	17.0(6)
C35	8543(5)	4194(3)	8284.0(11)	15.6(6)
C36	10083(5)	5021(3)	8138.2(12)	21.5(7)
C37	11678(5)	4532(4)	7918.2(13)	26.2(8)
C38	11724(5)	3225(4)	7842.2(13)	26.1(8)
C39	10207(6)	2402(4)	7990.6(13)	26.2(8)
C40	8611(5)	2881(3)	8207.7(13)	21.1(7)



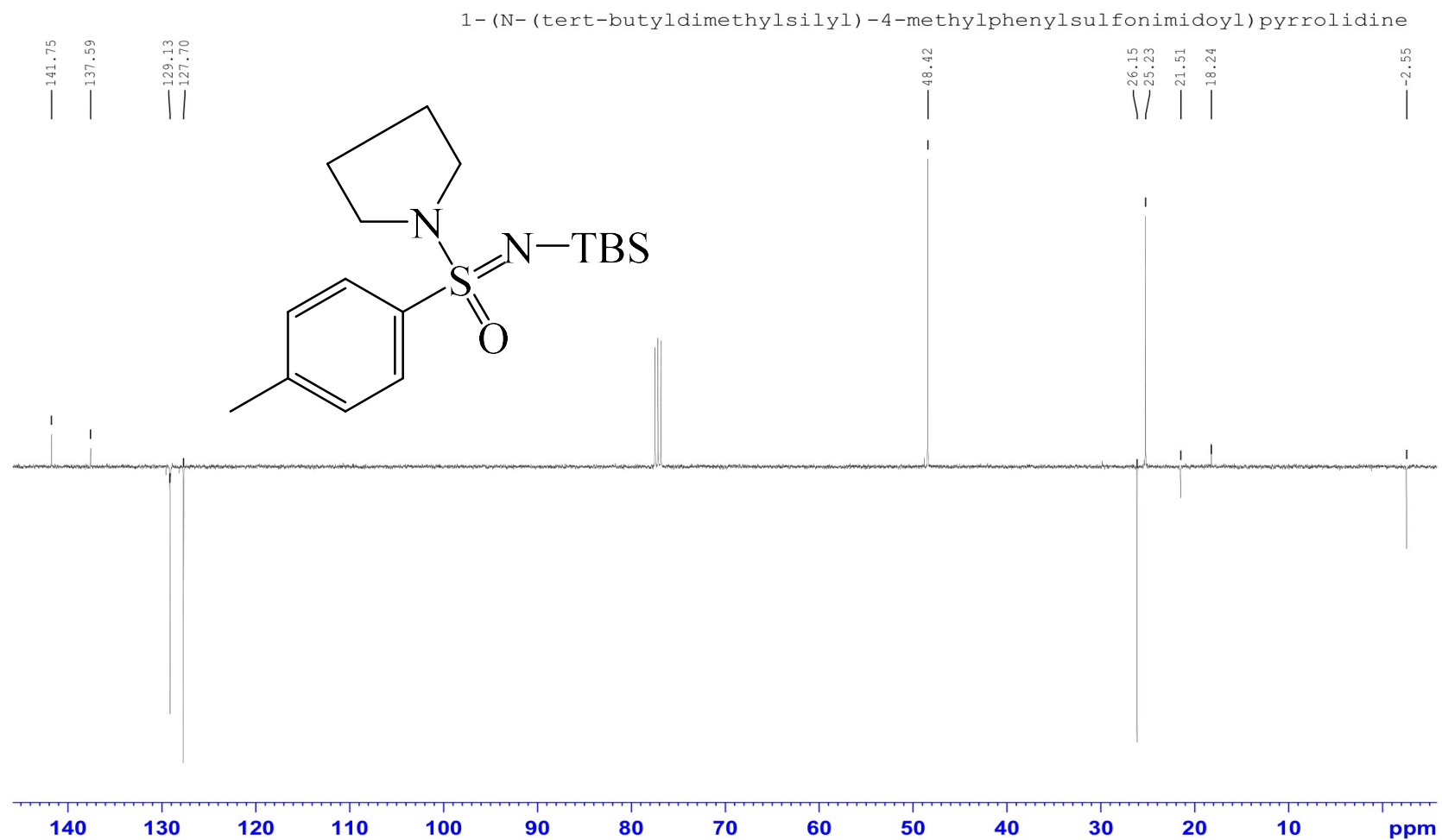
¹H NMR of 4-(N-(tert-butyldimethylsilyl)-4-methylphenylsulfonimidoyl)morpholine in CDCl₃ (4e)



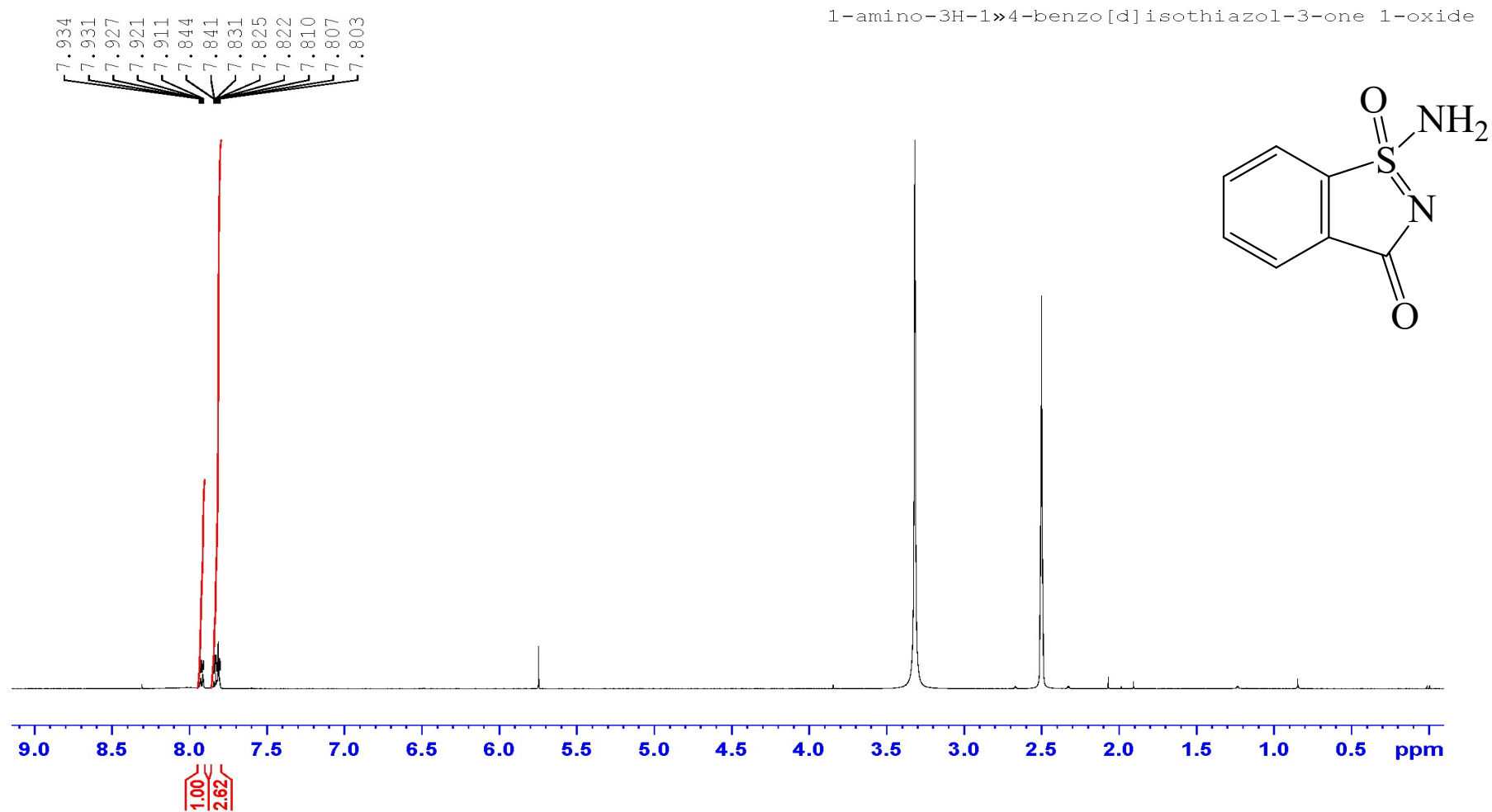
^{13}C NMR of 4-(N-(tert-butyldimethylsilyl)-4-methylphenylsulfonimidoyl)morpholine in CDCl_3 (4e)



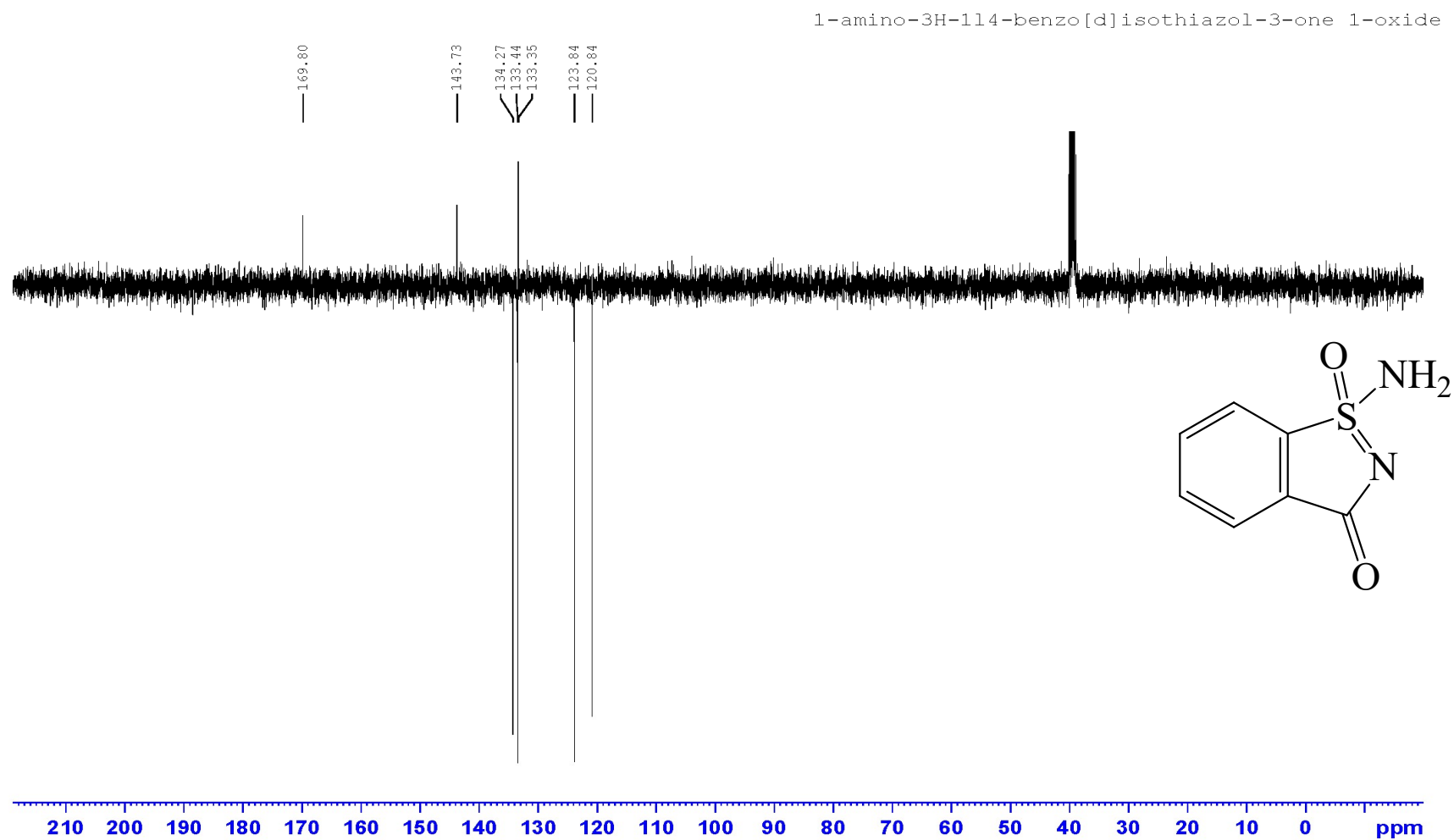
¹H NMR of 1-(N-(tert-butyl dimethylsilyl)-4-methylphenylsulfonimidoyl)pyrrolidine in CDCl₃ (4f)



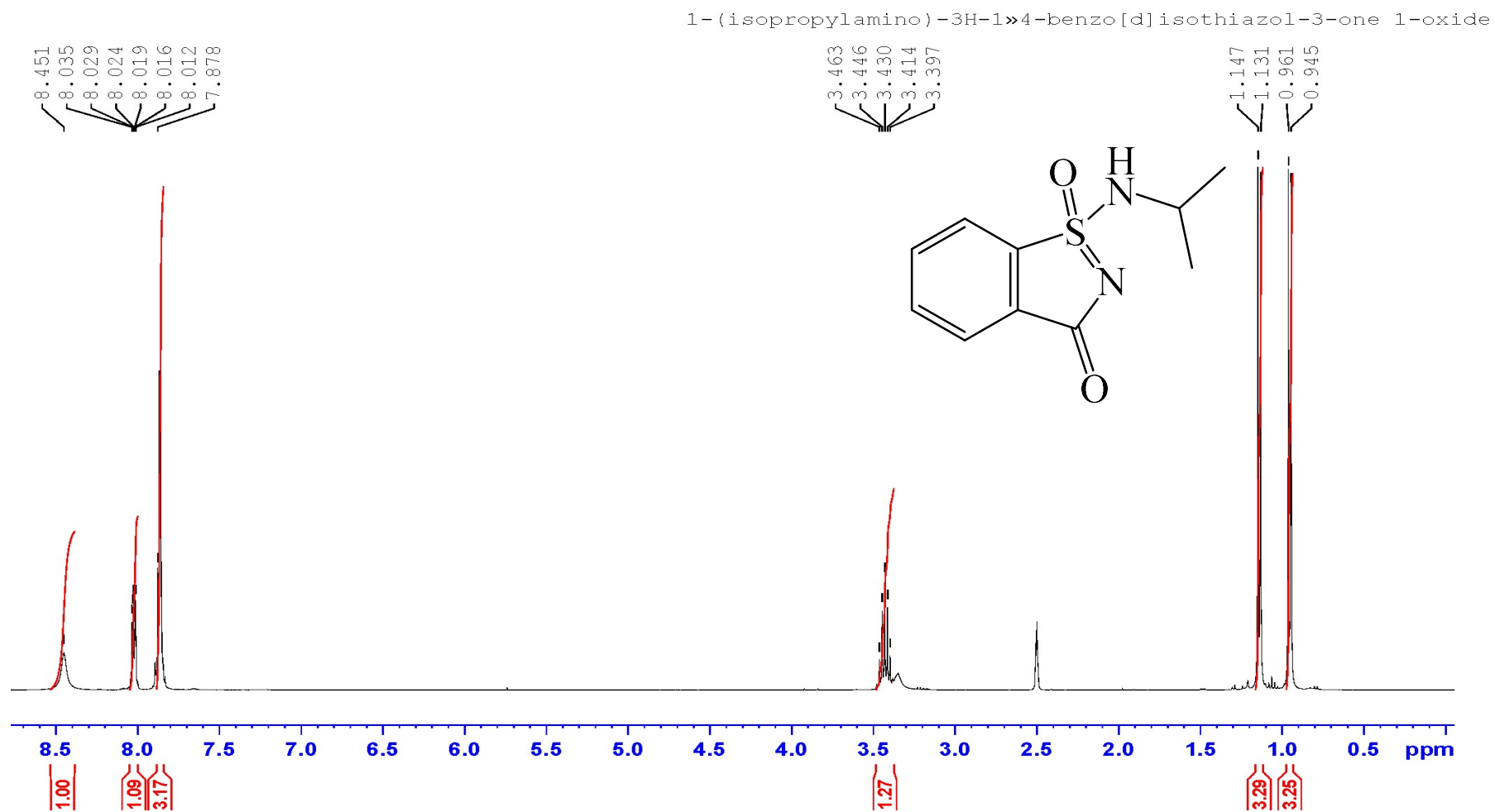
¹³C NMR of 1-(N-(tert-butyldimethylsilyl)-4-methylphenylsulfonimidoyl)pyrrolidine in CDCl₃ (4f)



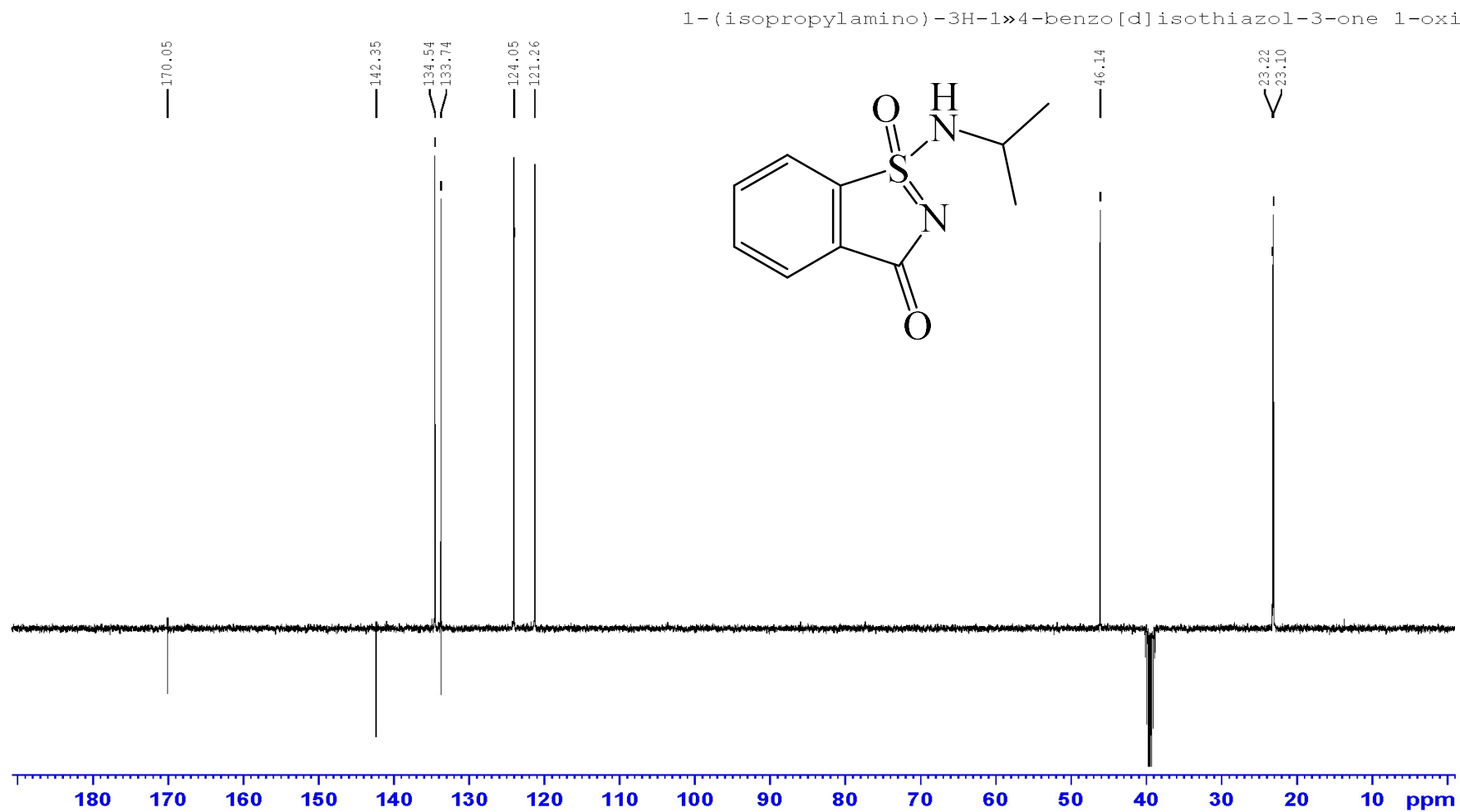
¹H NMR of 1-amino-3H-1,4-benzo[d]isothiazol-3-one 1-oxide in DMSO-d₆ (5a)



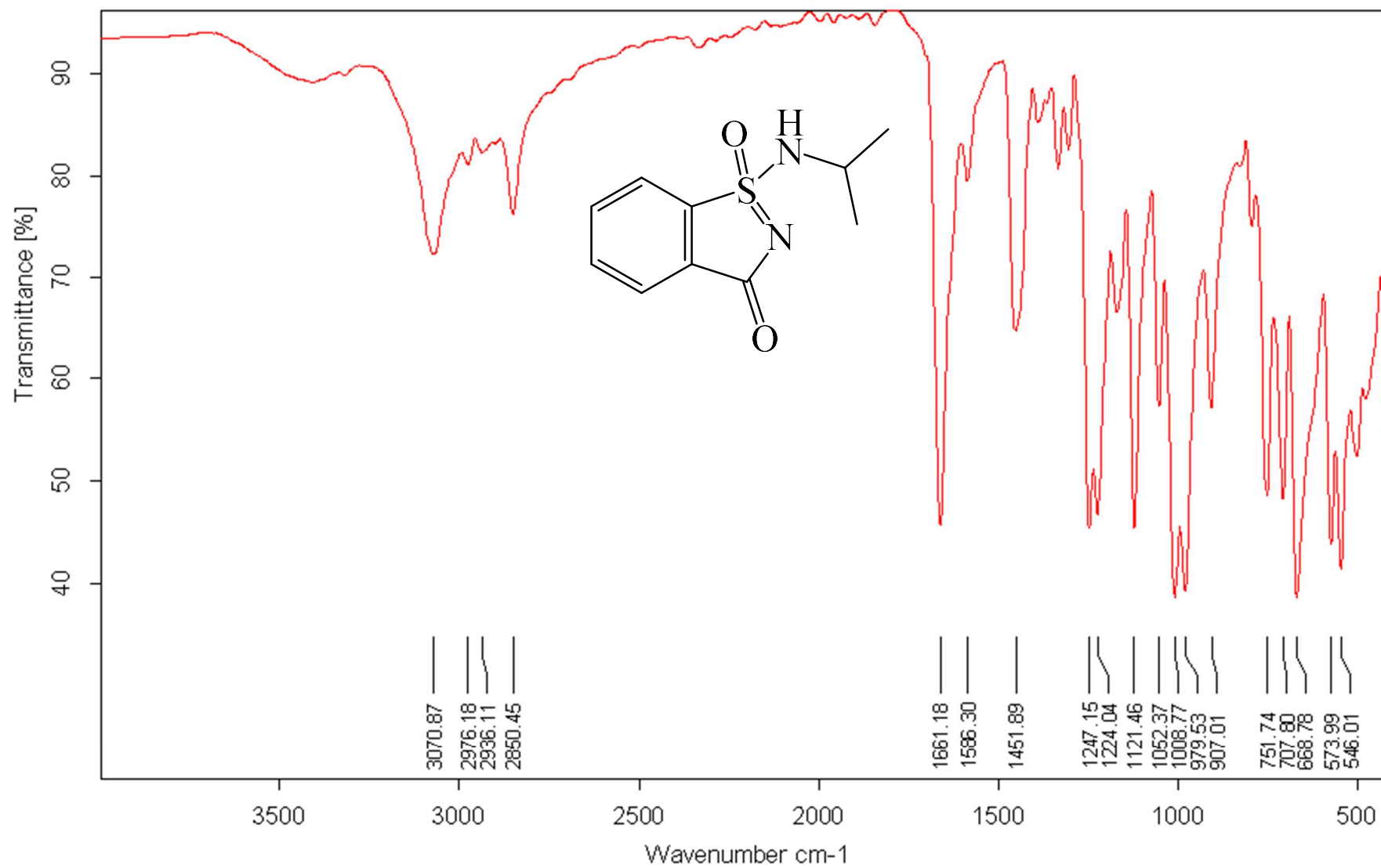
¹³C NMR of 1-amino-3H-1λ⁴-benzo[d]isothiazol-3-one 1-oxide in DMSO-d₆ (5a)



^1H NMR of 1-(isopropylamino)-3H-1,4-benzo[d]isothiazol-3-one 1-oxide in $\text{DMSO}-d_6$ (5b)



¹³C NMR of 1-(isopropylamino)-3H-1,4-benzo[d]isothiazol-3-one 1-oxide in DMSO-d₆ (5b)



IR of 1-(isopropylamino)-3H-1λ⁴-benzo[d]isothiazol-3-one 1-oxide (5b)

Display Report

Analysis Info

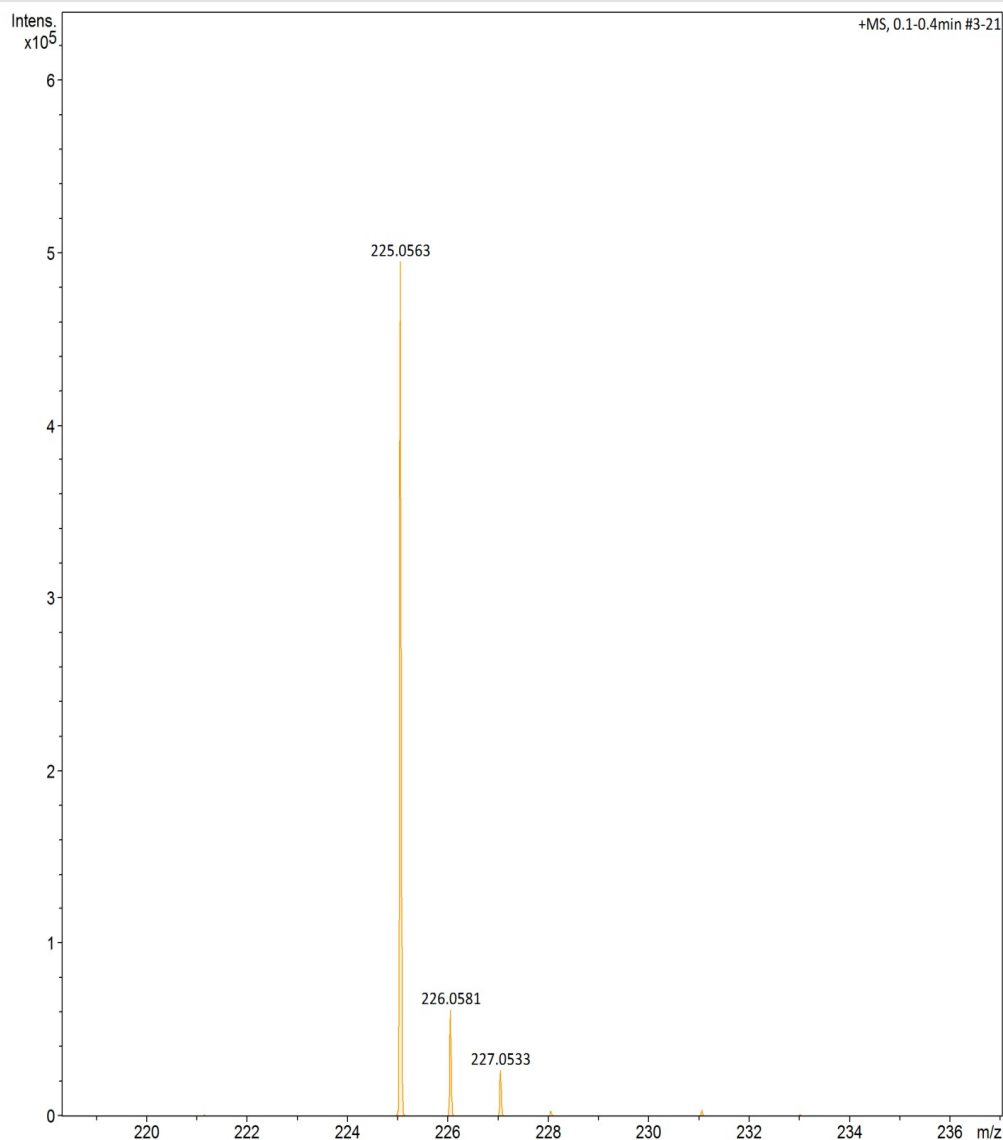
Analysis Name C:\Data\Arno\Loyd 1_02.d
Method tune_pos_mid_new.m
Sample Name 1
Comment

Acquisition Date 1/28/2020 10:24:49 AM

Operator @BLADE
Instrument micrOTOF-Q 228888.10139

Acquisition Parameter

Source Type	ESI	Ion Polarity	Positive	Set Nebulizer	0.3 Bar
Focus	Not active	Set Capillary	4500 V	Set Dry Heater	200 °C
Scan Begin	50 m/z	Set End Plate Offset	-500 V	Set Dry Gas	4.0 l/min
Scan End	3000 m/z	Set Collision Cell RF	200.0 Vpp	Set Divert Valve	Source



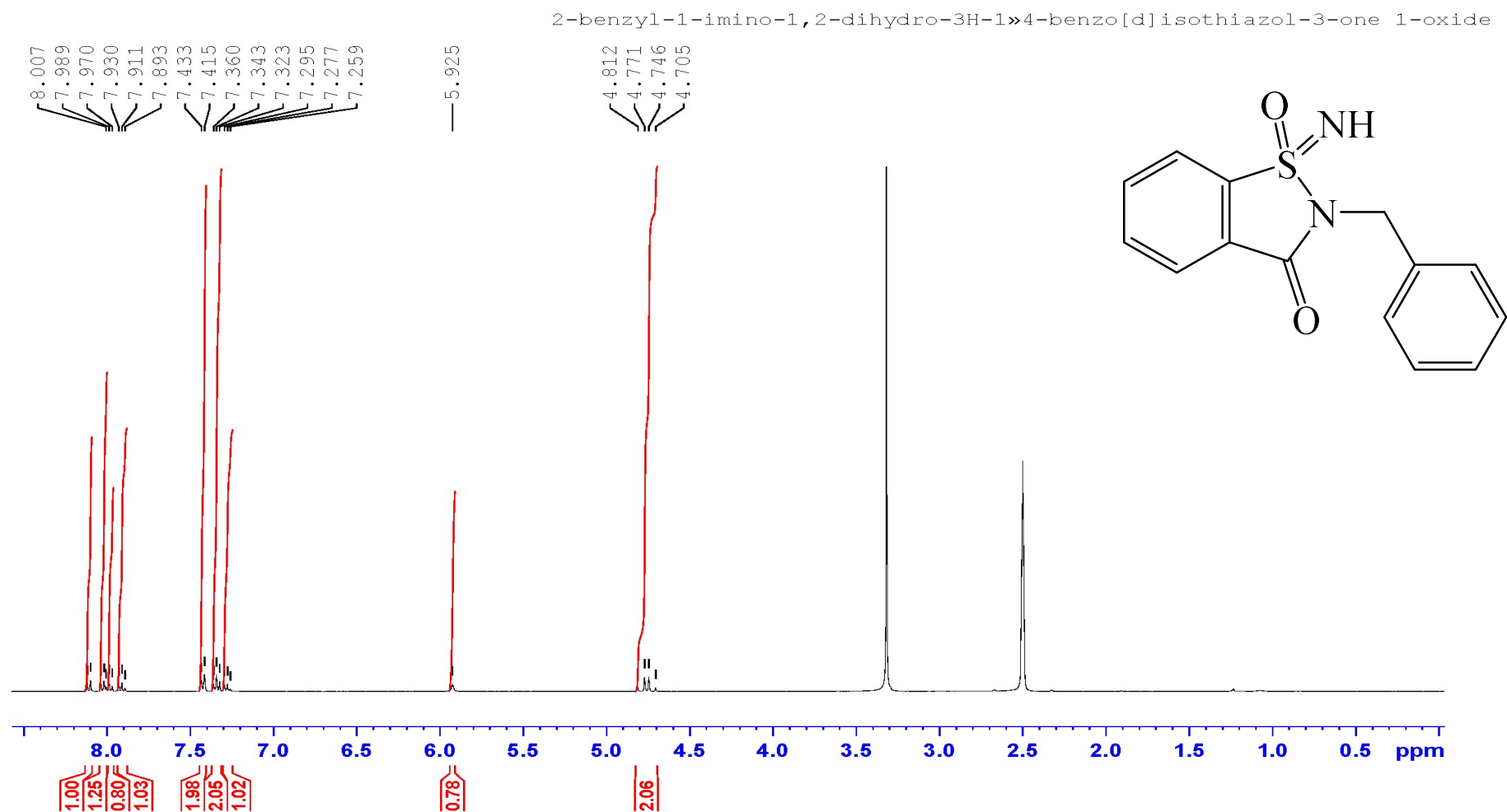
HRMS spectrum of 1-(isopropylamino)-3H-1λ⁴-benzo[d]isothiazol-3-one 1-oxide (5b)

Table 5: Crystal data and structure refinement for 1-(isopropylamino)-3H-1 λ ⁴-benzo[d]isothiazol-3-one 1-oxide.

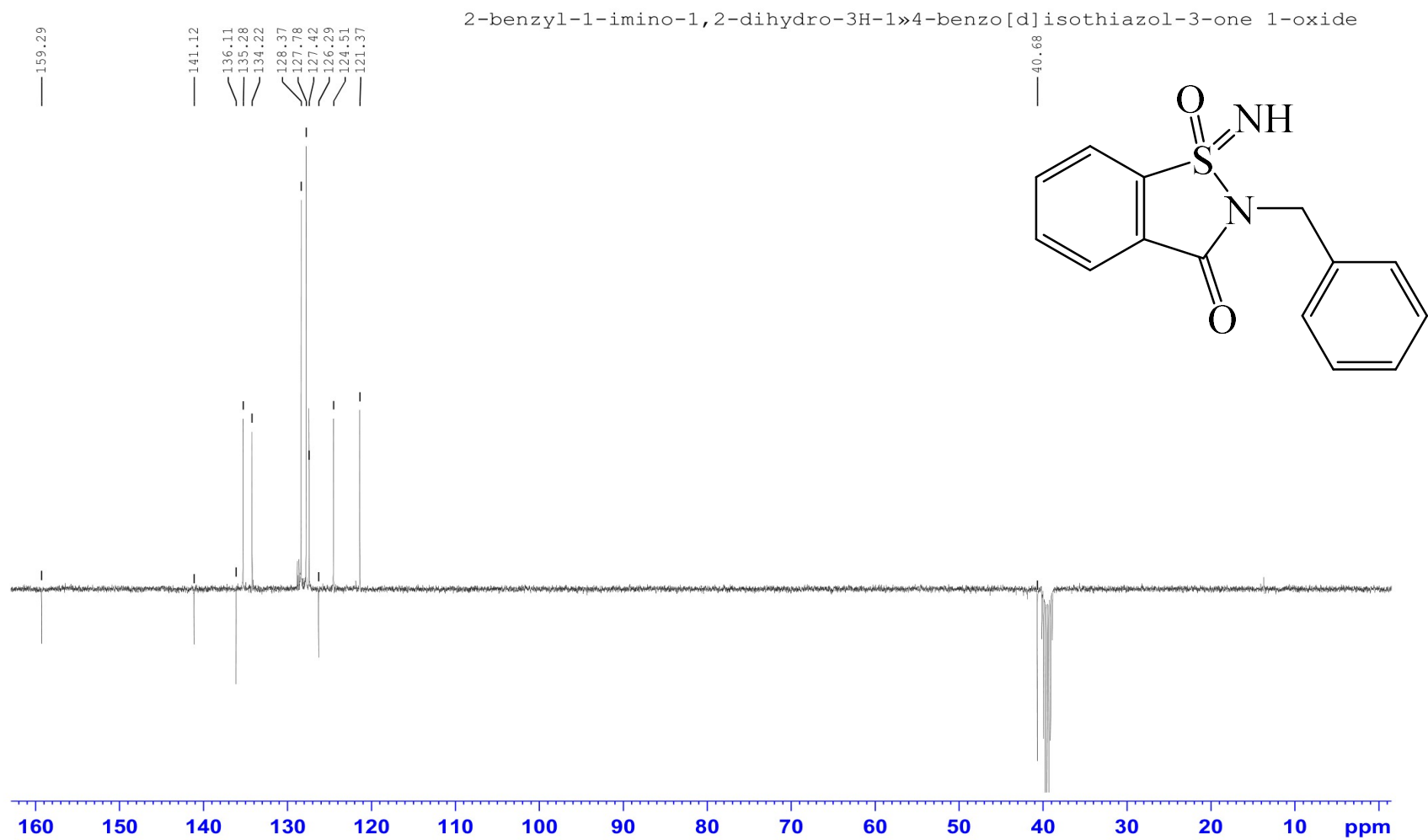
Empirical formula	C ₁₀ H ₁₂ N ₂ O ₂ S
Formula weight	224.28
Temperature/K	99.98
Crystal system	monoclinic
Space group	P21/c
a/Å	10.2429(4)
b/Å	8.4574(3)
c/Å	11.9931(4)
α /°	90
β /°	98.409(2)
γ /°	90
Volume/Å ³	1027.77(6)
Z	4
$\rho_{\text{calc}}/\text{cm}^3$	1.449
μ/mm^{-1}	0.295
F(000)	472.0
Crystal size/mm ³	0.33 × 0.28 × 0.21
Radiation	MoK α (λ = 0.71073)
2 Θ range for data collection/°	4.02 to 56.8
Index ranges	-13 ≤ h ≤ 13, -11 ≤ k ≤ 11, -16 ≤ l ≤ 15
Reflections collected	15575
Independent reflections	2521 [R_{int} = 0.0319, R_{sigma} = 0.0218]
Data/restraints/parameters	2521/0/142
Goodness-of-fit on F ²	1.233
Final R indexes [$I \geq 2\sigma(I)$]	R_1 = 0.0442, wR_2 = 0.1057
Final R indexes [all data]	R_1 = 0.0463, wR_2 = 0.1066
Largest diff. peak/hole / e Å ⁻³	0.39/-0.47

Table 6: Fractional atomic coordinates ($\times 10^4$) and equivalent isotropic displacement parameters ($\text{\AA}^2 \times 10^3$) for 1-(isopropylamino)-3H-1 λ 4-benzo[d]isothiazol-3-one 1-oxide. U_{eq} is defined as 1/3 of the trace of the orthogonalised U_{ij} tensor.

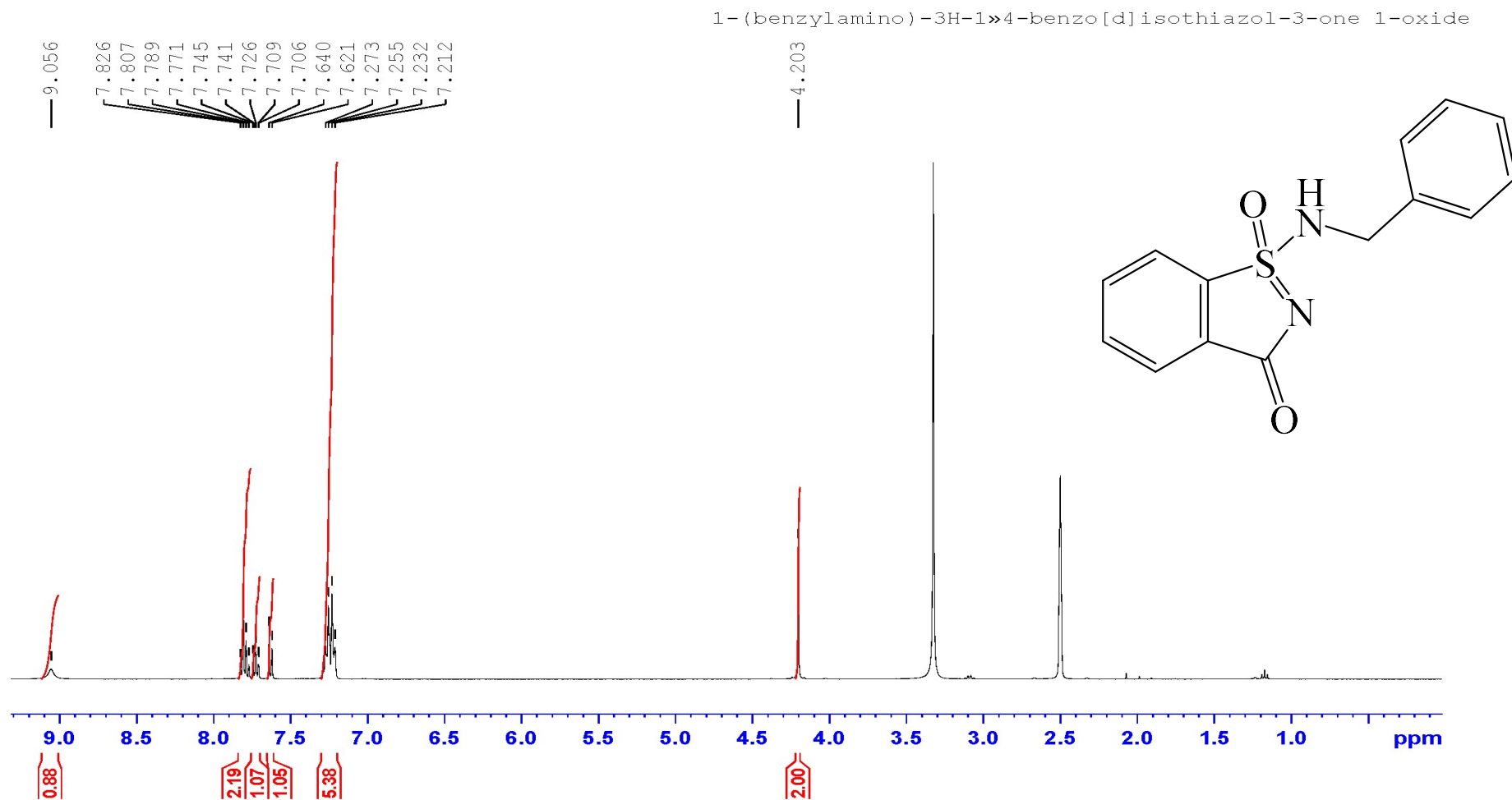
Atom	x	y	z	U(eq)
S1	7837.3(4)	7844.5(6)	4323.1(4)	14.11(13)
O1	7481.6(14)	5110.9(18)	6575.8(11)	20.3(3)
O2	8879.9(13)	8976.6(17)	4324.0(12)	20.0(3)
N1	7418.3(16)	7354(2)	5486.9(13)	17.1(3)
N2	6565.3(16)	8543(2)	3545.0(14)	15.9(3)
C1	7668.3(18)	5770(2)	5703.1(15)	15.8(4)
C2	8173.6(17)	4928(2)	4746.9(15)	14.4(4)
C3	8512.0(18)	3356(2)	4655.7(16)	16.4(4)
C4	8954.8(18)	2863(2)	3663.1(16)	18.2(4)
C5	9054.3(19)	3928(3)	2792.3(16)	18.8(4)
C6	8716.3(18)	5510(3)	2876.0(15)	17.2(4)
C7	8287.1(17)	5967(2)	3872.1(15)	14.1(4)
C8	5302.9(19)	7634(2)	3371.0(16)	18.1(4)
C9	4306(2)	8372(4)	4030(2)	33.6(6)
C10	4796(2)	7591(3)	2126.0(18)	30.4(5)



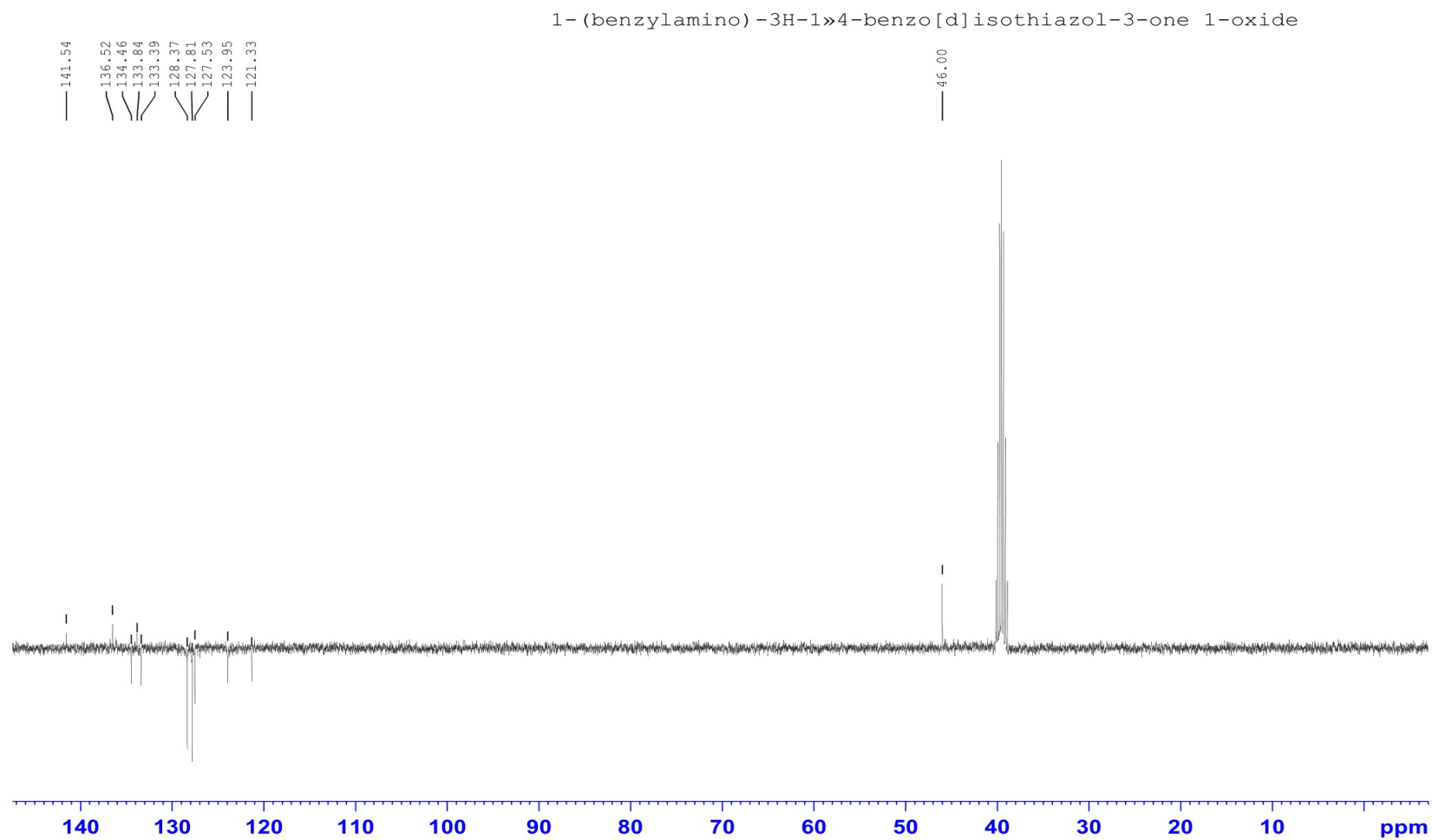
¹H NMR of 2-benzyl-1-imino-1,2-dihydro-3H-1λ⁴-benzo[d]isothiazol-3-one 1-oxide in DMSO-d₆ (5c)



¹³C NMR of 2-benzyl-1-imino-1,2-dihydro-3H-1λ⁴-benzo[d]isothiazol-3-one 1-oxide in DMSO-d₆ (5c)



¹H NMR of 1-(benzylamino)-3H-1λ⁴-benzo[d]isothiazol-3-one 1-oxide in DMSO-d₆ (5d)



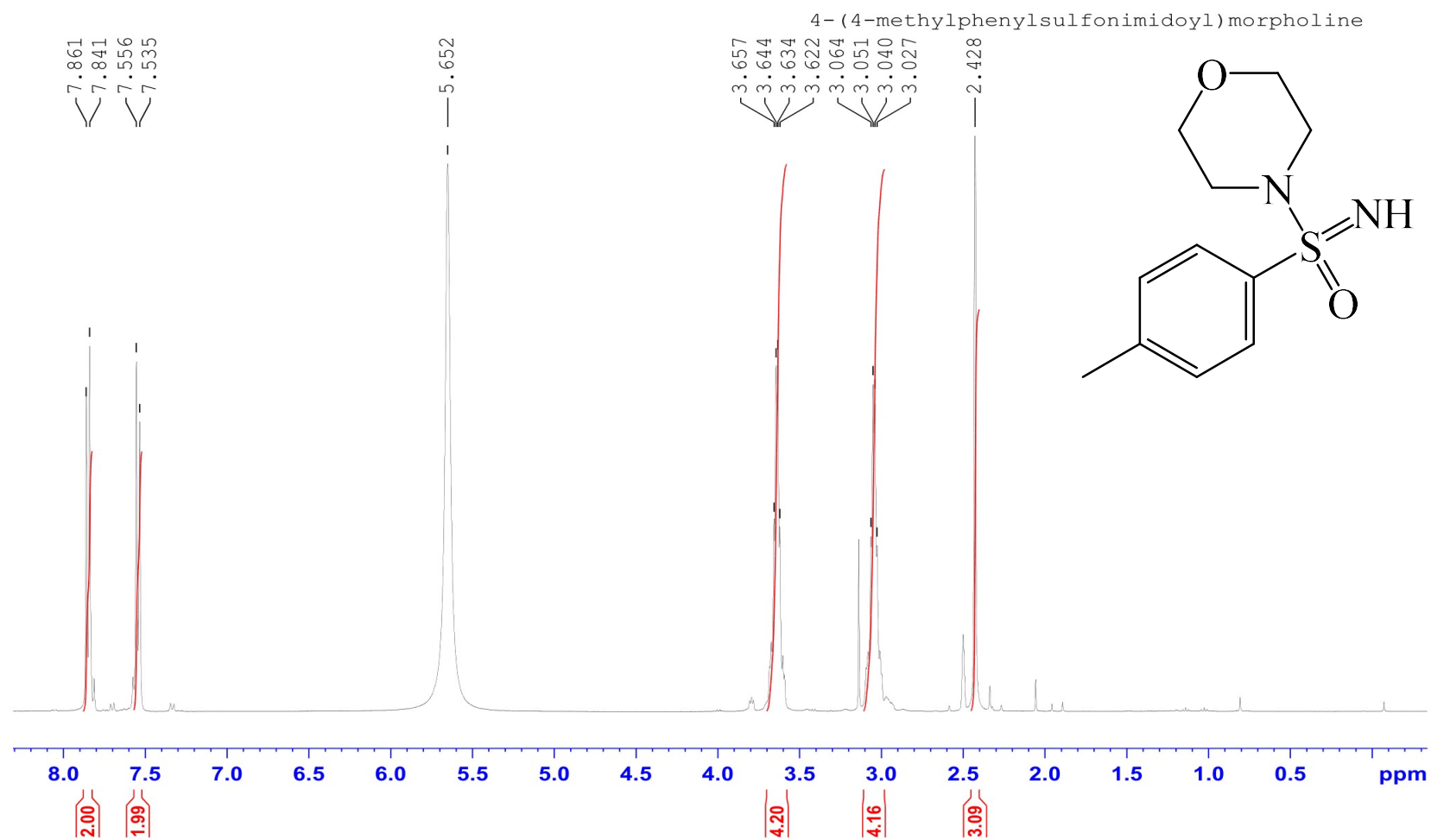
^{13}C NMR of 1-(benzylamino)-3H-1,4-benzo[d]isothiazol-3-one 1-oxide in DMSO-d_6

Table 7: Crystal data and structure refinement for 1-(benzylamino)-3H-1λ4-benzo[d]isothiazol-3-one 1-oxide.

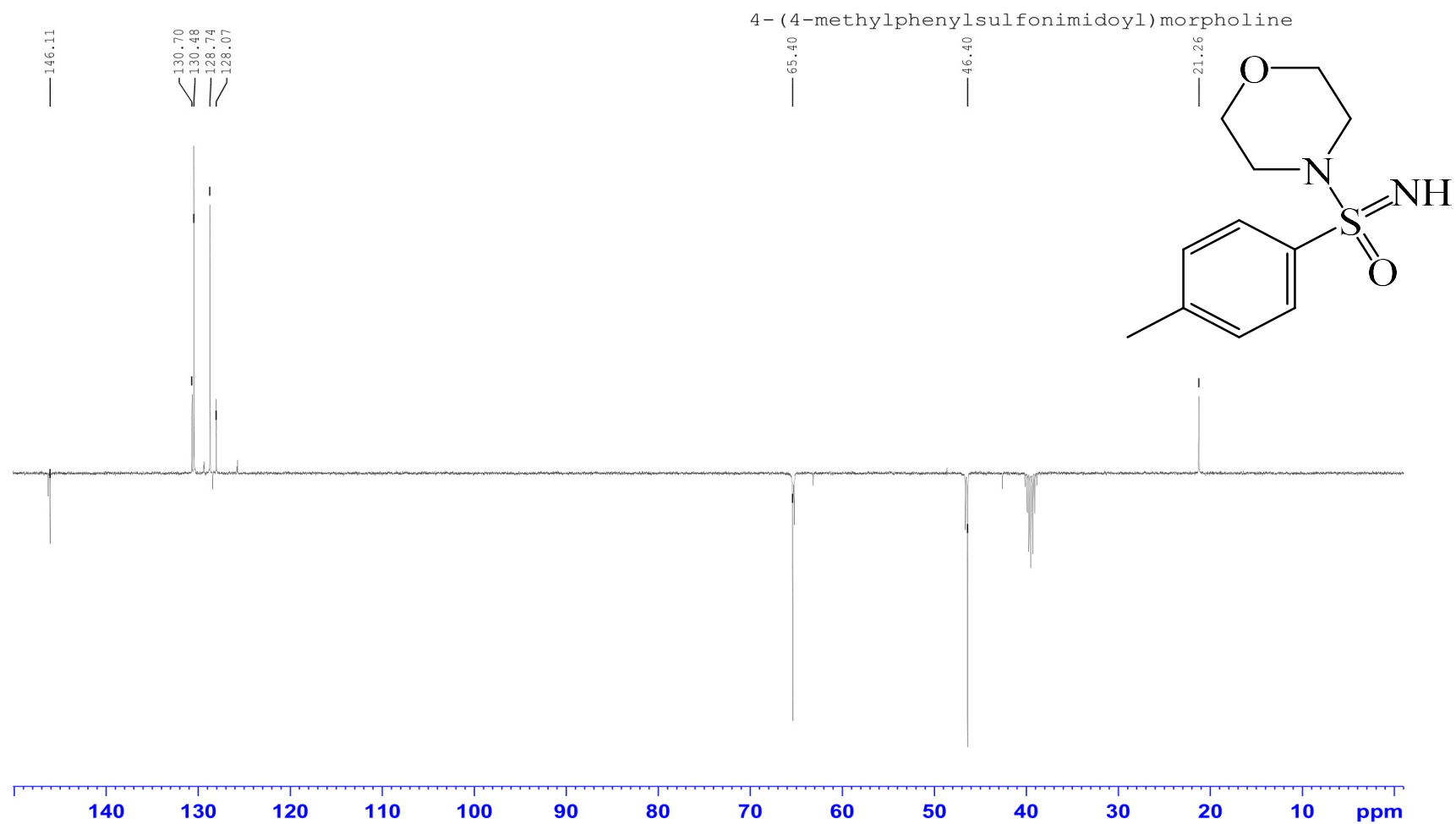
Empirical formula	C ₁₄ H ₁₂ N ₂ O ₂ S
Formula weight	272.32
Temperature/K	100.03
Crystal system	monoclinic
Space group	P21/c
a/Å	8.9031(2)
b/Å	10.2561(2)
c/Å	14.2232(3)
α/°	90
β/°	102.9750(10)
γ/°	90
Volume/Å ³	1265.58(5)
Z	4
ρ _{calc} /cm ³	1.429
μ/mm ⁻¹	0.254
F(000)	568.0
Crystal size/mm ³	0.33 × 0.21 × 0.14
Radiation	MoKα (λ = 0.71073)
2Θ range for data collection/°	4.696 to 56.728
Index ranges	-11 ≤ h ≤ 11, -13 ≤ k ≤ 12, -18 ≤ l ≤ 18
Reflections collected	14000
Independent reflections	3129 [R _{int} = 0.0146, R _{sigma} = 0.0119]
Data/restraints/parameters	3129/1/176
Goodness-of-fit on F ²	1.062
Final R indexes [I ≥ 2σ (I)]	R ₁ = 0.0299, wR ₂ = 0.0801
Final R indexes [all data]	R ₁ = 0.0330, wR ₂ = 0.0829
Largest diff. peak/hole / e Å ⁻³	0.46/-0.40

Table 8: Fractional atomic coordinates ($\times 10^4$) and equivalent isotropic displacement parameters ($\text{\AA}^2 \times 10^3$) for 1-(benzylamino)-3H-1 λ 4-benzo[d]isothiazol-3-one 1-oxide. U_{eq} is defined as 1/3 of the trace of the orthogonalised U_{ij} tensor.

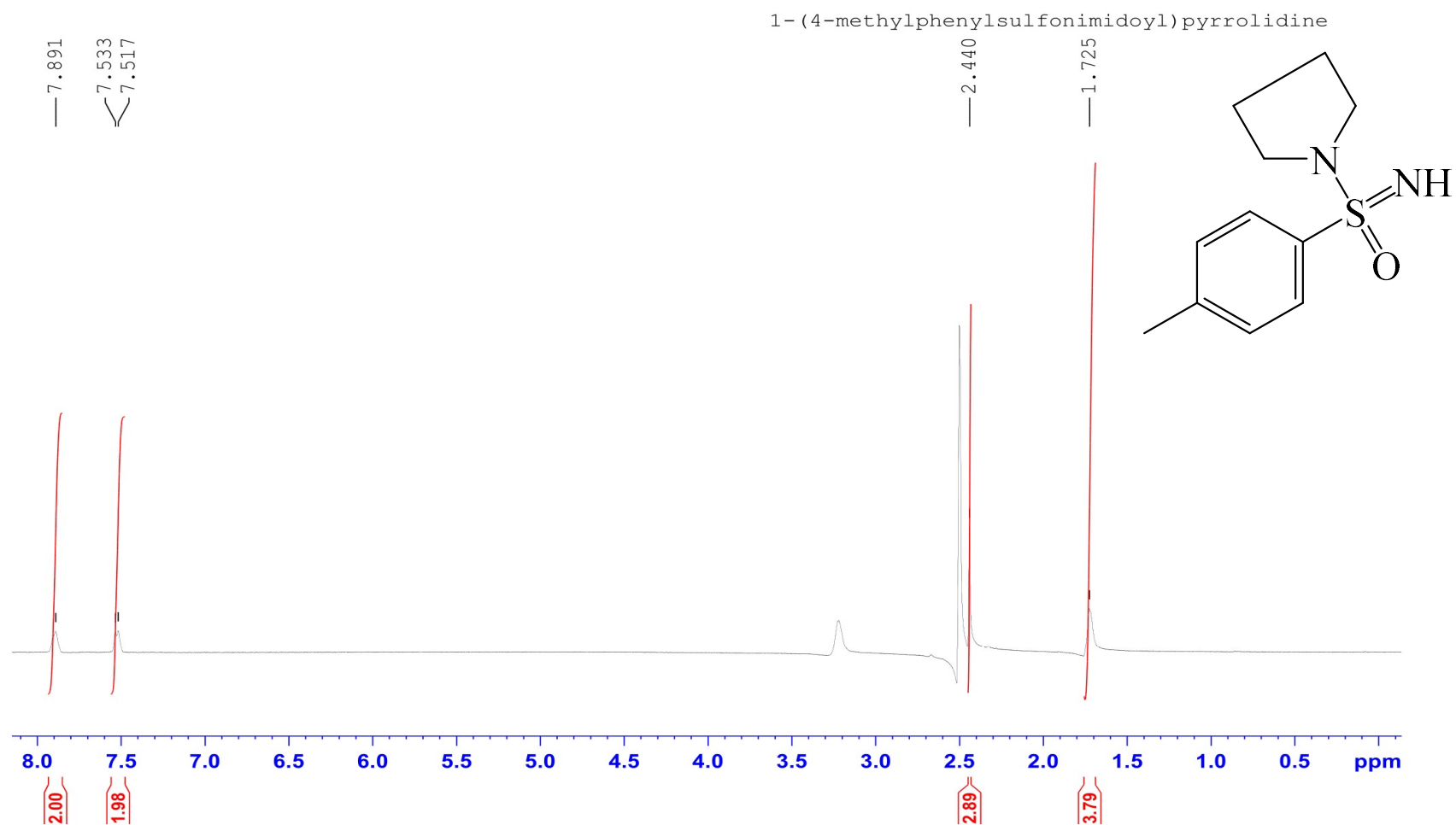
Atom	x	y	z	U(eq)
S1	5352.3(3)	5232.8(3)	2830.2(2)	13.01(9)
O1	4666.0(10)	8003.7(8)	4250.4(6)	18.27(18)
O2	6679.3(9)	4392.7(8)	3021.7(6)	17.87(18)
N2	4742.2(11)	5283.0(9)	1686.6(7)	14.91(19)
N1	5556.5(11)	6691.0(9)	3183.8(7)	15.94(19)
C2	3743.9(12)	5800.6(10)	4029.2(8)	13.6(2)
C7	3963.6(12)	4739.1(10)	3471.9(8)	13.6(2)
C1	4691.2(13)	6945.2(11)	3852.1(8)	14.5(2)
C8	3356.8(13)	6044.4(11)	1238.0(8)	16.8(2)
C6	3223.7(13)	3556.6(11)	3492.6(8)	16.3(2)
C9	1872.4(13)	5410.6(11)	1341.0(8)	16.4(2)
C3	2760.3(13)	5711.2(11)	4654.4(8)	16.1(2)
C4	2007.2(13)	4525.3(12)	4694.6(8)	18.1(2)
C5	2224.6(13)	3472.5(11)	4119.5(8)	18.0(2)
C14	894.5(15)	6040.5(12)	1832.2(9)	21.6(2)
C10	1493.9(14)	4166.8(12)	971.4(9)	22.2(2)
C11	150.6(15)	3565.4(14)	1088.4(10)	27.9(3)
C13	-450.2(15)	5431.4(14)	1951.5(10)	27.1(3)
C12	-823.2(15)	4198.2(14)	1578.3(11)	28.7(3)



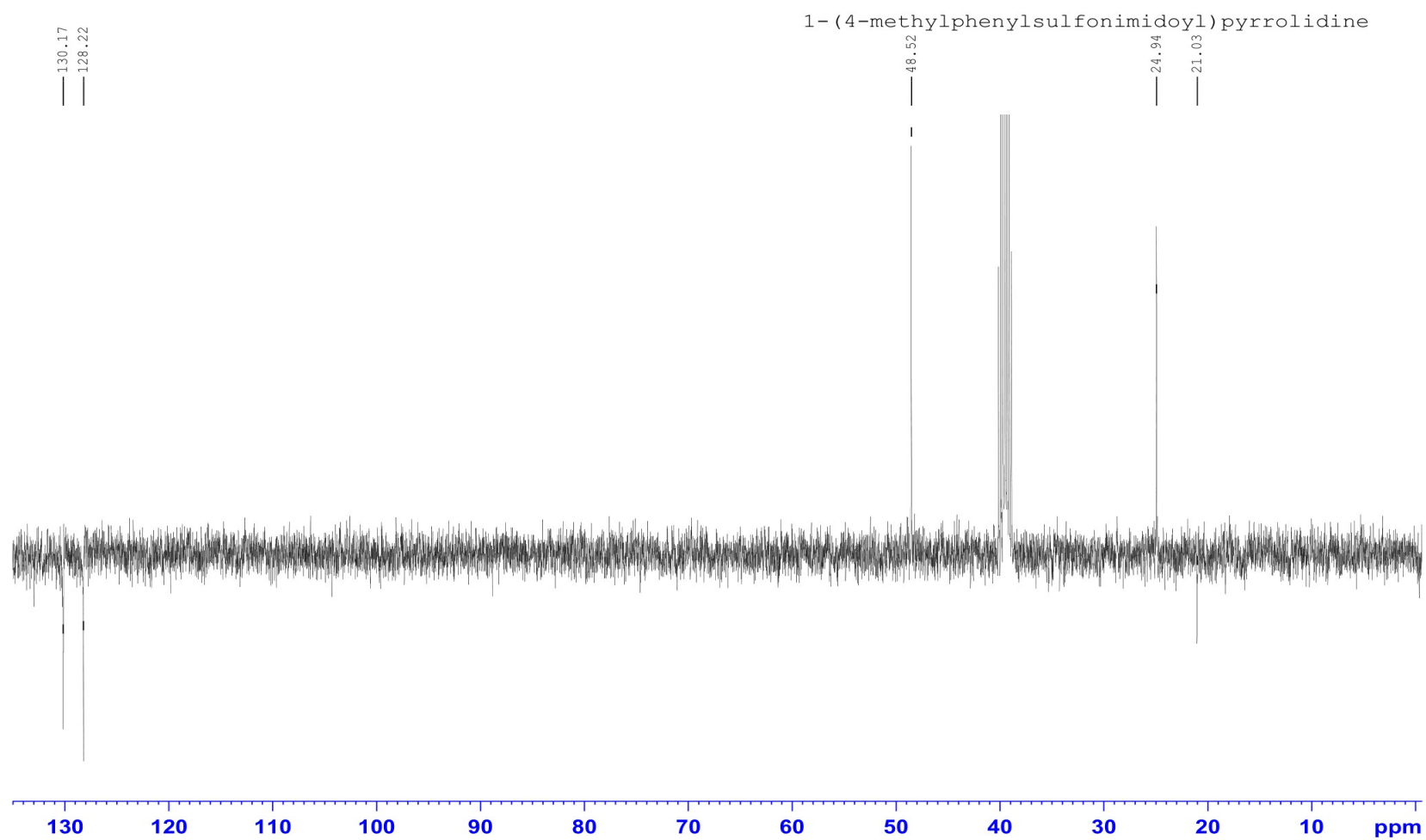
¹H NMR of 4-(4-methylphenylsulfonimidoyl)morpholine in DMSO-d₆ (5e)



¹³C NMR of 4-(4-methylphenylsulfonimidoyl)morpholine in DMSO-d₆ (5e)

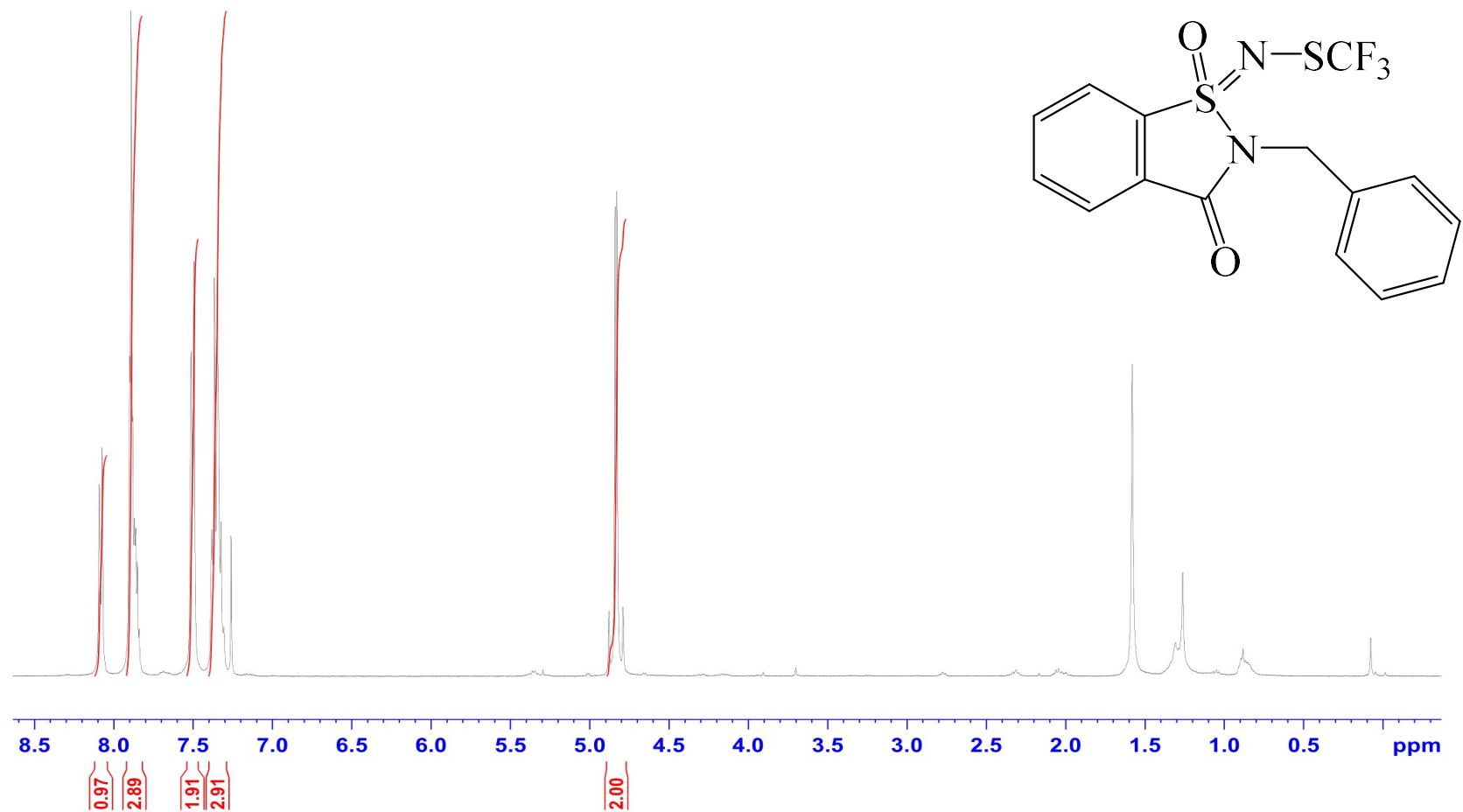


¹H NMR of 1-(4-methylphenylsulfonimidoyl)pyrrolidine in DMSO-d₆ (5f)

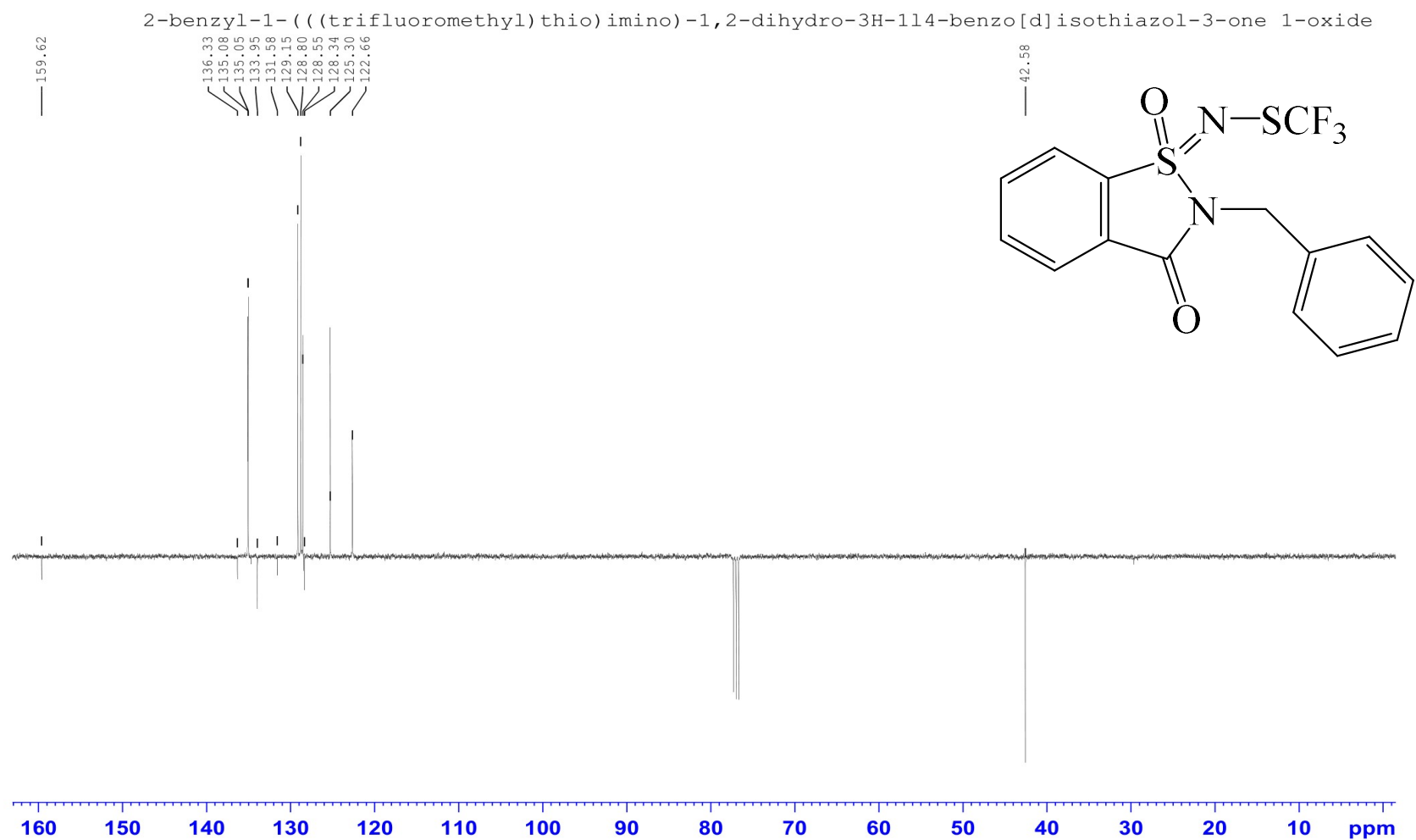


^{13}C NMR of 1-(4-methylphenylsulfonimidoyl)pyrrolidine in DMSO- d_6 (5f)

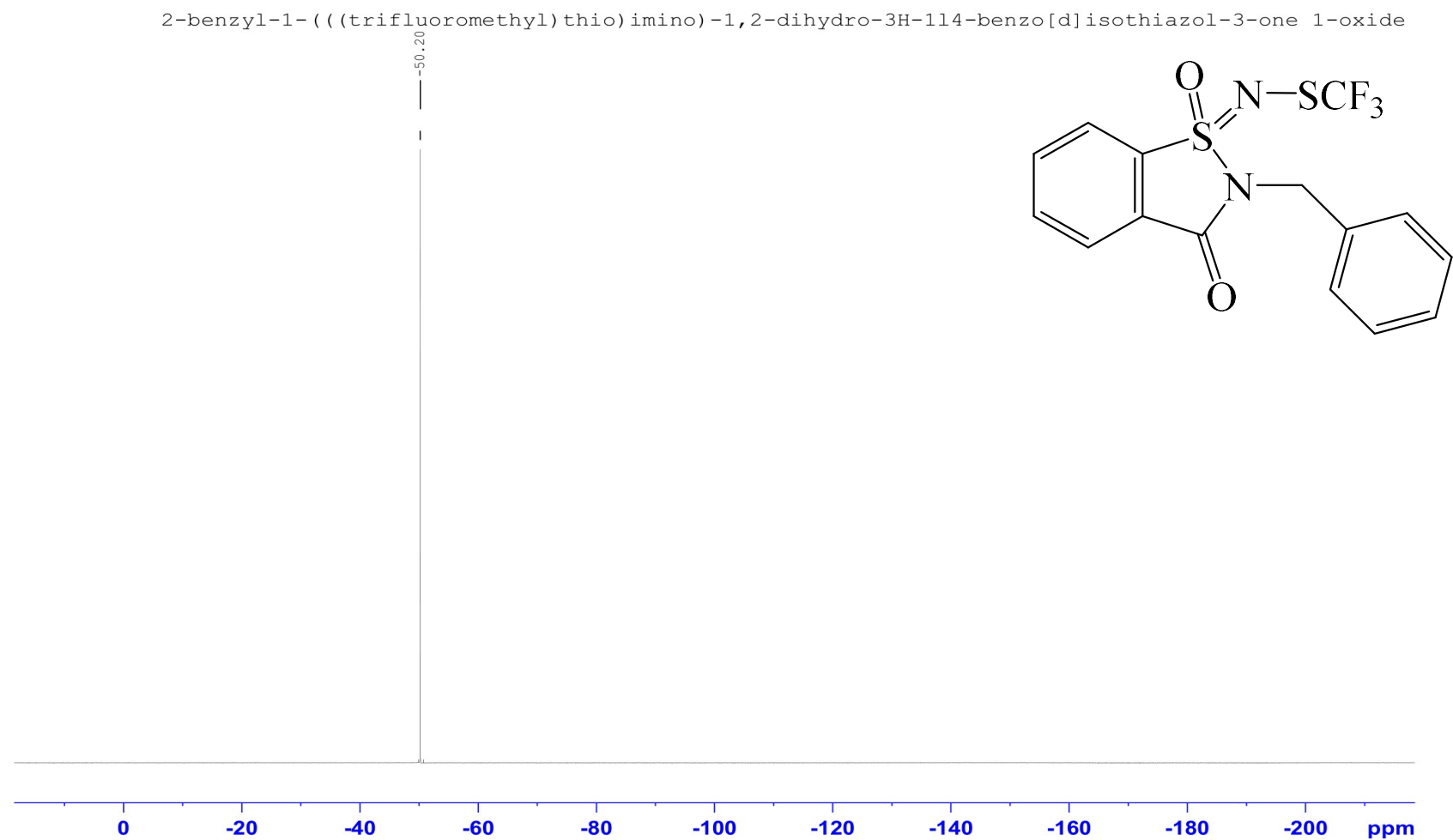
2-benzyl-1-(((trifluoromethyl)thio)imino)-1,2-dihydro-3H-114-benzo[d]isothiazol-3-one 1-oxide



¹H NMR of 2-benzyl-1-(((trifluoromethyl)thio)imino)-1,2-dihydro-3H-114-benzo[d]isothiazol-3-one 1-oxide in CDCl₃ (7c)



¹³C NMR of 2-benzyl-1-(((trifluoromethyl)thio)imino)-1,2-dihydro-3H-114-benzo[d]isothiazol-3-one 1-oxide in CDCl₃ (7c)



^{19}F NMR of 2-benzyl-1-(((trifluoromethyl)thio)imino)-1,2-dihydro-3H-14-benzo[d]isothiazol-3-one 1-oxide in CDCl_3 (7c)

Display Report

Analysis Info

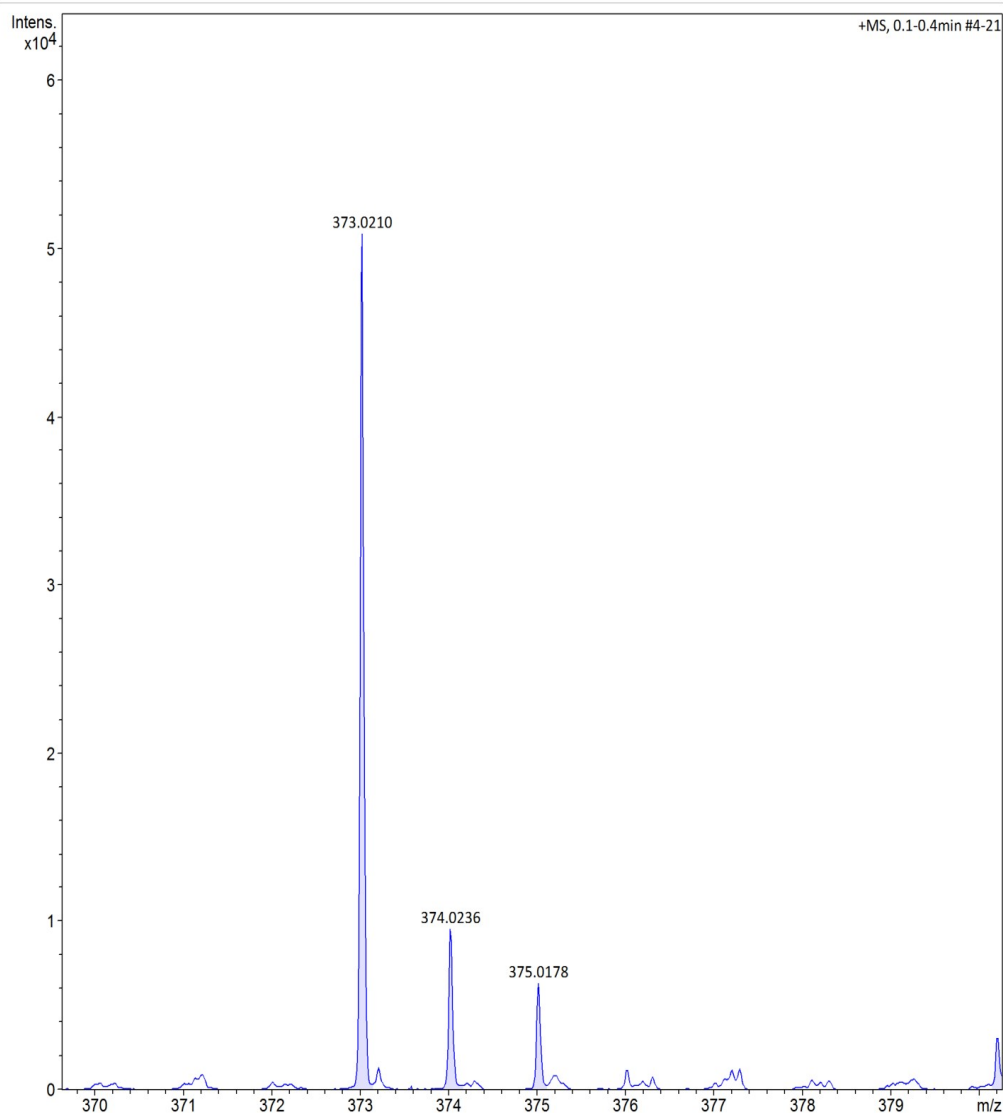
Analysis Name C:\Data\Arno\Loyd 2_01.d
Method tune_pos_mid_new.m
Sample Name 1
Comment

Acquisition Date 1/28/2020 10:30:14 AM

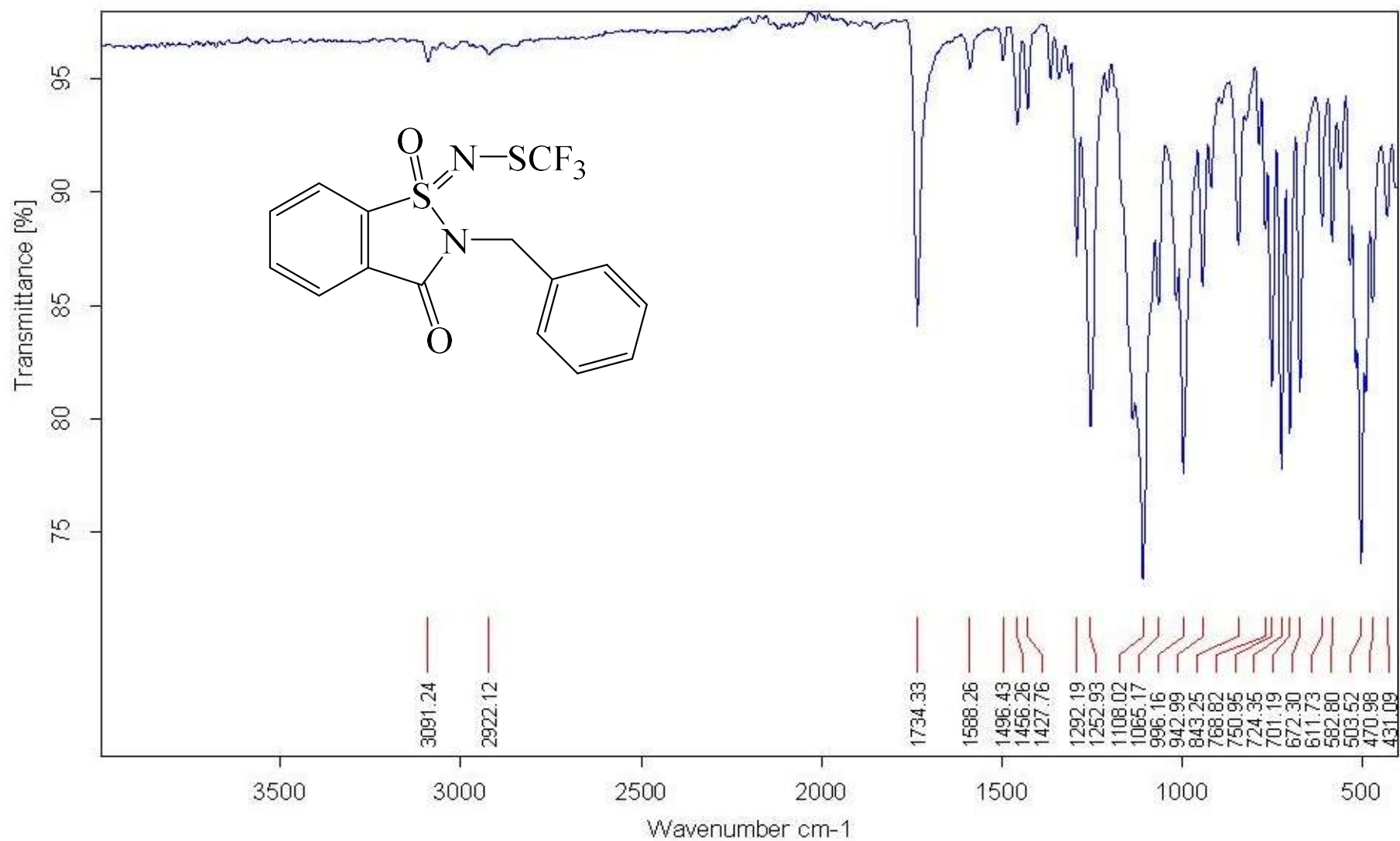
Operator @BLADE
Instrument micrOTOF-Q 228888.10139

Acquisition Parameter

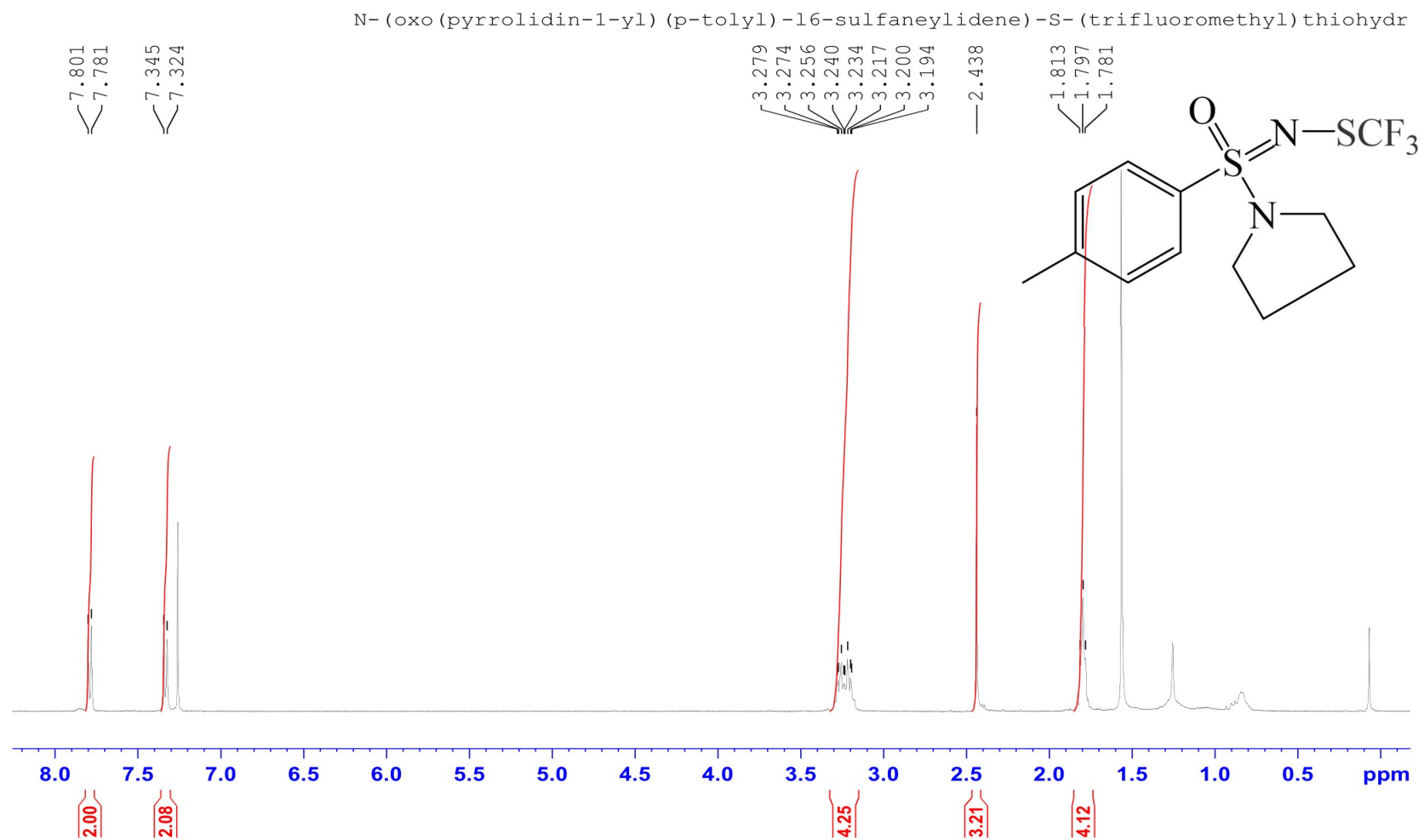
Source Type	ESI	Ion Polarity	Positive	Set Nebulizer	0.3 Bar
Focus	Not active	Set Capillary	4500 V	Set Dry Heater	200 °C
Scan Begin	50 m/z	Set End Plate Offset	-500 V	Set Dry Gas	4.0 l/min
Scan End	3000 m/z	Set Collision Cell RF	400.0 Vpp	Set Divert Valve	Source



HRMS spectrum of 2-benzyl-1-(((trifluoromethyl)thio)imino)-1,2-dihydro-3H-114-benzo[d]isothiazol-3-one 1-oxide (7c)

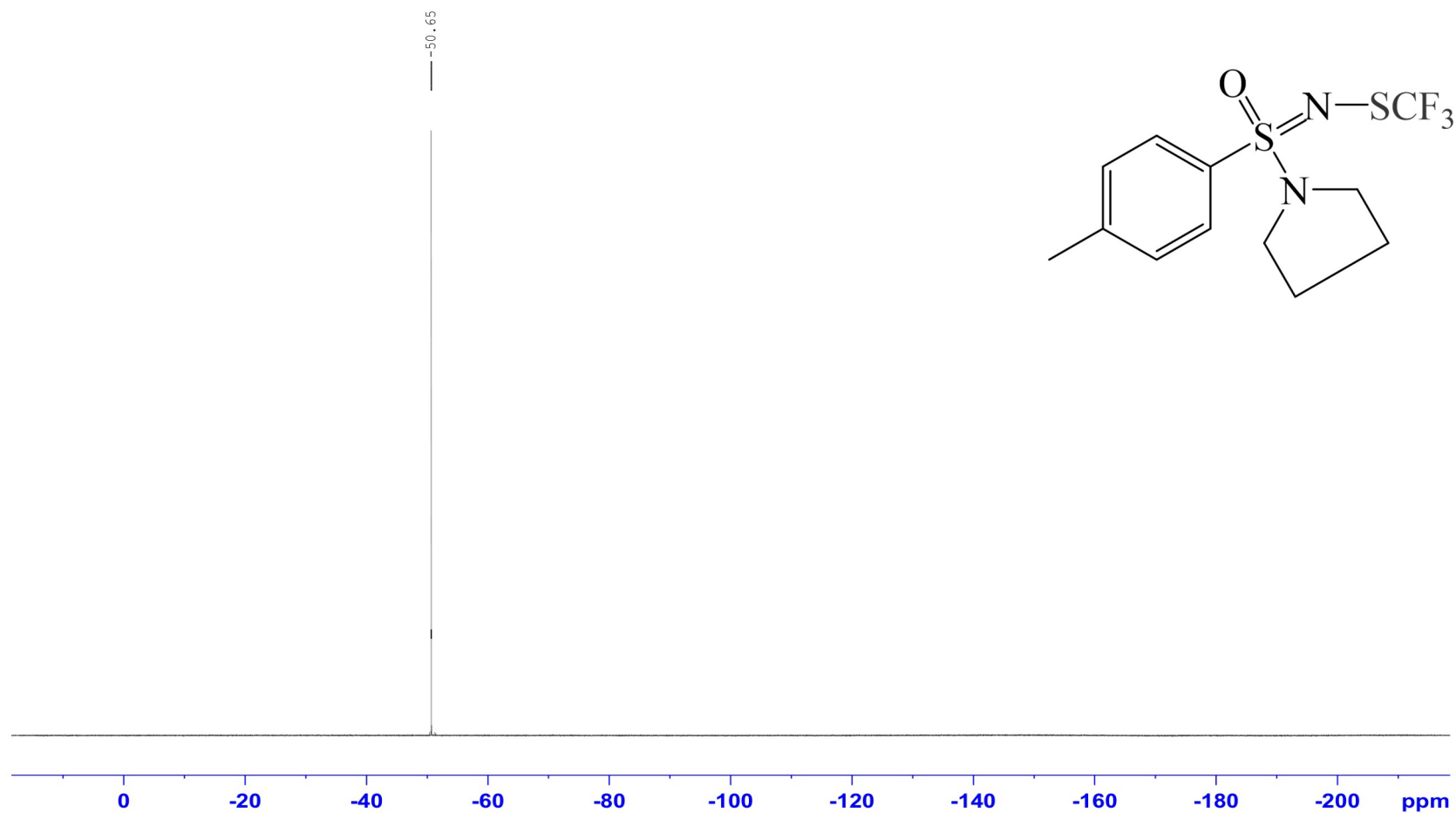


IR of 2-benzyl-1-(((trifluoromethyl)thio)imino)-1,2-dihydro-3H-114-benzo[d]isothiazol-3-one 1-oxide (7c)



¹⁹F NMR of N-(oxo(pyrrolidin-1-yl)(p-tolyl)-l6-sulfaneylidene)-S-(trifluoromethyl)thiohydroxylamine in CDCl₃ (7f)

N-(oxo(pyrrolidin-1-yl)(p-tolyl)-l6-sulfaneylidene)-S-(trifluoromethyl)thiohydroxylamine



^{19}F NMR of N-(oxo(pyrrolidin-1-yl)(p-tolyl)-l6-sulfaneylidene)-S-(trifluoromethyl)thiohydroxylamine in CDCl_3 (7f)